NASA CR-167956

R81AEG597

NASA

National Aeronautics and
Space Administration

ENERGY EFFICIENT ENGINE

LOW PRESSURE TURBINE TEST HARDWARE DETAILED DESIGN REPORT

By
D.G. Cherry
C.H. Gay
D.T. Lenahan

GENERAL ELECTRIC COMPANY
AIRCRAFT ENGINE BUSINESS GROUP
ADVANCED TECHNOLOGY PROGRAMS DEPT.
CINCINNATI OHIO 45215

Prepared for

NATIONAL AERONAUTICS AND SPACE ADMINISTRATION
LEWIS RESEARCH CENTER
21000 BROOKPARK ROAD
CLEVELAND, OHIO [illegible]135

NASA - LEWIS RESEARCH CENTER
Contract NAS3-20643

1 Report No	2 Government Accession No	3 Recipient's Catalog No
NASA CR-167956		

4 Title and Subtitle
Energy Efficient Engine
Low Pressure Turbine Test Hardware
Detailed Design Report

5 Report Date
August 1982

6 Performing Organization Code

7 Author(s)
D.G. Cherry
C.H. Gay
D.T. Lenahan

8 Performing Organization Report No
R81AEG597

10 Work Unit No

9 Performing Organization Name and Address
General Electric Company
Aircraft Engine Business Group
Cincinnati, Ohio .5215

11 Contract or Grant No
NAS3-20643

13 Type of Report and Period Covered
Topical Report

12 Sponsoring Agency Name and Address
National Aeronautics and Space Administration
Washington, D.C. 20546

14 Sponsoring Agency Code

15 Supplementary Notes
NASA Project Manager: C.C. Ciepluch
NASA Project Engineer: R.P. Dengler
Project Manager: R.W. Bucy

16 Abstract

The low pressure turbine for the Energy Efficient Engine is a five-stage configuration with moderate aerodynamic loading incorporating advanced features of decambered airfoils and extended blade overlaps at platforms and shrouds. Mechanical integrity of 18,000 hours on flowpath components and 36,000 hours on all other components is achieved along with no aeromechanical instabilities within the steady-state operating range. Selection of a large number (156) of Stage 4 blades, together with an increased Stage 4 vane-to-blade gap, assists in achieving FAR 36 acoustic goals. Active clearance control (ACC) of gaps at blade tips and interstage seals is achieved by fan air cooling judiciously applied at responsive locations on the casing. This ACC system is a major improvement in preventing deterioration of the 0.0381 cm (0.015 in.) clearances required to meet the integrated-core/low-spool turbine efficiency goal of 91.1% and the flight propulsion system efficiency goal of 91.7%.

17 Key Words (Suggested by Author(s))
Energy Efficient Engine
Low Pressure Turbine
Five Stage Turbine
Active Clearance Control

19 Security Classif (of this report)	20 Security Classif (of this page)	21 No of Pages	22 Price*
Unclassified	Unclassified	141	

[redacted]

NASA-C-168 (Rev 10-75)

ORIGINAL PAGE IS
OF POOR QUALITY

TABLE OF CONTENTS

PRECEDING PAGE BLANK NOT FILMED

LIST OF ILLUSTRATIONS

LIST OF ILLUSTRATIONS (Continued)

LIST OF ILLUSTRATIONS (Continued)

LIST OF ILLUSTRATIONS (Continued)

LIST OF ILLUSTRATIONS (Concluded)

LIST OF TABLES

SYMBOLS AND ABBREVIATIONS

ACC	Active Clearance Control
Accel	Acceleration (from Low- to High-Power Engine Operation)
Amb	Ambient
AR	Aspect Ratio, h/d_o or h/AW
AW	Airfoil Axial Width, cm (in.)
CH	Airfoil Chord
CF6	General Electric Commercial Turbofan Engine
D	Diameter, cm (in.)
d_o	Airfoil Throat Dimension, cm (in.)
DOC	Direct Operating Cost
Decel	Deceleration (from high- to Low-Power Engine Operation)
DDR	Detailed Design Review
E^3	Energy Efficient Engine
F	Force, N (lbf)
FADEC	Full Authority Digital Electronic Control
FIDLE	Flight Idle
FPS	Flight Propulsion System - The fully developed configuration of the E^3 which would be suitable for installation on an airframe.
GIDLE	Ground Idle
H	Hub
h	Airfoil Height at the Trailing Edge, cm (in.)
HCF	High Cycle Fatigue
HDTO	Hot-Day Takeoff [(50° C (122° F)]
HLFT	Highly Loaded Fan Turbine

I	Moment of Inertia
ICLS	Integrated Core/Low Spool - the Turbofan Configuration of the E^3
Inco	Inconel
K_t	Stress Concentration Factor
ℓ	Extended Aerodynamic Overhang
L	Airfoil Length, cm (in.)
LCF	Low Cycle Fatigue
LE	Leading Edge
LP	Low Pressure
LPT	Low Pressure Turbine
M	Mach Number
MXCR	Maximum Cruise Operating Point
N	Turbine Speed, rpm
n	Number of Airfoils per Blade Row
P	Pressure, Pa (psi)
P_T	Total Pressure, Pa (psi)
R	Rotor
R1	Stage 1 Rotor
R2	Stage 2 Rotor
R3	Stage 3 Rotor
R4	Stage 4 Rotor
R5	Stage 5 Rotor
Rev	Revolution
sfc	Specific Fuel Consumption, kg/N • hr (lbm/lbf • hr)
S	Stator

SS	Stainless Steel
S1	Stage 1 Stator
S2	Stage 2 Stator
S3	Stage 3 Stator
S4	Stage 4 Stator
S5	Stage 5 Stator
SLTO	Sea Level Take-off
t	Thickness, cm (in.)
T	Total Temperature, Temperature, K, °C (°R, °F)
TE	Trailing Edge
TIG	Tungsten Inert Gas
u or U	Rotor Tangential Velocity at the Mean Radius, m/sec (ft/sec)
V	Absolute Velocity, m/sec (ft/sec)
W	Flow, kg/sec (lbm/sec)
α	Absolute Flow Angle, Degrees from Axial
β	Relative Flow Angle, Degrees from Axial
Γ	Turbine Exhaust Swirl, Degrees
Δ	Differential or Incremental Value (Prefix)
Δh	Energy Extraction, J/g (Btu/lbm)
ΔT_{amb}	Temperature above Ambient, 15° C (59° F), on a Standard Day
ζ	Blade Tip Shroud Interlock Angle, Degrees
η	Turbine Efficiency
θ	Blade Tip Shroud Angle Denoting Direction of Shroud First-Flexural Vibration
μ	Coefficient of Friction
σ	Stress
ϕ	Assembly Pretwist Rotation of Blade Tip Shroud, Degrees

ψ Turbine Loading, $\Delta h/$[illegible]

ν Flutter Index

<u>Subscripts</u>

0	Turbine Stator Inlet Plane
1	Turbine Stator Exhaust/Rotor Inlet Plane, Also Bloderow Exit Plane in Figures 9-18
2	Turbine Rotor Exhaust Plane
25,2.5	Core Compressor Inlet Plane Cycle Designation
42,4.2	HPT Exhaust Plane, Cycle Designation
49,4.9	LPT Inlet Plane, Cycle Designation
50,5.0	LPT Exit Plane Cycle Designation
Alt	Alternating
amb	Ambient
c or C	Coolant Air
Eff	Effective (Combined effective stress per the Hinkey Von Mises theory)
L	Leakage
Max	Maximum Local Value
Mean	Mean Value of Stress Range
Nom	Nominal (i.e. without K_t)
R	Relative
Rad	Radial
p or P	Pitchline (mean radius), or peak
S	Static
T	Total
TT	Denotes Condition Based on Total-To-Total Properties (P_{T_0}/P_{T_2})
Z	Axial
z	Denotes Zweifel
θ	Tangential (as in tangential stress)

1.0 INTRODUCTION AND SUMMARY

This report describes the detailed aerodynamic, heat transfer, and mechanical design of the low pressure turbine (LPT) for the Energy Efficient Engine (E^3). The LPT configuration in Figure 1 was selected after investigation of alternate designs, tradeoff studies, payoff evaluations, and extensive preliminary design analyses aimed at achieving high aerodynamic efficiency while maintaining maximum mechanical integrity.

The E^3 LPT is a five-stage, moderately loaded, low-through-flow design with a high outer wall slope of 25°. The LPT is close-coupled to the high pressure turbine (HPT) via a 7.62-cm (3-in.) axial length transition duct. The flowpath has been sized to match the fan characteristics and to achieve performance goals for the flight propulsion cycle. Provisions have been made to accommodate a potential growth application. The aerodynamic design point is the maximum-climb power setting at Mach 0.80 and 10.67-km (35,000-feet) altitude.

The design-point gas flow rate through the LPT is 22.7 kg/s-m^2 (4.6 lbm/sec-ft^2). The Stage 1 rotor has a tip radius of 0.45 m (17.55 in.) and a tip speed of 168.6 m/s (553 ft/sec). The Stage 5 rotor has a tip radius of 0.59 m (23.28 in.) and a tip speed of 223.7 m/s (734 ft/sec).

An assessment of the performance of the LPT has been made based on a series of scaled air-turbine tests divided into two phases: Block I and Block II. The transition duct and the first two stages of the turbine were evaluated during the Block I phase from March through August 1979. The full five-stage scale model, representing the final integrated core/low spool (ICLS) design and incorporating redesigns of Stages 1 and 2 based on Block I data analysis, was tested as Block II in June through September 1981.

Results from the scaled air-turbine tests, which will be reviewed briefly herein, indicate that the five-stage turbine designed for the ICLS application will attain an efficiency level of 91.5% at the Mach 0.8/10.67-km (35,000-ft), max-climb design point. This is relative to program goals of 91.1% for the ICLS and 91.7% for the flight propulsion system (FPS).

In order to improve roundness control and radial clearances, the casing is a full 360° structure, rather than two 180° halves, with nozzle stators attached in multivane segments. The LPT rotor assembly employs high-aspect-ratio, tip-shrouded blading in disks connected by bolted flanges in low-stress attachment areas. The rotor assembly is supported by a single bearing cone. The Stage 4 rotor-to-stator spacing employs a wide gap (1.4 blade chord lengths) to minimize turbine noise.

Cooling requirements have been minimized so that only the Stage 1 nozzle employs controlled purge air from the fifth-stage compressor bleed for seal blockage and disk rim purge.

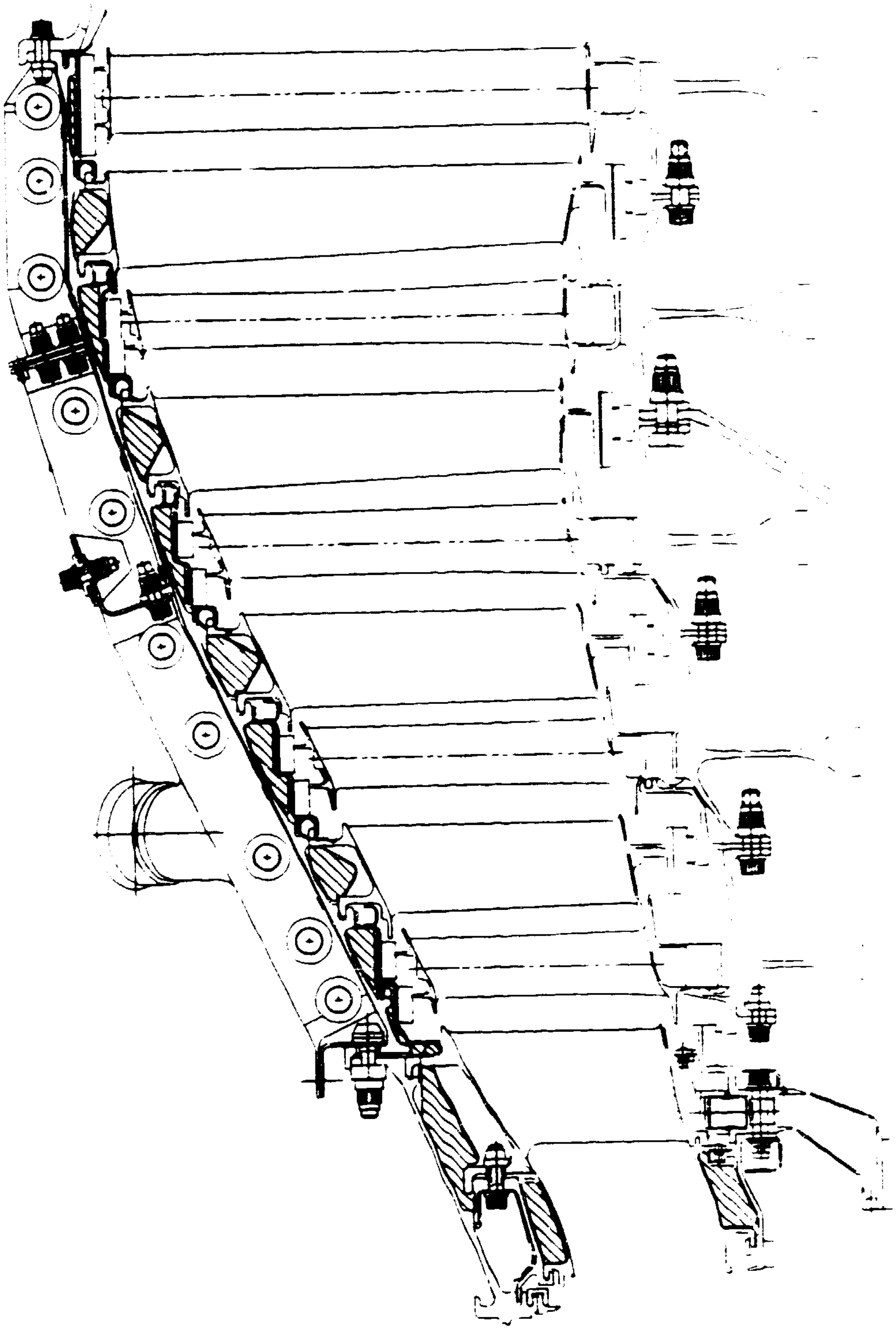

Figure 1. LPT Flowpath, ICLS Configuration.

Active clearance control (ACC) is an integral part of the LPT design. The ACC uses fan bleed air routed from pylon scoops to a distribution manifold for impingement on the casing. The ACC system reduces blade-tip and interstage-seal radial clearances at selected high-performance operating points.

Mechanical integrity is assured by designing airfoils for a service life of 18,000 missions and 18,000 stress cycles. The casing and rotor are sized for 36,000 missions and 72,000 stress sycles, respectively. Airfoil quantities and characteristics have been selected so that no resonances are predicted in the range of engine steady-state operating speed. All material-property design data are based on average-minus-three standard deviations (-3σ) and include section size considerations.

The capability of the LPT configuration to meet design and operating requirements in each technical area is discussed, and the technical details are presented in depth, in the following pages.

2.0 AERODYNAMIC DESIGN

2.1 DESIGN REQUIREMENTS

Historically in prototype engines, turbomachinery component efficiencies fall short of design goals by significant amounts. The consequent cycle rebalance causes components to operate off-design, further reducing efficiency. In an attempt to obviate this trend, the ICLS cycle was devised with appropriate derates on component efficiencies. Depending on the accuracy of the efficiency derates, turbomachinery components designed to the requirements of the resultant cycle will avoid off-design penalties.

Table I presents LPT cycle data for the ICLS max-climb aerodynamic design point and, for comparison, data for the FPS maximum climb, maximum cruise, and sea level takeoff points. Note the relatively small differences between climb and cruise for the FPS. Note further that the ICLS has been designed to a flow function approximately 4% higher at climb than the FPS. This reflects the derated component efficiencies and estimated instrumentation losses in the ICLS.

Efficiency goals at Mach 0.8/10.67 km (35,000 ft) maximum climb are 0.911 (or 91.1%) for the ICLS and 0.917 (91.7%) for the FPS.

2.2 NUMBER OF STAGES

The selection of a five-stage configuration for the E^3 LPT was based in part on results obtained during the IR&D-funded Highly Loaded Fan Turbine (HLFT) technology development program and also on system studies aimed at minimizing direct operating cost (DOC). These system studies evaluated the impact of turbine loading, weight, and cost on DOC and indicated a relative optimum at a loading level attainable in five stages. Further, significant performance gains at this loading level had been demonstrated in the HLFT program, indicating that the ICLS goal could be met with a five-stage turbine.

2.3 INITIAL FLOWPATH SELECTION (BLOCK I)

Maximum tip diameters for the HPT and LPT were set by mechanical and configuration control requirements at 76.2 cm (30 in.) and 118.1 cm (46.5 in.), respectively. In addition, the LPT flowpath outer-wall slope was limited to 25° through Stage 3, transitioning to cylindrical by the Stage 5 exit.

The initial (Block I) five-stage flowpath was defined through an iterative technique whereby a candidate outer-wall contour was selected (within the limitations on wall slope and exit diameter), and the inner wall contour and stage energy distribution were iterated concurrently to yield acceptable levels of loading ($gJ\Delta h/2u^2$) and flow coefficient (V_z/u) for each stage. The

Table I. Critical LPT Operating Point Data.

Parameter	Units	ICLS	FPS		
		Max. Climb	Max. Climb	Max. Cruise	Sea Level Takeoff +27° F
Inlet Temp., T49	K	1099.8	1083.2	1054.6	1128.7
	° R	1979.7	1949.8	1898.2	2031.6
Energy, $\Delta h/T$	J/kg/K	318.1	326.5	322.3	306.3
	Btu/lbm/° R	0.07597	0.07798	0.07697	0.07315
Speed, $N/\sqrt{T}$	rad/sec$\sqrt{K}$	11.07	11.26	11.08	10.61
	rpm/$\sqrt{°R}$	78.82	80.14	78.86	75.53
Corrected Flow, $W\sqrt{T}/P$	g$\sqrt{K}$/sec·Pa	4.098	3.936	3.947	3.967
	lbm$\sqrt{°R}$/sec·psi	83.57	80.27	80.33	80.90
Loading, $\Delta h/2u^2$	---	1.292	1.283	1.308	1.355
Efficiency, η	---	0.911	0.917	0.916	0.921

best candidate flowpaths were selected based on a stage-by-stage efficiency estimate which accounted for the effects of loading, flow coefficient, tip slope, aspect ratio, and clearance.

2.4 BLOCK I AIR TURBINE DESIGN AND TEST

The detailed aerodynamic design of Stages 1 and 2 of the Block I flowpath was executed according to HLFT design philosophy in a 0.67-scale test rig. The configurations tested, along with the approximate test dates, were as follows:

- Stage 1 nozzle annular cascade (March 1979)
- Stage 1 (April 1979)
- Stage 1 with Stage 2 nozzle annular cascade (June 1979)
- Two-stage group (August 1979).

The rig flowpath for the two-stage group is shown in Figure 2. Note that the HPT to LPT transition duct is an integral part of the Stage 1 vane assembly.

Total-to-total efficiency for the Block I two-stage build, as tested in the two-stage group, was below the pretest prediction. The following items were identified as possible contributors to the deficiency.

1. An area of secondary flow over the outer 40% of span of the Stage 1 vane was identified during the Configuration 1 test. This loss core, caused by the combination of a weakened inlet boundary layer (from the diffusing outer wall of the transition duct) and the high vane tip slope, induces deviation from the design-intent efficiency near the stator tip. Figure 3 presents the measured efficiency for Stator 1. Note that the transition duct loss is included in the cascade efficiency definition.

2. Similar secondary flow effects were noted during Configuration 3 testing over the outer 20% span of the Stage 2 vane.

3. Both rotating tests revealed unexpectedly poor performance in the region of the rotor hubs. Figure 4 presents the Stage 1 efficiency profile. Note that, in addition to the severe dropoff at the hub, performance in the outer half of the annulus is depressed due, in part, to the Stage 1 vane tip losses.

A stage-by-stage performance stackup for the ICLS turbine, using the trend and the level of the stage efficiency versus loading characteristic established by the Block I test series, indicated a status efficiency of 90.4% versus the ICLS goal of 91.1%, a 0.7% deficiency.

Based on extensive posttest data matching and data analysis, the following were identified as crucial items to be addressed during the Block II redesign:

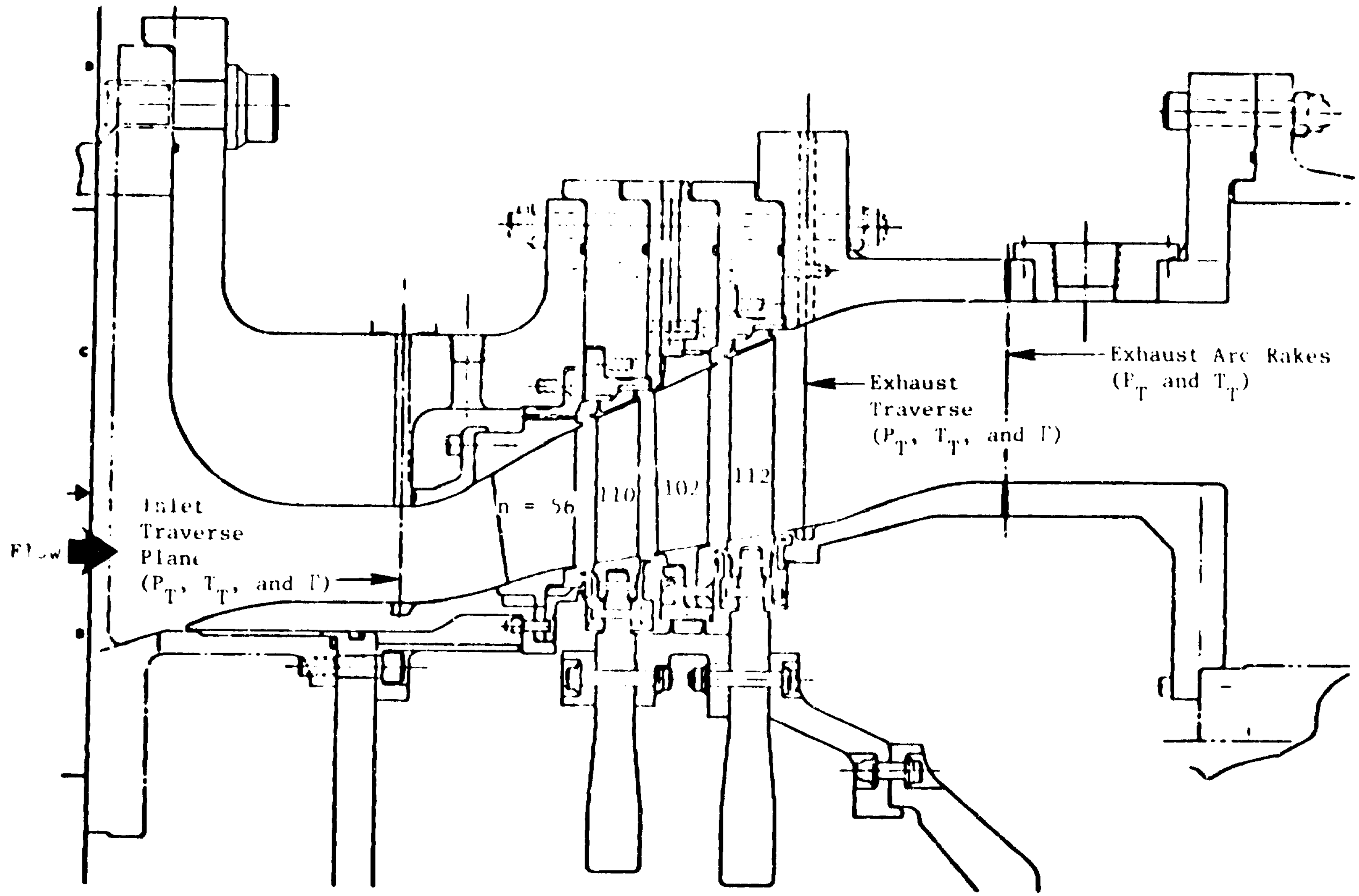

Figure 2. Scaled Test Vehicle Flowpath, Block I Two-Stage Build.

ORIGINAL PAGE IS
OF POOR QUALITY

ORIGINAL PAGE IS
OF POOR QUALITY

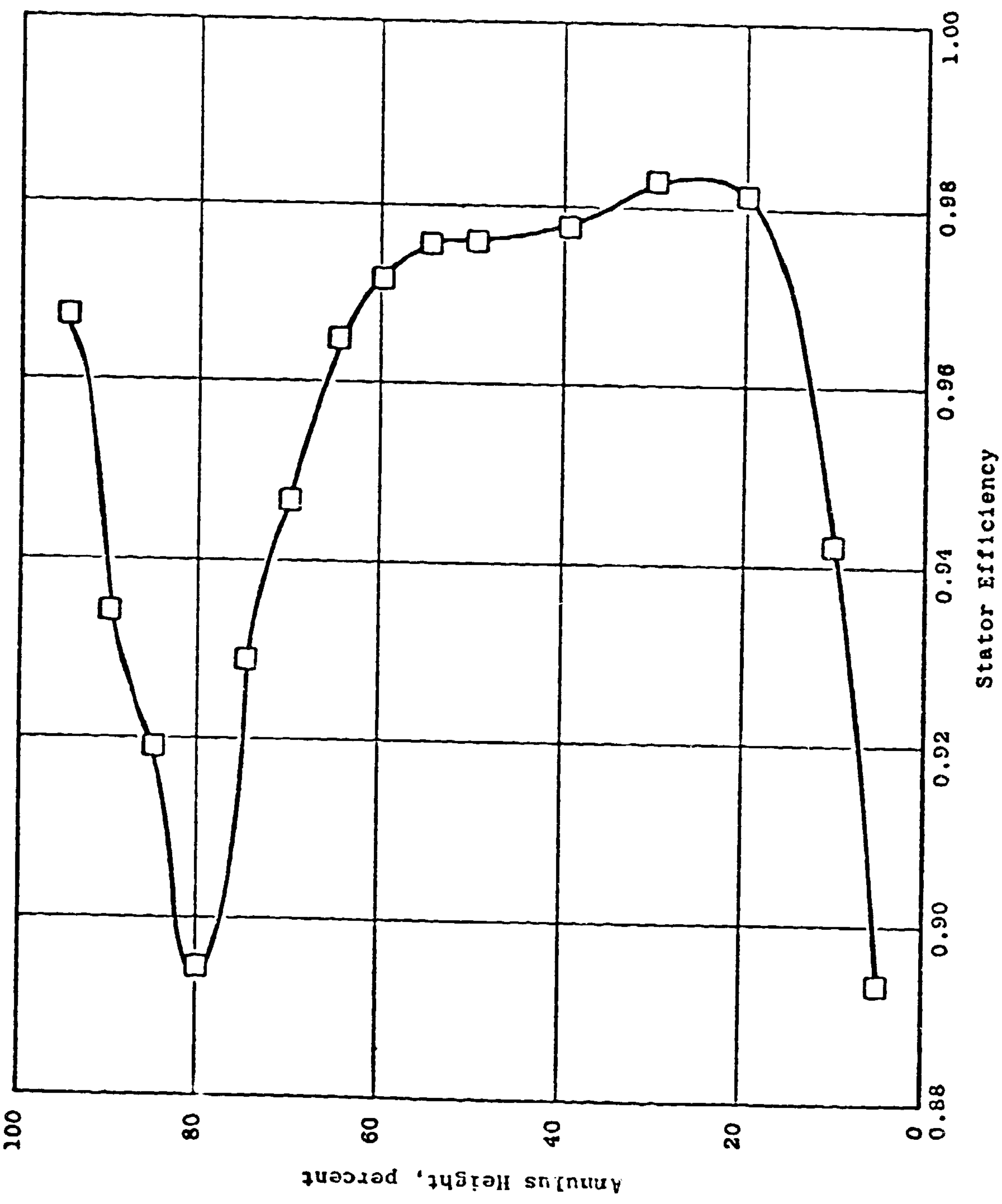

Figure 3. Block I, Stage I Vane Kinetic Energy Efficiency.

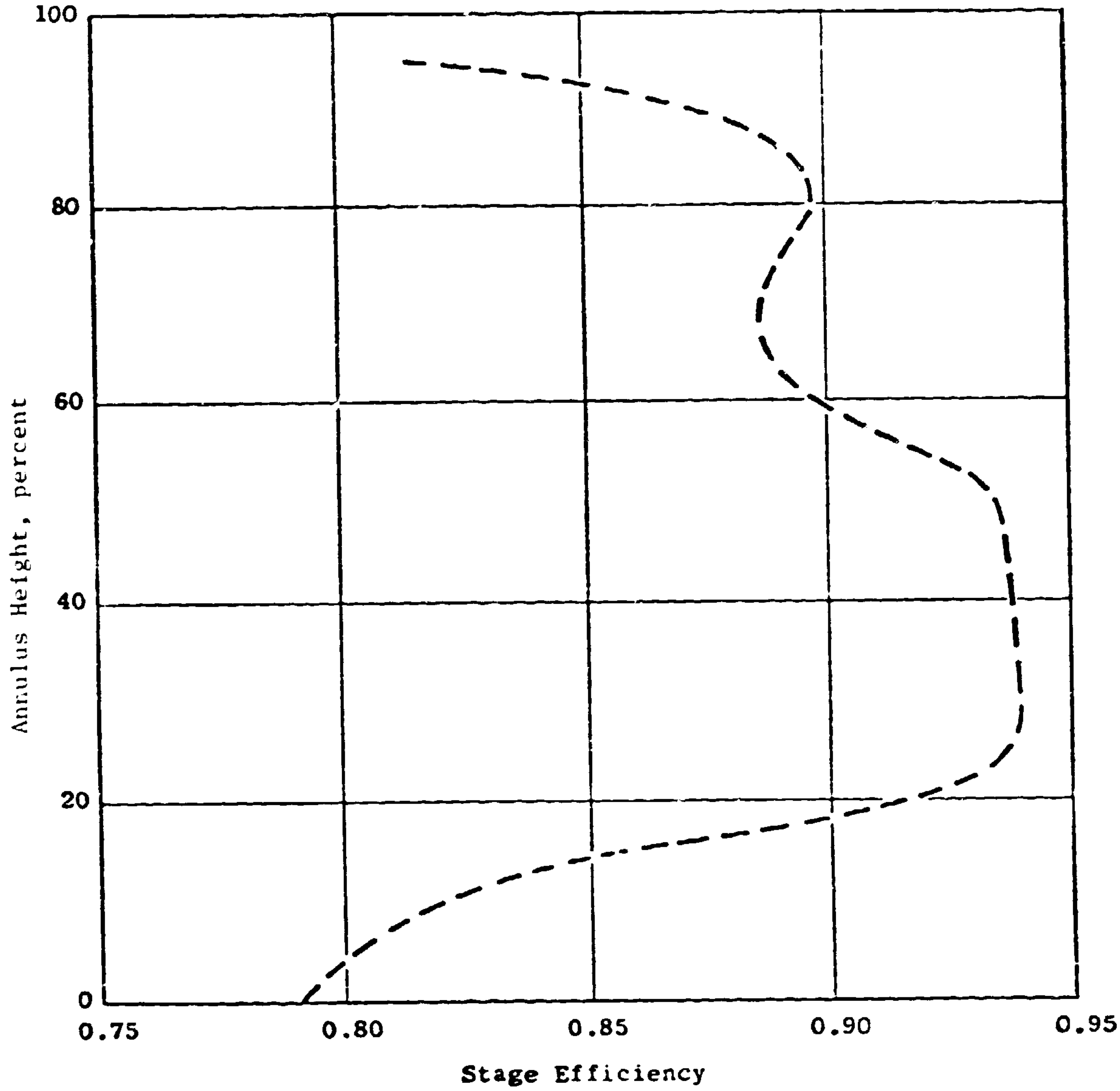

Figure 4. Block I, Stage 1 Total-to-Total Efficiency.

- o Stage 1 vane solidity is low, especially at the hub.

- o Stage 1 vane aspect ratio is low, especially near the tip.

- o The solidity of rotor blade hubs is low, and there is excessive pressure-side diffusion near the leading edges.

- o A severe performance penalty is incurred by the increase in outer wall slope from 22° (HLFT) to the current 25°. This is especially true in the vicinity of low-aspect-ratio-vane tips.

- o Inner and outer-wall overlap geometry is degraded relative to HLFT. This refers specifically to the amount (or lack) of axial overlap between the stator bank and the rotor platforms/tip-shroud extensions.

2.5 FINAL FLOWPATH SELECTION (BLOCK II)

In order to address the issue of outer-wall slope and the influence it has on performance, several alternate flowpaths were developed and analyzed by those methods previously described. One ground rule that was enforced in the course of this alternate-flowpath study was that the overall length and diameter remain unchanged. Results of the study indicated that configurations which reduce wall slope via an increase in loading or through-flow velocity show a net loss relative to the base Block I flowpath. Consequently, the Block II (final aero) flowpath has remained essentially unchanged from the Block I status. However, the following modifications were incorporated to address the specific problems identified during Block I testing:

- o A higher aspect ratio, higher solidity version of the Stage 1 vane has been added, along with a modified transition duct, to accommodate the new vane design. Figure 5 shows a comparison of the Block I duct/vane with that of Block II. Note that the solidity was increased by raising the airfoil count from 56 [illegible], this also increases the airfoil-throat aspect ratio (he[illegible] throat). The chordal aspect ratio was increased by reduc[illegible]e axial chord at the outer wall.

- o An effort to improve flowpath overlaps resulted in the Block II five-stage flowpath shown in Figure 6. A comparison of typical inner-wall overlap geometry for Block II with that of Block I (inset, Figure 6) shows that the rotor platforms have been extended to lap under the stator inner bands. Note also that the flow near the outer wall is effectively shielded from the open honeycomb of the tip shrouds; this was not the case in Block I (see Figure 2). The poor performance of the Block I stages near the walls is partly attributable to the overlap geometry, which is more open relative to past General Electeric AEBG (Aircraft Engine Business Group) air turbine rig flowpaths.

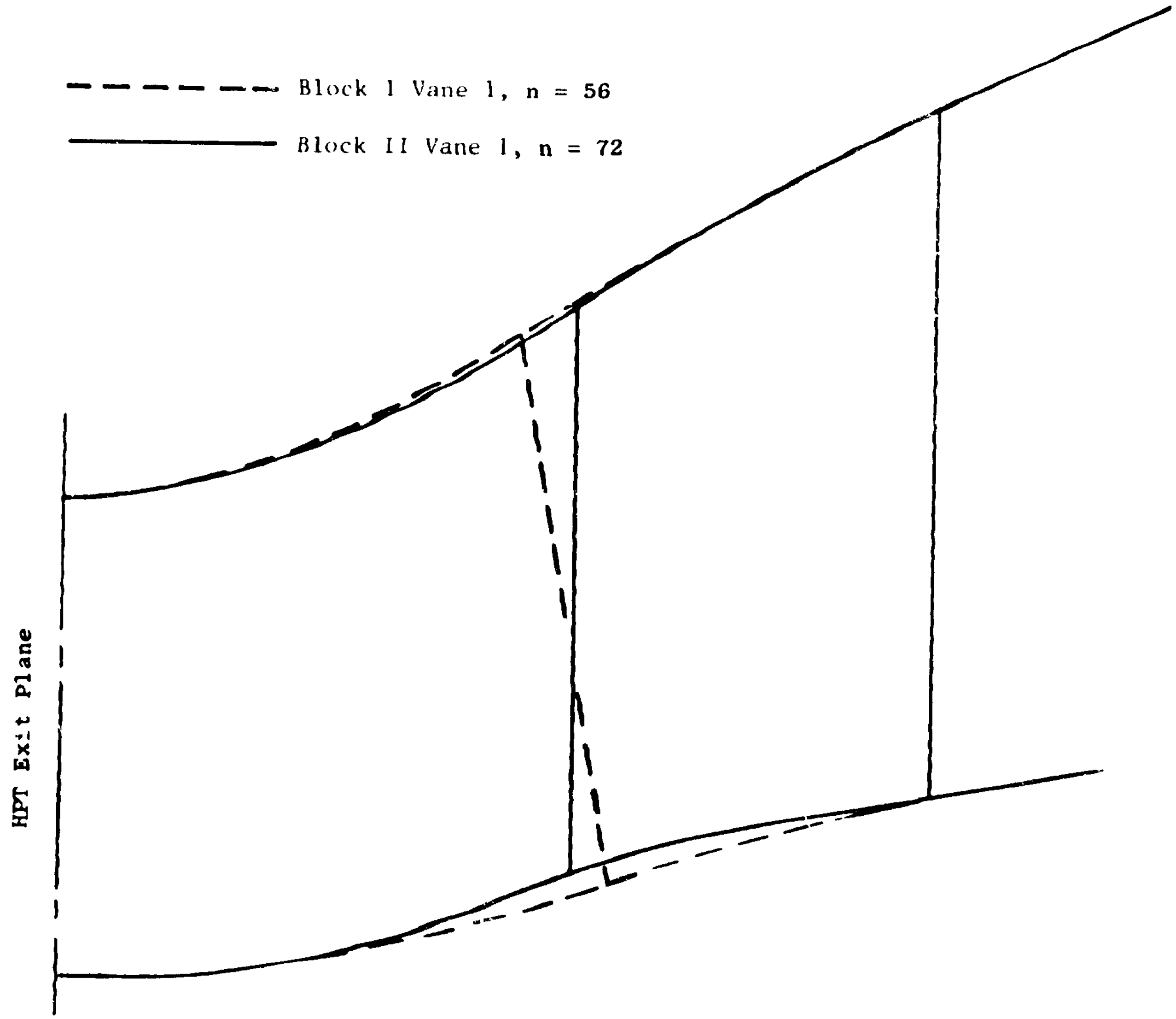

Figure 5. Block II Stage 1 Stator and Transition Duct Compared to Current Block I Design.

ORIGINAL PAGE IS
OF POOR QUALITY

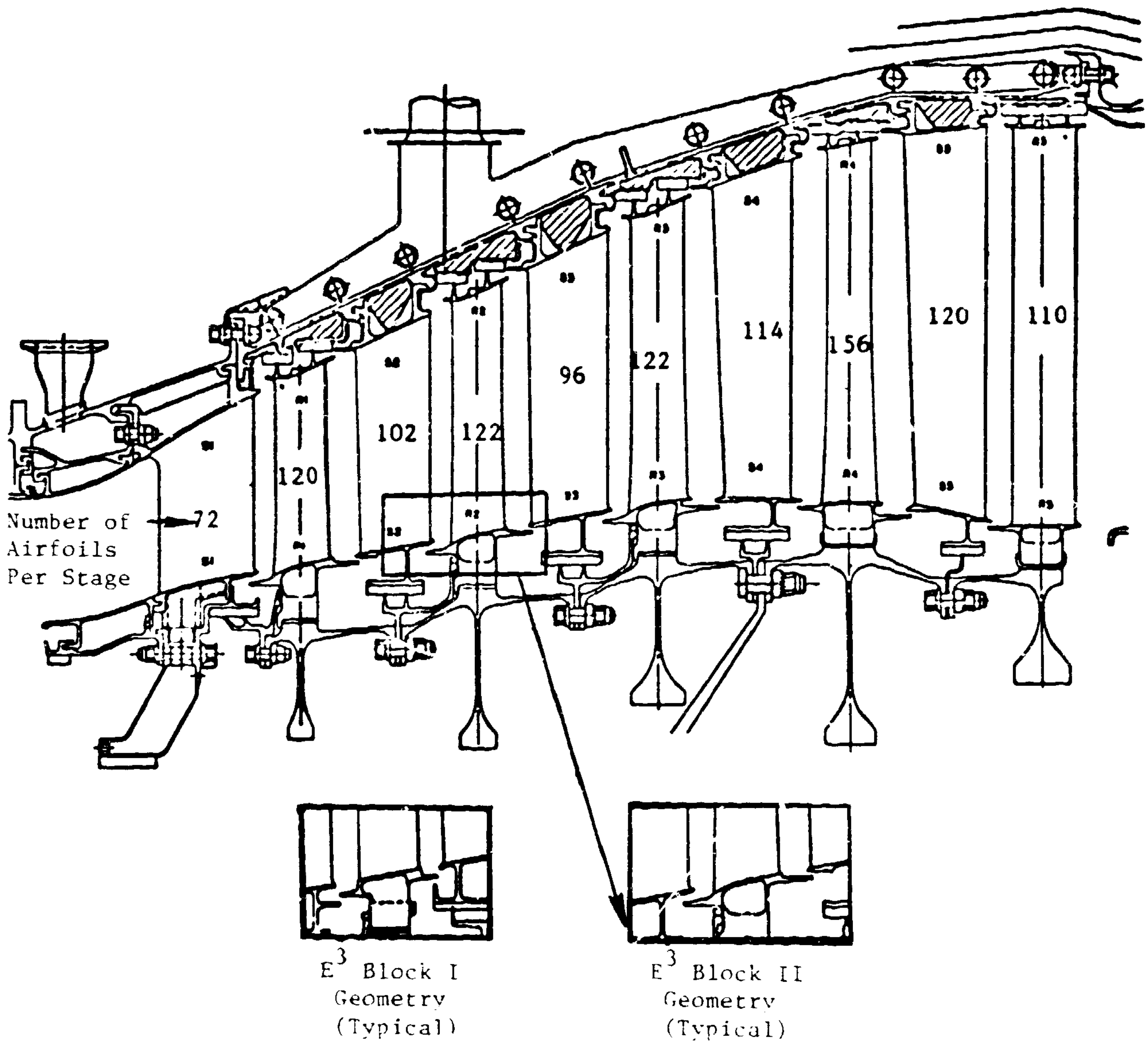

Figure 6. LP Turbine Flowpath Final for Block II.

- In an effort to increase blade hub solidity locally without a significant weight increase, rotor hub axial widths were retained at the Block I levels while the numbers of blades for each rotor were increased to yield the desired solidity at the hub, and the axial widths from the pitch line to the tip were reduced to get solidities there back to Block I levels.

Figure 7 presents the results, including inner- and outer-wall Mach number distributions, from an axisymmetric analysis of the final transition duct. Note that two additional lines have been added on the outer wall in the vicinity of the vane leading edge to show stagnation and midchannel streamline Mach numbers as they approach the leading edge. Also included is a plot of a "separation parameter." This is an indicator of the sensitivity of a turbulent boundary layer (on the outer wall in this case) to separation in the presence of an adverse pressure gradient.

2.6 FINAL VECTOR DIAGRAMS

The gas path through-flow or vector diagram analysis was accomplished by using a calculation procedure that solves the full, three-dimensional, radial-equilibrium equation for axisymmetric flow accounting for (1) streamline slope and curvature, (2) the effects of radial-component blade force due to airfoil sweep and dihedral, and (3) airfoil blockage and radial gradient of flow properties. Calculations were made with radial gradients of blading losses to simulate end-loss effects. The calculation model for the E^3 LPT showing meridional streamlines and intrablade-row calculation stations is shown on Figure 8. Table II presents final Block II vector diagram data. These data served as boundary conditions for the airfoil design analysis.

2.7 AIRFOIL DESIGN ANALYSIS

Airfoil aerodynamic design analysis was initiated using vector diagram data from the through-flow analysis, Table II, and preliminary solidities determined during design studies. A tabulation of blading aerodynamic geometry is presented in Table III. The design process was initiated by generating approximate airfoil shapes using a numerical procedure which applies a thickness distribution to a mean camber line as a function of flow angles and appropriate input coefficients. These preliminary airfoil shapes were analyzed by a procedure that calculates the compressible flow along the stream surfaces determined from the through-flow analysis which accounted for the variation in stream tube thickness.

The undesirable features of the resultant surface-velocity distributions were corrected, and modified surface Mach number distributions were input to the analysis procedure which, in turn, made the necessary modifications to airfoil shapes in order to produce the desired velocity distribution. Final airfoil shapes and velocity distributions are shown in Figures 9 through 18 for stream surface sections at 10%, 50%, and 90% from the inner wall. The

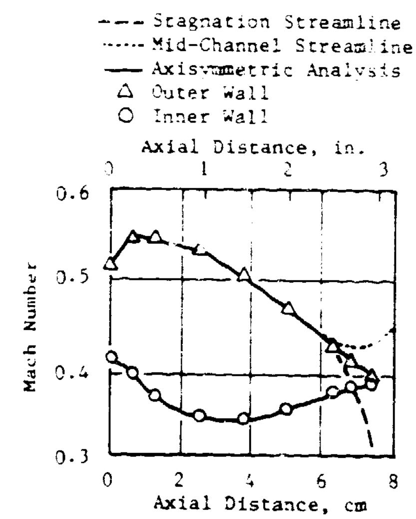

(a) Block II Duct Mach Number

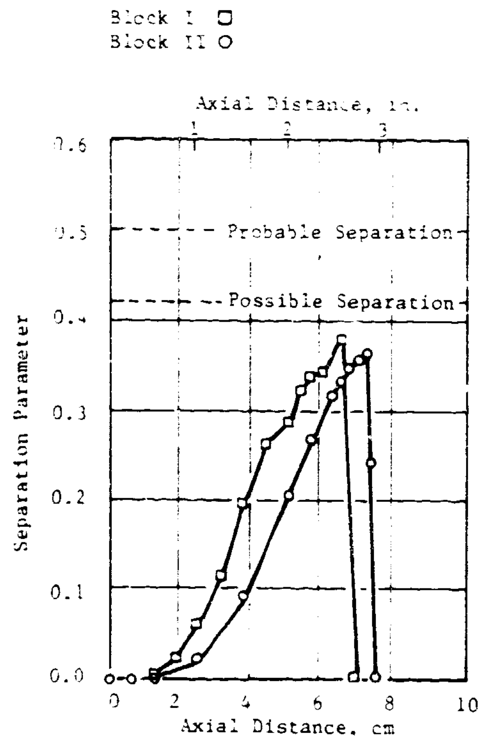

(b) Outer Wall Separation Parameter Comparison

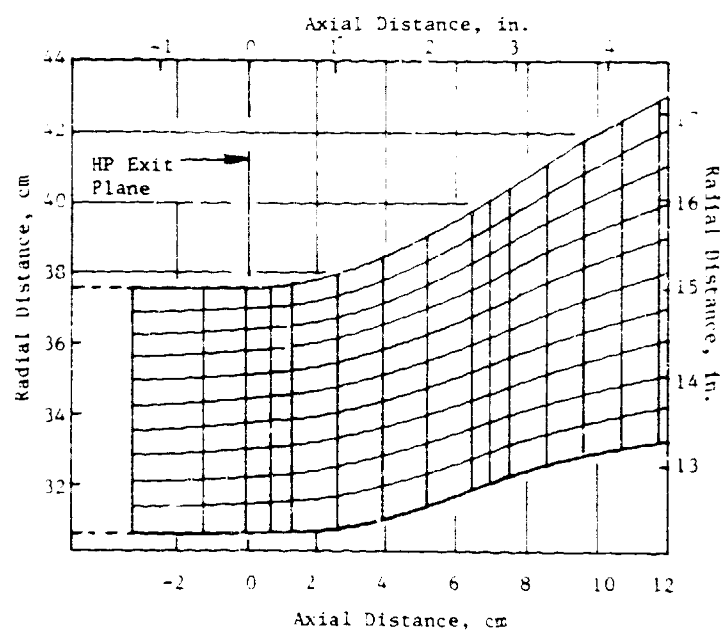

(c) Block II Flowpath Streamlines

Figure 7. Axisymmetric Flow Analysis of Stage 1 Vane Including Outer Wall Separation Sensitivities.

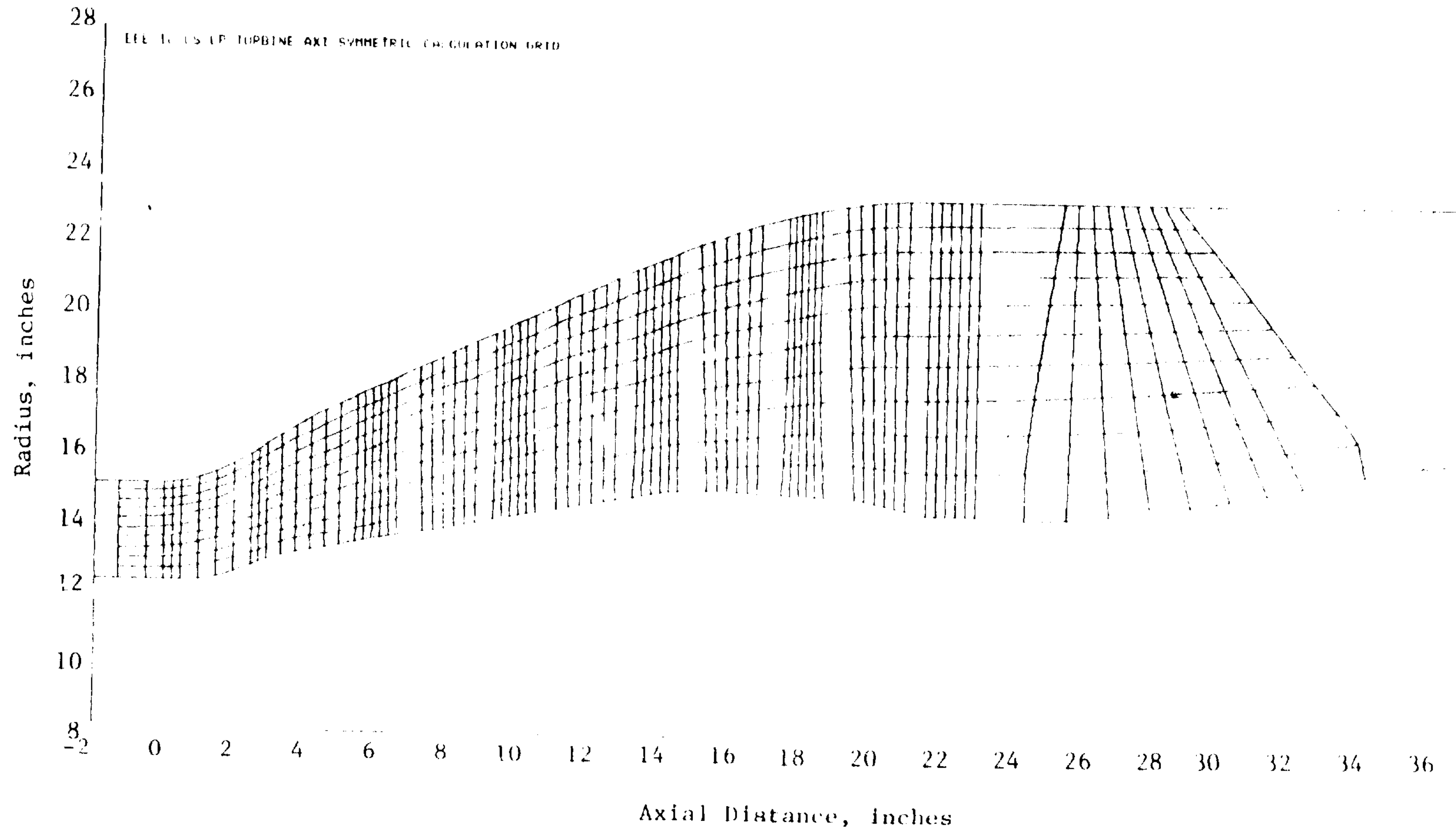

Figure 8. E^3 ICLS LP Turbine Axisymmetric Calculation Model.

Table II. LPT Final Block II Vector Diagram Summary.

	Stage 1			Stage 2			Stage 3			Stage 4			Stage 5		
Energy Extraction, Δh	31.4			34.0			35.3			30.2			21.2		
Pressure Ratio, P_T/P_T	1.30			1.35			1.40			1.36			1.26		
Aero Loading, $\Delta h/2u^2$	1.71			1.58			1.43			1.13			0.80		
Flow Coefficient, V_z/u	1.25			1.08			1.04			0.98			1.07		
	H	P	T	H	P	T	H	P	T	H	P	T	H	P	T
Reaction	0.256	0.305	0.390	0.280	0.351	0.422	0.312	0.372	0.440	0.255	0.385	0.481	0.205	0.330	0.476
Stator Exit Angle, α_1 (degrees)	53.7	61.0	60.0	55.8	64.1	62.9	56.3	64.8	63.7	56.2	62.3	59.7	55.4	56.0	46.5
Stator Exit Mach Number, M_1	0.660	0.633	0.550	0.669	0.625	0.553	0.711	0.641	0.538	0.686	0.593	0.490	0.575	0.531	0.452
Rotor Relative Inlet Angle, β_1 (degrees)	43.0	47.9	35.7	44.5	49.3	37.0	44.7	47.8	31.1	44.3	40.0	10.0	40.5	24.2	-8.0
Rotor Relative Inlet Mach Number, M_{R_1}	0.485	0.430	0.368	0.475	0.407	0.330	0.508	0.397	0.290	0.474	0.344	0.253	0.365	0.323	0.305
Rotor Relative Exit Angle, β_2 (degrees)	55.6	61.3	60.0	55.8	63.8	62.8	55.7	63.8	62.7	55.4	60.5	58.2	48.5	50.0	48.4
Rotor Relative Exit Mach Number, M_{R_1}	0.600	0.601	0.572	0.619	0.623	0.585	0.670	0.646	0.564	0.619	0.600	0.544	0.464	0.503	0.542
Stage Exit Swirl, degrees	41.2	47.6	37.0	40.0	49.1	36.8	39.7	47.7	31.0	36.5	37.0	16.5	20.0	12.5	2.0
Stage Exit Axial Mach Number	0.335	0.261	0.303	0.349	0.255	0.283	0.400	0.261	0.257	0.364	0.280	0.291	0.302	0.319	0.365

...L PAGE IS
OF POOR QUALITY

Table III. Turbine Blading Solidity and Aspect Ratio Tabulations.

Blade Row	S1	R1	S2	R2	S3	R3	S4	R4	S5	R5
AW/t	1.55	1.33	1.44	1.26	1.47	1.24	1.46	1.23	1.48	1.30
t_z	0.606	1.094	0.924	1.069	0.884	1.065	0.966	1.079	0.984	1.023
TE Blockage	0.043	0.070	0.058	0.070	0.055	0.065	0.054	0.072	0.045	0.041
AR, h/d_o	5.96	11.04	10.51	13.93	12.13	15.61	14.51	20.82	13.87	12.80
AR, h/AW	1.92	4.02	3.27	5.02	3.64	5.74	4.77	8.62	5.41	6.36

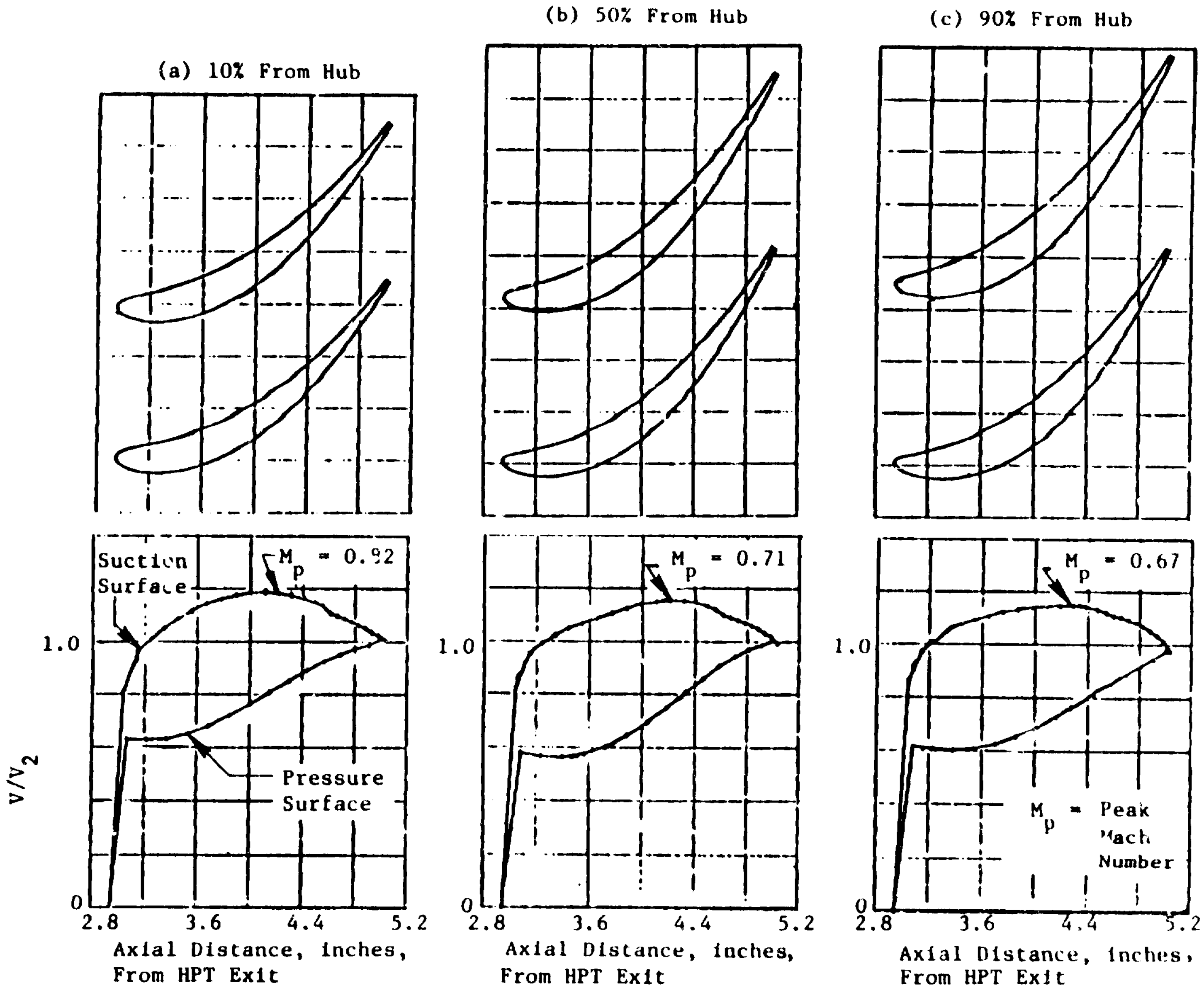

Figure 9. Block II Stage 1 Vane Shapes and Stream Surface Velocity Distributions.

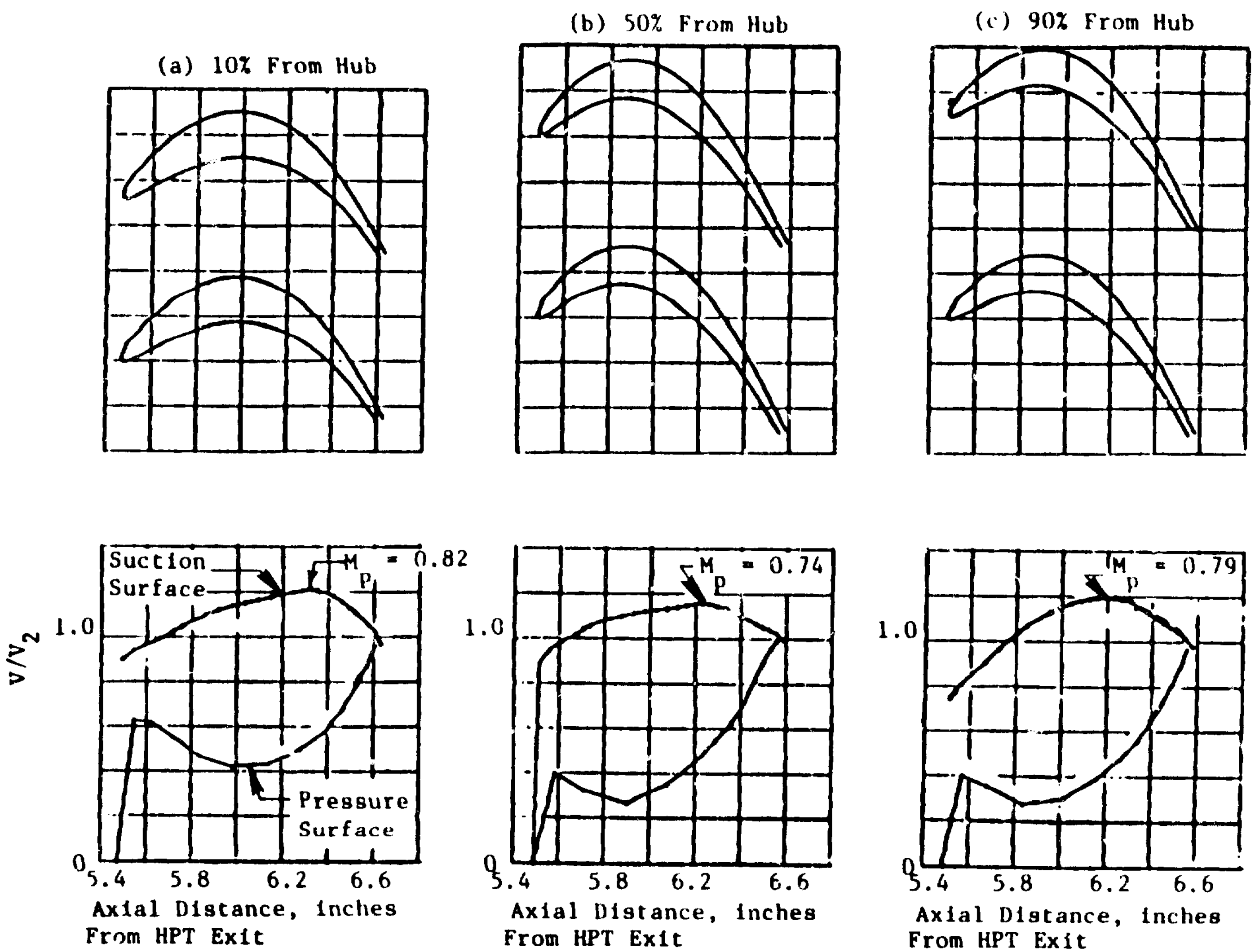

Figure 10. Block II Stage 1 Blade Shapes and Stream Surface Velocity Distributions.

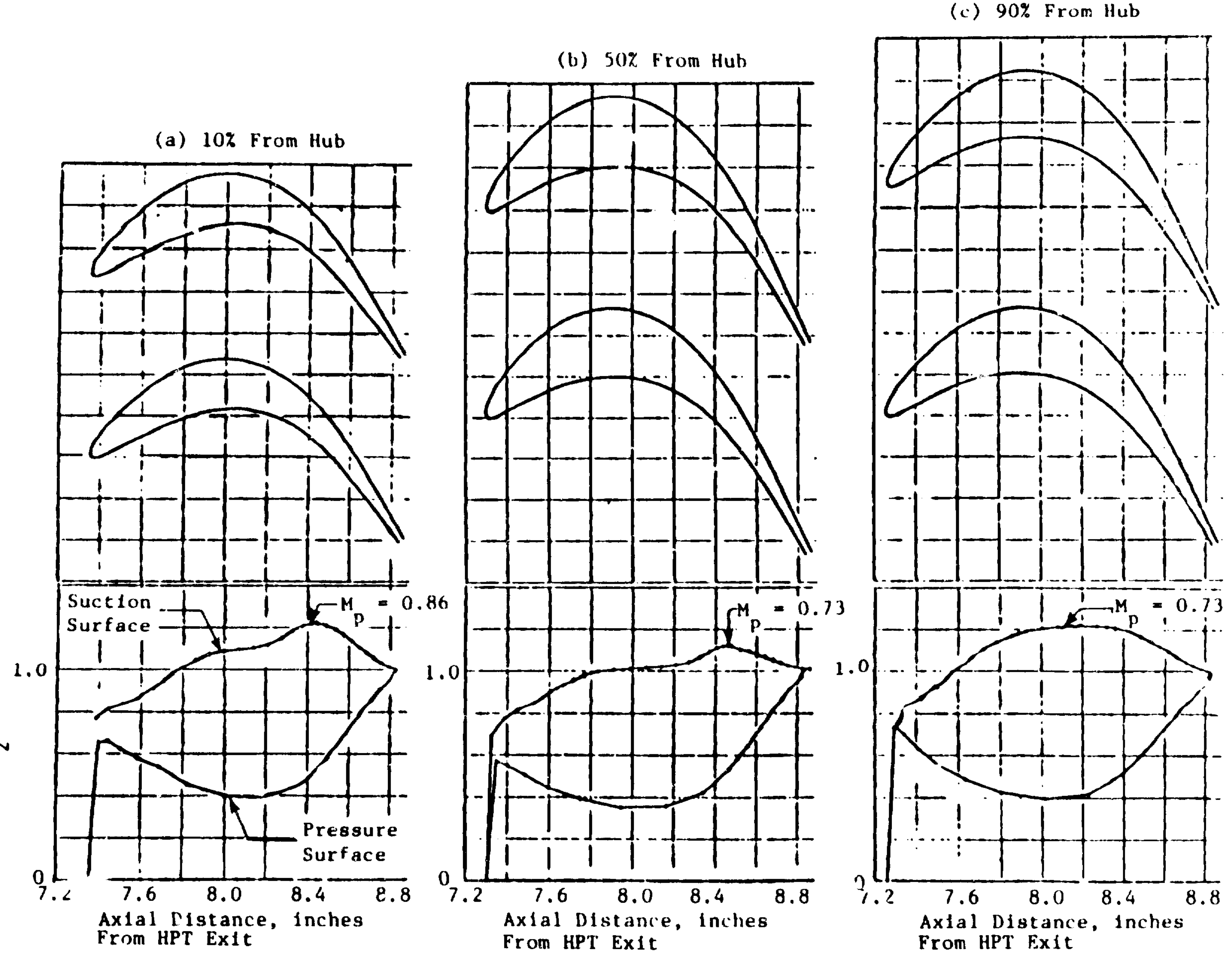

Figure 11. Block II Stage 2 Vane Shapes and Stream Surface Velocity Distributions.

ORIGINAL PAGE OF POOR QUALITY

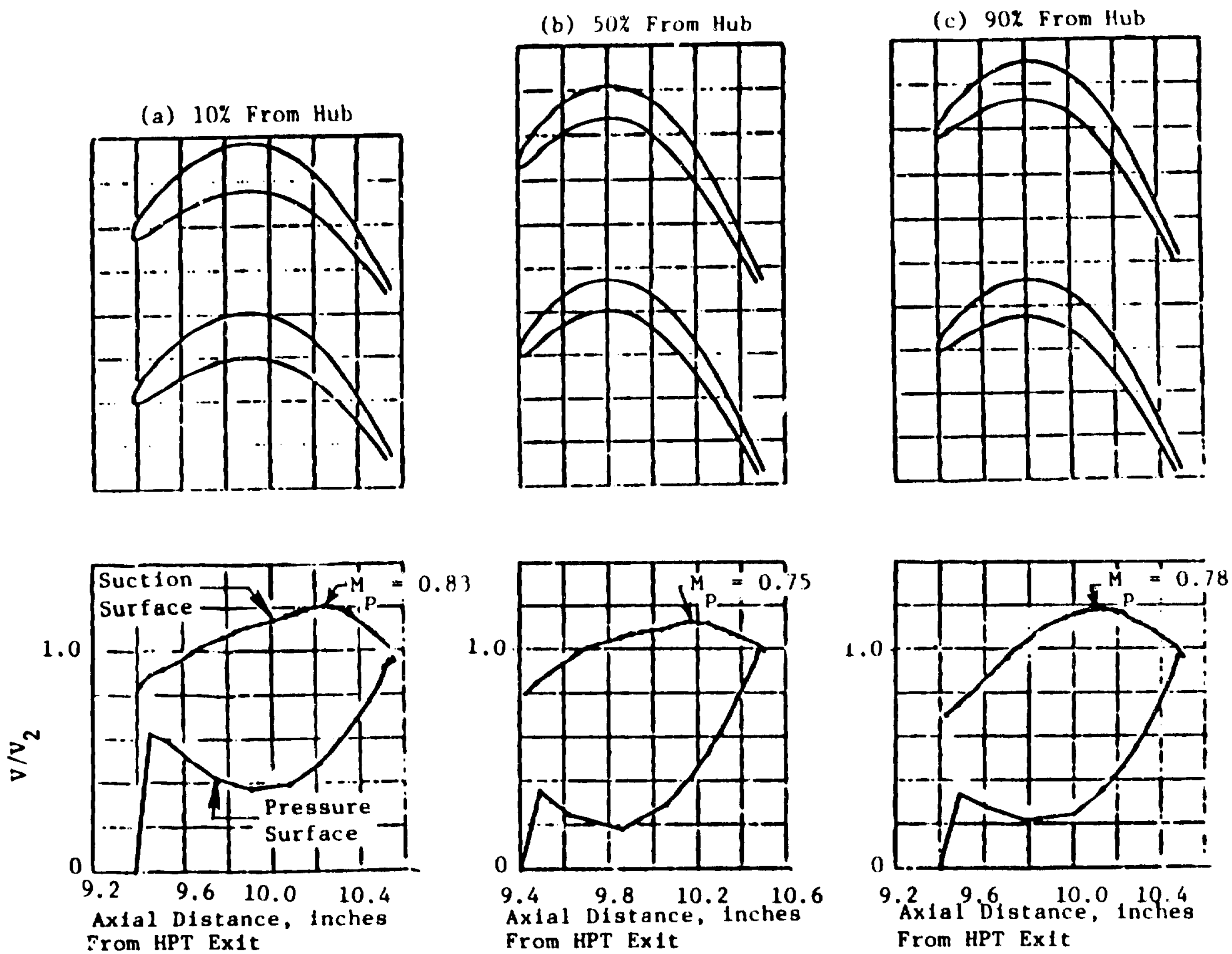

Figure 12. Block II Stage 2 Blade Shapes and Stream Surface Velocity Distributions.

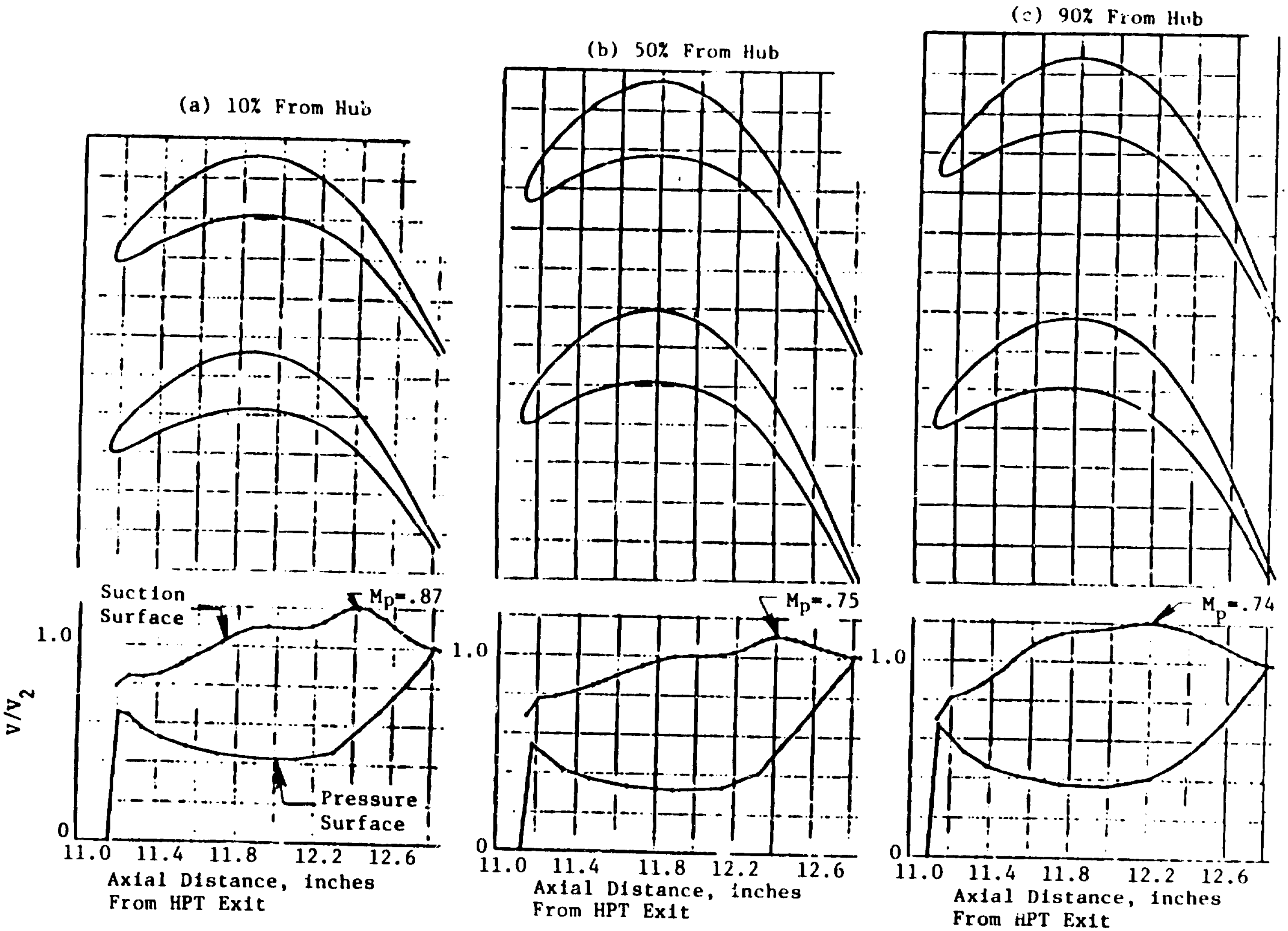

Figure 13. Block II Stage 3 Vane Shapes and Stream Surface Velocity Distributions.

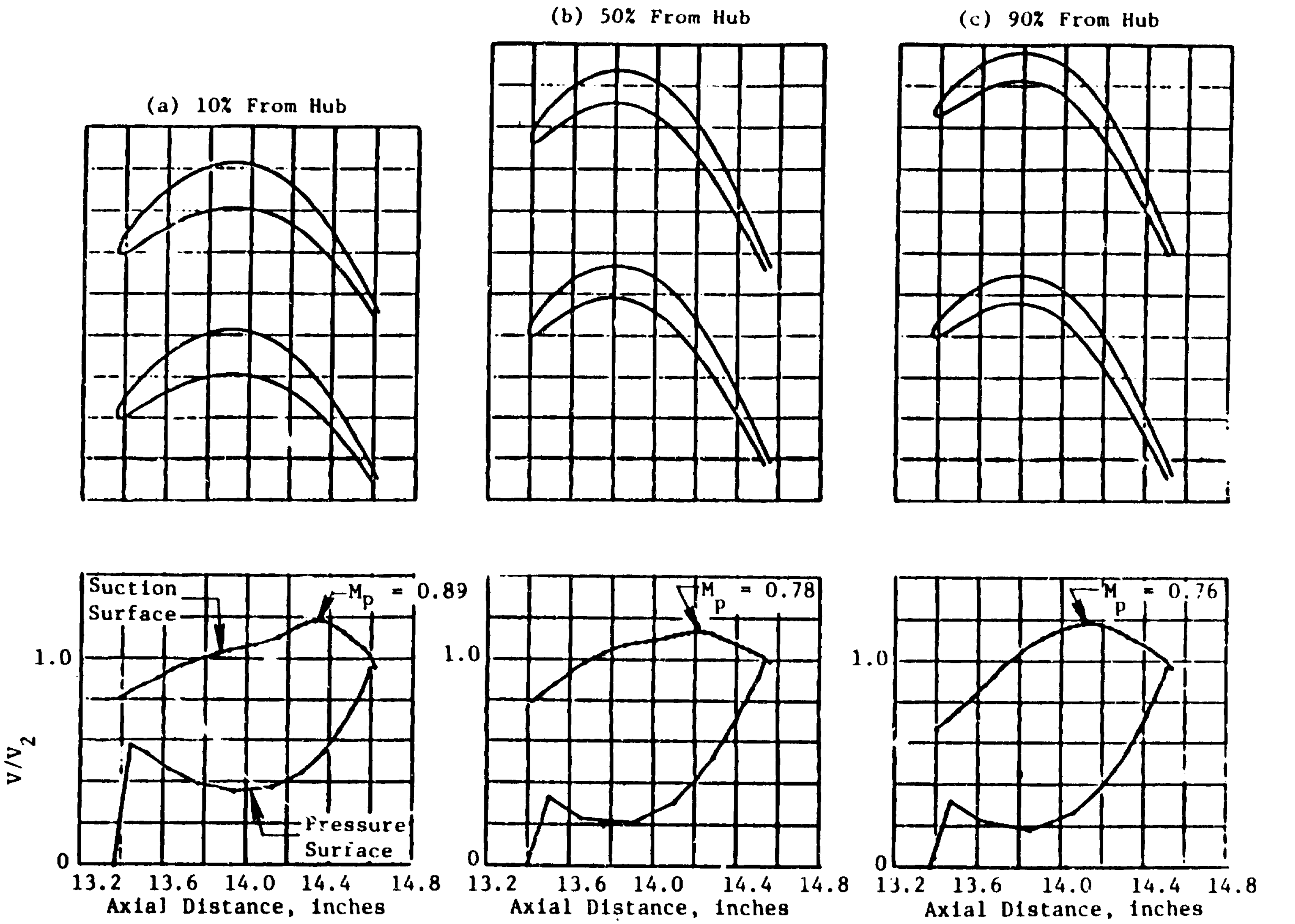

Figure 14. Block II Stage 3 Blade Shapes and Stream Surface Velocity Distributions.

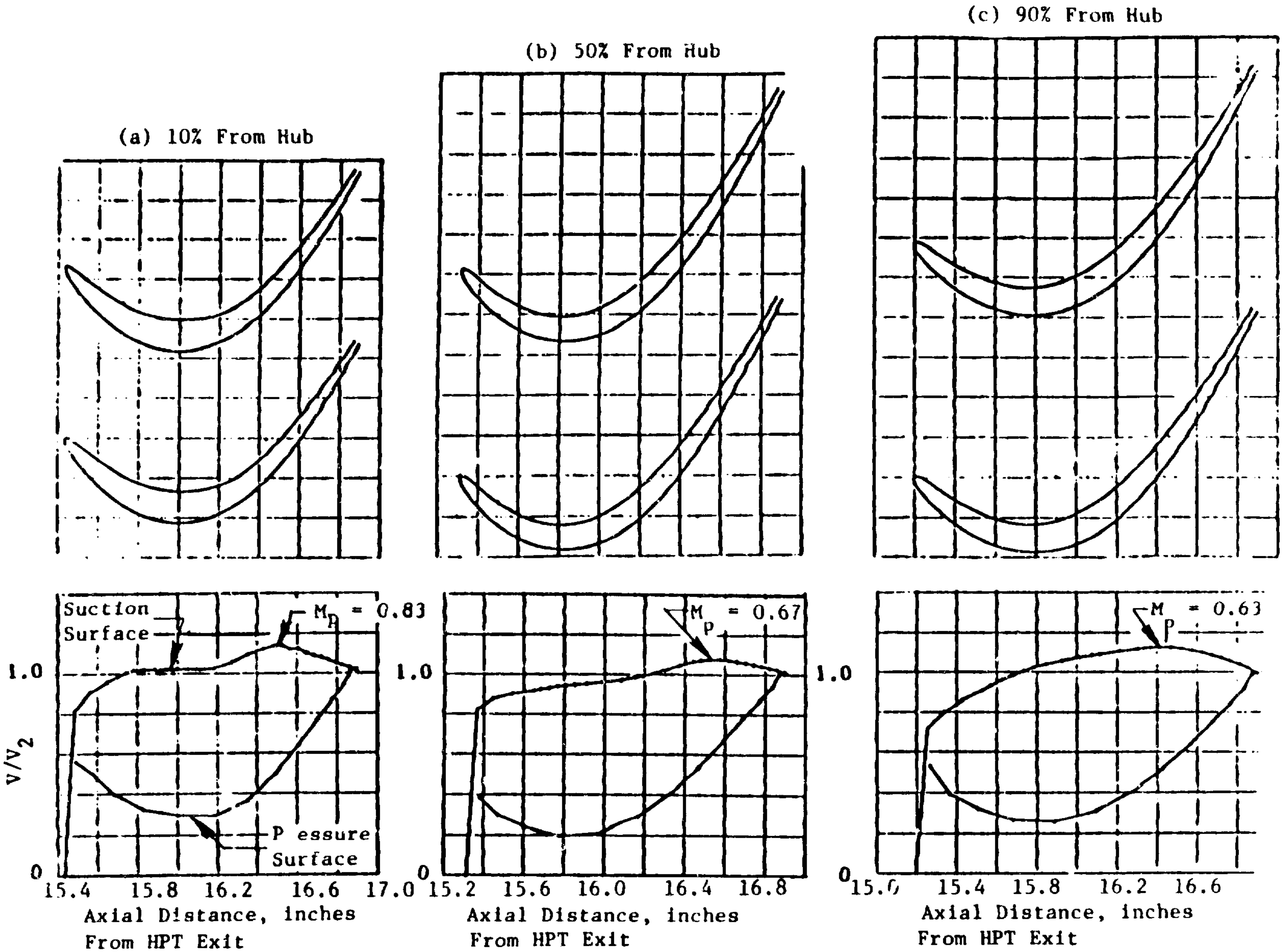

Figure 15. Block II Stage 4 Vane Shapes and Stream Surface Velocity Distributions.

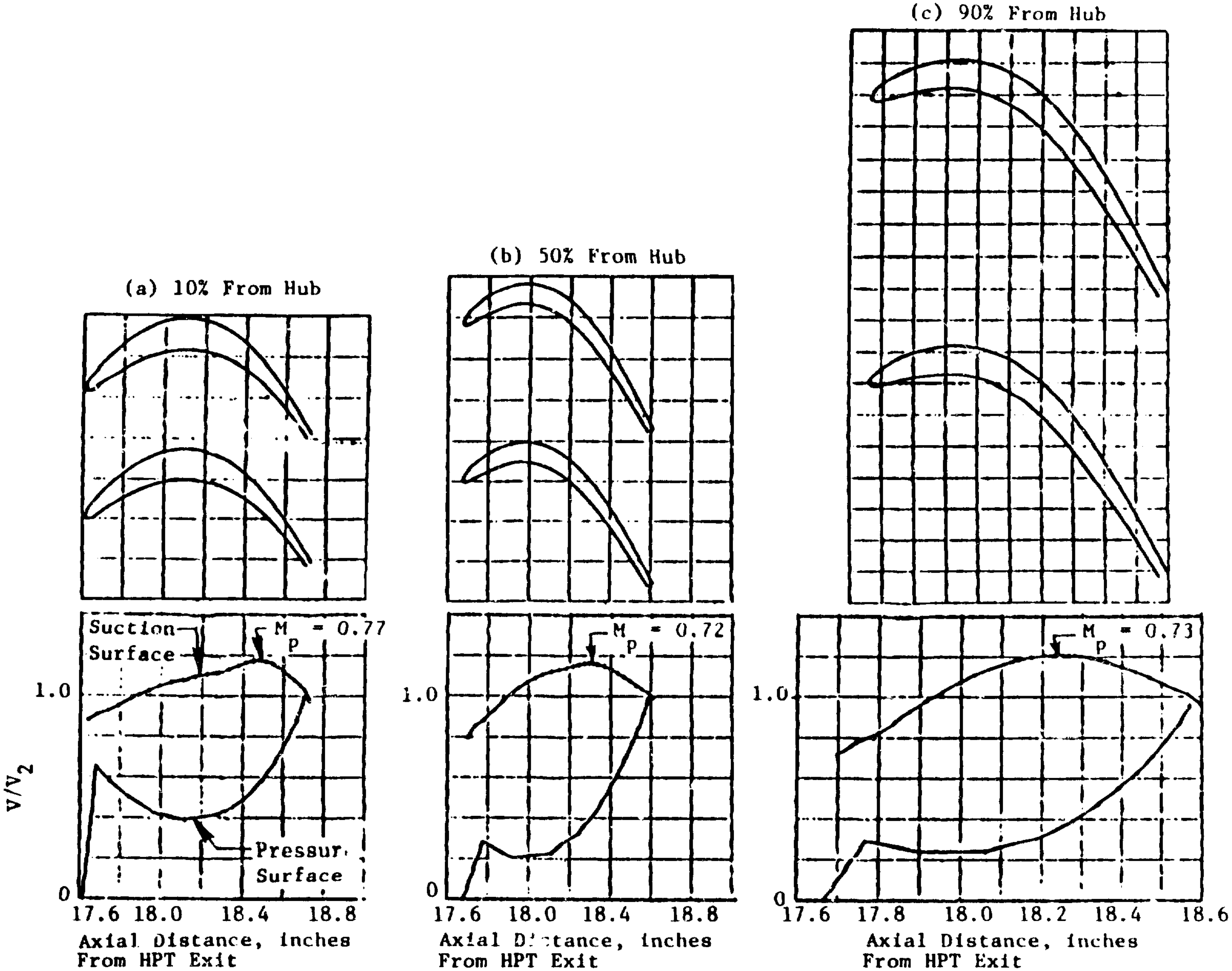

Figure 16. Block II Stage 4 Blade Shapes and Stream Surface Velocity Distributions.

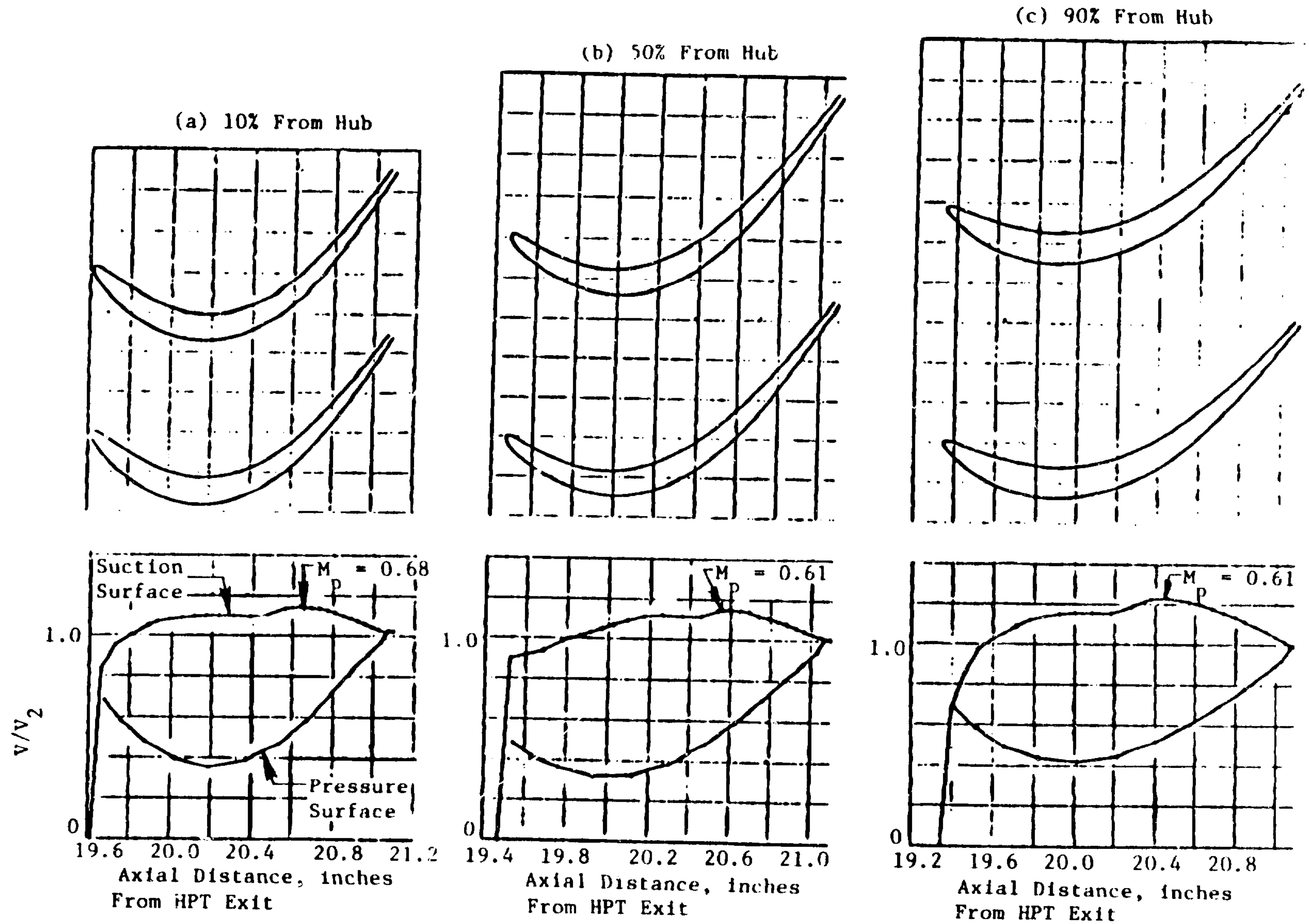

Figi re 1/. Block II Stage 5 Vane Shapes and Stream Surface Velocity Distributions.

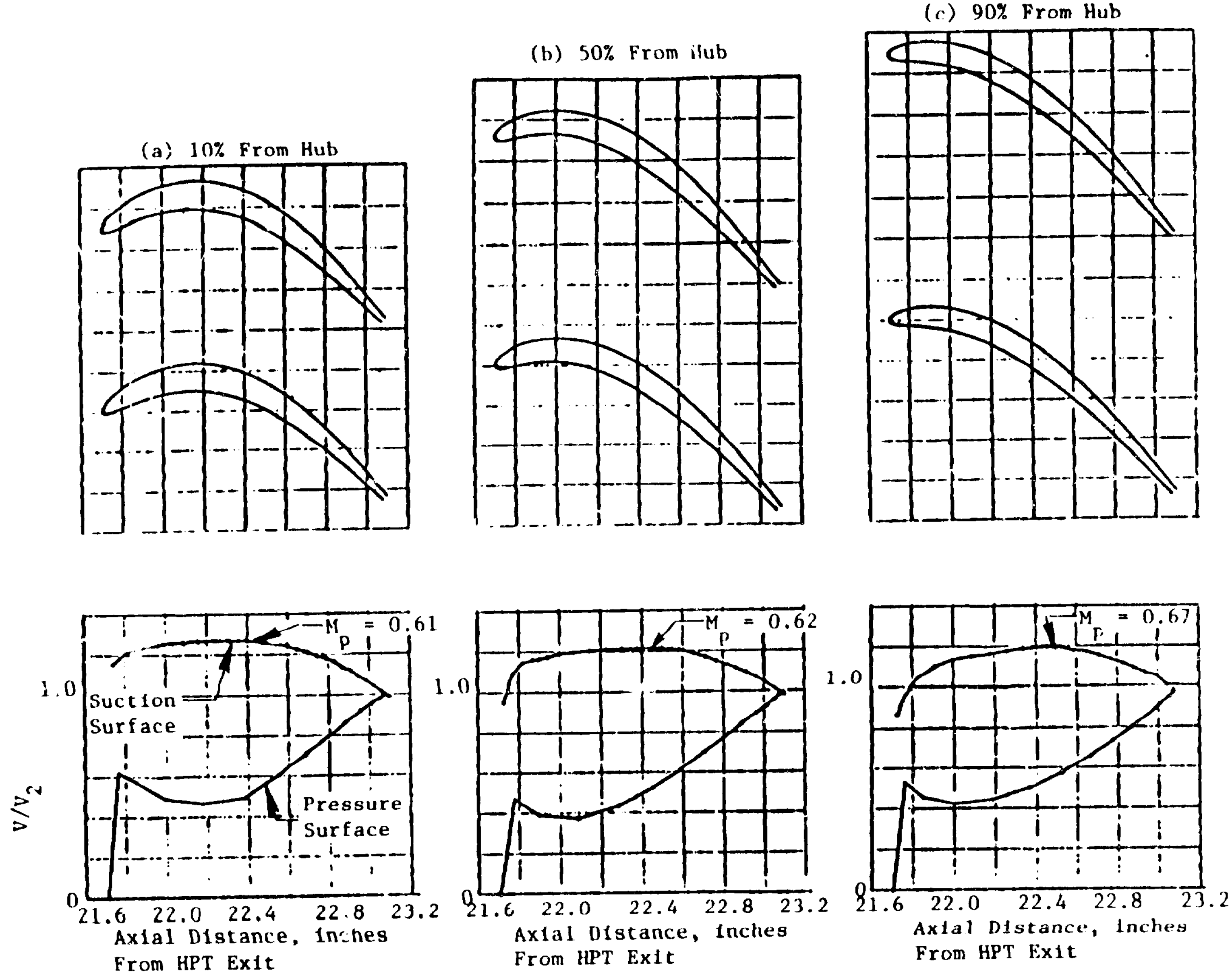

Figure 18. Block II Stage 5 Blade Shapes and Stream Surface Velocity Distributions.

ORIGINAL PAGE IS
OF POOR QUALITY

data are represented by plots of local surface velocity normalized by downstream exit velocity. The peak Mach number (Mp) is indicated on each velocity distribution. Airfoil coordinates for each of the sections in Figure 9 through 18 are presented in the Appendix.

2.8 BLOCK II AIR TURBINE TEST

The performance status of the Block II aerodynamic design was assessed through scaled rig testing of the following configurations (given with the approximate test dates):

- Two-stage group (June 1981)
- Five-stage group (September 1981)

Results of the Block II two-stage test are compared to the Block I two-stage test results in Figure 19; group efficiency versus group loading is presented at design pressure ratio. Note that the redesign features incorporated into Block II have improved the efficiency at design loading by 0.75%. Note further that the Block II airfoils have improved tolerance to negative incidence, as evidenced by the increasing efficiency improvement at the lower loadings. Design-point loading for the Block II two-stage group is 89.1%.

The flowpath for the Block II five-stage rig is shown in Figure 20. Results of the five-stage test are presented in Figure 21 as group efficiency versus group loading at design pressure ratio. Note that the turbine design-point efficiency is 92.0%. The following tabulation compares this result with a pretest estimate (based on extrapolation from Block I test results) made for the 1980 Detail Design Review (DDR):

	1980 Estimate	1981 Rig Test
η_{TT}	91.5%	92.0%
$\Delta\eta$ edge blockage		+0.1
$\Delta\eta$ purge air	+0.1	+0.1
$\Delta\eta$ Reynolds number	-0.7	-0.7
η_{TT} at Mach 0.8/10.67 km (35,000 ft), max climb	90.9%	91.5%

These are relative to program goals [at the Mach 0.8/10.67 km (35,000 ft), max-climb condition] of 91.1% for the ICLS and 91.7% for the FPS.

The correction for edge blockage accounts for the fact that all Block II rotor blades were received from the vendor with trailing edge diameters which were, on the average, 25% oversized relative to design intent.

The $\Delta\eta$ for purge air reflects the availability of extra power from the inner-cavity purge as it enters the LPT flowpath in the front stages and expands through downstream stages. This was not simulated in the rig.

The $\Delta\eta$ for Reynolds number is based on a Reynolds number excursion done on five-stage rig and verifies the 0.7% pretest prediction. This is the penalty for altitude operation.

The performance status of the E[3] LPT at the Mach 0.8/10.67 km (35,000 ft), max-climb design point is 91.4%, exceeding the ICLS goal by 0.3%.

ORIGINAL PAGE IS OF POOR QUALITY

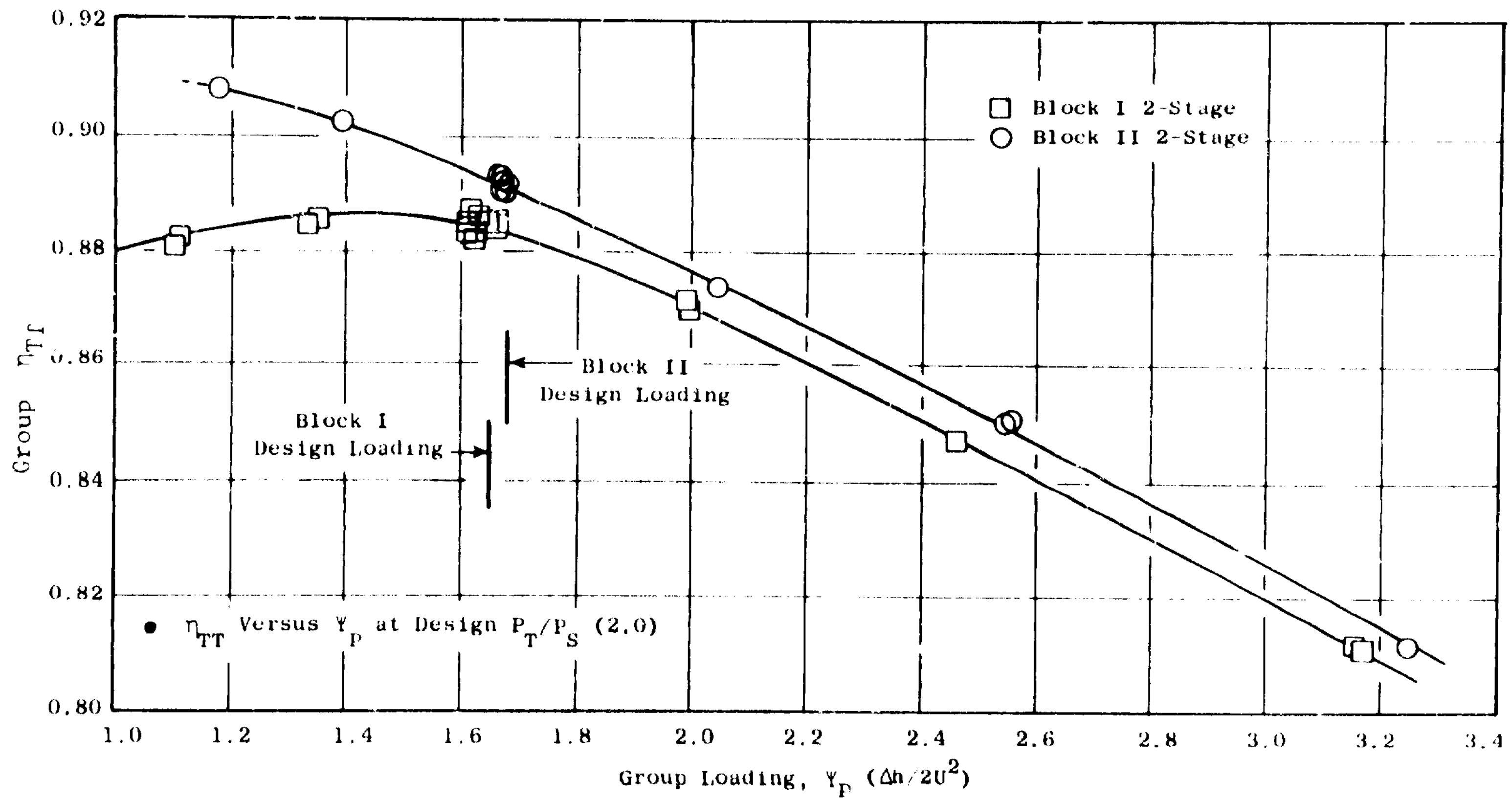

Figure 19. Efficiency Vs. Loading for Two-Stage LPT.

ORIGINAL PAGE IS
OF POOR QUALITY

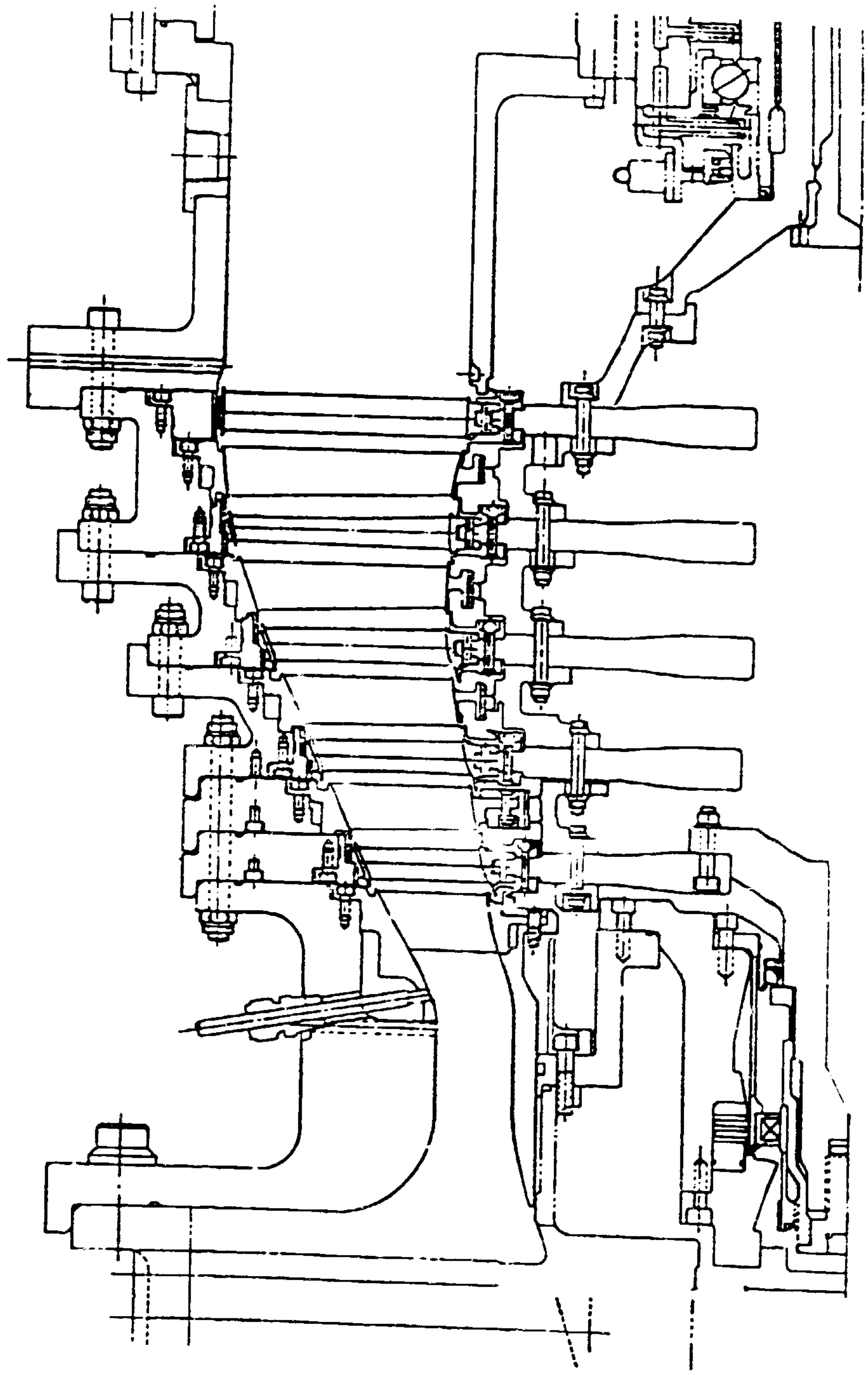

Figure 20. Scaled Test Vehicle, Five-Stage Configuration.

ORIGINAL PAGE IS
OF POOR QUALITY

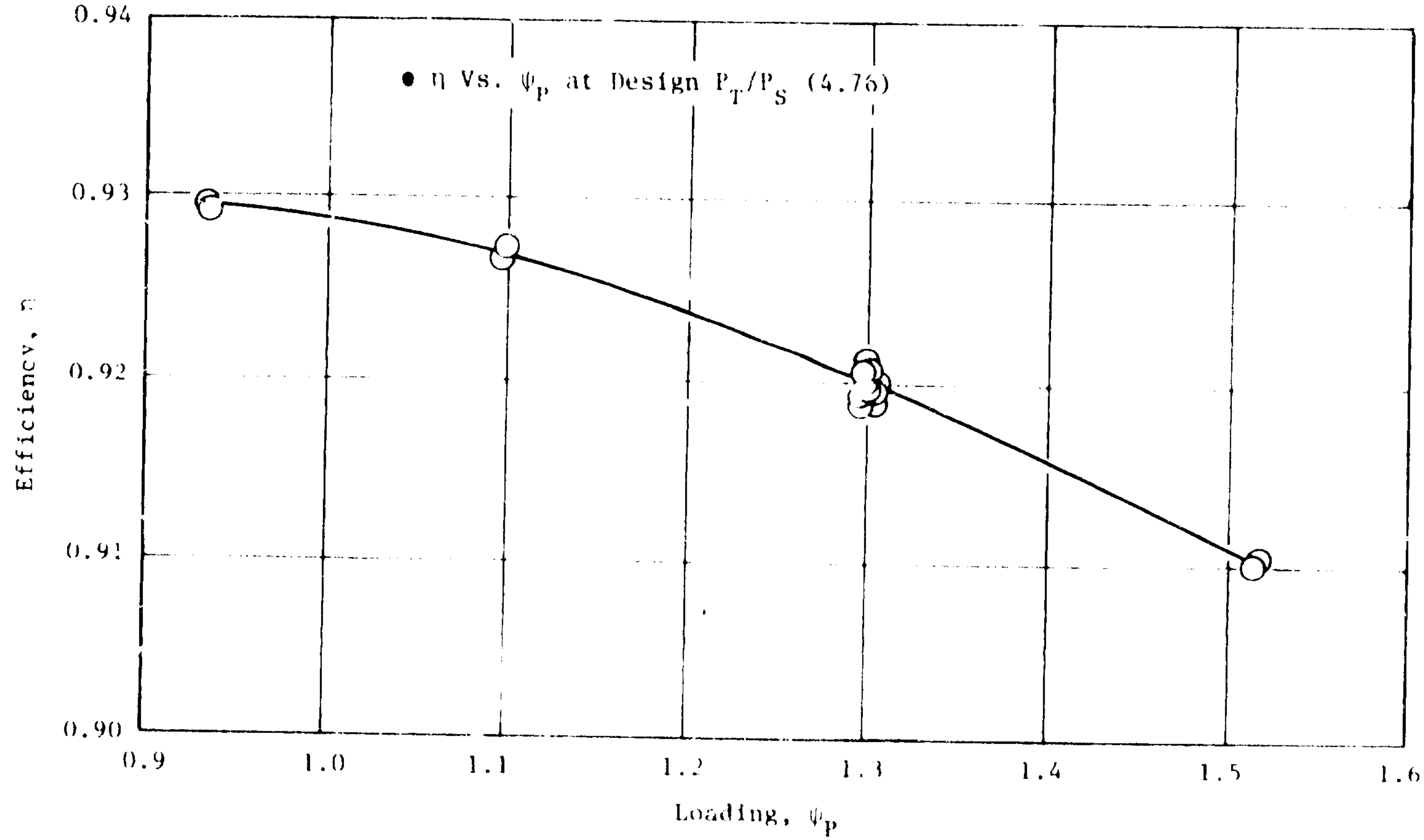

Figure 21. Efficiency Vs. Loading for Five-Stage LPT.

3.0 HEAT TRANSFER DESIGN

3.1 OBJECTIVE

To meet the stringent requirements for high performance in the E^3 design, the development of a high-efficiency LPT is essential. An important factor in this development is limiting the amount of cooling air bled from the high-pressure compressor (HPC) so the overall cycle performance is not unduly penalized but reasonable and acceptable temperatures are maintained for the LPT components. Initial design effort was directed at defining the cooling airflow requirements to keep the rotor and casing below the temperature limit for Inconel 718. During the detailed analysis, each component was analyzed in an effort to assure that the proper rupture and low-cycle fatigue (LCF) lives were obtained. Other efforts were directed at the ACC and the Stage 1 nozzle transient temperatures for both rupture and LCF analyses. The seal-blockage flow requirements also had to be defined by first looking at the relative rotor/stator transient growth in order to define the maximum clearance and the potential rub problem.

The rotor and casing cooling airflows were defined by first establishing the limit temperatures and seal-blockage airflows required to cool the casing and purge the rotor of any hot gases, thereby preventing ingestion. In order to achieve this, thermal transient analyses of both the rotor and stator were required. Also, ACC requirements had to be included in the analyses. The cooling air-delivery system, the impingement manifold, spent-impingement-air rejection system, and engine system performance payoff were also considered in the LPT cooling-design analysis.

3.2 DESIGN CONDITIONS

In most commercial engine applications the greatest thrust requirements occur at takeoff power. The large amount of thrust at takeoff is accomplished through high flow and high temperatures in the core engine. The high flow and temperature drive the LPT which in turn drives the fan to generate most of the thrust. It is this high flow rate and high temperature of the gases entering the LPT during takeoff power that cause most observed distress. That is why the heat-transfer design point was established as the hot-day, max-power-takeoff cycle point.

The LPT heat transfer design for this engine study has been established by the overall engine cycle parameters. The most severe temperature and pressure conditions occur at maximum-power takeoff.

Table 1' and Figure 22 present the base FPS engine LPT design parameters. The design cycle condition was chosen as 50° C (122° F) day, maximum-power takeoff, sea level, at Mach 0.3. This represents the highest gas and coolant temperature condition. In order to prevent the LPT from being growth-limited,

Table IV. E^3 LPT Heat Transfer Design Parameters.

● 50° C (122° F) Day Max. Sea Level Takeoff at Mach = 0.3.

Parameter (See Figure 22)	Base Engine FPS	ICLS**
T_{42} (Cycle)	859° C (1578° F)	897° C (1647° F)
T_{42} + Margin*	920° C (1688° F)	920° (1638° F)
T_5 (Cycle)	578° C (1073° F)	601 (1113° F)
P_{42}	509.4 kPa abs (73.88 psia)	565.2 kPa abs (81.97 psia)
P_{42}/P_5	3.589	3.782
T_C 5th Stage Compressor Bleed Port	393° C (740° F)	379° C (714° F)
W_C 5th Stage Compressor Bleed Port	1.40% W_{25}	1.40% W_{25}
P_{C_S} 5th Stage Compressor Bleed Port	794.7 kPa (113.8 psia)	861.9 kPa abs (125 psia)
P_{C_S} - LP Turbine Casing	522.6 kPa abs (75.80 psia)	574.1 kPa abs (83.26 psia)
RPM	3289	3419

*110° F T_{42} Margin (Based on Commercial Engine Experience)

**86° F Day SLS Max. Takeoff (Hottest Ambient Conditions that the First Test Engine is Expected to Experience)

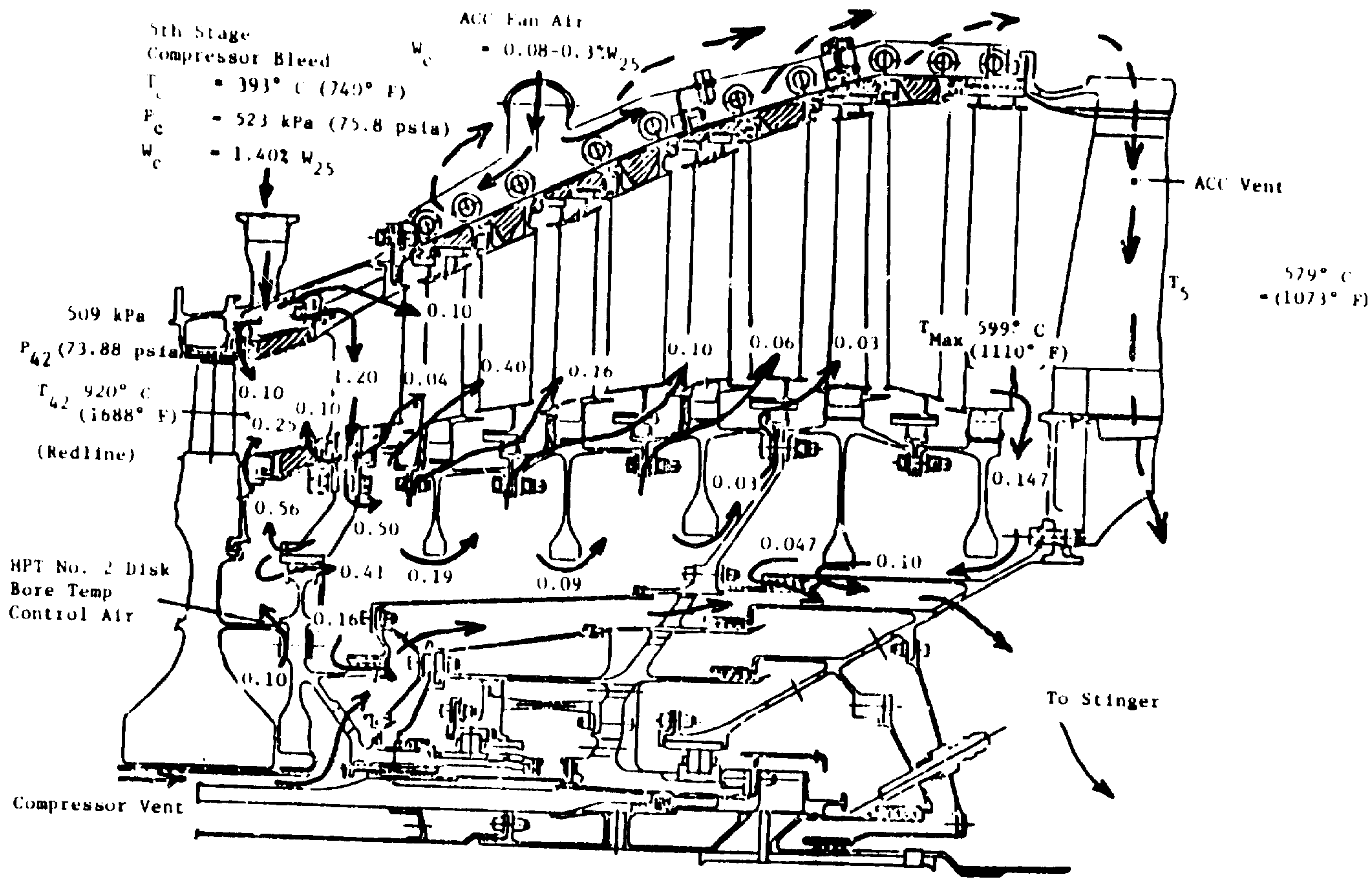

Figure 22. E^3 LPT Cooling Air Requirements for the Base Engine.

a design was required which ensured that the turbine structure could accommodate higher operating temperatures. This was accomplished by designing the rotor and stator casing for the growth-cycle environment. However, the flowpath components were designed to meet the base engine design objectives. The LPT inlet cycle-average design gas temperature, $T_{4.2}$, for the base engine is 859° C (1578° F), to which 61° C (110° F) of margin is added. The $T_{4.2}$ margin includes the effects of deterioration, engine-to-engine variation, transient overshoot, open clearances at takeoff, and control-system tolerance. Including margins, redline average LPT inlet temperature is 920° C (1688° F) for the base engine and 966° C (1771° F) for the growth engine.

LPT design parameters for the FPS base engine and a growth-engine design are also presented in Table IV for comparison with the ICLS cycle data. The tabulation indicates that, for the assumed component efficiencies, the ICLS engine represents a deteriorated FPS base engine. Thus, the ICLS data will yield a good comparison with the FPS analysis (which was also done for a deteriorated engine).

The maximum peak temperature is defined as the highest local temperature that might be encountered on a stationary component. Based on CF6 engine experience, the maximum predicted peak radial gas temperature profile at each LPT vane stage inlet at hot-day takeoff power for a deteriorated base engine is presented in Figure 23. The maximum peak gas-temperature radial profile at the inlet to the LPT is defined through analysis and utilization of commercial engine experience. The temperature drop through each stage in the turbine is determined from the normalized work extraction as defined by the detailed aerodynamic design at each stage.

Based on CF6 experience, the radial temperature distribution that the LPT rotor blade stages of the base engine will be subjected to during hot-day takeoff is presented in Figure 24. These radial temperature profiles are also defined with the use of commercial engine data and the aerodynamic vector diagram at each stage. Since there is no cooling in any of the five rotor stages, and since the relative blade Mach numbers are low, the blade metal temperature is assumed to be identical to the relative gas temperature. Radial conduction within the blades is also neglected.

In order to define the LCF life of the various flowpath components, it is necessary to evaluate the typical thermal transient from idle to maximum power. In order to accomplish this, the gas-temperature profile at idle power was defined. The maximum and average temperature profiles at the inlet and exit of the LPT at the idle power setting are presented in Figure 25. Because there is very little work extraction in the LPT at idle conditions, there is virtually no temperature drop of the gases. The profile is also peaked at the 75% span, as could be expected, because the combustor is lit on the pilot dome only.

3.3 COOLING AIR SUPPLY SYSTEM

The airflow that is used for cooling the LPT internal structure, Stage 1 nozzle, and rotor is extracted at the fifth stage of the compressor. Mechanical restrictions, such as the variable compressor vanes, prevented moving the

ORIGINAL PAGE IS
OF POOR QUALITY

- $M = 0.3$, - 18° C, (65° F) Day, SLTO
- Cycle
  T_{41} = 1343° C, (2450° F)
  T_{42} = 859° C, (1578° F)
- ΔT_{42} Margin = 61° C, (110° F)

(Based on CF6 LPT Inlet Profile Experience)

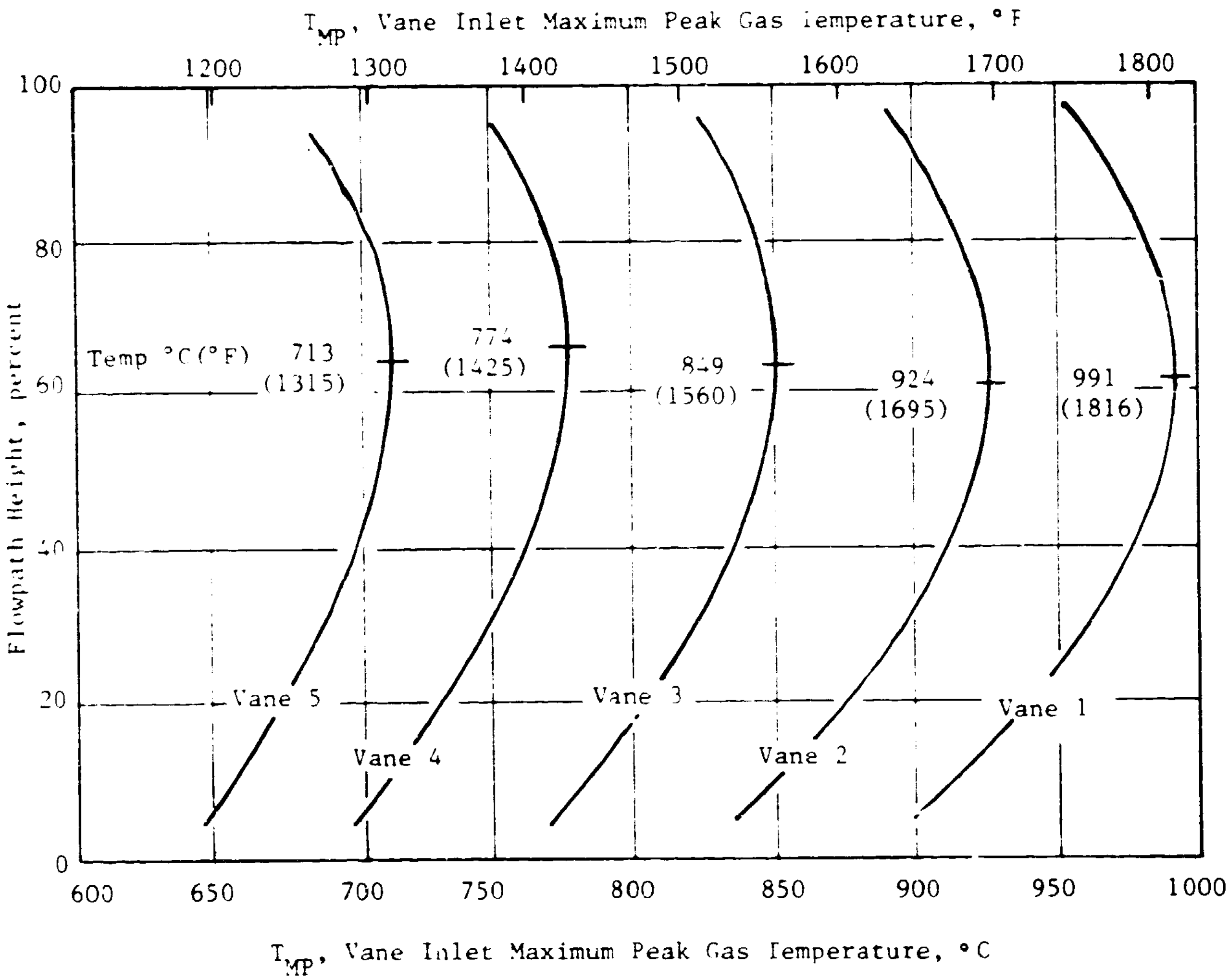

Figure 23. LPT Base Engine Stator Gas Temperature Profile.

- $M = 0.3$, + 17° C, (63° F) Day, SLTO

- Cycle
  T_{41} = 1343° C, (2450° F)
  T_{42} = 859° C, (1578° F)
- ΔT_{42} Margin = 61° C, (110° F)

(Based on CF6 LPT Inlet Profile Experience)

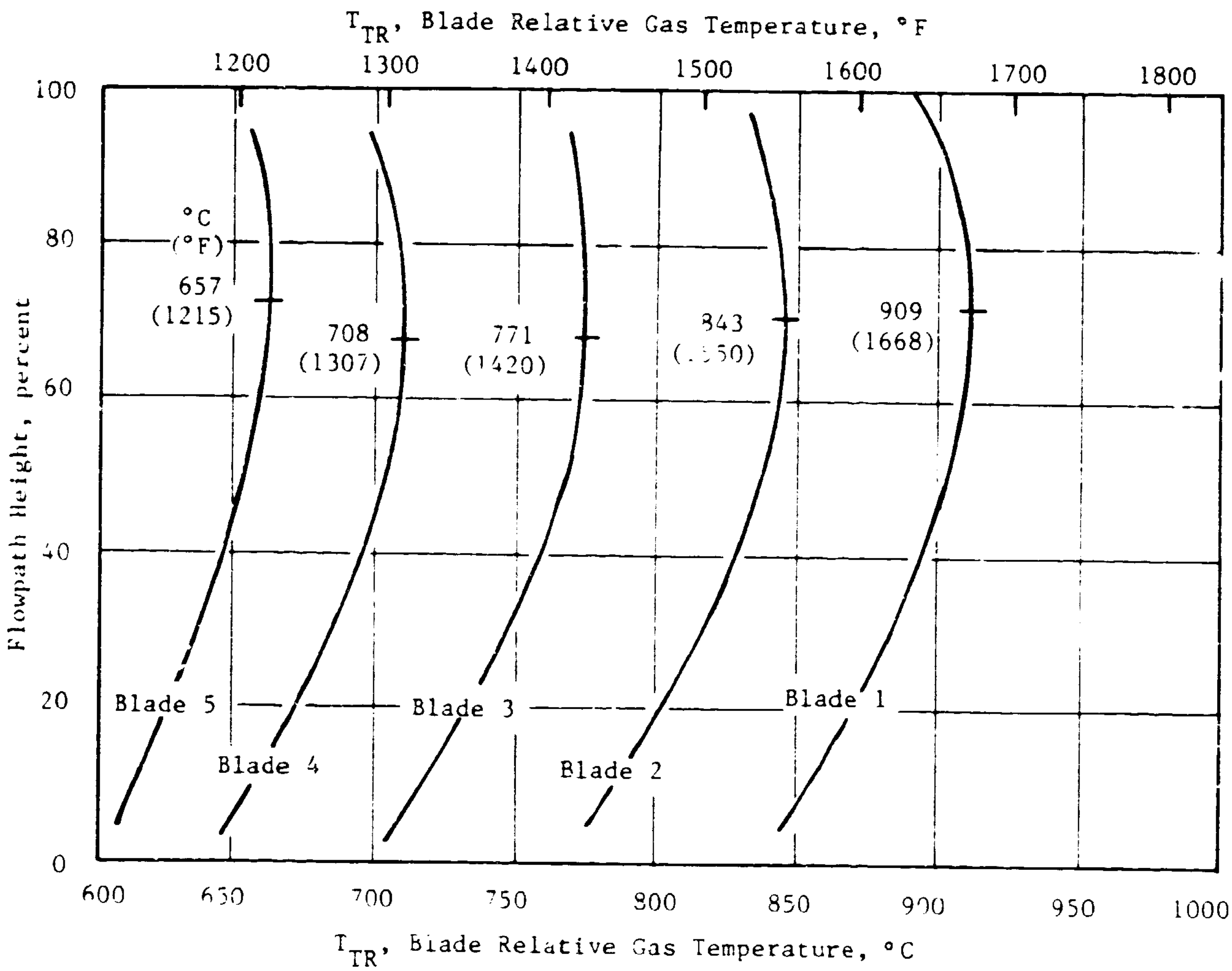

Figure 24. LPT Base Engine Blade Relative Gas Temperature Profile.

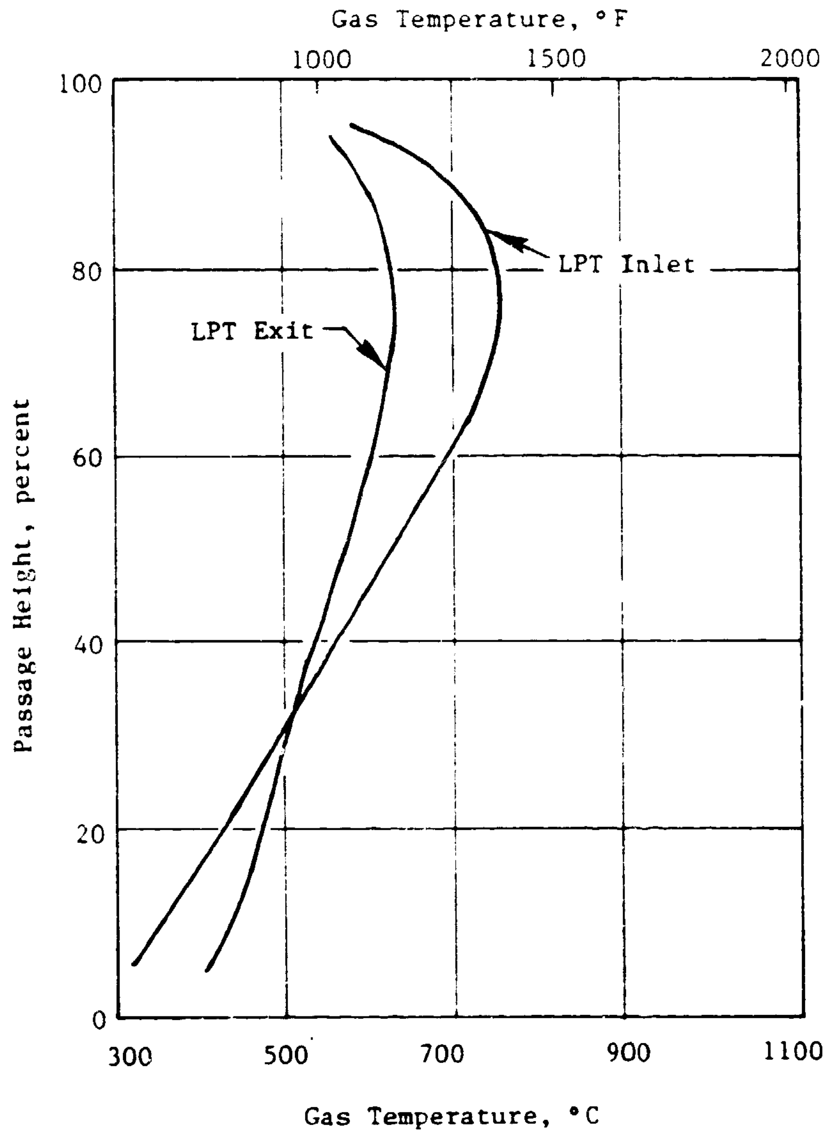

Figure 25. LPT Gas Temperature Profiles 50° C (122° F) Day, Steady-State Idle Without Bleed.

compressor bleed location to the fourth stage of the compressor even though it would have been adequate. The extra pressure associated with Stage 5 bleed enabled this air to be used in the compressor ACC cooling circuit. After the fifth-stage compressor bleed air has been routed through the compressor ACC system and into the low pressure casing manifold, the pressure is 3% above the gas stream total pressure at the LPT inlet. This pressure is high enough to cool and purge the rotor but is not so high as to cause excessive leakage and degrade engine performance.

During an engine start cycle, the compressor pumping at the fifth stage is not adequate to yield a satisfactory cooling/purge-supply pressure for the LPT. For this reason, the compressor exit air is used to augment the LPT cooling/purge air. A check valve is used in the compressor discharge circuit so that backflow into the fifth-stage compressor bleed system will not occur. This compressor discharge bleed augmentation system will be activated at any subidle power setting.

The LPT casing is cooled with fan air extracted from the fan bypass duct. The air enters a pair of scoops, one on each side of the pylon. After entering the scoops, the air is diffused before entering a 270° plenum surrounding the LPT. From this plenum, the fan air enters an array of tubes and then impinges on the outside of the LPT casing in order to cool the structure. The spent impingement air discharges through the rear frame struts and out the center vent. Air leaving the center vent mixes with the primary-nozzle gases and yields a small amount of thrust.

The air temperature rise resulting from cooling the LPT casing is adequate to offset the attendant pressure loss; this eliminates any significant loss in thrust when the cooling air reenters the main gas stream.

The LPT ACC system is also combined with the primary casing cooling system. This is done by incorporating a cooling-flow-modulation valve between the fan-duct scoop and the 270° manifold that surrounds the LPT.

3.4 DESIGN MISSION

The first step in the detailed thermal analysis of the LPT was to define the flight mission. The mission that was analyzed consisted of a 24-minute takeoff climb cycle and a 24-minute descent cycle. The takeoff/climb cycle presented in Figure 26 incorporated a 2-minute takeoff and a 22-minute climb. During climb, the aircraft is gradually accelerating to the maximum speed of Mach = 0.8 at 9.1 km (30,000 ft).

Because the engine does not reach the high ram Mach numbers until high altitude, the LPT does not achieve maximum rpm until 10.67 km (35,000 ft) at the maximum-climb power conditions. Figure 27 presents the LPT rpm excursions for a typical flight cycle. The takeoff mission starts at 1000 seconds and continues until about 2500 seconds at which point the aircraft has achieved a maximum-cruise condition. The landing mission starts at 3000 seconds and proceeds through flight idle, approach, touchdown, thrust reverse, and back to ground idle at the 4600-second point.

ORIGINAL PAGE IS
OF POOR QUALITY

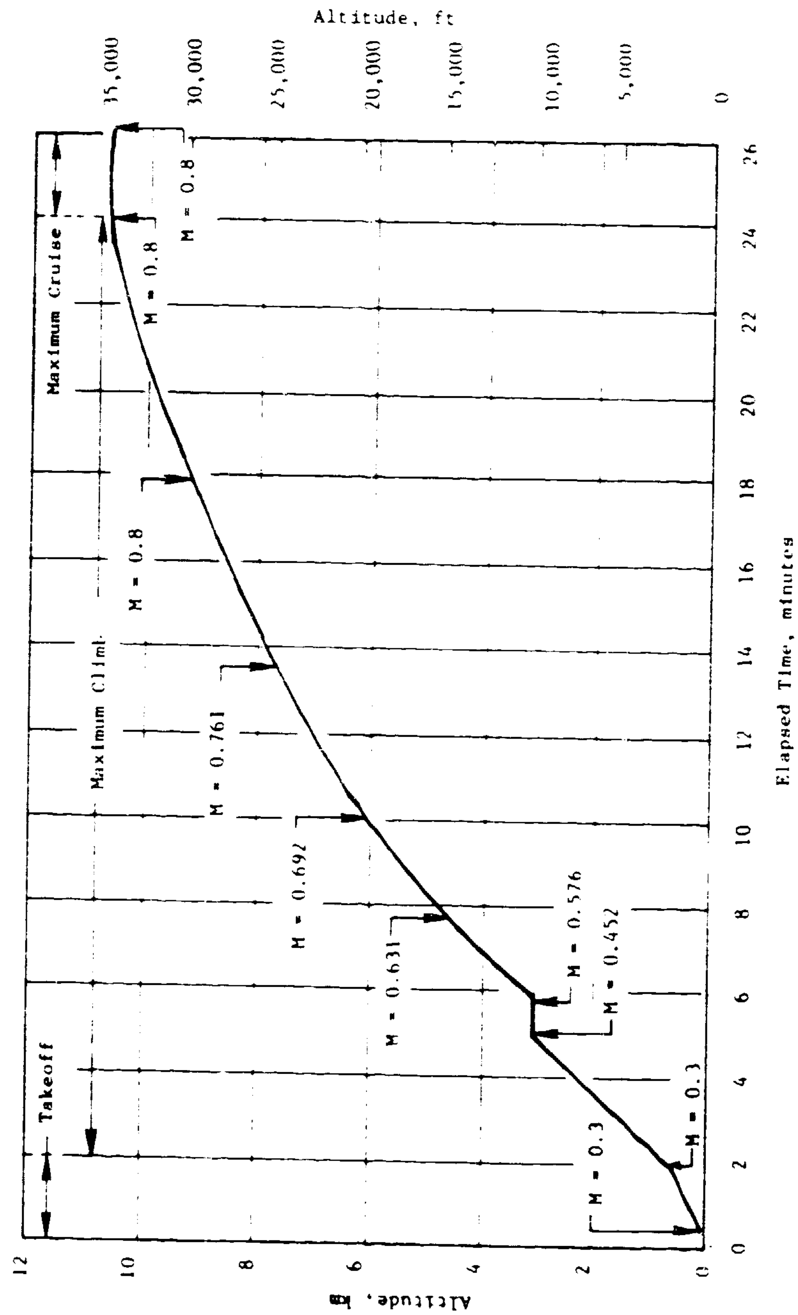

Figure 26. Takeoff - Climb - Cruise Flight Mission.

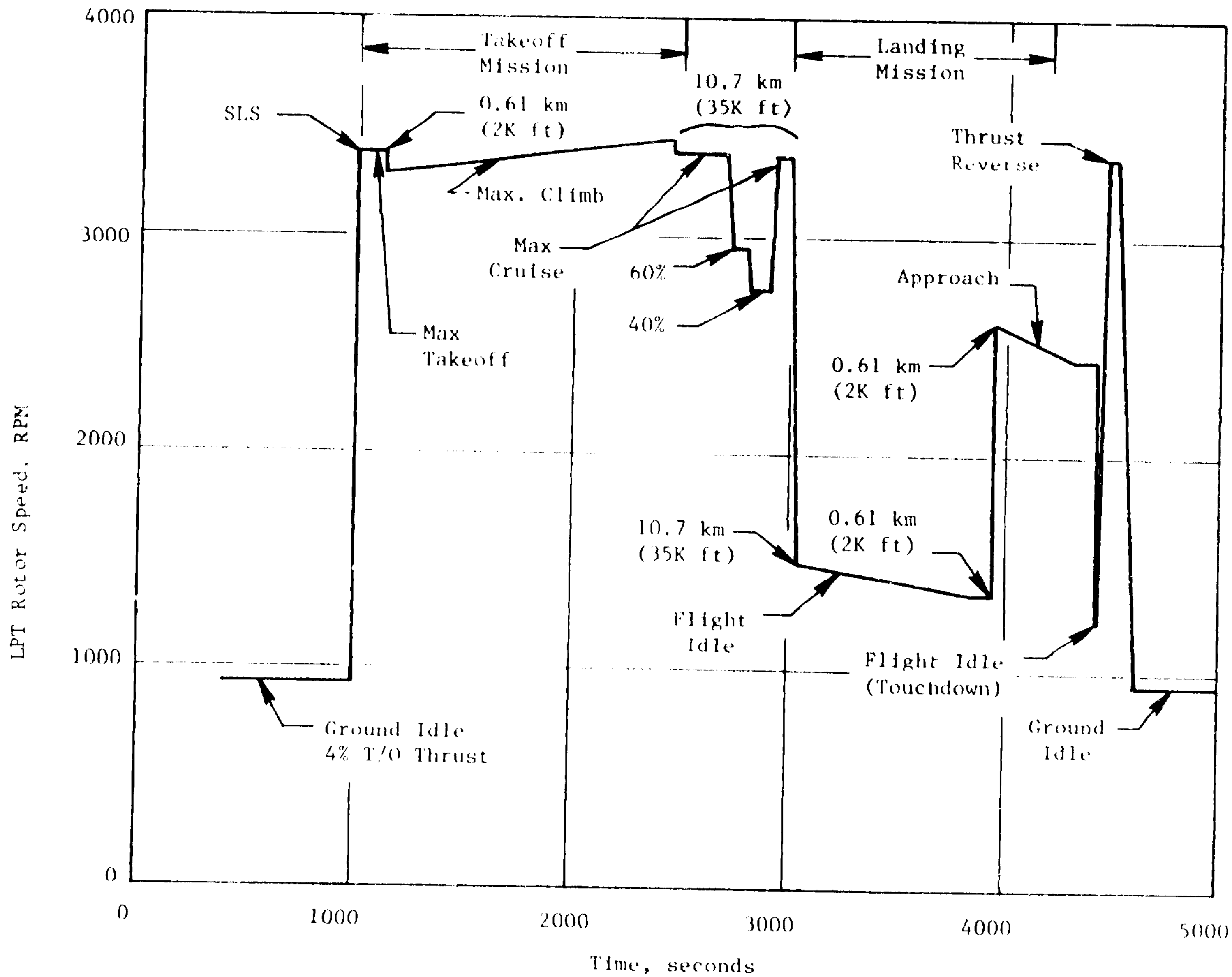

Figure 27. E^3 LPT Rotor Speed Over Typical Flight Cycle.

3.5 COOLING FLOW DEFINITION

The required cooling air is presented in Figure 22 for the base engine and in Figure 28 for the growth engine. The major portion of the rotor purge air is defined by the estimates of the seal clearances and the required flow to block the seals and prevent the flowpath gases from being injected into the rotor cavity. To accomplish this, 1.40% of the fifth-stage compressor bleed air is used to purge the outer and inner bands of the Stage 1 nozzle, cool the vane approximately 56° C (100° F), block the HPT rotor balance seal, and purge the LPT rotor cavity. A small portion of the rotor purge air leaks into the sump purge cavity and eventually exits through the center vent of the primary exhaust nozzle. But the majority of the flow returns to the LPT flowpath; work is recovered as the purge air expands through the remaining stages and out through the exhaust nozzle. The flow through the Stages 1, 2, and 3 rotor spacer arm flanges is defined by the required spacer arm temperatures.

The aft rotor cavity is purged with LPT exhaust gas. This is a significant change from the preliminary design where fifth-stage compressor bleed air was used to purge the cavity. The prime reason for purging the cavity with warm air was to improve engine performance and reduce thermal gradients in the rear frame hub and in the rotor disks of Stages 4 and 5. This system allowed a reduction in fifth-stage bleed air by 0.1% W_{25} and provided better temperature matches in the frame hub and between the bores and rims of the disks.

The outer casing will be kept under the design objective metal temperature of 677° C (1250° F) by impingement cooling with fan air. The ACC and the casing impingement-cooling scheme are combined into one system. The cooling of the casing requires 0.1% W_{25}; this will be increased to 0.3% for maximum cooling in order to achieve the greatest clearance reduction.

To incorporate growth capability in the LPT rotor, it was necessary to increase the rotor cavity flows so that the disk spacer arms were kept within temperature limits. For the growth engine, cooling for the LPT was increased from 1.4% to 1.57% of the core compressor inlet airflow.

The LPT gas stream and cavity pressures at the 30° C (86° F) ambient temperature, maximum-takeoff, base-engine cycle point are presented in Figure 29. These cavity pressures were used to define the seal-blockage flow rates and various sink pressures for the cooling air.

The prime source of LPT cooling air is fifth-stage compressor bleed delivered to the turbine through six pipes equally spaced around the Stage 1 LPT nozzle cooling-supply manifold. This manifold, which is integral with the casing and outer transition duct hanger, distributes the cooling air uniformly around the inside of the casing. Next, cooling air is fed into the 72 nozzle vanes and across the flowpath to the inner nozzle support structure shown in Figure 30. The cooling air warms to about 72° C (130° F) while flowing through the vanes. The rotor cavity need not be cooled significantly below 593° C (1100° F), and this will happen when fifth-stage compressor bleed is used as coolant. Most nozzle cooling is done near the leading edge where the

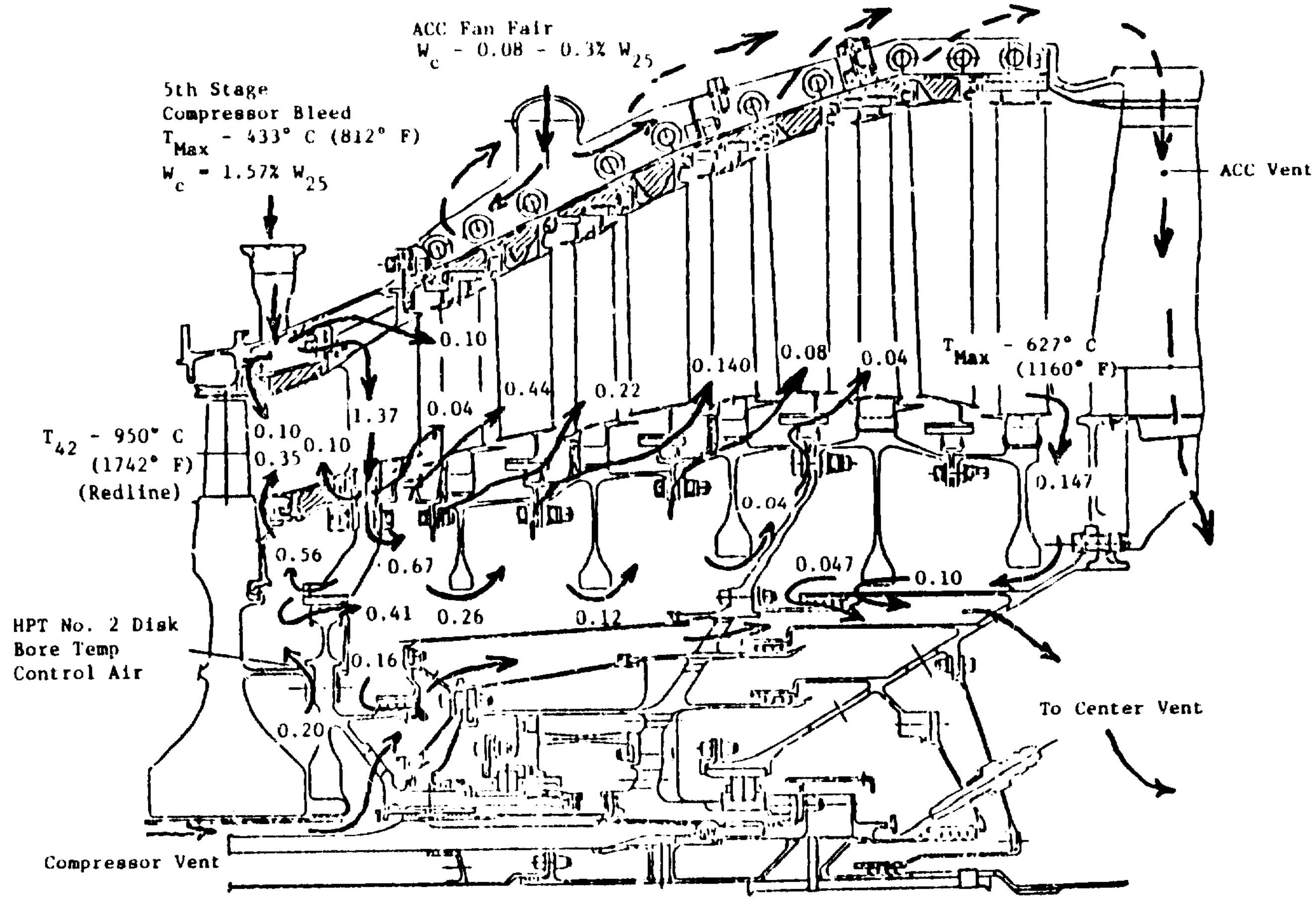

Figure 28. E^3 LPT Cooling Air Requirement for the Growth Engine.

ORIGINAL PAGE IS
OF POOR QUALITY

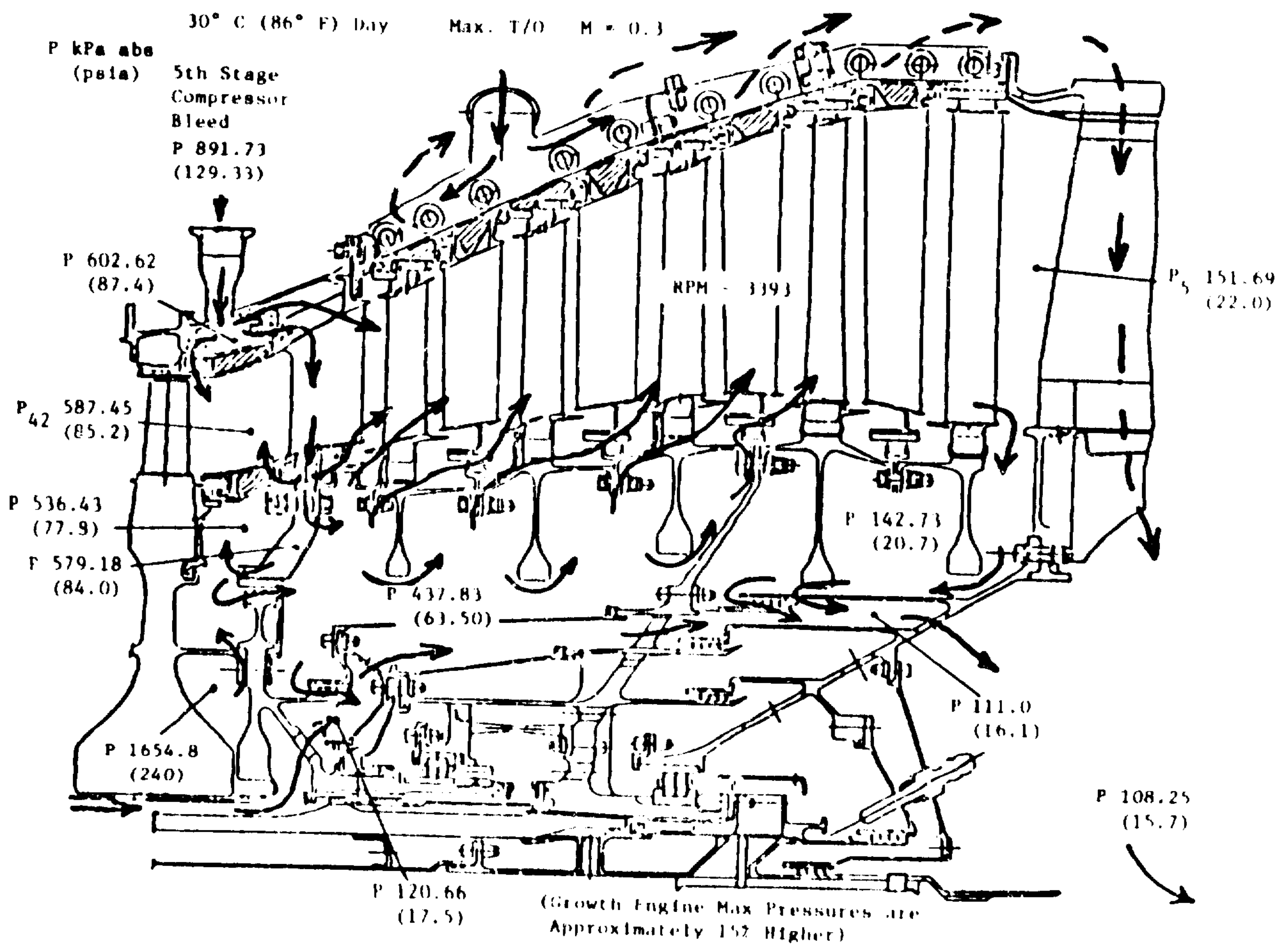

Figure 29. F^3 LPT Base Engine Max Pressures.

ORIGINAL PAGE IS
OF POOR QUALITY

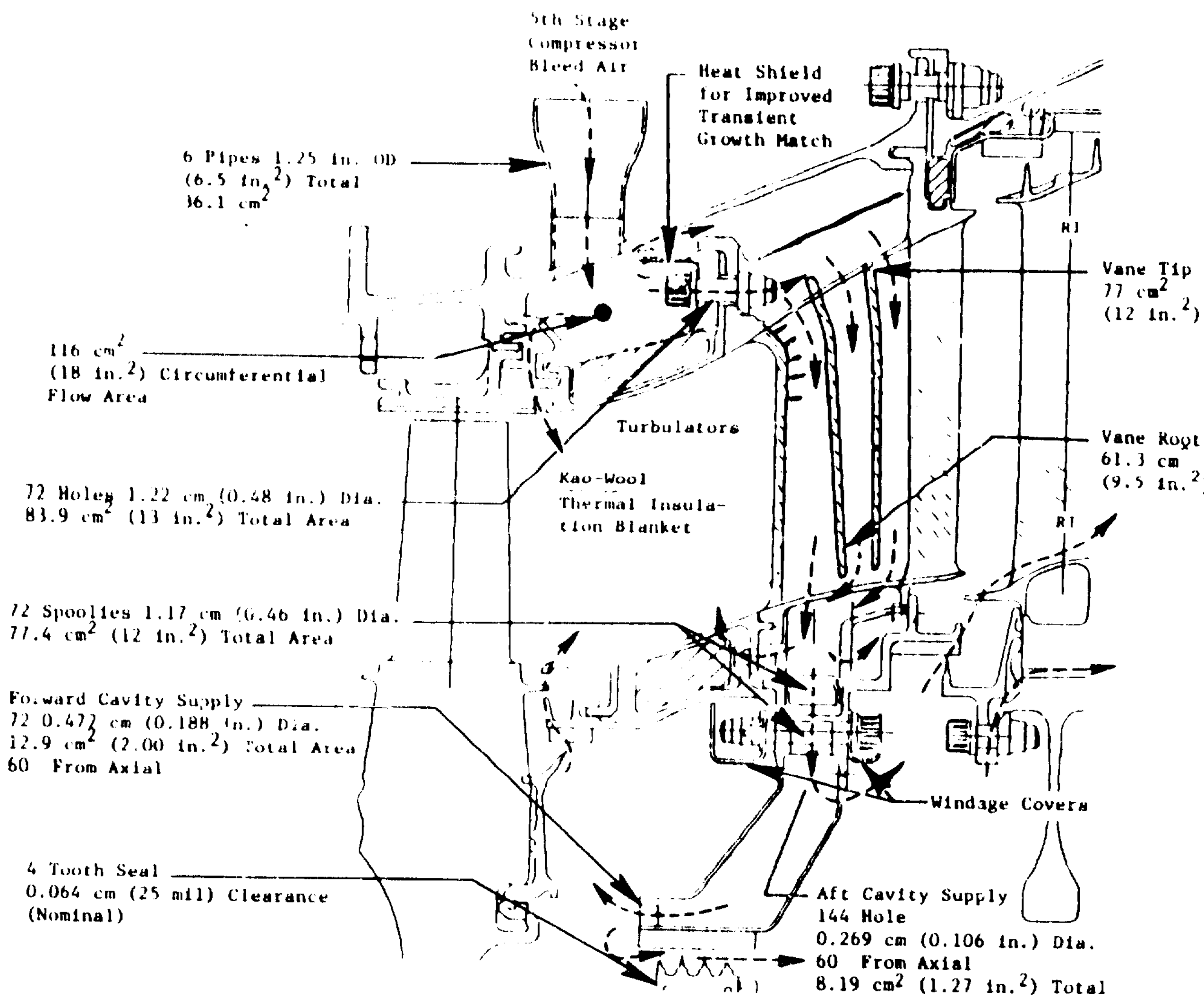

Figure 30. E^3 LPT Cooling Supply and Nozzle Cooling System.

highest stresses occur. Once the cooling air reaches the nozzle hub it is delivered into the wheel-space supply plenum by 72 spoolies. The total cooling air passing through the nozzle is 1.2% W_{25}, of which 0.14% is used to help purge the nozzle inner-flowpath structure. Of the remaining 1.06% that enters the 360° wheel-space supply plenum, 0.56% is supplied to the forward wheel-space cavity, and 0.5% is supplied to the aft wheel-space cavity. The plenum supply pressure is 545 kPa abs (79 psia) while the forward wheel space cavity pressure is 488 kPa abs (70.8 psia) as shown in Figure 31. This yields a 1.08 pressure ratio across the wheel-space injection holes. The holes are angled 60° from the circumferential direction and yield a tangential velocity of 149 m/sec (488 ft/sec). This tangential velocity reduces the amount of boundary layer pumping that the HPT rotor must do. The wheel-space cavity pumping analysis indicates that the velocity of the air should be about 50% of wheel speed. Since the aft cavity is at a pressure of 410 kPa abs (59.5 psia), the cooling-air injection pressure ratio is higher, and a higher tangential velocity is achievable. The LPT rotor is rotating at less than 30% of the HPT rotor speed; therefore, the tangential velocity leaving the injection holes is better than twice the LPT rotor wheel speed. With this system, a substantial amount of work will be obtained from the injected air as it is pumped up on the rotor disks.

Of the 0.56% W_{25} that is injected into the forward wheel-space cavity, 0.4% leaks back through the interturbine seal and into the LPT rotor cavity. Extensive seal-clearance studies have been conducted on the interturbine seal to define the proper quantity of blockage air. Over the engine operating range, it is expected that the seal clearance will vary between 0.025 cm (10 mils) and 0.068 cm (27 mils) as shown in Figure 32. The tightest clearance occurs during cold-start takeoff transients with a new seal; the most open clearance occurs at nominal cruise power with a deteriorated seal. The seal will flow 0.67% W_{25} when the clearance has opened up to 0.09 cm (36 mils). This could only occur as part of an engine failure, and only then would hot flowpath gases be injected into the HPT aft rotor cavity. In conclusion, the seal blockage air is satisfactory from an engine safety standpoint and yields the best overall performance. During the ICLS test, important information on the windage temperature rise and vortex pressure gradients will be obtained in the wheel-space cavities. These data will be very beneficial in developing the seal design for the FPS.

The LPT rotor cooling/purge air supply consists of interturbine seal leakage air and air that is injected tangentially into the rotor cavity from the wheel-space-cooling-supply plenum. The total cooling-air supply to the rotor cavity will be 0.91% W_{25} for the base engine and 1.08% for the growth engine. The extra cooling flow of 0.17% W_{25} for the growth engine is required in order to dilute the 36° C (64° F) hotter gas around the rotor spacer arms. The disk spacer arms are exposed to higher gas temperatures; thus, more wheel-space purge air is required to dilute the gases and keep the metal within acceptable limits. The wheel-space purge air requirements were defined by evaluating the allowable gas temperatures in a detailed thermal model. Then dilution airflow requirements were defined in order to bring the gas temperatures down to the allowable level. This cooling scheme will also allow the

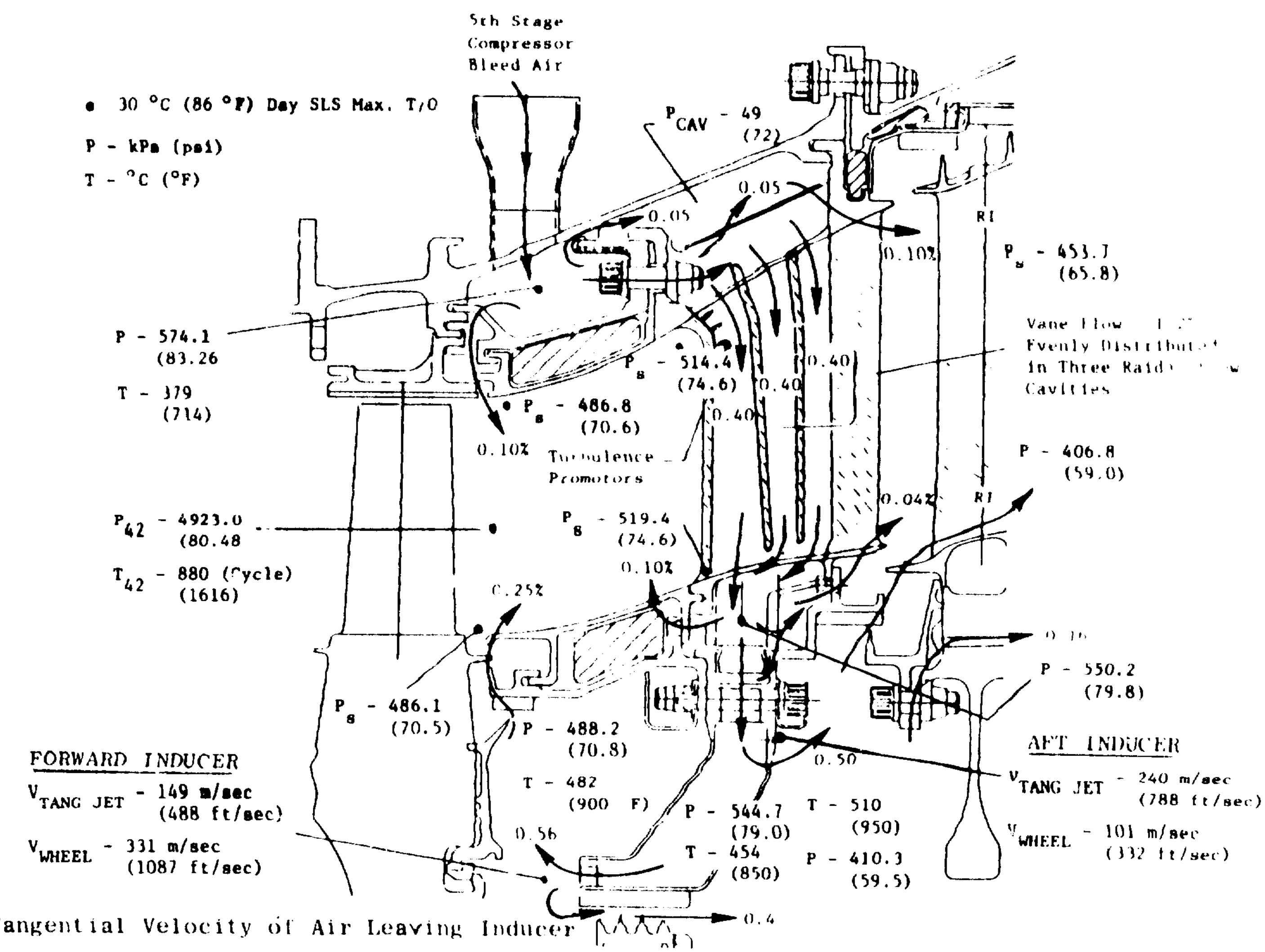

$V_{TANG\ JET}$ - Tangential Velocity of Air Leaving Inducer

V_{WHEEL} -Tangential Velocity of Wheel at Radius of Inducer

Figure 31. E^3 LPT Cooling Supply System (ICLS).

ORIGINAL PAGE IS
OF POOR QUALITY

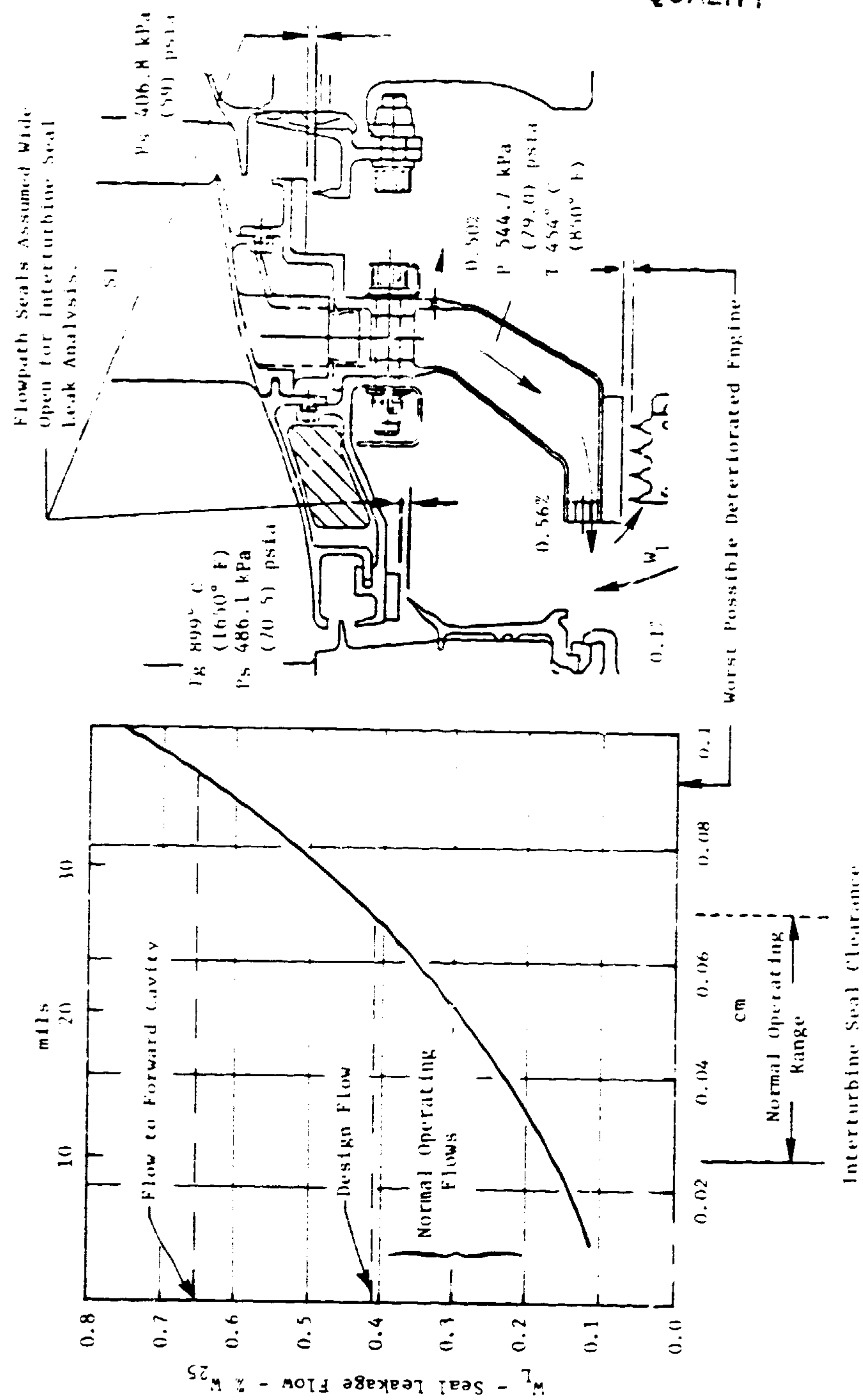

Figure 32. E^3 LPT/HPT Interturbine Seal Blockage.

cool dilution air to circulate through the taps between dovetails and disk posts and keep those components within limits. The wheel-space purge air is metered through slots in the upstream spacer arm bolt flange. This will yield a consistently small flow area needed to meter the flow. The purge airflows (Figure 22) are 0.16, 0.10, and 0.06 % W_{25} for the first, second, and third wheel-space cavities, respectively. An additional 0.03% is supplied through the main torque-bolt flange. This helps to define the flow under the Stage 3 disk and the through-flow in the cavity bounded by the Stage 3 disk and the main torque cone. Of the 0.91% W_{25} that dumps into the rotor cavity, 0.16% leaves through the sump bypass seal. This air then flows around the aft sump and dumps into the centerbody at the back of the engine. From there it flows out through the primary-nozzle center vents, recovering a portion of the thrust. An extensive analysis has been conducted in an effort to keep the sump bypass leakage seal as small in diameter as possible to keep the clearance to a minimum.

The remaining rotor-cooling flow (0.4% W_{25}) is supplied to the seal ahead of the Stage 1 rotor. This flow is more than adequate to cool and purge the Stage 1 forward wheel-space cavity. The quantity of flow must be kept at a high level to compensate for significant variations in seal clearance during normal operation. The flow tolerance of the interturbine seal is 0.16 to 0.41% W_{25}, and the flow tolerance of the sump bypass seal is 0.05 to 0.20% W_{25}. The wheel-space-metering-slot tolerance could shift the flow from 0.25 to 0.45% W_{25}. When the worst tolerance stackup clearance arrangement is evaluated, there will still be a small quantity of wheel-space air flowing through the Stage 1 rotor forward seal.

As mentioned previously, no cooling air is used to purge the aft rotor cavity. The aft cavity, Rotors 4 and 5, is now purged with LPT exhaust gas at the hub of the fifth-stage rotor exit; 0.147% W_{25} of this gas is allowed to circulate down around the two disks in the aft cavity before dumping into the aft sump bypass cavity. Not only does this reduce the temperature gradients in the rear frame hub and between the bore and rim of the Stages 4 and 5 disks during transients, it also improves engine performance. The fifth-stage compressor bleed air used to purge this cavity is now allowed to flow through the complete engine before being extracted at the LPT rotor exit. In transient operations, the hot gas is used to heat the forward, inner-hub structure of the turbine rear frame more quickly during engine accelerations; thus, thermally induced stresses in the frame struts are mitigated. The maximum gas temperature at the hub of the five-stage rotor is 599° C (1110° F) for a deteriorated FPS engine. This is not a severely high temperature, and the gas can be used for disk temperature control. Between idle power and maximum takeoff power, this gas temperature changes by only 111 to 167° C (200 to 300° F); therefore, thermal gradients at high rpm are moderate.

3.6 ROTOR TEMPERATURE DISTRIBUTION

A detailed heat-transfer analysis of the total rotor structure has been completed. This analysis included both the FPS and the growth engine. The transient analysis considered a complete mission from steady-state ground idle through takeoff and climb to maximum cruise. Included in the transient was a throttle chop from maximum at 6.09 km (20,000 ft) climb to flight idle. After holding to flight idle for 320 seconds the engine was taken back to maximum-climb power. This maximum-climb, hot-rotor reburst was analyzed to determine the relative clearance between the rotor and casing.

The rotor gas temperatures at idle and maximum power were defined by using commercial engine data. At idle power the combustor is burning on the pilot dome only; this generates a spiked profile that persists even into the LPT. The spiked profile does mix out as the gases flow through the five stages of the LPT. But since there is not much work extraction in the LPT at idle power, temperature drop through the five stages is insignificant. The profile effect combined with the low-work-extraction effect causes the hub temperature to increase as the gas flows through the turbine. This is typified by the idle profile at the LPT inlet and exit as presented in Figure 25.

A detailed thermal model of the rotor structure was constructed. It contained 532 nodes, as shown in Figure 33, and extended from the Stage 1 disk forward seal back through the fifth-stage rotor. A generous portion of the torque cone was included so that boundary effects could be evaluated. The heat-transfer model also included 192 separate time-dependent boundary conditions, 173 metal-to-metal contact resistances, and 4 separate temperature-dependent material property tables. Rotor temperatures throughout the mission were defined for both the base and the growth engines. Figure 34 shows rotor temperatures at various locations for the growth engine 120 seconds into a hot-day takeoff. The spacer arm reached a temperature of 616° C (1141° F), well within the temperature limits of the Inco 718 material. But the seal reached a temperature of 668° C (1235° F); this made it the temperature-limiting item in the rotor assembly. However, the seal temperature was still within the design limit of 677° C (1250° F).

3.7 CASING COOLING SYSTEM

The LPT is cooled with fan air impinging on the outside of the casing from an array of holes located in a manifold surrounding the complete casing. Commercial experience has shown this approach to be reliable and the least costly from a performance standpoint since LPT fan air is used. Thrust is also recovered from the fan air as it is ejected out the primary-nozzle center vent. As shown in Figure 35, the impingement holes are located over the vane/seal hangers. These areas are the hottest part of the casing and need the most cooling. The objective is to keep the maximum Inco 718 casing temperature below 677° C (1250° F) and meet the life objectives at the same time. The detailed transient temperature analysis indicates that this is feasible when the contact area between vanes and casing is kept to a minimum. It was also necessary to minimize the length of the hangers and to increase the conduction area between the hanger and casing. Blankets of low-conductivity material were placed between the flowpath components and the casing. This insulation helps reduce the radiation and gas circulation between the hot

Input

- 532 Nodes
- 192 Boundary Conditions
- 4 Materials
- 173 Contact Resistances

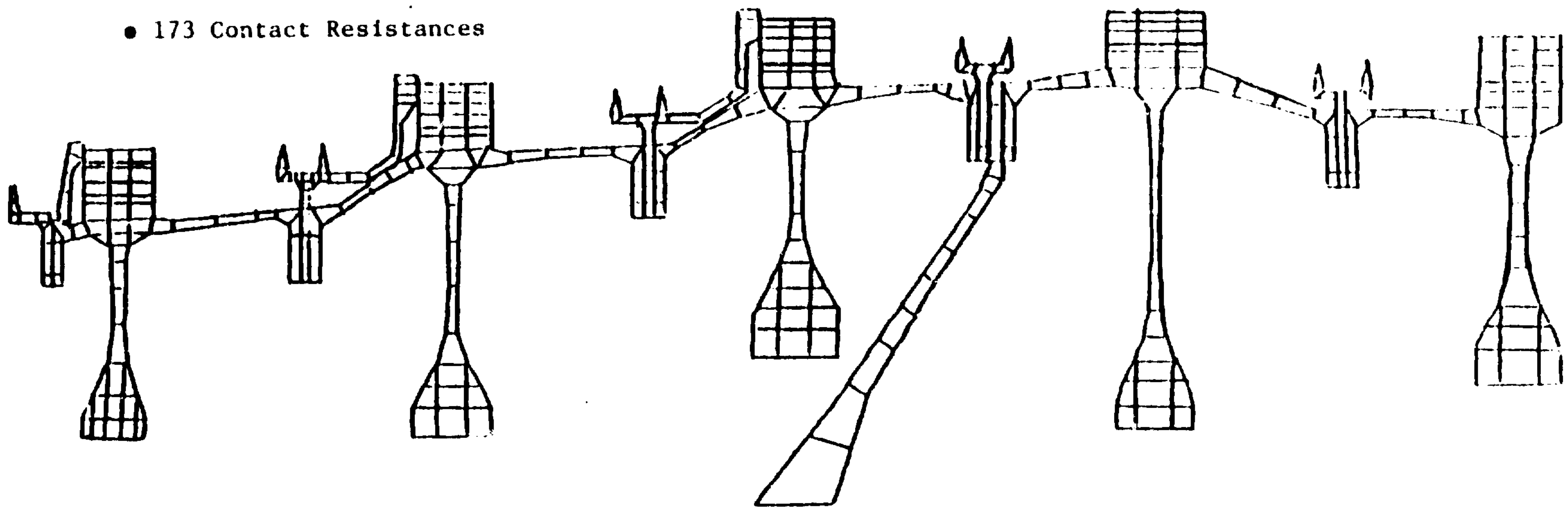

Results

- Transient Temperature Distribution

  Takeoff (Idle - Takeoff - Climb - Cruise)

  Descent (Thrust Reverse - Idle Cruise - Descent - Approach - Touchdown)

Figure 33. E^3 LPT Rotor Structure Heat Transfer Model.

- 50° C (122° F) Day Max T/O Growth Engine Temperature Distribution 120 Seconds into Takeoff

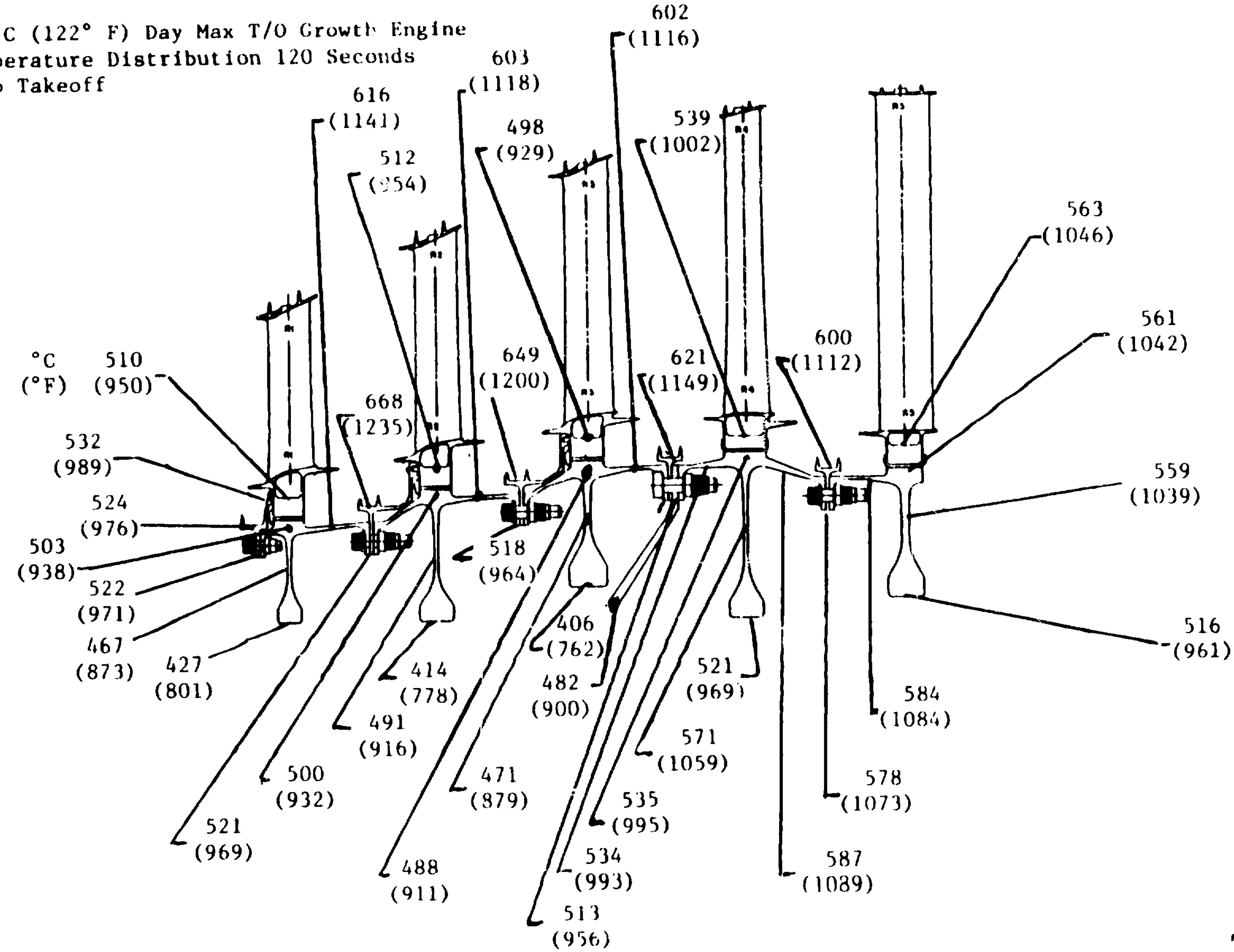

Figure 34. E^3 LPT Rotor Structure.

ORIGINAL PAGE IS OF POOR QUALITY

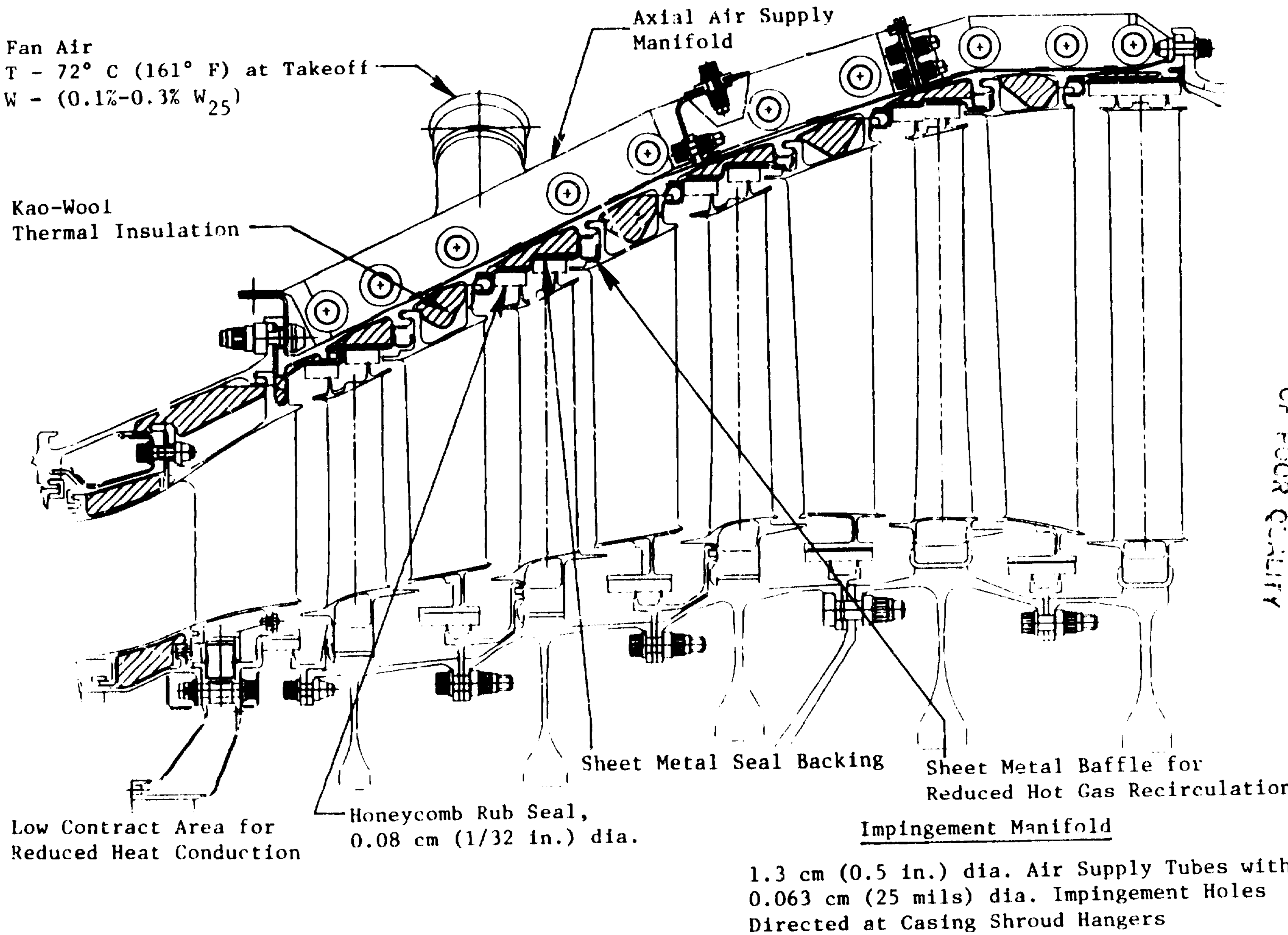

Figure 35. E^3 LPT Casing Cooling System.

flowpath and the casing. Each insulation blanket is covered with 0.005 to 0.008 cm (2 to 3 mil) thick Inco 600 metal foil to help maintain the integrity of the insulation material between overhauls. Where the foil might be exposed to hot, high-velocity flowpath gases, the foil thickness has been increased to 0.015 cm (6 mils).

Casing cooling is accomplished by means of an impingement manifold extending around the complete LPT casing. The coolant is collected by a scoop located in the fan bypass duct. The cooling air is then fed through a circumferential duct to the LPT casing impingement manifold. The impingement manifold consists of four 90° sectors with one axial distribution plenum per section as shown in Figure 36; 1.27-cm (0.5-in.) diameter tubes distribute the cooling air circumferentially around the casing. The cooling air leaves the tubes through 0.064-cm (25-mil) diameter impingement holes evenly distributed in each circumferential tube. The 0.064-cm (25-mil) impingement hole is the minimum size that extensive commercial engine experience has shown to have no plugging problems. The hole spacing in each ring has been adjusted to give the desired cooling for each turbine stage. The spacing parameter (distance ÷ diameter) varies from 9 to 16, and the total number of holes yields a total impingement flow area of 13.97 cm^2 (2.165 in^2). This impingement flow area is the minimum flow area in the cooling-supply system. All other pipes and ducts have flow areas at least three times larger than the impingement flow area.

In order to complete the detailed heat-transfer analysis of the casing, a thermal model was constructed. Figure 37 illustrates the detailed thermal model; it consists of 534 nodes, 5 different materials, 121 metal-to-metal contact resistances, and 56 time-dependent boundary conditions of temperature and heat-transfer coefficients. The thermal model extended from ahead of the Stage 1 LPT nozzle flange to beyond the Stage 5 shroud aft-support flange.

The high heat transfer coefficients associated with the LPT gas flowpath and the low heat-transfer coefficients associated with the casing external impingement cooling system were input into the detailed thermal model. Radiation from the casing was also factored into the detailed thermal model. The gas temperatures along the casing flowpath, with only the combustor pilot stage burning, were factored into the idle-temperature definition. A complete flight transient analysis was conducted. The most severe temperature distribution occurs at the end of the maximum takeoff segment of the flight mission and last for 2 minutes. After this point, the engine is throttled back to maximum-climb power setting, and the LPT inlet temperature drops by 56° C (100° F).

Since the LPT ACC is combined with the casing cooling system, two analyses were conducted on the casing. The two analyses consisted of the casing cooling extremes: (1) minimum cooling to keep the casing temperatures within limits and (2) maximum cooling to define the closure capability of the cooling system and worst temperature gradients. The temperature distribution in the casing at 2 minutes into the takeoff transient is presented in Figure 38 for the minimim cooling of 0.08% W_{25}. The temperature distribution at the end of

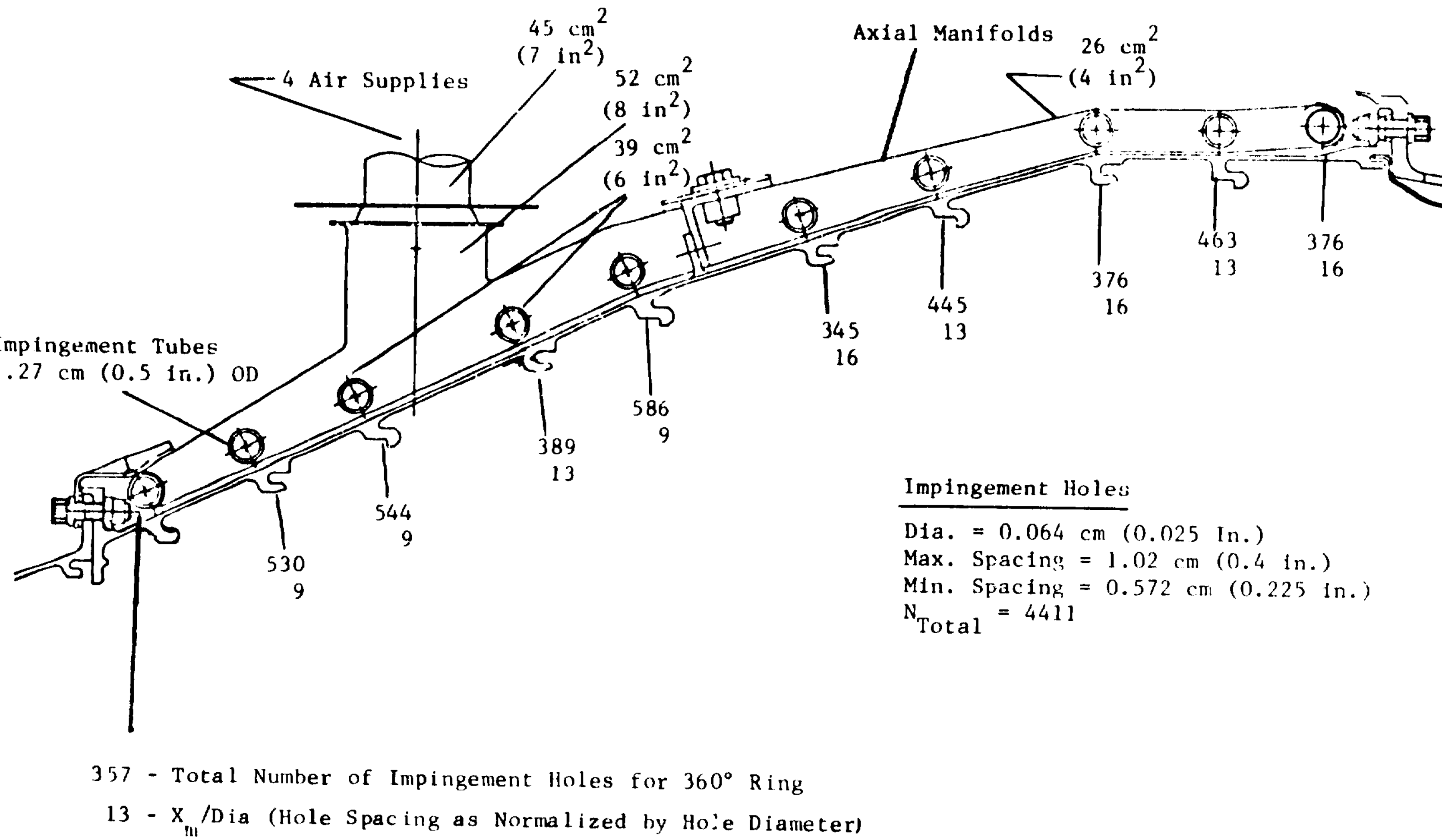

Figure 36. E^3 LPT Cooling/ACC Impingement Manifold.

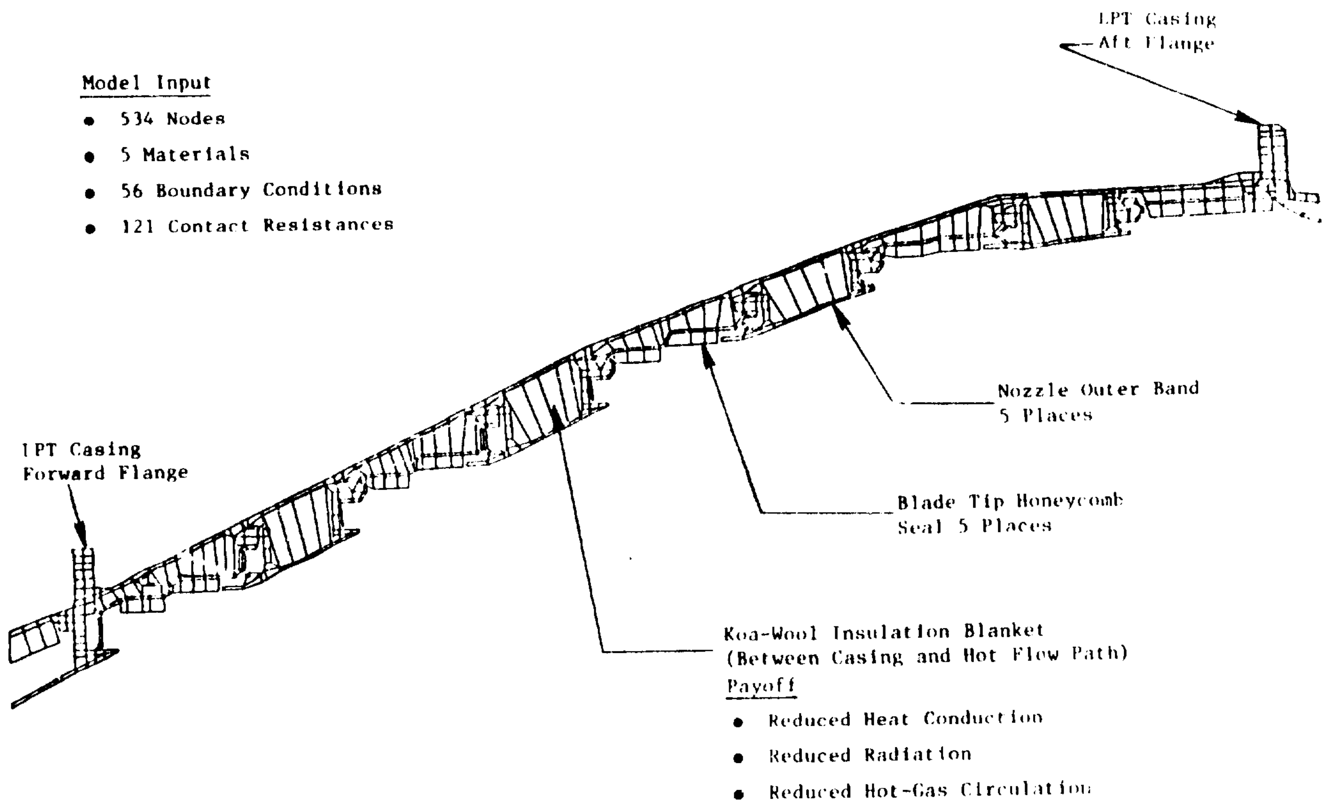

Figure 37. E^3 LPT Casing Detailed Thermal Transient Model.

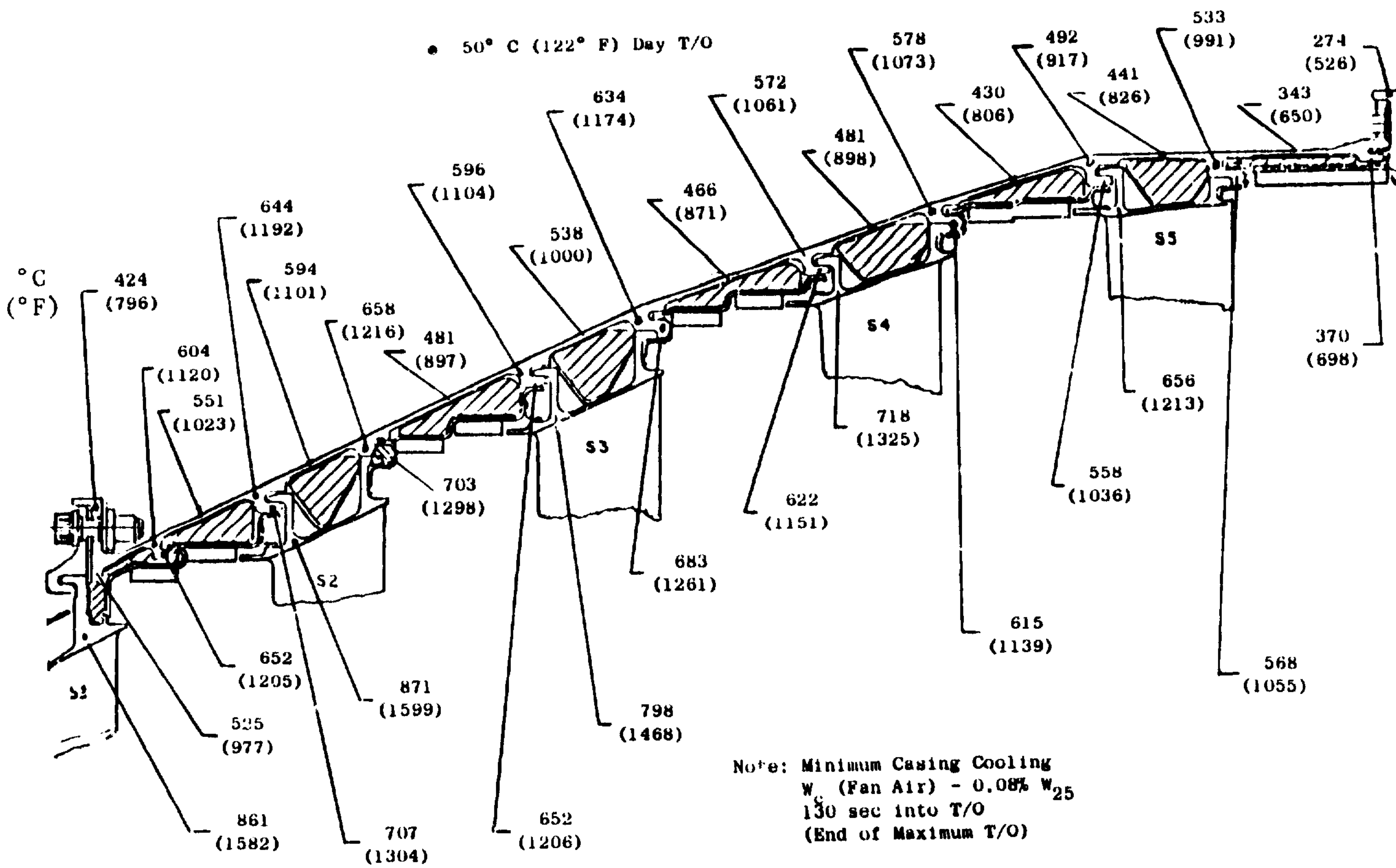

Figure 38. LPT Casing Transient Temperature Distribution.

takeoff with the maximum cooling of 0.3% is presented in Figure 39. The analyses indicated that 0.08% W_{25} casing cooling at the second-stage nozzle hangers may not be enough. With the maximum cooling of 0.4% W_{25}, the stage 2 nozzle hangers are well below the 677° C (1250° F) temperature. These areas will be watched closely in the ICLS test in order to find out if additional flow will be required to keep the casing hanger temperatures at an acceptable level.

3.8 STAGE 1 NOZZLE

Extensive analysis on the heat transfer design of the Stage 1 nozzle has been completed. This analysis includes the outer casing and flowpath structure, the Stage 1 vane, and the inner flowpath structure (see Figure 30). Because of the critical nature of the nozzle support structure, the HPT aft wheel-space purge, the interturbine seal blockage, and the LPT rotor blockage, a detailed temperature analysis has been made of each of these areas.

The analysis of the outer flowpath structure included the casing, the nozzle support ring, the transition flowpath, and the HPT Stage 2 aft shroud-support ring. Several changes were made in the design of the nozzle support structure during the detail design phase. Most of these changes were directed toward establishing an effective, reliable means of supplying rotor cooling air while keeping air leakage to a minimum and meeting the hardware life requirements. The final design meets these objectives. A detailed transient heat-transfer analysis of the final design has been completed. The thermal model (Figure 40) contains 375 nodes of 4 different materials, 37 contact resistances, and 27 time-dependent boundary conditions of temperature and heat-transfer coefficients. Also, radiation from the casing was factored into the model. The complete flight mission was analyzed thermally. The analysis included the effects of ACC cooling on the HPT/LPT casing. The point in the engine mission exhibiting the most severe thermal gradients occurred 30 seconds after the 10-second accel from ground idle to full-power takeoff on a hot day.

One of the concerns with the design was the rabbet seal between the nozzle support ring and the casing. It is imperative that the rotor cooling supply system seal leakage be kept to a minimum. Extensive investigative analysis was done to assure that the seal stayed tight under all transient conditions. The critical takeoff portion of the mission presented no problems. The internal nozzle support structure quickly heated while the casing was somewhat slower to respond. The thermal coefficient of expansion is comparable for both rings and results in a tight fit since the fast-responding inner ring grows outward against the slow-responding casing. Some leakage occurs during the descent transient from maximum cruise to flight idle where the seal has a tendency to open up. The fast-responding inner ring cools faster than the casing, and eventually the inside ring is cooler than the casing. The worse condition occurs at about 450 seconds after the throttle chop from maximum cruise to flight idle. In order to overcome this leak problem, a 360° heat shield was placed over the rabbet seal ring. Because the heat comes from the rotor purge air, the heat shield reduces the effective heat transfer coefficient, thus slowing the rate of response. The shield eliminates the temperature-gradient reversal during the descent transient. The detailed temperature

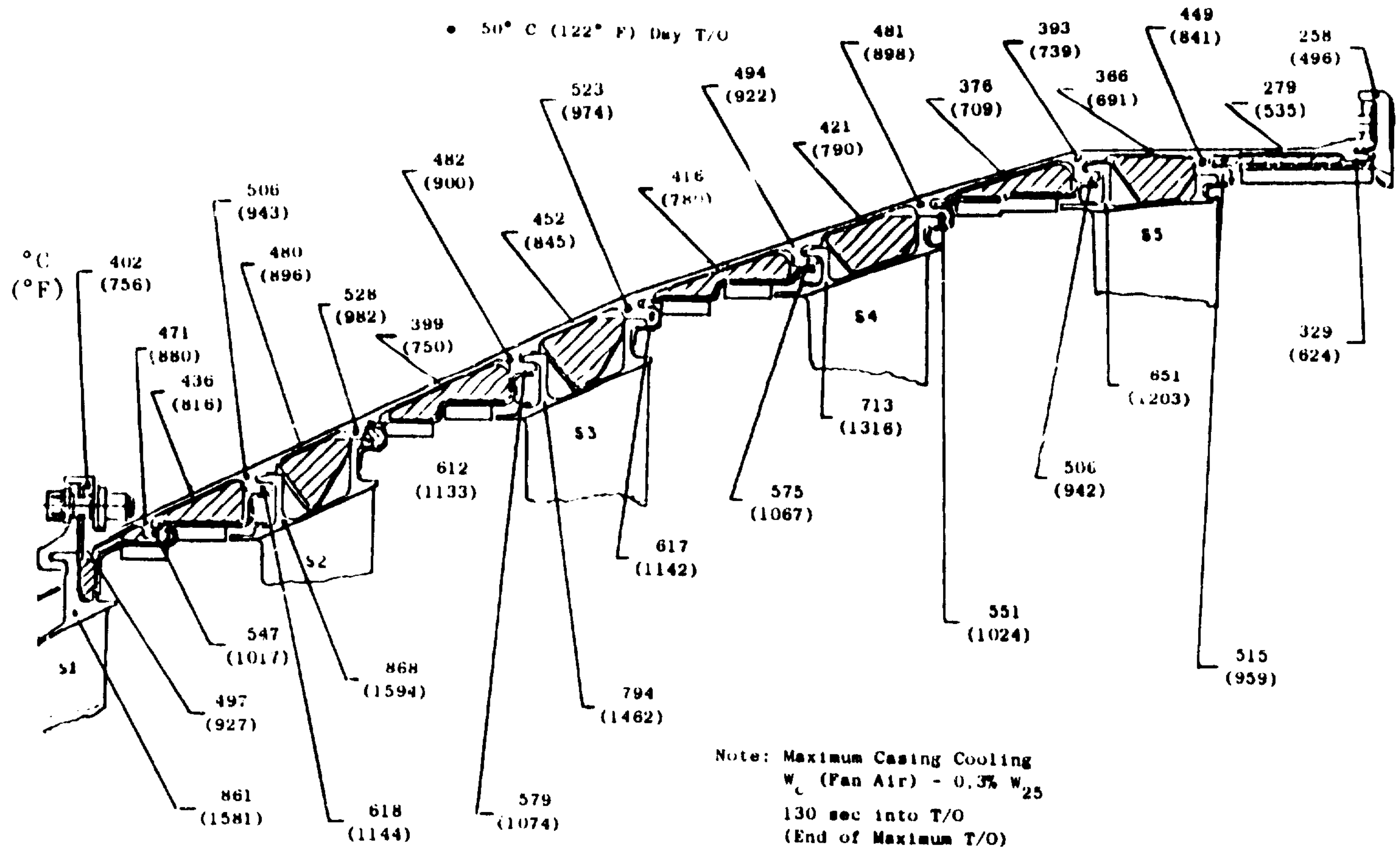

Figure 39. E^3 LPT Casing Transient Temperature Distribution.

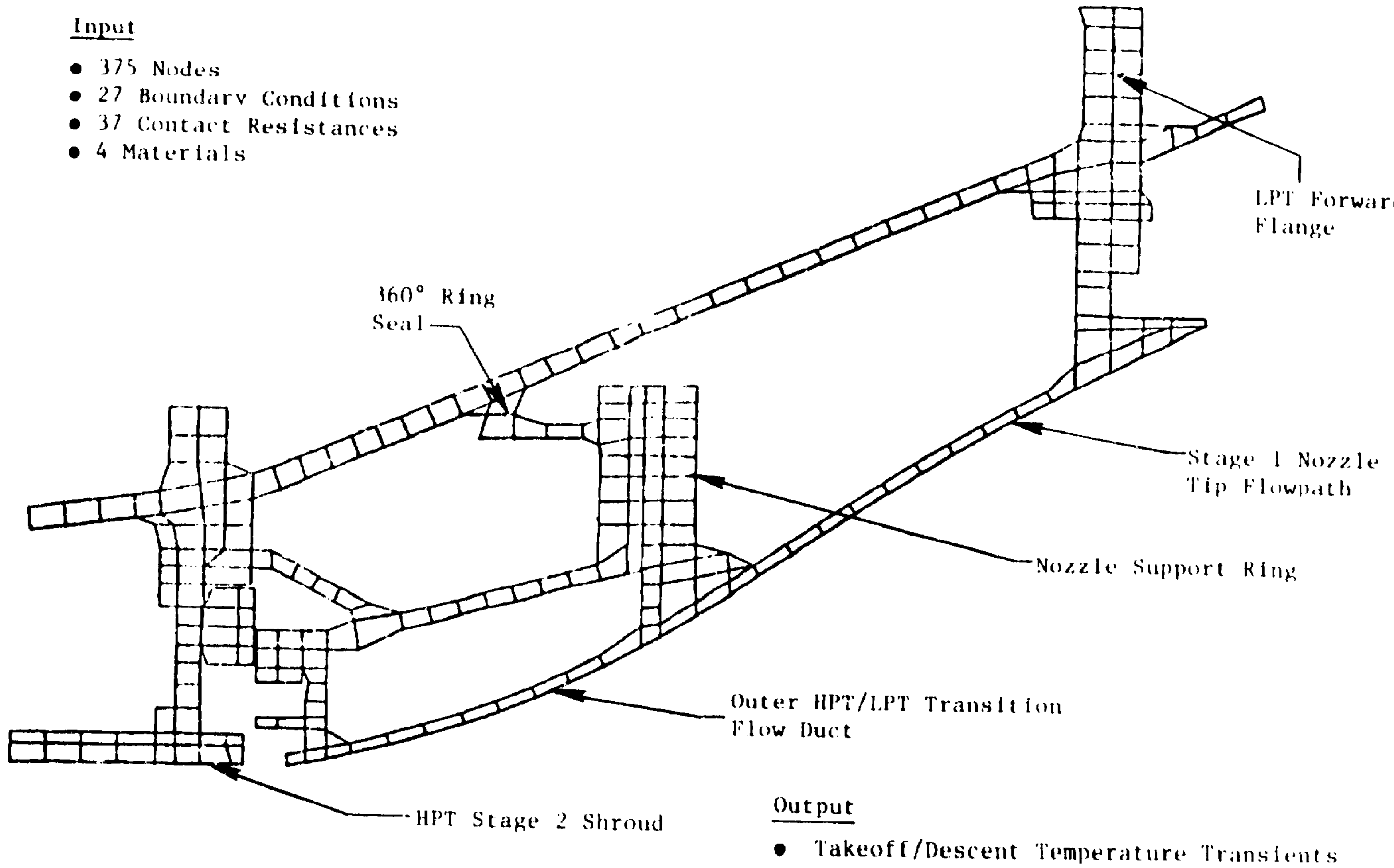

Figure 40. E^3 LPT Stage 1 Nozzle Support Structure Detailed Thermal Model.

distribution was defined and mechanical loads were evaluated at the 450-second point into the descent transient in an effort to evaluate the seal gap. The temperature distribution at the critical time is given in Figure 41. Although the seal ring is 12° C (22° F) warmer than the adjacent casing, the seal will open to 0.013 cm (5 mils). This results in a 0.22% W_{25} leak through the gap. Inasmuch as this occurs during the flight descent, no service problems will result, but efforts have continued in order to further reduce the gap. The prime thermal mismatch is caused by the other sections of the 360° plenum cooling, by as much as 83° C (150° F), faster than the casing. The biggest problem was caused by the cooling air impinging on the 360° manifold at six locations around the casing where the LPT cooling air entered the through-pipes in the casing. To further improve the clearance between the casing and seal ring, a heat/splash shield was placed under each of the six pipes entering the casing. The splash shield is 15.2 cm (6 in.) wide in the circumferential direction and fastened to the nozzle support ring by two bolts. The improvement produced by the heat/splash shield will cut seal leakage virtually to zero. The end result is a plenum that has a good thermal match with the casing to keep the seal leakage to a minimum over the complete mission. The interference fit between the seal ring and the casing during accel will also be reduced. This will diminish the possibility of wear due to transient axial-growth variation when there is a large interference fit at the seal. In addition, the Stage 1 vane was analyzed because it is the prime load-carrying member for the inner flowpath structure and the flowpath for the rotor cooling air. From previous engine experience, the highest stress point is the vane leading edge (LE). Early in the detail design, the preliminary heat-transfer calculations indicated that it was reasonable to reduce the LE temperature 28° C (50° F) below gas stream. Since the gas-stream temperature at the 90% vane span was 949° C (1740° F) for a hot streak on a deteriorated engine, the LE had to be cooled below 921° C (1690° F). At the same time, the pressure drop required to maintain sufficient cooling flow through the nozzle had to be kept to a minimum. Temperature reduction and pressure-loss objectives were achieved by adding two ribs in the vane. The ribs were slanted so that the flow was restricted in the forward cavity at the outer band; the flow was diffused by tilting the rib aft and gradually increasing the flow area at the hub. This resulted in LE cavity with the minimum flow area at 90% span and maximum flow area at the hub. The flow area distribution in the two aft cavities were reversed from the LE cavity. The maximum flow area was at the vane 90% span, and the minimum flow area was at the hub. This design approach resulted in a high-velocity cooling flow at the vane outer flowpath LE cavity and a high heat-transfer coefficient. Turbulence promoters were also added to the inside of the LE radial cavity as a means of further enhancing the coolant heat transfer.

A detailed thermal model was set up to assess the temperature distribution in the vane at the LE and in the rest of the vane, including the trailing edge. The gas-side heat transfer was defined by using the design velocity distribution and heat-transfer design practice for this type of airfoil with no film holes and low Reynolds number. Local metal and steady-state temperatures at maximum takeoff are presented in Figure 42. The maximum LE temperature was reduced by more than 28° C (50° F) below gas stream to 918° C (1684° F). The bulk metal temperature dropped to 871° C (1599° F); this kept the

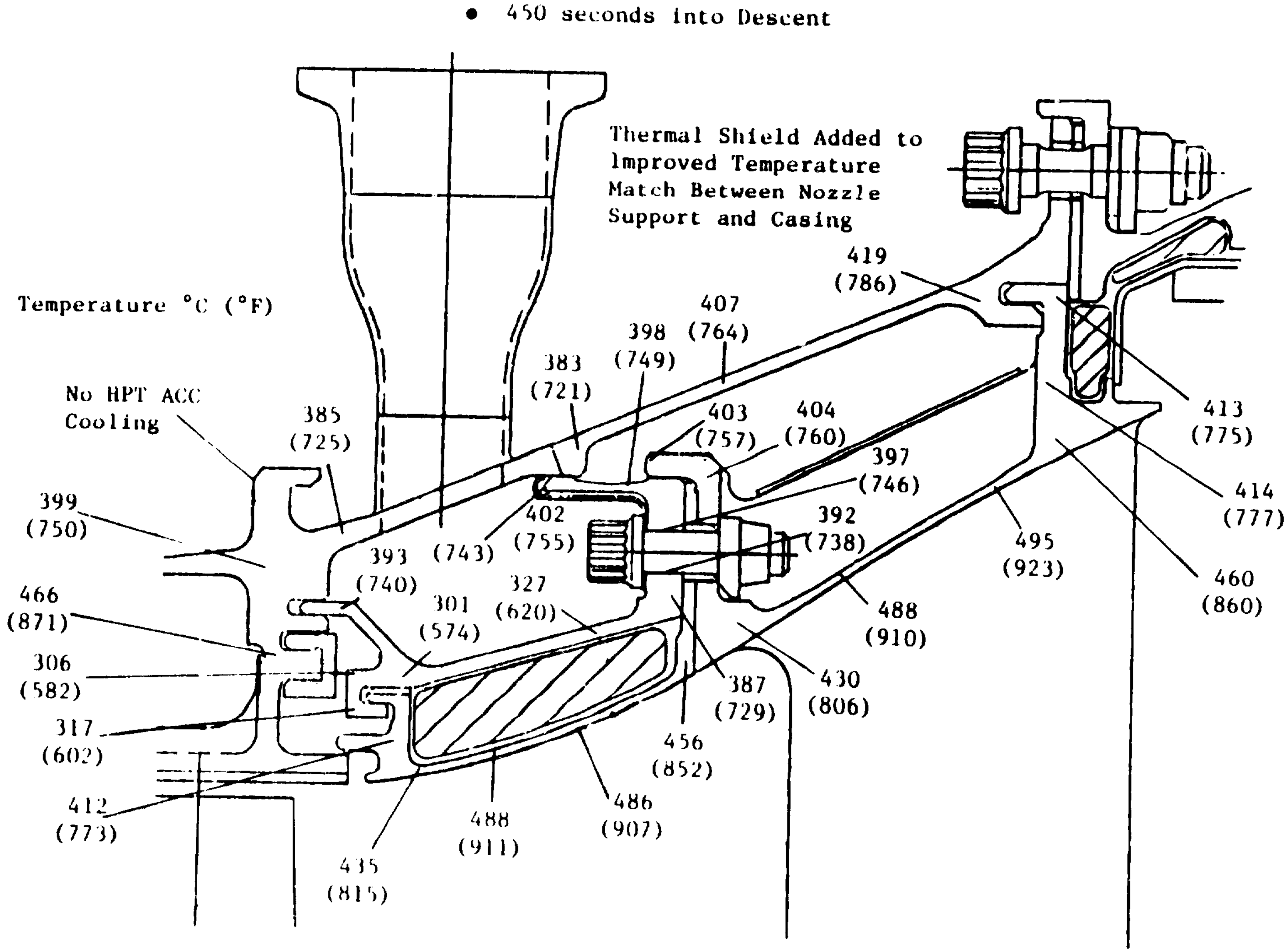

Figure 41. LPT Stage 1 Vane/Transition Duct/Support THT Temperatures at 3450 Seconds (Decel).

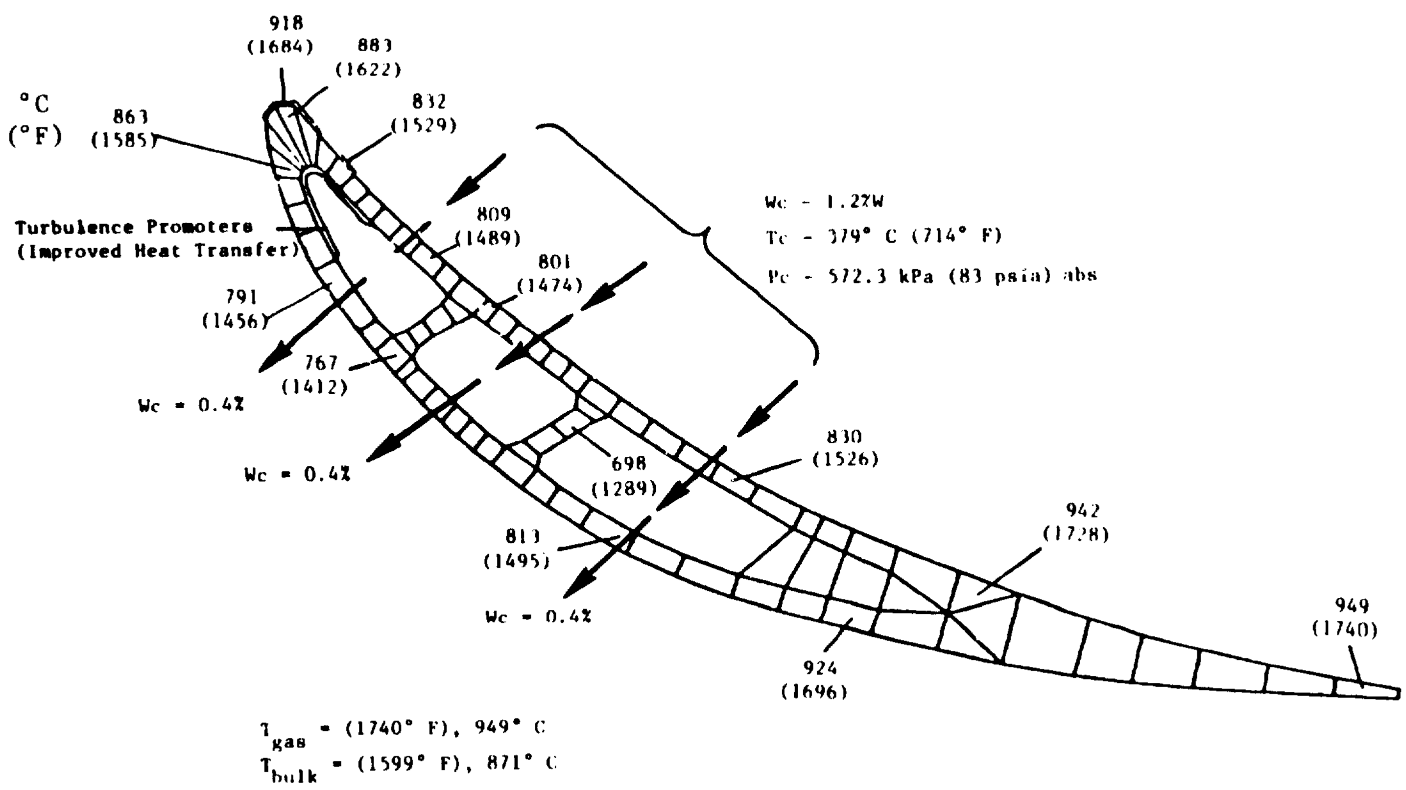

Figure 42. Stage 1 Vane 90% Span Steady State Max Takeoff Temperature Distribution.

maximum LE-to-bulk-temperature difference to 47° C (85° F). Due to the low cooling at the trailing edge, that section of the airfoil will be effectively the same as the gas temperature. Even with the worst possible temperature profile, at the 60 to 70% span, the gas temperature will not get much above 982° C (1800° F) and therefore will not cause any significant life problem with the René 125 material in the FPS nozzles or René 77 in the ICLS nozzles.

Because of the critical nature of the load-carrying capability of the Stage 1 vane LE, investigation was extended to the fillet region of the vane and outer band. The vane wall thickness was kept the same as the maximum thickness at the 90% span. But, because the curvature of the LE was greater, the gas-side heat transfer was reduced, and the area ratio ($A_{gas}/A_{coolant}$) went down. Although the coolant heat-transfer coefficients went down due to the reduced flow velocity, net cooling was improved because the cooling surface area increase had the dominating effect. This resulted in a lower metal temperature at the LE.

The next item in the rotor cooling-air-supply system is the inner nozzle support structure and the inner HPT/LPT transition-duct flowpath and rotor cavity air-supply plenum. Of the air that is supplied through the vanes, 1.06% is fed through the spoolies into the rotor supply plenum, and 0.14% is used for structure purge and spoolie leakage in the inner nozzle cavity, as shown in Figures 30 and 31. The purge air will help prevent any hot-gas leakage from circulating into the cavities around the nozzle inner flowpath cavity. This will help the nozzle aerodynamic performance by keeping the high-momentum gases in the flowpath and will improve the hardware life by preventing high thermal stresses associated with high temperature gradients around the structure delivering the rotor cooling air.

In order to define the temperature distribution in the nozzle inner flowpath structure, a detailed thermal model was constructed. This model (Figure 43) included the 10% vane span, the transition structure, the vane and seal support structure, and the rotor air-supply plenum. The thermal model contained 238 nodes of 4 materials and 32 contact resistances. There were 25 different time-dependent boundary conditions of temperature and heat-transfer coefficients included in the model. The most severe temperatures occurred 30 seconds after takeoff from ground idle power. Selected temperatures at this particular time are presented in Figure 44. A transient analysis was carried out from takeoff through cruise in an effort to define the interturbine seal growth for clearance definition in order to assure proper rotor cavity purge at all cycle conditions.

3.9 ACTIVE CLEARANCE CONTROL

In the design of a high-performance engine like the E^3, component efficiencies must be maintained at a high level. Each component was examined to define which factors contributed to potential deterioration of engine performance. It was found that blade tip clearances had a significant impact on compressor and HPT/LPT performance. No matter how close the clearances are

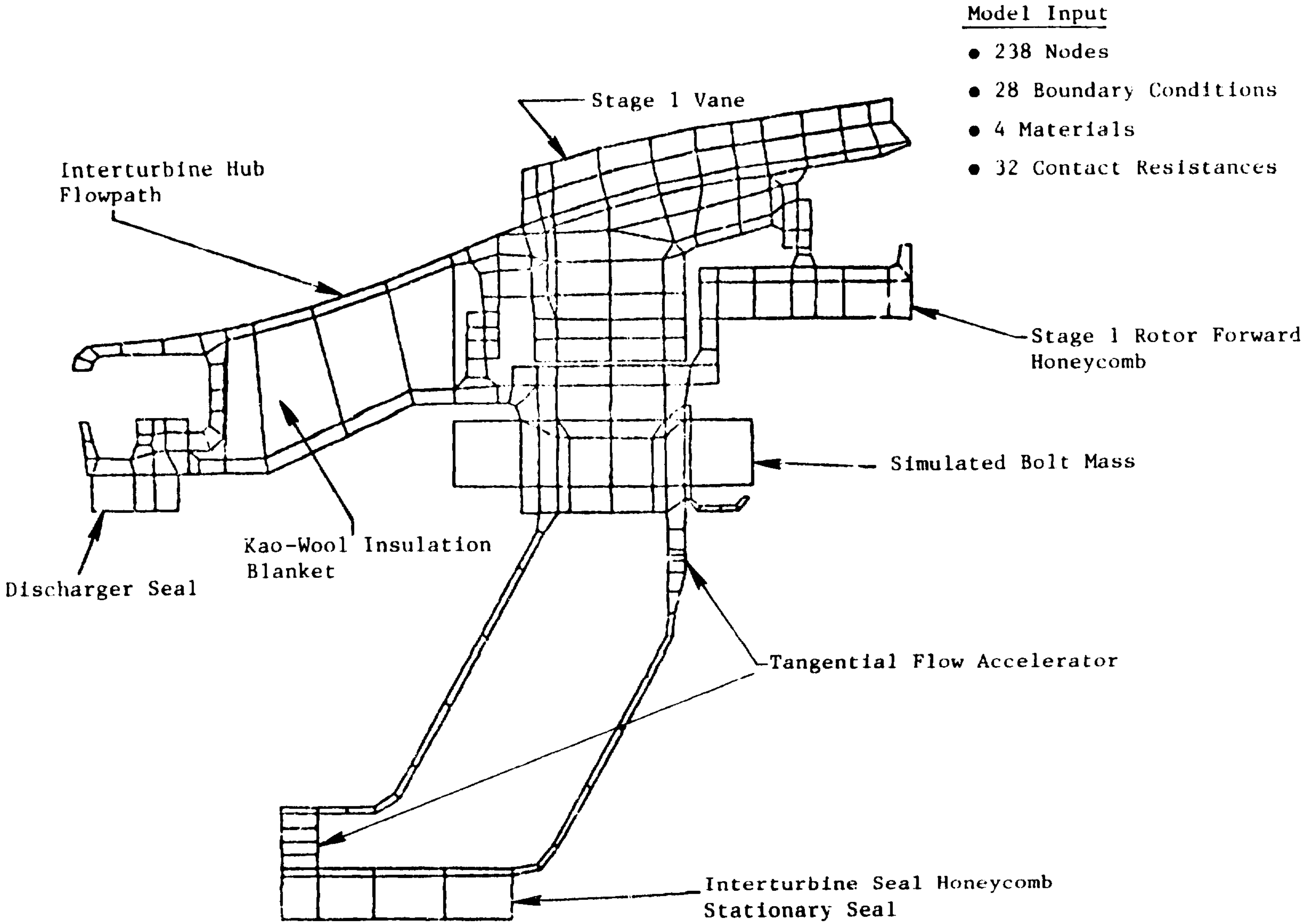

Figure 43. Stage 1 Nozzle Hub Structure Detailed Thermal Transient Model.

ORIGINAL PAGE IS
OF POOR QUALITY

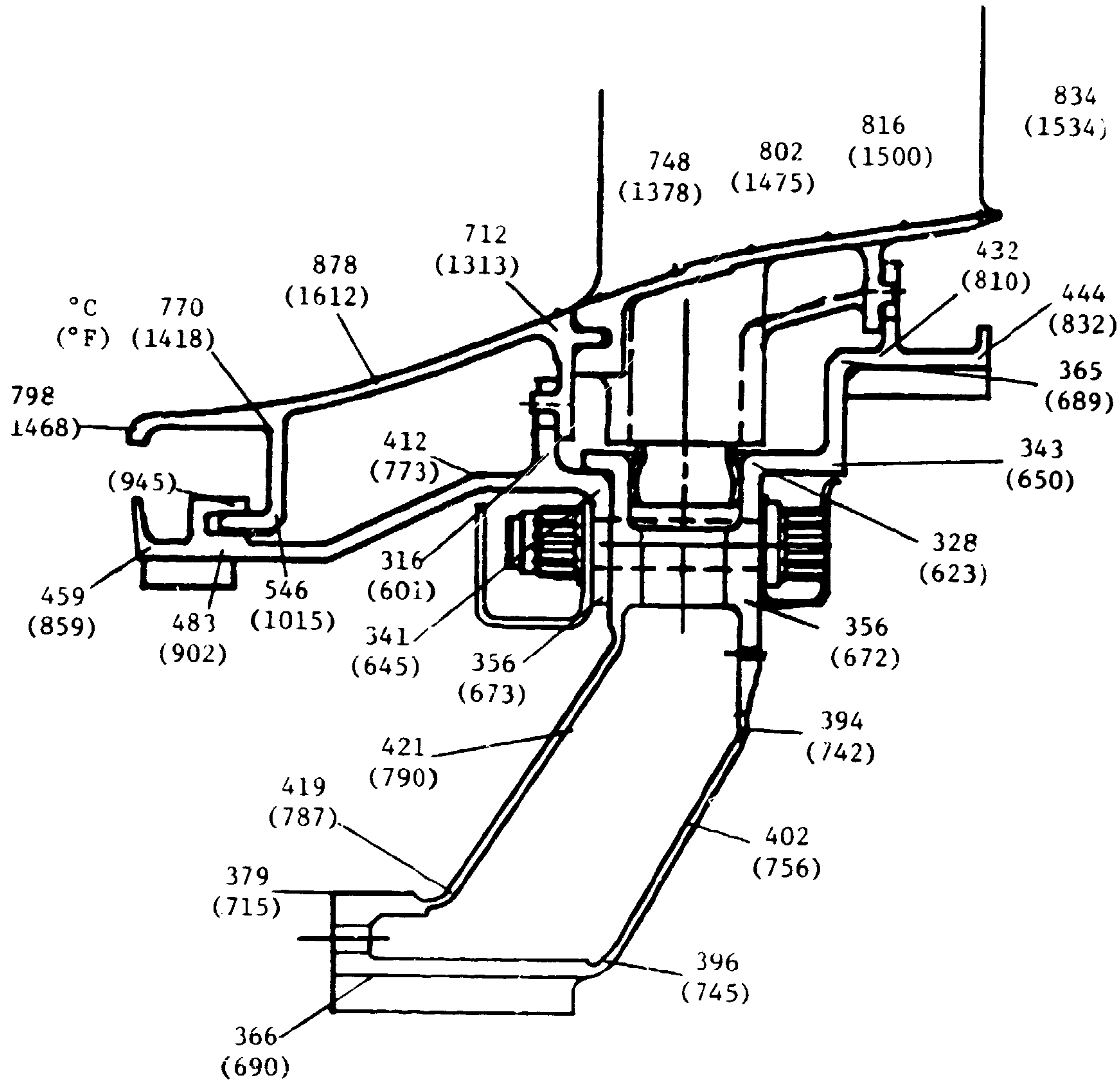

Figure 44. LPT Stage 1 Vane Inner Seal Temperatures at 30 Seconds into HDTO.

set at engine assembly, they cannot be kept to a minimum at all engine operating conditions without an independant means of control. Various factors contribute to increased blade tip clearance, thereby reducing component/engine performance. In the LPT, the items that contribute to tip clearance deterioration are:

1. Transient Thermal/Mechanical Growth - Mechanical growth of the rotor structure and mechanical-plus-thermal growth of the airfoils occur within 10 to 20 seconds after start of a typical accel from ground idle to maximum-power takeoff. Thermal growth of the casing is significantly slower. Such growth will cause the blade tip clearance to transiently close, possibly causing a tip rub. In the LPT the stationary shrouds are constructed of metal honeycomb which can be rubbed out very easily by the blade tip-seal teeth. However, as the casing heats up, it moves rapidly out and away from the rotor and leaves a gap between the stationary shroud and the blade seal teeth.

2. Engine Bending - Engine bending occurs because thrust reaction must be carried out of the engine to the airframe through the engine mounts. Thrust at sea level static, maximum-power takeoff is six times higher than cruise thrust. The high takeoff thrust reaction causes the casing to distort and go out of round. Sections of the stationary shrouds will rub while other sections will have larger than normal clearance and will not rub. When the thrust loads are reduced, the casing returns to a normal, round configuation. The sections of the shrouds that were subjected to a rub now have a larger clearance between the honeycomb seal and the blade seal teeth. Flight maneuver loads can also cause a rub. Because of the mass and inertia of the rotor, a rub can occur when a sudden flight maneuver is transmitted to the rotor through the roller and thrust bearings. There will be bending in the rotor structure between bearings; this will result in a rub between the blades and stationary shrouds. The magnitude and location of the rub will depend on the severity and direction of the maneuver. Once the rub has occurred and the flight maneuver ceases, the rotor will return to the normal position relative to the casing, and locally the clearances will be larger. Larger clearances will also be available during takeoff and climb, when the maximum distortions are expected.

3. Rotor and Stator Vibrations - The rotor will be subjected to various levels of vibration depending on the natural frequencies and excitations that might exist in the engine. The vibration will increase when the frequency of the stimulus approaches the natural frequency of the rotor or a component in the rotor structure. Similarly, the casing or stationary components also can vibrate and can enhance the possibility of a blade rub.

If the performance of an engine is to be improved by reducing the LPT blade tip clearance, the above-mentioned distortions must be reduced, or the configuration must be designed to accommodate them. Both methods of improvement are being incorporated in the E^3. Distortions are being reduced by evaluating better methods of transmitting engine loads. Vibrations are being kept to a minimum through the judicious location of the bearings designed to transmit loads with a minimum of structural distortion. At cruise, once the distortion loads and vibration have diminished, the clearances are closed down by the ACC system.

ACC in the E^3 LPT is accomplished by shrinking the casing that supports the stationary seals. During steady-state cruise conditions, the casing skrinkage is accomplished by cooling the metal - taking advantage of the high coefficient of thermal expansion of Inco 718. By cooling the casing 167°C (300° F) it is quite possible to reduce the casing diameter by 0.304 cm (120 mils). This temperature reduction will reduce the clearance by 0.152 cm (60 mils) and is more than adequate to accomplish the objective of active clearance control. The casing-cooling system relies heavily on experience with the CF6-50 LPT casing impingement-cooling system. In this system the low-pressure, low-temperature fan air is used as coolant and is impinged on the outside of the LPT casing by means of an array of manifolds. In the E^3 system, fan air is extracted from the fan duct by means of a scoop. The air is routed to the impingement manifold through a control valve and 270° core-cowl manifold. Clearance control is accomplished by adjustment of the impingement cooling flow by means of an air valve. By judiciously setting the valve, by means of the engine control system, the quantity of impingement-cooling flow to the LPT casing can be controlled. The controlled flow rate, in turn, controls the amount of casing temperature reduction; this defines the casing shrinkage and thus blade-tip clearance. As the control-valve flow area is increased, reducing the flow restrictions, more air will flow from the fan stream to the impingement manifold, cooling the casing to a lower temperature. As the casing temperature is reduced, the diameter shrinks, and the blade tip clearance becomes smaller.

The ACC valve in the FPS will be controlled by the full-authority, digital electronic control (FADEC). Fan speed, fuel flow, and compressor exit temperature and pressure will be the FADEC input used to control the LPT ACC system. The FADEC will define the best clearances for a particular flight condition. The thermal history of the rotor and casing will be factored into the control so that the required cooling for the casing can be defined. The valve setting required to achieve the desired cooling flow will then be met.

The ACC fan scoop (Figure 45) is a split design combining the HPT and LPT ACC air supplies. This design was chosen over the separate-scoop design as a means of keeping the amount of fan-duct blockage and scoop drag to a minimum. The fan-duct scoop is split down the middle into the HPT and LPT sections by a sheet metal divider. This divider segregates the HPT and LPT cooling air from the inlet of the scoop unit after impingement. Separate valves are provided to control the amount of cooling air delivered to the HPT and the LPT.

The scoop is mounted away from the wall to avoid ingestion of the boundary layer flow. After the air enters the scoop it is diffused in an effort to recover as much of the fan-duct dynamic pressure as possible. After the air

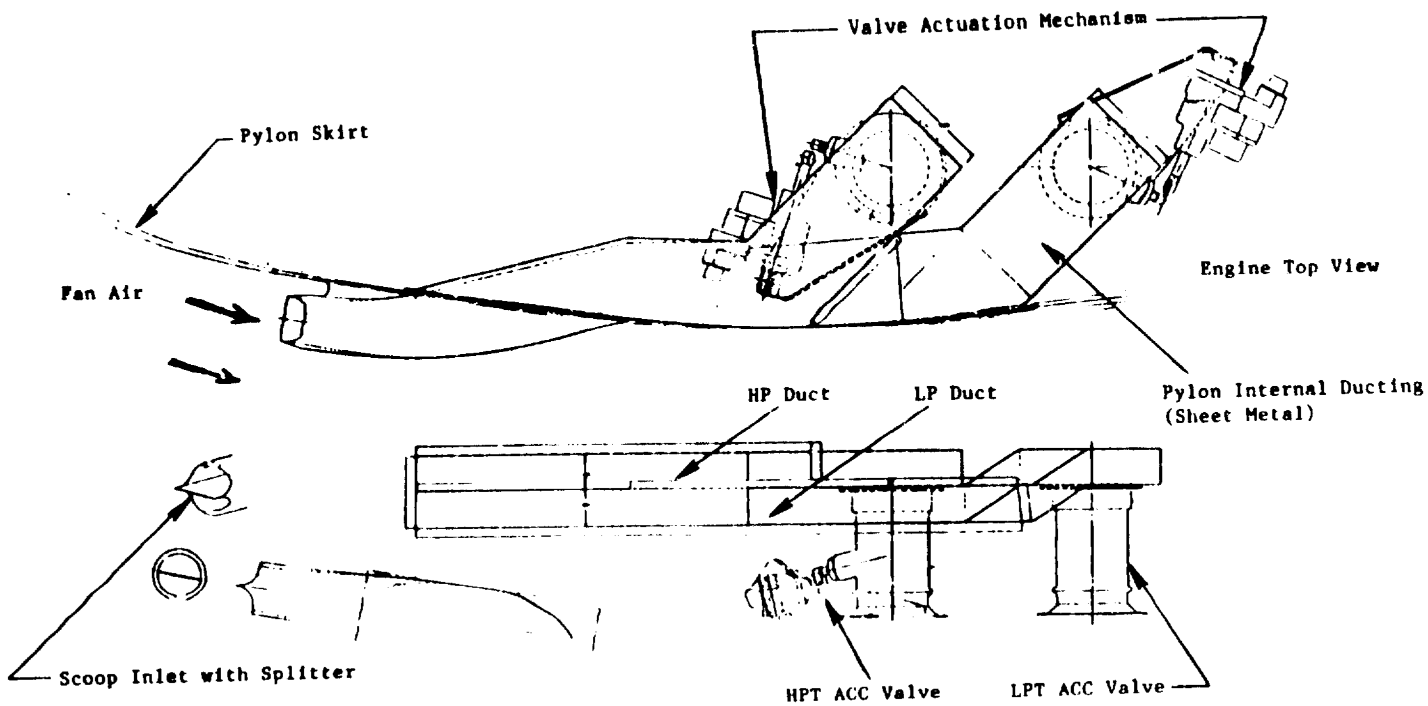

Figure 45. E^3 HPT/LPT Turbine Active Clearance Control Fan Duct Scoop.

diffuses to a 2:1 area ratio, it dumps into a rectangular duct that directs the air to the control valve (Figure 46). After flowing through the valve the air dumps into a 270° sector manifold inside the core engine cowl. The flow splits and flows circumferentially around the LPT in the rectangular duct. The flow divides and flows circumferentially around the LPT in the rectangular duct. The flow is bled off the rectangular core-cowl plenum at four locations (two on each side of the engine) and into the LPT casing impingement manifold. After the air impinges on the casing, it discharges through the rear frame and out the primary-nozzle center vent. A bulkhead is required to segregate the core-cowl purge air from both the HPT and the LPT ACC air. This is located ahead of the HPT casing and extends from the casing to the core cowl. An extensive effort has been made to seal all possible leaks into the core cowl in order to maintain the performance of the ACC cooling system.

To evaluate the ACC, it was first necessary to look at the required casing cooling at various engine cycle conditions. Shown in Figure 47 are several engine cycle conditions that were evaluated. At ground idle, the casing cooling will be reduced to a minimum value. This will allow the casing to be at a higher temperature during takeoff transients but still keep it within the material limiting temperature of 677° C (1250° F). Maximum rotational loads occur after the engine has undergone acceleration to full takeoff power and after liftoff has occurred; then casing cooling can be initiated. The ACC will open the valve and admit 0.15% W_{25} of fan airflow to the impingement manifold where it cools the casing and closes the clearances to the required range. Since the rotor rpm and blade metal temperatures are at the highest level, very little clearance closure is required. As the engine is throttled back to maximum-climb power, the metal temperatures drop. When this occurs, more casing clearance closure, and thus more cooling, is required. At maximum cruise, 66% of the maximum clearance closure is required; at 60% maximum cruise, all of the ACC cooling is required. Of course, there are few cycle points in the engine mission below 60% maximum cruise where the ACC will be needed. During approach and flight idle the ACC cooling will be shut off in anticipation of a throttle burst to a higher power setting.

The performance payoff of the ACC system was defined at the LPT design point: maximum-climb power at an altitude of 10.67 km (35,000 ft). The clearances with minimum casing cooling ranged between 0.112 cm (44 mils) on the last stage to 0.022 cm (48 mils) on the first three stages. Since these clearances can be reduced to 0.041 cm (16 mils) at this power setting, the potential clearance reduction is between 0.07 cm (28 mils) on the last stage to 0.08 cm (32 mils) on the first three stages, as shown in Figure 48. This can be accomplished with the use of about two-thirds of the cooling capability of the system. The performance payoff for each stage was evaluated, and the overall LPT efficiency increase was 0.5%. When the cost of the fan air is factored in, the net payoff is a 0.33% reduction in specific fuel consumption (sfc). It should be noted that this improvement in performance is not only due to the reduction in blade tip clearance but also to the hub interstage seal clearances. In cooling the casing, the nozzle diaphragm moved radially inward and closed down the interstage seal clearances as well. The interstage seal clearances represent about one-third of the overall system payoff.

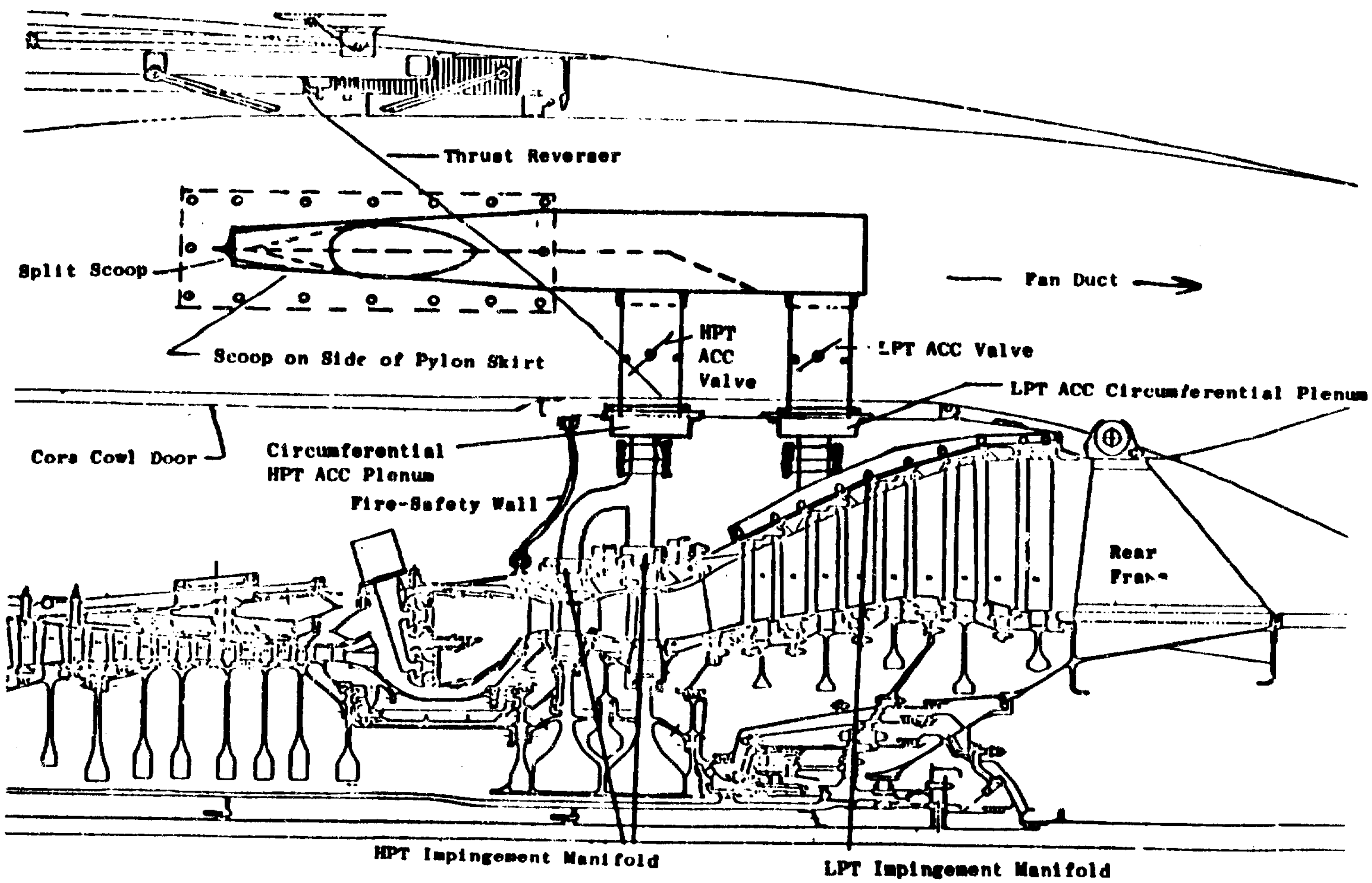

Figure 46. E^3 HPT/LPT Active Clearance Control Design Features.

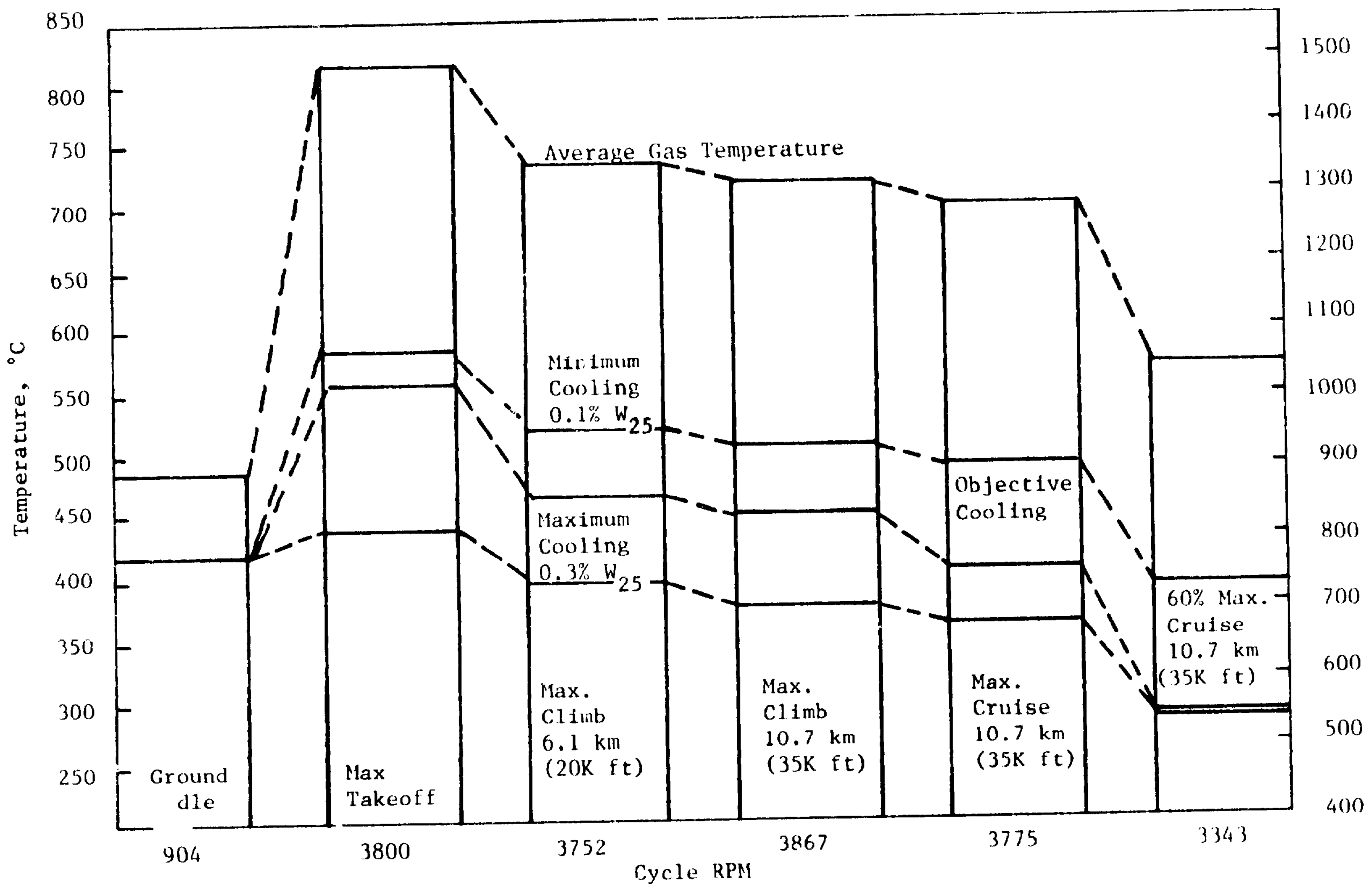

Figure 47. E^3 LPT Active Clearance Control Casing Cooling Objective.

STAGE	1	2	3	4	5	
$\Delta\eta_T$/10 MILS	.033	.043	.038	.030	.016	
CLOSURE MILS	.032	[illegible]	.032	.030	.028	
$\Delta\eta_T$/STAGE	.105	.130	.121	.090	.045	$\rightarrow$ .5% $\Delta\eta_T$ - TOTAL

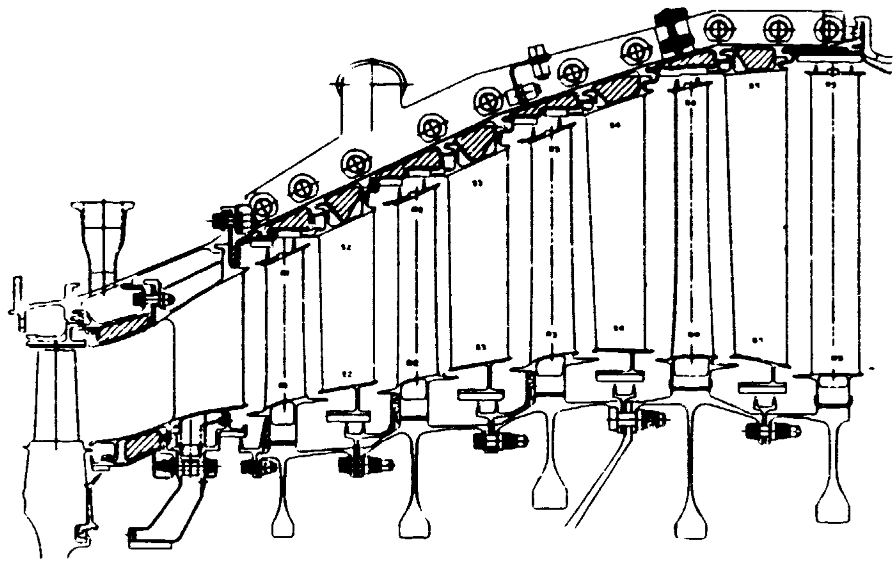

SYSTEM PAYOFF

	CLEARANCE REDUCTION	FAN AIR COST	TOTAL PAYOFF
ΔSFC	-.35%	+.02%	= -.33% ΔSFC

Max. Cruise 10.67 km (35 K Ft.)

Figure 48. E^3 Low Pressure Turbine Active Clearance Control Payoff Potential

3.10 START ANALYSIS

In the development of the E^3, the compressor has continued to be a critical item. The 23:1 pressure ratio, single-spool compressor is truly an advancement in the state of the art for axial-flow compressors. However, the high pressure ratio of the compressor necessitated several features The variable stators in the first five stages had to have more control during start-up and low-power conditions. The compressor also was designed to provide stall margin in the front stages during starting conditions. Without bleed, the aft end of the compressor cannot pass the flow that the front stages are delivering. The compressor bleed is extracted at the seventh stage where it has the greatest payoff in terms of flow stability during start. The seventh-stage bleed air is dumped overboard.

During the early E^3 program start analysis, the required bleed flow was defined at a maximum of 30% of the compressor inlet flow. This flow required the turbine inlet temperature to be set at 1149° C (2100° F) if the engine was to be started and accelerated to idle speed within the designated start time. Several assumptions had to be made in conducting the early start analysis. These assumptions addressed

- Compressor efficiency at subidle
- Turbine efficiency at subidle
- Compressor stall margin at subidle

All these factors have a significant impact on the required turbine inlet temperature and on compressor-bleed requirements.

During 1980-1981, both the 2-stage HP air turbine test and the 10-stage compressor test were completed. The results from these two tests had a significant impact on the engine start analysis. The factors that affected the engine start analysis are:

- Ten-point compressor efficiency improvement during start
- Five-point HPT efficiency improvement during start
- Stall margin achieved with reduced seventh-stage bleed
- HPT flow function decrease during start

These improvements during start conditions allow the engine to be accelerated to idle speed within the required time at a reduced turbine inlet temperature. The HPT inlet temperature reduction amounts to a 200° C (360° F) drop to 949° C (1740° F). The LPT inlet temperature reduction amounts to a more impressive 289° C (520° F) drop to 627° C (1160° F). This was attributable to the improvement in turbine efficiency and a reduction in the turbine flow function.

With the substantial reduction in cycle average temperature entering both the HPT and the LPT, the engine could be started and accelerated to idle speed with only the pilot combustor burning. This causes a substantial outward skewing of the combustor exit profile. The maximum (peak) pattern factor at the HPT vane inlet is 1.26, and the circumferential-average pattern factor is 0.63. Although this results in local gas-stream temperatures above the maximum design value, the steady-state metal temperature does not become excessive. This is due to the reduced cooling-air temperature and the heat-flux environment (low pressure) during engine start conditions. By the time the hot streak has reached the LPT, the temperature has attenuated by mixing and work extraction; the maximum peak pattern factor at the LPT is down to 0.27, and the circumferential pattern factor is down to 0.21. The attenuation factors for the double-annular combustor, burning on the pilot stage only, were defined in the CF6-50 double-annular combustor program. After the 49° C (88° F) $T_{4.9}$ design margin is added to the 627° C (1160° F) $T_{4.9}$ cycle temperature, the peak pattern factor yields a hot-streak temperature of 801° C (1474° F). This is the highest temperature that the LPT Stage 1 vane will be exposed to during start. Because the trailing edge (TE) of this vane is uncooled, a temperature gradient is set up between the bulk metal and the TE. The maximum temperature gradient on the vane will not exceed 779° C (138° F) under steady-state conditions. The maximum transient temperature gradient has been estimated to be 203° C (365° F). This is within acceptable limits.

With an average circumferential pattern factor of 0.21, the LPT vane inlet yields a 777° C (1431° F) temperature. This is the highest temperature that the first-stage blade might be exposed to during engine start. There is no cooling in the blade, so the only temperature gradients are set up during the transient. The highest gradient between the TE and the bulk metal temperature during the start transient is 172° C (310° F) and occurs 40 seconds after start. Beause the LPT rotor spool is at a very low speed at this point, no significant mechanical-load stresses occur. Therefore, the combined thermal and mechanical stresses are not excessive.

A review of component life, based on updated start temperatures and thermal gradients, showed that full-life goals can be expected. The start-transient thermal gradients in the LPT vanes are less severe than the steady-state, hot-day-takeoff gradients in the highly cooled HPT Stage 1 vane and occur at a substantially lower temperature. The blade transient metal temperature gradients have been found to be less severe than an earlier analysis indicated. In the early analysis, which was based on the original dynamic start model, the full blade life for the required flight missions was achieved. Only a small percentage of the blade life was used up during the start cycle. These factors lead to the conclusion that the LPT life objectives can be achieved with the current start cycle.

The effects of engine starting on HPT and LPT temperatures will be monitored closely during the E^3 program. As information is obtained from tests of the compressor, the HPT/LPT air turbines, and the core engine, it will be factored into the engine-start dynamic model to assure the reliability of both the ICLS and the FPS.

4.0 MECHANICAL DESIGN

4.1 OVERALL DESIGN APPROACH

4.1.1 Description

The LPT to be used in the ICLS test is a moderately loaded, close-coupled, five-stage turbine with uncooled airfoils. Mechanical features are shown in the Figure 49 cross section.

The LPT casing is a continuous, no-split-flange design with wall insulation and local impingement cooling for improved clearance control. The Stage 1 nozzle is a conventionally cast, four-vane segment attached by a hooked tang at the outer flowpath. Stages 2 through 5 nozzle vanes are cast, multivane segments attached by hook tangs to the outer-case supports. Outer honeycomb seals are brazed to sheet metal backing strips that hook into the outer casing and assist in the radial retention of the Stages 2 through 5 nozzles. The inner diameters of these vanes have integral seals which consist of honeycomb brazed to the cast vane seal support. A full-ring inner seal is bolted to the Stage 1 vane and consists of three sections of honeycomb brazed to a sheet metal structure.

Material selections for the LPT static parts are shown in Figure 50 and listed in Table V.

Table V. LPT Materials.

Component	ICLS	FPS
Stator		
Vane 1	René 77	René 125
Vanes 2-5	René 77	René 77
Casing	Inco 718	Inco 718
Manifold	321 SS	321 SS
Seals	Hastelloy X	Hastelloy X
Bolts	Inco 718	Inco 718
Nuts	Waspaloy	Waspaloy
Rotor		
Blades 1-5	René 77	René 77
Disks 1-5	Inco 718	Inco 718
Blade Retainers	Inco 718	Inco 718
Bolts	Inco 718	Inco 718
Nuts	Waspaloy	Waspaloy

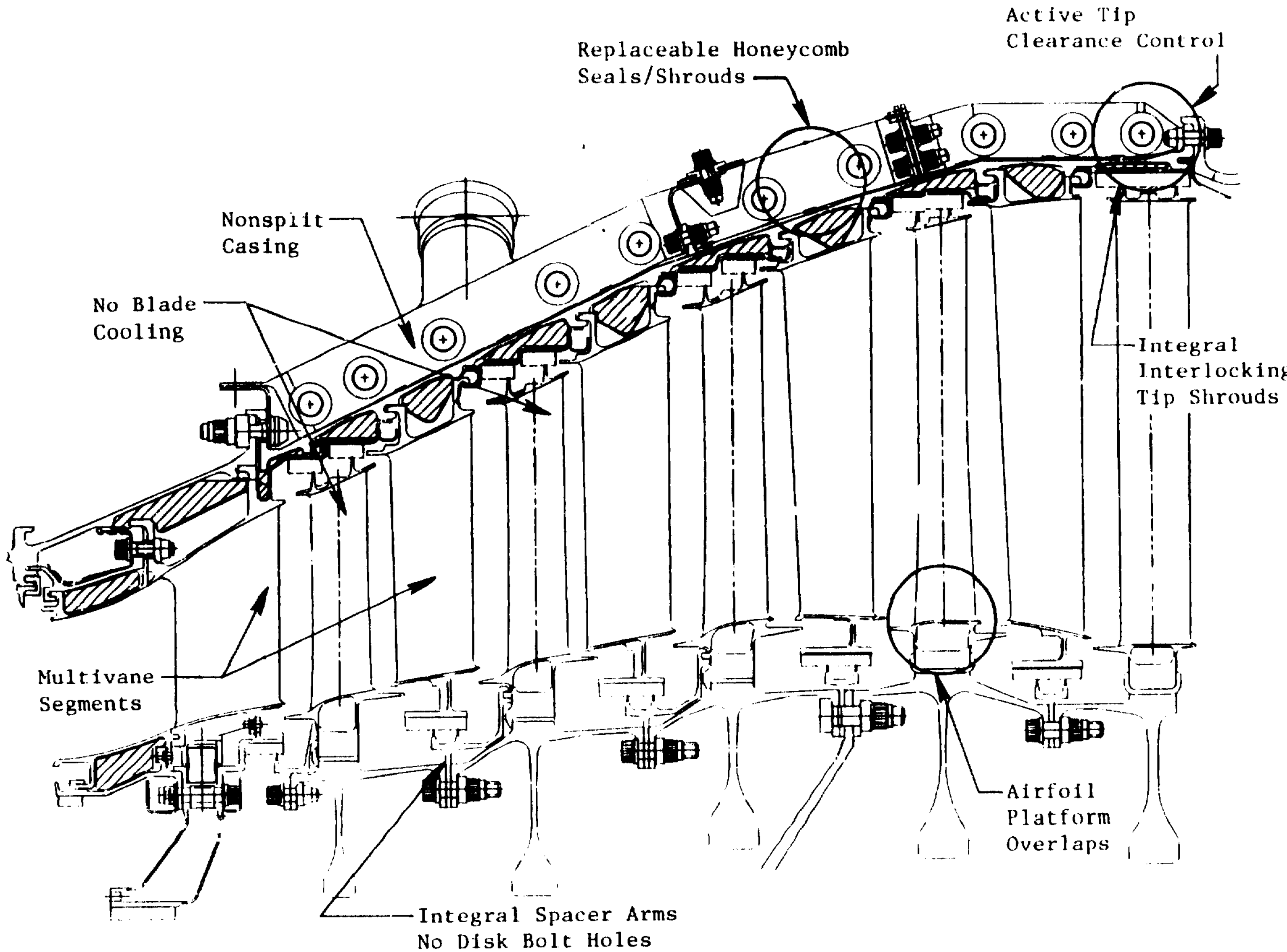

Figure 49. E^3 LP Five-Stage Turbine Features.

The LPT rotor is an uncooled design comprising disks with integral spacer arms and bolted joints between each stage. The main support cone extends from the sump between the HPT and LPT rotors and attaches at the LPT spool between the Stage 3 and Stage 4 disks. LPT blading is a proven, cast design with tip shrouds and multitang dovetails. Inner stage seals of the LPT spool are repairable, two-tooth designs and are attached at the bolted flange joints between the disk spacer connections. They provide good performance (low leakage) and easy replacement. The rotor materials are shown in Figure 50 and listed in Table V.

Overall, the selected LPT configuration is a balanced design with a strong emphasis on high efficiency and performance while retaining good maintenance features and low cost.

4.1.2 Design Loads and Limits

The LPT is designed to meet the mechanical loads and limits that are defined in the E^3 technical requirements and according to GE design practices. Basic engine cycle performance parameters defining the aerodynamic design point and the maximum rotor speeds are given in Table VI. The ICLS engine hardware is designed to meet two levels of requirements. The blades are designed for FPS conditions, and the rotor spool and support structures are designed for growth conditions. Basic aerodynamic design parameters for Stages 1 and 5 rotors are shown in Table VII and indicate the range between LPT inlet and exit characteristics.

Design limit stresses are set by the -3σ material properties. For high-cycle fatigue (HCF) life evaluation, a Goodman diagram is used to predict the maximum allowable vibratory stress where infinite life can be achieved. Low-cycle fatigue (LCF) stress levels are based on limits as set by parts usage on 36,000 aircraft missions with two stress cycles per mission for rotor parts. This results in requirements of 72,000 stress cycles for rotor parts and 36,000 stress cycles for all other components. In addition, the disks must be designed to provide a residual life of 6,000 cycles when the disk has a defect of the size: 0.025 x 0.076 cm (0.01 x 0.03 in.).

Acoustic considerations imposed separate requirements on the Stage 4 rotor where a 1.4-chord, axial, blade-to-vane gap and a rotor with 156 blades were needed.

The typical mission with the major time-lapse increments denoted is shown in Figure 51.

4.1.3 Design Goals

The LPT mechanical configuration is based on meeting the overall engine requirements of sfc and DOC within the following goals:

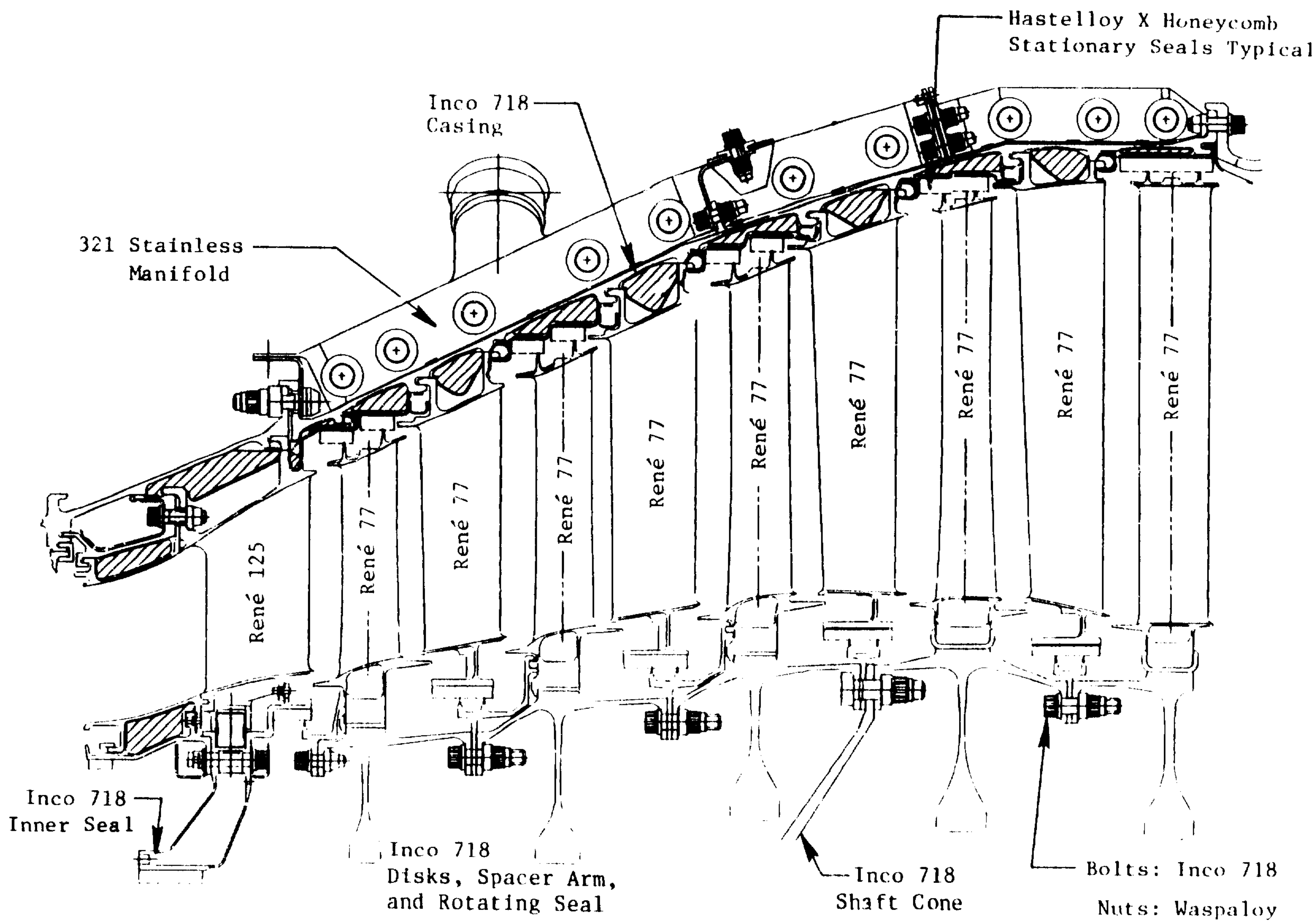

Figure 50. LPT Materials for FPS Major Components.

ORIGINAL PAGE IS
OF POOR QUALITY

Table VI. LPT Design Cycle Performance Parameters.

	FPS	Growth
I. Flowpath and Clearance Calculation		
Cycle Case No. 41		
Altitude	10,668 m (35,000 ft)	10,668 m (35,000 ft)
Mach No.	0.80	0.80
ΔT_{amb}	+10° C (+18° F)	+10° C (+18° F)
Rating	Max. Climb	Max. Climb
Fan Physical Speed	3539 rpm	3939 rpm
II. Maximum Stress Calculations		
Cycle Case No. 72		
Altitude	5791 m (19,000 ft)	5791 m (19,000 ft)
Mach No.	0.30	0.30
ΔT_{amb}	+35° C (+63° F)	+35° C (+63° F)
Rating	Takeoff	Takeoff
Rotor Physical Speed	3611 rpm	4079 rpm
(at 2.6% Overspeed)	(3707 rpm)	(4160 rpm)
Cycle Case No. 27		
Altitude	Sea Level Static	Sea Level Static
Mach No.	0.30	0.30
ΔT_{amb}	+35° C (+63° F)	+35° C (+63° F)
Rating	Takeoff	Takeoff
Rotor Physical Speed	3289 rpm	3679 rpm
(at 2.6% Overspeed)	(3376 rpm)	(3777 rpm)

Table VII. LPT Design FPS Aerodynamic Parameters, Design Point.

Parameter	Stage 1 Rotor	Stage 5 Rotor
Tip Diameter	89.1 cm (35.1 in.)	118.3 cm (46.56 in.)
Tip Speed	168.6 m/sec (553 ft/sec)	23.7 m/sec (734 ft/sec)
Airflow	67.8 kg/sec (149.5 lb/sec)	67.o kg/sec (149.5 lb/sec)
Inlet Radius Ratio	0.76	0.64
Aspect Ratio	3.54	5.72
P_T/P_T	1.30	1.26
Numbers of Blades	122	110

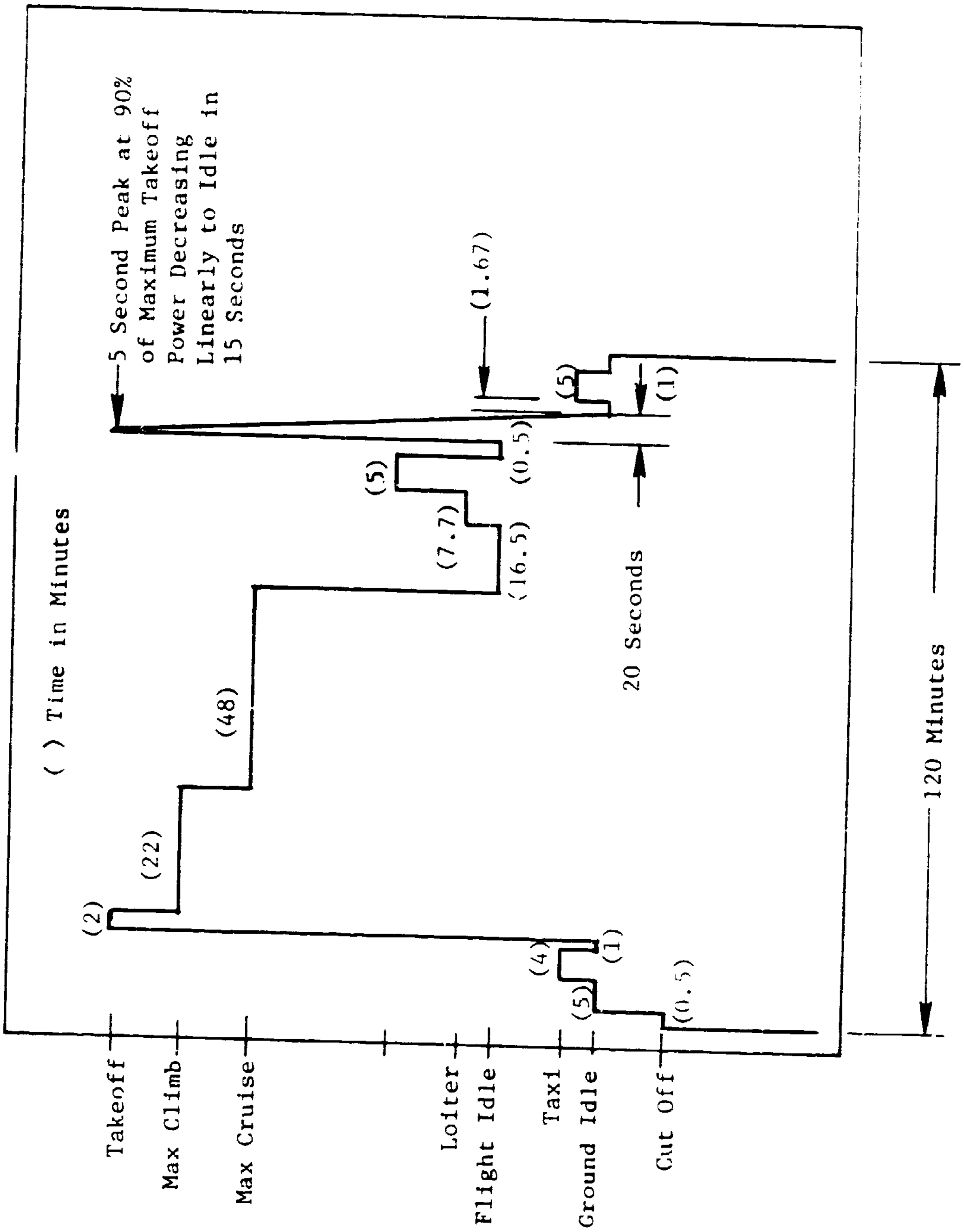

Figure 51. Typical Flight Cycle.

1. Performance

- Provide a loading parameter of 1.29 at a physical speed of 3457 rpm at a fully developed efficiency of 91.7% at the Mach 0.8/10.7 km (35,000 ft) cruise match point.

2. Life

- 18,000 hours/18,000 flight cycles for cold (nonflowpath) parts
- 9,000 hours/9,000 flight cycles for hot (flowpath) parts
- Minimize potentially damaging airfoil vibrations
- Rotor structures unaffected by blade-out-induced vibrations
- Rotor structure designed to 122% of maximum-rated growth physical speed

3. Reliability

- Elimination of bolt holes in live disk
- Proven blade design

4. Turbine Development

- Develop the aerodynamic efficiencies of the blading by a systematic building-block-approach, air-turbine test program.
- Design the rotor and blading systems to achieve cost, aerodynamic, and aeromechanical requirements as well as initial reliability equal to or better than current high-bypass turbofans.

4.2 Rotor

4.2.1 Blade Design

The Block IIB air turbine blade features shown in Figure 52 reflect successful commercial engine experience. All five stages of the blades are solid and uncooled and have two-tang dovetails. The tip shrouds are cast integrally with the airfoils and have two-tooth seals to prevent leakage past the blade.

The blade airfoils were designed (quantity, chord, shape, size) initially to meet aerodynamic requirements and then modified (quantity or shape) as needed to meet additional mechanical-stress or frequency requirements. Figure 52 shows the major airfoil geometry features. The blade airfoils range in length from 10.90 cm (4.29 in.) on Stage 1 to 22.58 cm (8.89 in.) on Stage 5.

ORIGINAL PAGE IS
OF POOR QUALITY

	Number of Blades	C_H, Root Chord, cm (in.)	Tip Chord, cm (in.)	L, Blade Length, cm (in.)	Aspect Ratio
Stage 1	120	3.05 (1.20)	3.10 (1.22)	10.90 (4.29)	3.54
Stage 2	122	3.05 (1.20)	3.18 (1.25)	13.74 (5.41)	4.39
Stage 3	122	3.30 (1.30)	3.51 (1.38)	16.66 (6.56)	4.99
Stage 4	156	3.07 (1.21)	2.90 (1.14)	20.22 (7.96)	7.47
Stage 5	110	3.66 (1.44)	4.22 (1.66)	22.58 (8.89)	5.72

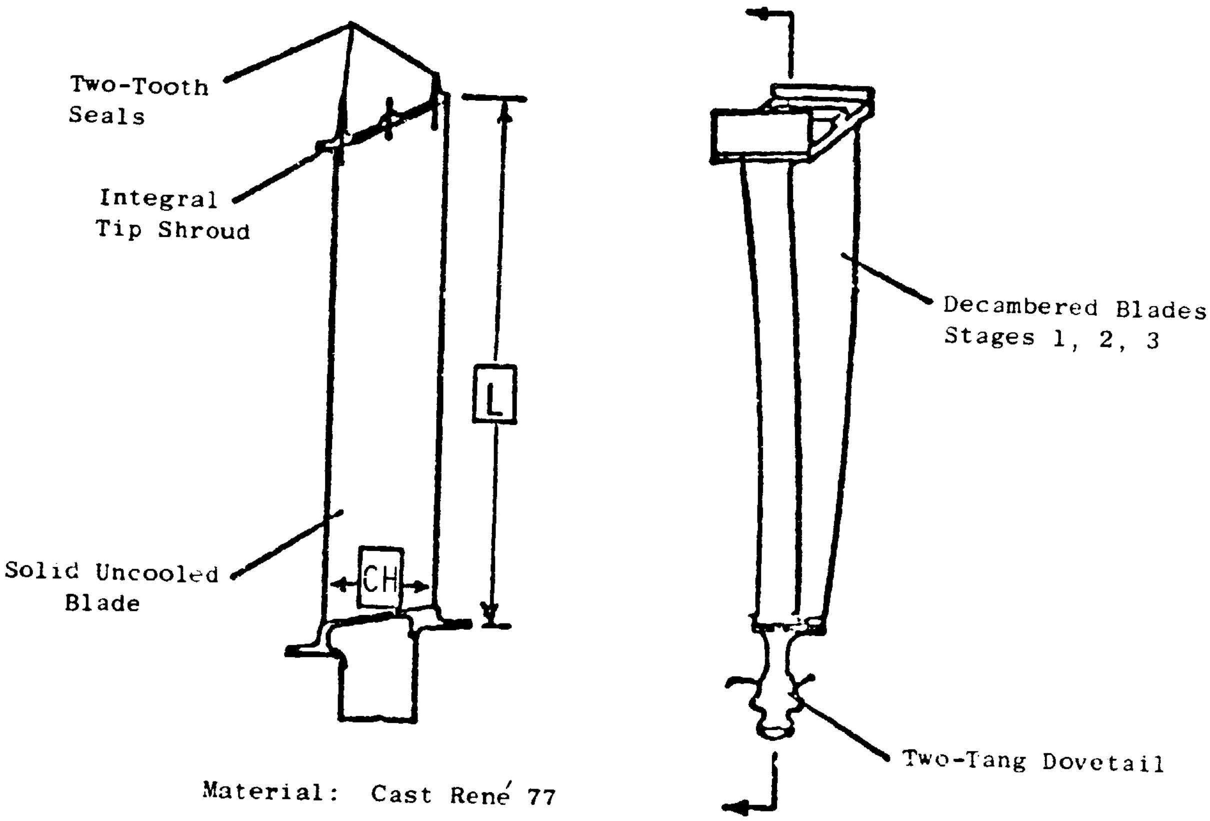

Figure 52. LPT Blade Features of Stages 1 Through 5.

The aspect ratios range from 3.54 on Stage 1 to 7.47 on Stage 4. The large aspect ratio on Stage 4 is due to the aerodynamic "flask" design of the airfoil. The chord dimension decreases from the root to the pitch and then increases from the pitch to the tip. The smaller chord at midspan produces a larger aspect ratio. Also, there are more blades in Stage 4 than in any other stage. The larger number of blades (156) was selected to improve acoustic emissions by increasing blade-passing frequency and by providing a larger nozzle-to-blade gap due to the shorter blade chord.

Additional typical airfoil geometry features are shown in Figure 53. Leading-edge and trailing-edge diameters are shown for the root, pitch, and tip sections. They range from 0.079 cm (0.031 in.) on Stage 1 to 0.048 cm (0.019 in.) on Stage 4. In addition, area and maximum thickness are plotted versus percent span. In all stages, the maximum thickness and area through the blade shank are larger than those through the airfoil in order to provide added strength adjacent to the dovetail attachment. An angled platform (5° from axial) was used on the Stage 4 blade to provide an adequate platform for the highly staggered airfoil shape (Figure 54).

Each blade airfoil was analyzed for combined spanwise stresses. Figure 55 shows these stresses for significant Stage 1 airfoil locations. The airfoil was tilted tangentially to balance the leading-edge and maximum-convex stresses. Axial and tangential offsets were provided at the blade root to reduce the peak stresses in the dovetail. A summary of airfoil stresses is presented in Table VIII.

Blade airfoil rupture life was calculated by using a mission-mix analysis. Seven operating points were chosen to represent the full range of engine/aircraft mission points (Table IX). The resulting rupture lives and HCF allowable stresses for the airfoils are shown in Figures 56 through 60. The minimum allowable vibratory stress value is based on GE engine experience. All blades were found to have adequate rupture lives and HCF vibratory capabilities.

LCF lives were calculated at maximum hot-day takeoff stresses. For each mission, it was conservatively assumed that there were two LCF cycles: one for takeoff and one for thrust reverse. Therefore, 36,000 cycles would result from 18,000 missions. All blades were found to have LCF life in excess of 100,000 cycles, versus 36,000 cycles required, as shown in Table X.

Vibration analyses were performed to ensure that there were no resonances of blade natural frequencies with major engine stimulation forces in the steady-state operating range. Typical mode shapes investigated were first flex, first torsion, first axial, and two-stripe (Figure 61).

Results of the resonance study for the Stage 1 blade are shown in Figure 62. The only cross points (intersections of forcing functions with blade natural frequencies) near the steady-state operating range are for the second torsional mode with both the Stage 1 vane line (72/rev) and the Stage 2 vane line (102/rev). (There are no known problems in the second torsional mode for previous engine designs; therefore, no problems are expected with this blade.)

ORIGINAL PAGE IS OF POOR QUALITY

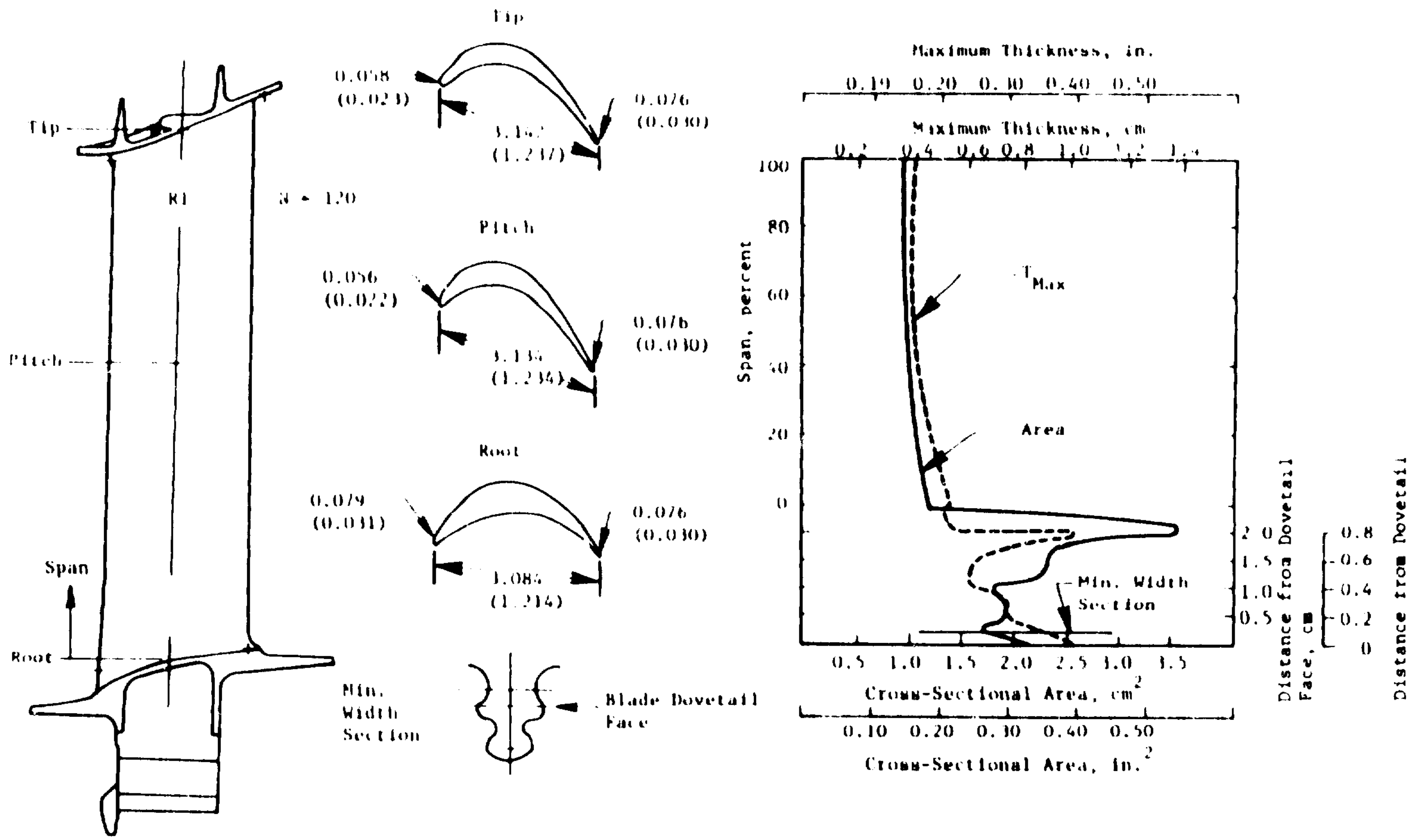

Figure 53. Stage 1 Blade Airfoil Configuration.

C-2

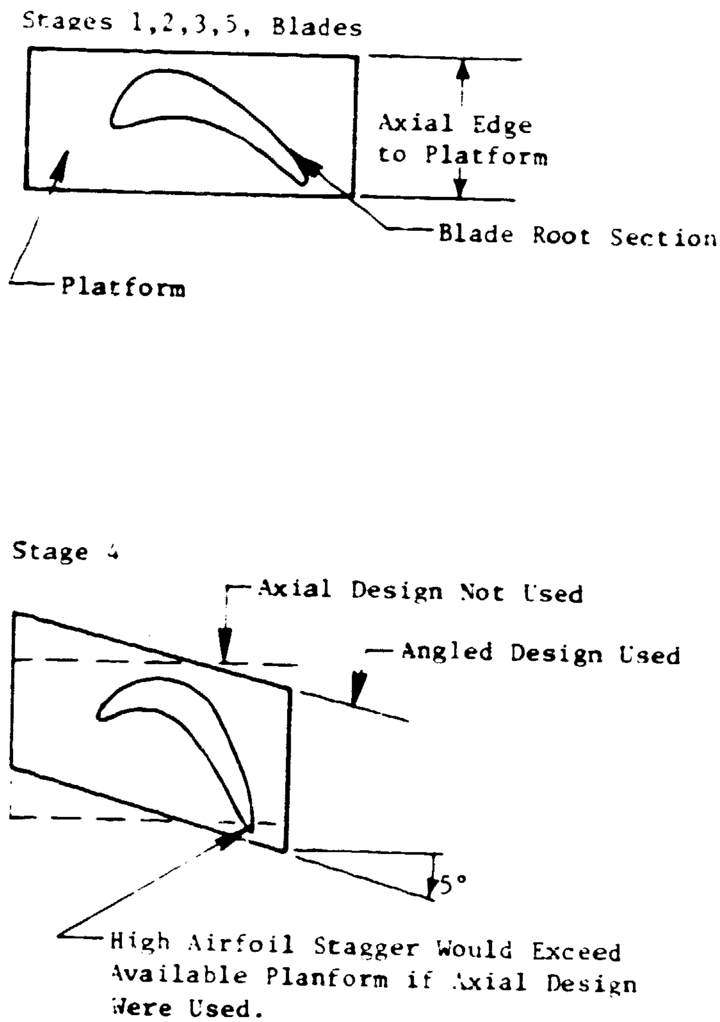

Figure 54. Blade Platform Planform Selection.

ORIGINAL PAGE IS
OF POOR QUALITY

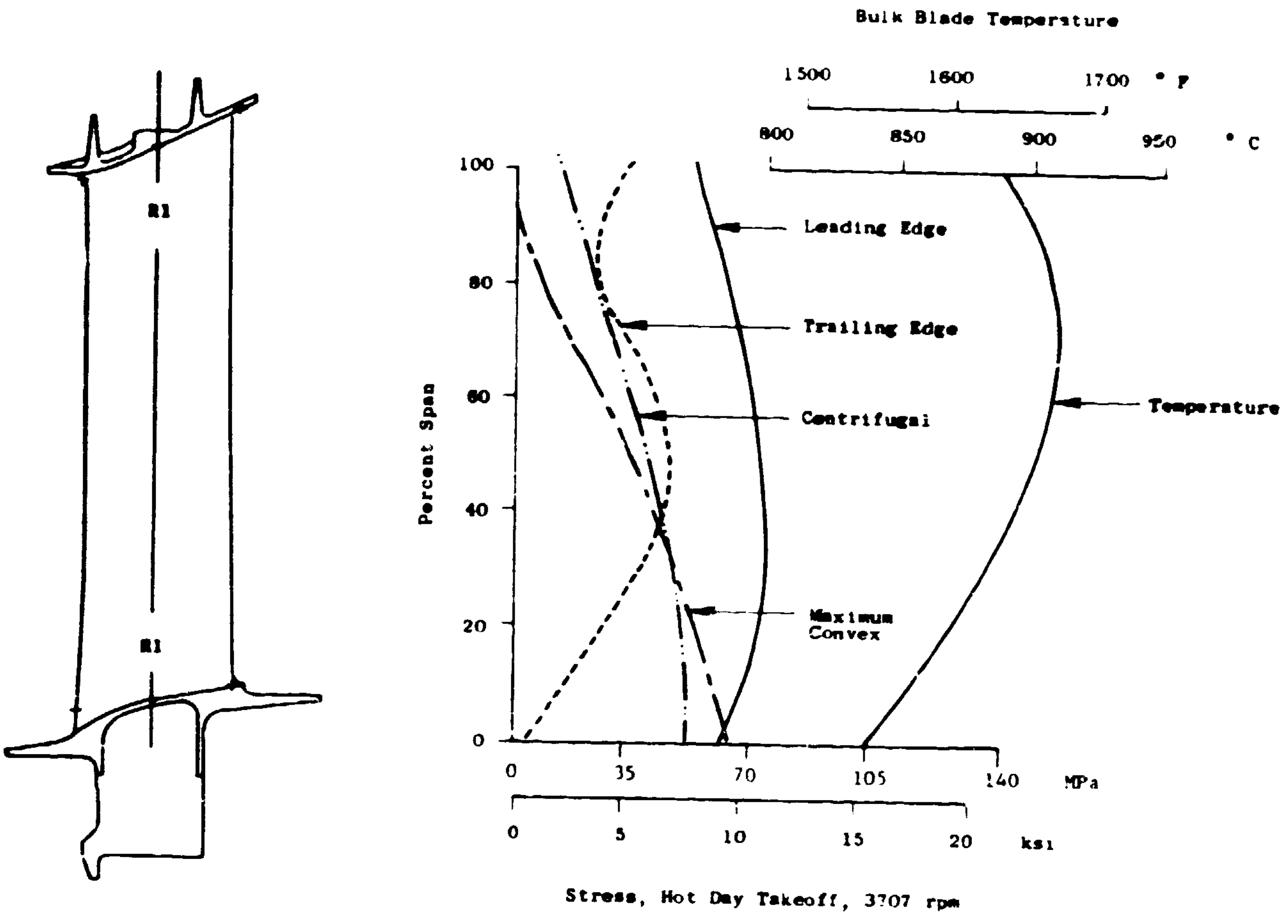

Figure 55. LPT Stage 1 Blade Stress and Temperature Distribution.

ORIGINAL PAGE IS
OF POOR QUALITY

Table VIII. Airfoil Stress Summary - Takeoff Condition.

Stage	1	2	3	4	5
Centrifugal Stress					
Pitch, MPa (ksi)	41.3 (6.0)	57.9 (8.4)	62.7 (9.1)	84.8 (12.3)	93.1 (13.5)
Root, MPa (ksi)	53.1 (7.7)	66.7 (9.7)	87.5 (12.7)	88.2 (12.8)	136.5 (19.8)
Leading Edge Resultant Stress					
Pitch, MPa (ksi)	73.8 (10.7)	101.3 (14.7)	104.1 (15.1)	124.1 (18.0)	106.9 (15.5)
Root, MPa (ksi)	62.7 (9.1)	59.3 (8.6)	96.5 (14.0)	88.9 (12.9)	134.4 (19.5)
Uncorrected Gas Bending Stress					
Root, MPa (ksi)	133.1 (19.3)	150.3 (21.8)	157.9 (22.9)	207.5 (30.1)	248.2 (36.0)

Table IX. LPT Mission Analysis Used for Airfoil Rupture Creep Life Calculations.

Power Setting	Time at Condition (hr)	Altitude, m(ft)	Mach No.	ΔT_{amb} °C (°F)	rpm	T_{49} °C (°F)	P_{49} Tot kPa (psi)
Max. Takeoff	159.5	0	0.3	+18 (+33)	3707	9?0 (?588)	586 (85)
Max. Takeoff	159.5	0	0.3	+3 (+6)	3707	873 (1604)	586 (85)
Max. Climb	1,685	3,048 (10,000)	0.453	+10 (+18)	3453	871 (1601)	462 (67)
Max. Climb	1,685	10,668 (35,000)	0.8	+10 (+18)	3633	870 (1599)	262 (38)
Max. Cruise	5,515	10,668 (35,000)	0.8	+10 (+18)	3526	843 (1549)	248 (36)
Max. Cruise	1,838	15,240 (50,000)	0.8	+10 (+18)	3477	844 (1552)	120 (17.4)
Approach Idle	6,958	0	0	+10 (+18)	2800	677 (1250)	207 (30)
	18,000						

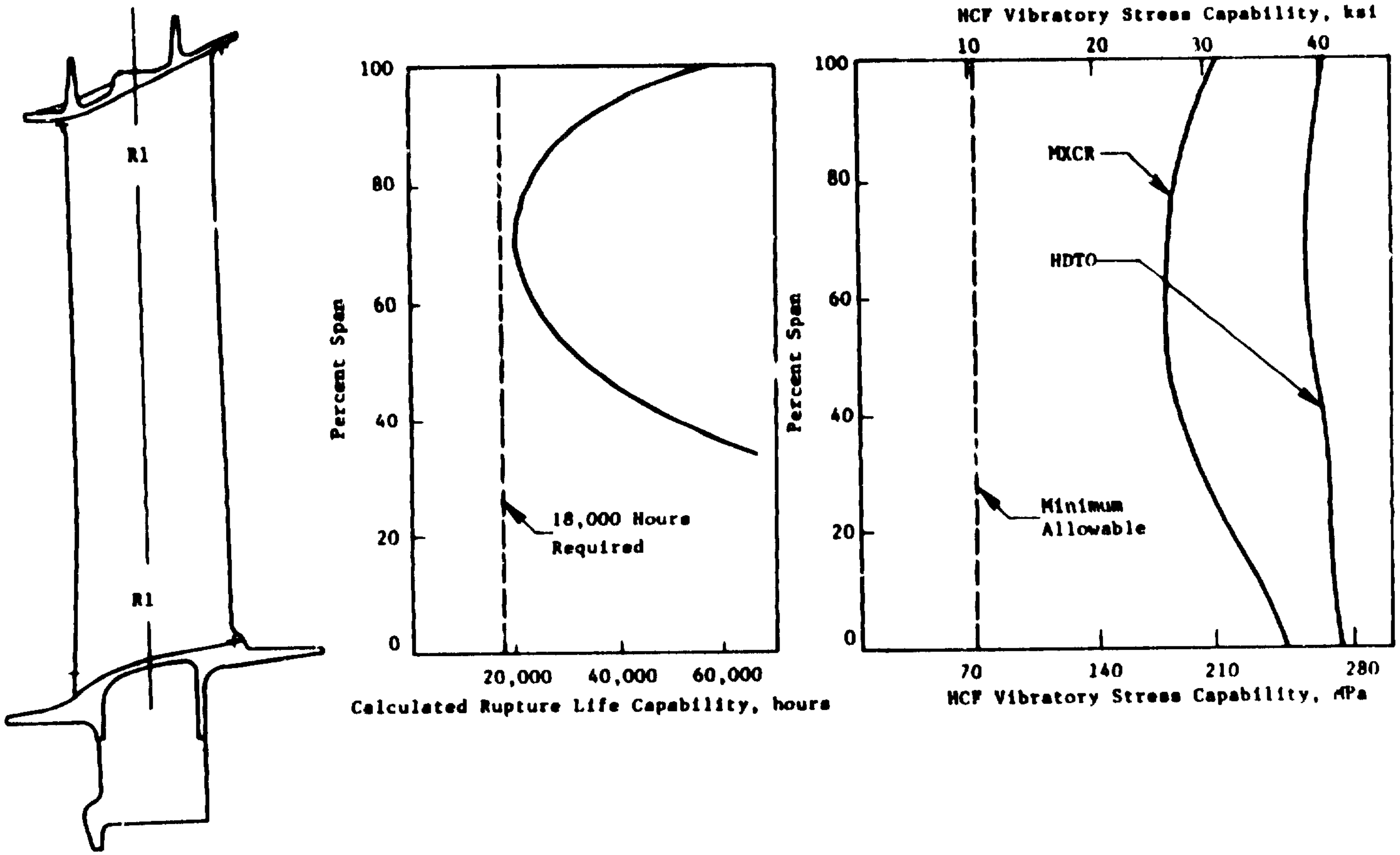

Figure 56. LPT Stage 1 Blade Airfoil Life Characteristics.

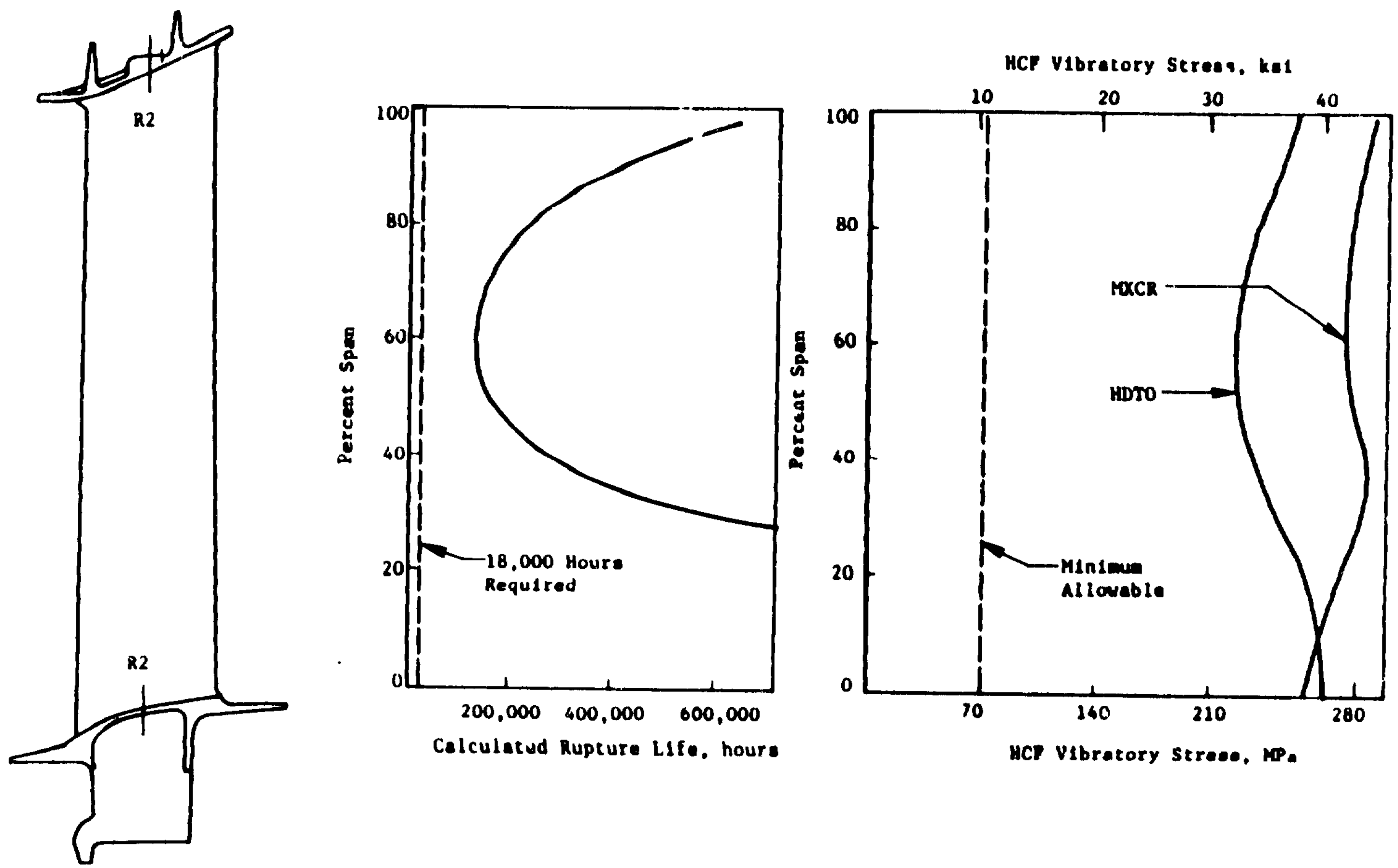

Figure 57. LPT Stage 2 Blade Airfoil Life Characteristics.

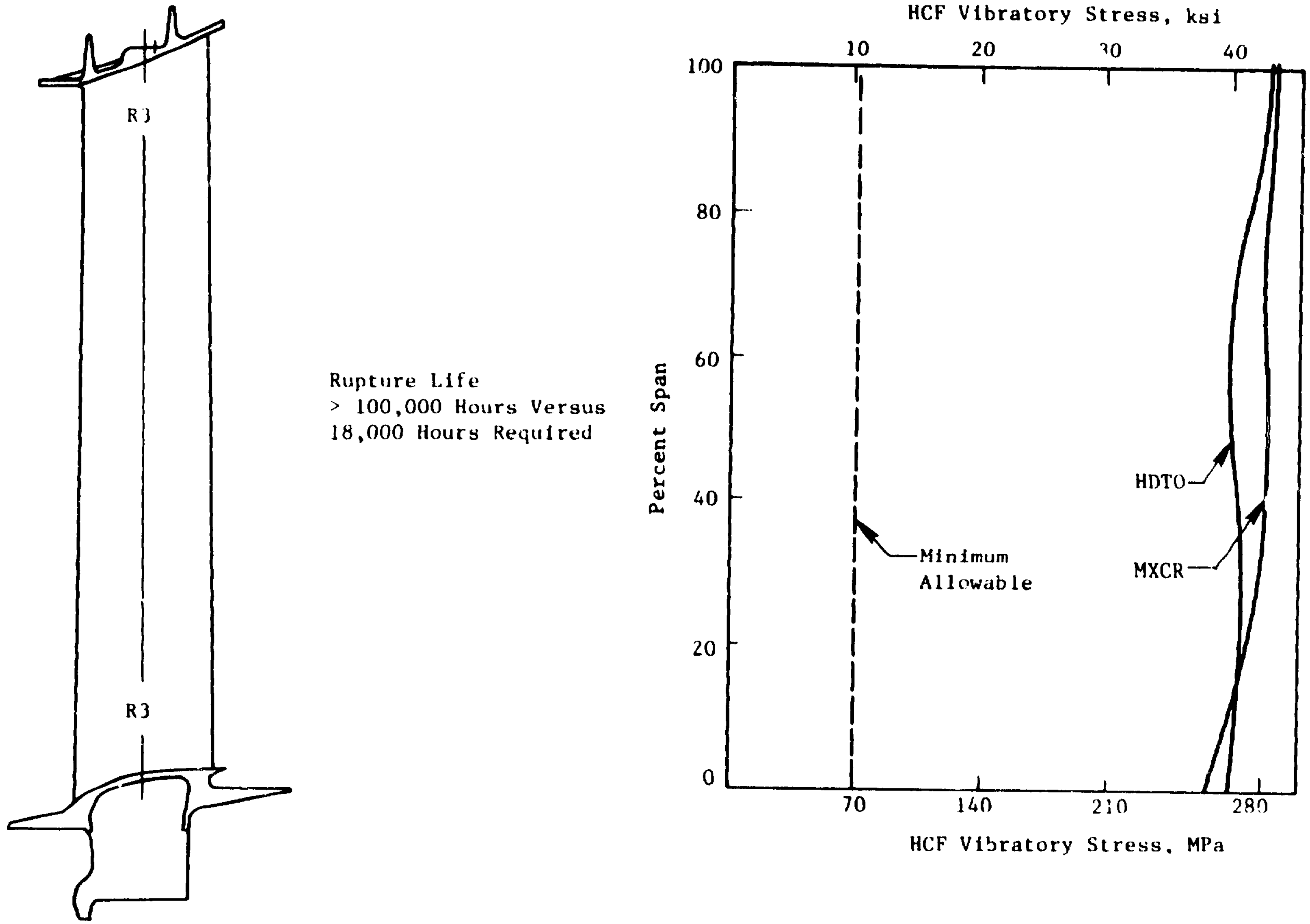

Figure 58. LPT Stage 3 Blade Airfoil Life Characteristics.

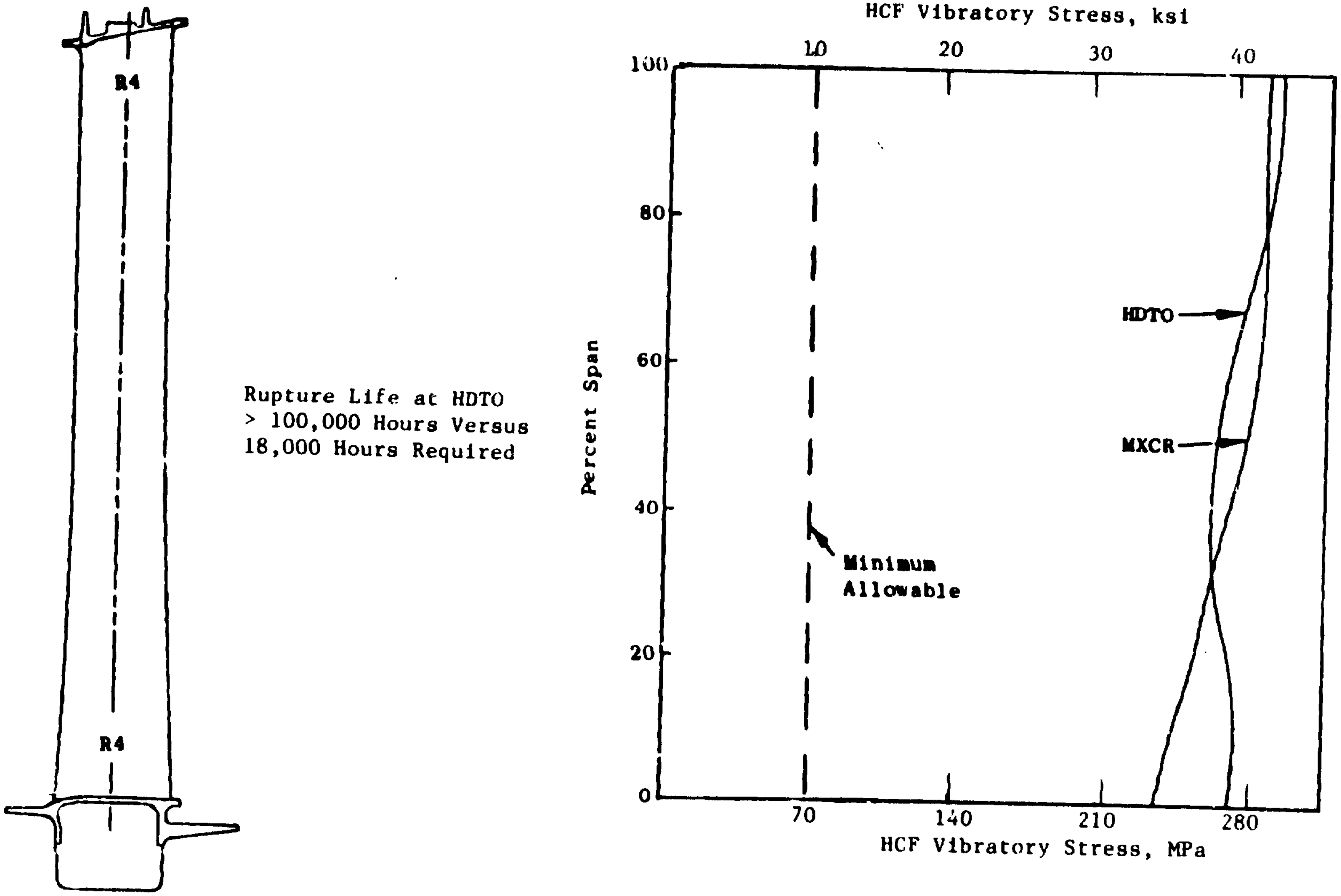

Figure 59. LPT Stage 4 Blade Airfoil Life Characteristics.

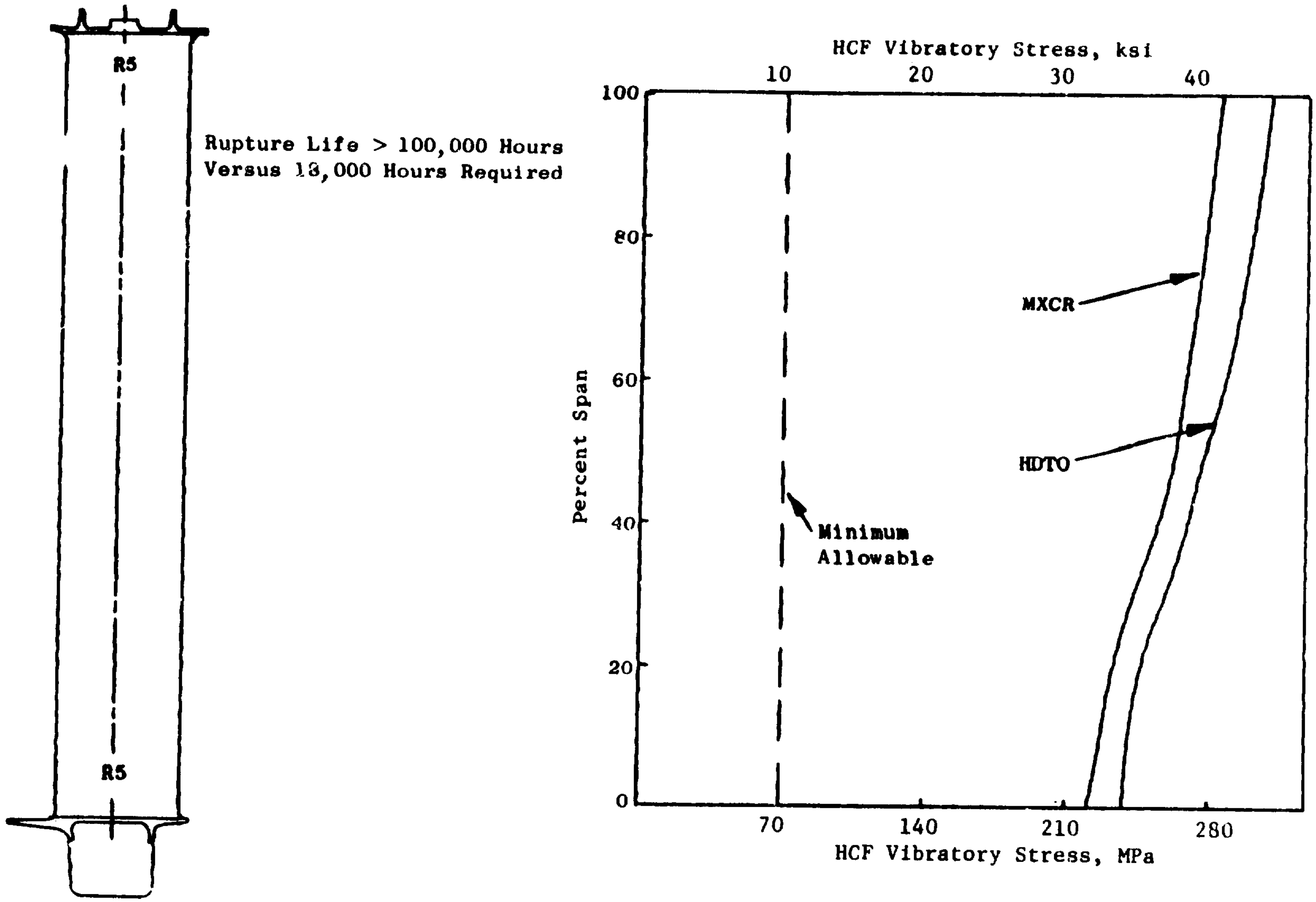

Figure 60. LPT Stage 5 Blade Airfoil Life Characteristics.

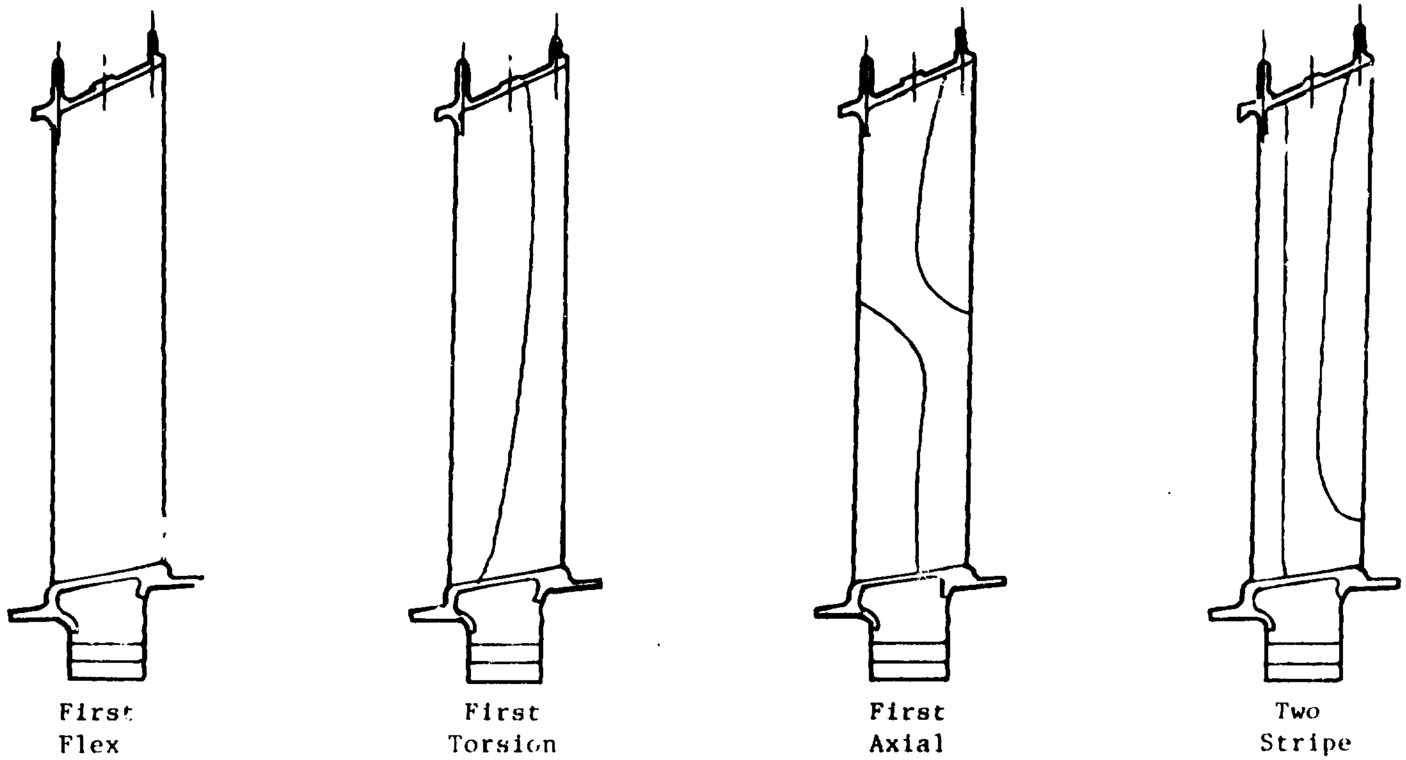

Figure 61. LPT Blade Natural Frequencies - Typical Mode Shapes.

ORIGINAL PAGE IS OF POOR QUALITY

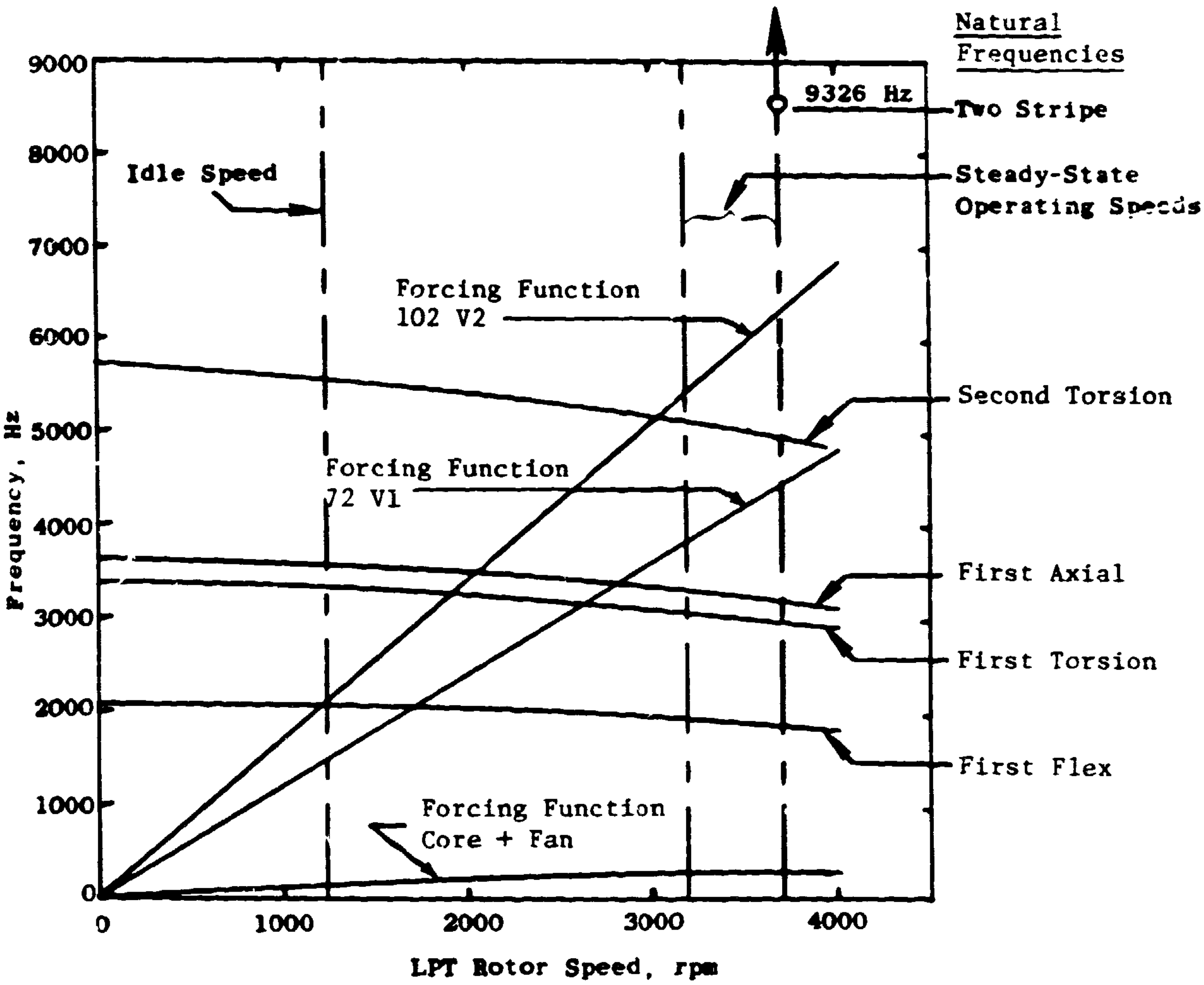

Figure 62. Stage 1 Blade (Pinned Tip) Resonant Frequency Analysis.

ORIGINAL PAGE IS
OF POOR QUALITY

Table X. Blade Airfoil LCF Life.

Stage	σ_{Max}, MPa (ksi)	% Span	Temperature, °C (°F)	LCF Life Cycles*
1	75.85 (11.0)	30	882 (1620)	$>10^5$
2	101.36 (14.7)	50	838 (1540)	$>10^5$
3	107.56 (15.6)	30	746 (1375)	$>10^5$
4	129.63 (18.8)	40	693 (1280)	$>10^5$
5	148.24 (21.5)	20	624 (1155)	$>10^5$

*Required Life = 36,000 Cycles

Thus, the vibration characteristics of the Stage 1 blade are completely satisfactory.

Similar analyses were performed on blade designs for Stages 2 through 5 blades; no indications of vibration problems were found.

The blades were also analyzed for sensitivity to flow-induced vibration (flutter). A flutter index was calculated for the torsional and flexural modes of vibration, and this index was compared with values obtained from prior GE engine evaluations. All blade designs met the flutter-vibration requirements as shown in Table XI.

Table XI. LPT Flutter Analysis.

Calculation

- Flutter Index = ν = $\dfrac{\text{Relative Flow Velocity}}{\text{1/2 Blade Chord} \cdot \text{Blade Natural Frequency}}$
- Check Both Flexural and Torsional Flutter
- Safety Factor = $\nu_{\text{Max. Allowable}}/\nu_{\text{Calculated}}$

Results

	Stage				
Safety Factor	1	2	3	4	5
• Torsion	2.3	1.8	1.6	1.0	1.3
• Flex	4.9	4.0	3.4	1.8	2.2

Conclusion

All Blades Meet Flutter Vibration Requirements (Factor $\geq$1)

Analyses were performed to determine combined blade/disk vibration frequencies in the operating range and to establish that there were no resulting detrimental excitations. The modes investigated were the 2, 4, and 6 diameter types. The combined blade/disk natural frequencies for each disk stage are plotted against existing engine excitations in Figure 63 for Stage 1. A review of this plot (Campbell diagram) showed that even the potentially limiting mode, the 2-diameter on Stage 1, has greater than the desired frequency margin with the 2/rev excitation line throughout the engine operating range. Thus, no vibration problems are indicated at any frequency.

The blade tip shrouds provide rotational fixity for resistance to vibration and also serve as tip seals against gas leakage. The tip shroud sizing and design considerations are listed in Figure 64. The tip shroud geometries were based on commercial engine experience with thicknesses set by stress and frequency requirements. Temperatures considered in the analyses were for the hot-day takeoff condition.

Figure 65 shows a typical view of two adjacent tip shrouds after assembly. Saw teeth are used on the seals so that they will cut into the stationary honeycomb seals rather than crushing into them. A hard coating, applied by flame-spraying, is used on the tip-shroud interlock surfaces to prevent excessive wear. CM64 hard coat will be used on Stages 1 and 2 because it has good high-temperature wear characteristics, and Triballoy T800 will be used on Stages 3, 4, and 5 because it has excellent wear characteristics at lower temperatures.

An LPT flowpath improvement in the Block IIB design provided axial lengthening in the upstream portion of the tip shrouds on Stages 1, 2, and 3 in order to achieve larger overlaps at the outer flowpath. This tip shroud extension, although improving performance, had adverse effects with respect to stresses and vibrations. Consequently, the first three stages of tip shrouds were thickened to ensure that they would meet the life requirements and that the lowest natural frequencies would be higher than vane-passing frequencies by sufficient margins.

Figure 66 shows the results of the Stage 1 blade tip-shroud analysis. The tip shrouds were analyzed for stress and frequency. A creep limit stress was calculated based on reaching plastic creep during the 18,000-hour mission shown in Table IX. The frequencies of the overhangs were calculated and compared to the vane-passing frequencies of the adjacent stages. As indicated in Figure 66, the Stage 1 tip shroud meets the creep limit stress criteria and has sufficient frequency margins over vane-passing frequencies. Similar analyses were made for the shrouds of Stages 2 through 5; again, no problems were found with vibration stresses.

One additional region, the blade platform angel wings, was checked for potential vibration problems. Short overlaps are used in current GE engines, and these angel wings have natural frequencies much higher than any stator vane-passing-frequency excitation. The E^3 LPT angel wings are much longer, for improved performance, so they have lower frequencies and, thus, greater potential for coincidence with stator excitation. The analyses performed on

ORIGINAL PAGE IS
OF POOR QUALITY

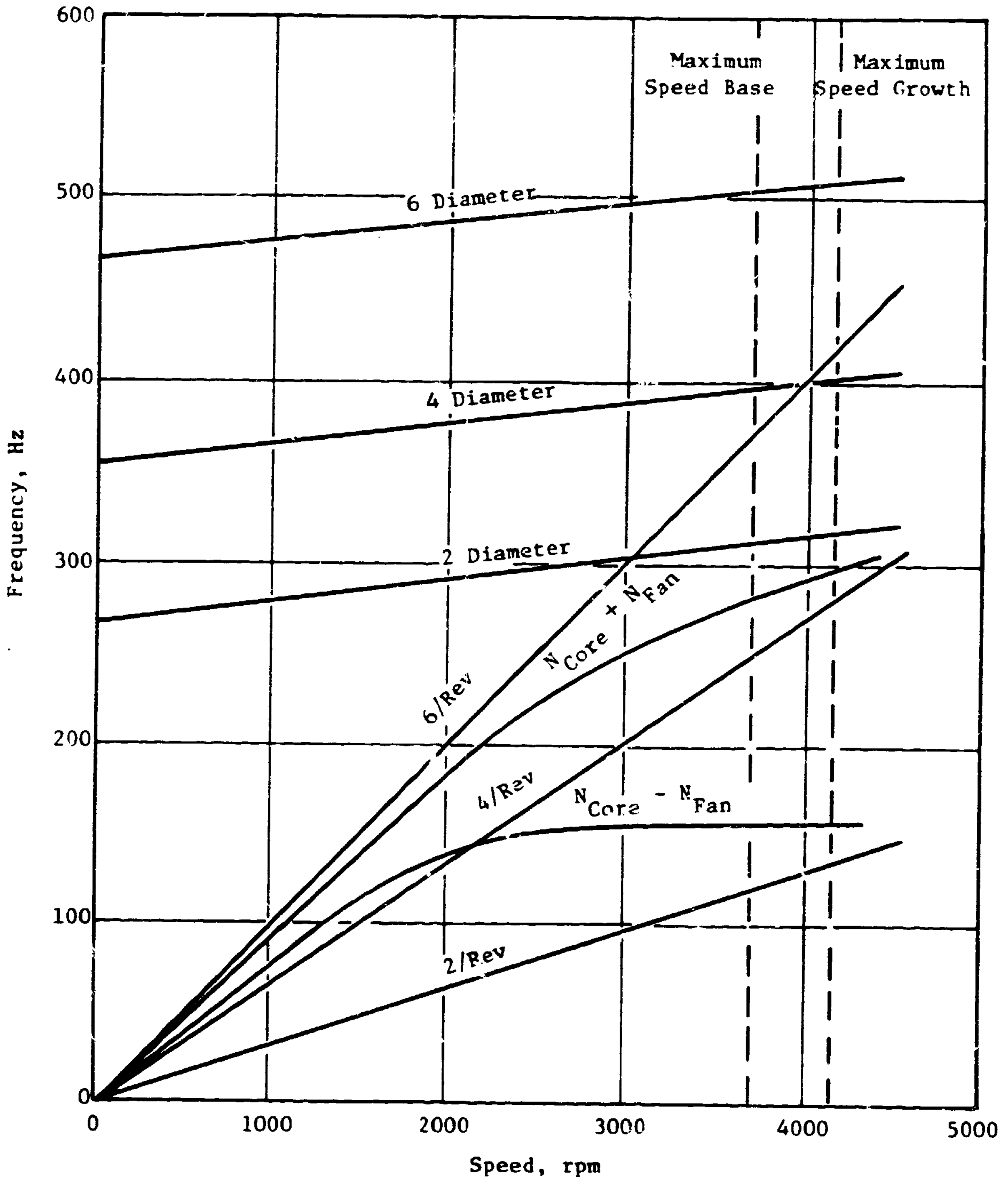

Figure 63. Stage 1 Coupled Blade Disk Cambell Diagram.

GEOMETRY

Sizing - Overhang: Balanced Over Airfoil

- Angle: Based on Commercial Engine Experience

  : Provides Tip Lockup

- Thickness: Set by Stress and Frequency Requirements

- Seal Teeth: Height Set by Flowpath Angles

TEMPERATURES - Considers Gas Profile

- Hot Day Takeoff

STRFSS - Meets Life Requirements

- Correlated with Commercial Engine Experience

VIBRATION - Overhangs have Sufficient Frequency Margins Over Vane Per Revs

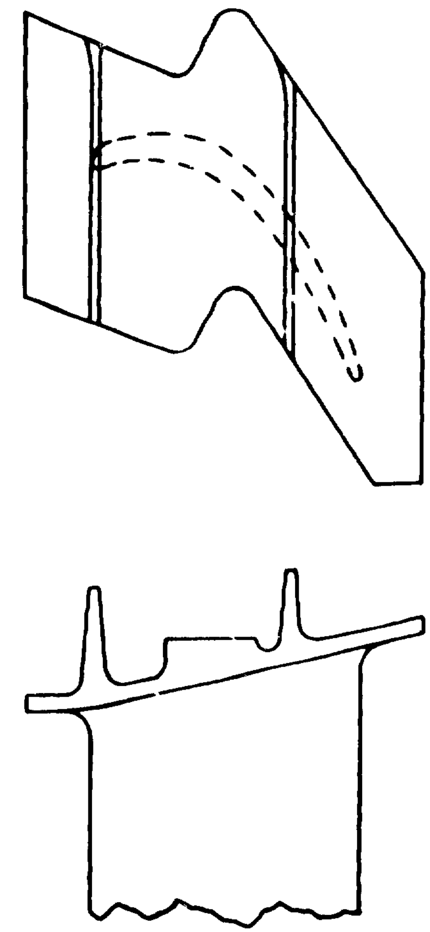

Figure 64. LPT Tip Shrouds.

Stage		1	2	3	4	5
Interlock Surface,	cm^2	0.142	0.206	0.193	0.116	0.193
	in^2	0.022	0.319	0.030	0.018	0.030
Pretwist,	Φ	0.8°	1.25°	1.25°	5.2°	3°
	β	25°	25°	30°	30°	30°
	θ	14.70	15.5	16.5°	17.5°	20.7°
ℓ	cm	0.767	1.01	0.988	-	-
	in	0.302	0.40	0.389	-	-
Interlock Contact Stress,	MPa	13.8	9.3	11.4	14.3	8.3
	(ksi)	2.0	1.3	1.7	2.1	1.2

Configuration

Thickness: Tapered, Stages 1, 2, and 3
: Constant, Stages 4 and 5

Features

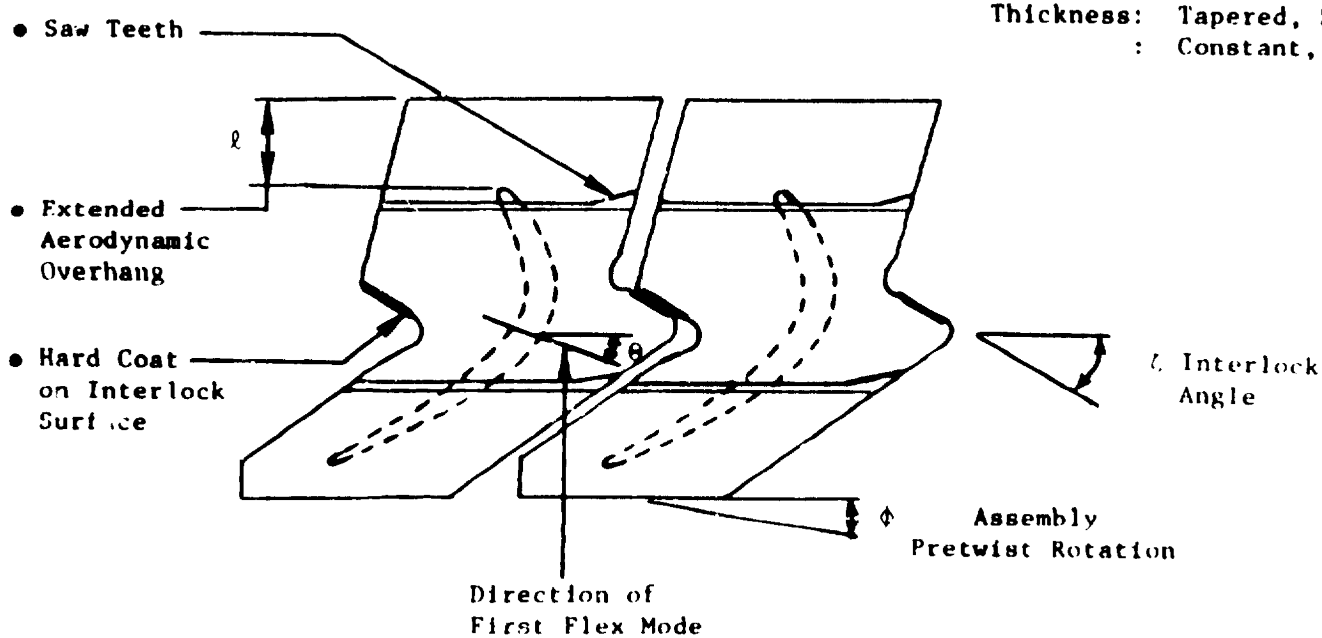

Figure 65. LPT Blade Tip Shroud Features and Configuration.

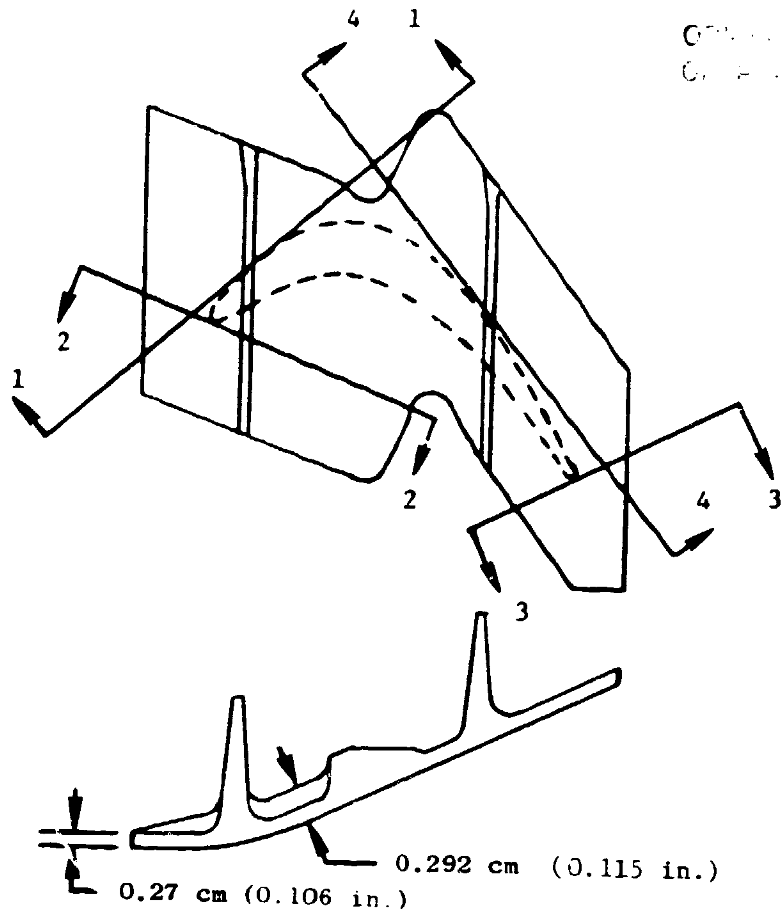

- Other Shrouds Also Meet Stress and Frequency Requirements

	Stress MPa (ksi)		Frequency	
Section	Actual	Creep Limit	Actual (Hz)	% Margin Over 102 S2*
1-1	82.7 (12.0)	87.6 (12.7)	10,490	40
2-2	78.6 (11.4)	87.6 (12.7)	14,620	57
3-3	51.0 (7.4)	87.6 (12.7)	15,800	60
4-4	75.8 (11.0)	87.6 (12.7)	15,310	59

*Stage 2 Vane Forced Vibration, 102 per Revolution

Figure 66. LPT Stage 1 Blade Tip Shroud Stress/Life and Frequency.

the blade angel wings were comparable to those for the tip shrouds described above. The angel wings were analyzed as cantilevered beams. Figure 67 shows that the Stage 1 angel wings met the creep limit stress criteria and that they had sufficient frequency margins over vane-passing frequencies. Similar analyses were made for Stages 2 through 5 angel wings. Again, no problems were indicated.

The LPT blades are retained in dovetail slots by two different methods. On Stages 1, 2, and 3, they are retained from aft movement by integrally cast retainers on the ends of the dovetails, as shown in Figure 68, and are retained against forward movement by the rotor seals. On Stages 4 and 5 the blades are retained against forward and aft movement by formed tab retainers as shown in Figure 69.

Stages 1, 2, and 3 blade retainers were designed so that they would not exceed material limits when a maximum design force (larger than the expected steady-state force) was applied at the end of the retainer. Figure 68 shows that all these retainers either meet or exceed the required strength.

The designs of the Stage 4 and 5 blade retainers were based on correlations with CF6 load tests. Thickening of the retainers was necessary for resisting axial transition (push-out) to meet requirements. The depths of the disk dovetail slots were increased slightly to allow room for the thickened retainers. The blade retainers are designed to withstand push-out force greater than the calculated applied loads.

As a result of these stress/life and frequency studies, the blade designs for all five stages are judged mechanically acceptable.

4.2.2 Dovetail Attachments

The dovetail design has been specifically tailored to the load conditions and design requirements of the E^3. Commonality in dovetail size was achieved by using the same size for Stages 1, 2, and 3; this provides a substantial saving in the cost of cutting tools. Stage 5 uses the same dovetail configuration except that the slot bottom was altered to permit a larger blade retainer. The Stage 4 dovetail is smaller due to the larger number of Stage 4 blades (required for acoustic considerations) which must fit into the same disk-rim circumference.

Detail stress distributions for the Stage 1 dovetail are shown in Figure 70. The peak stresses for the blade and disk are indicated by the "boxed" values and are the LCF life-limiting locations. A summary of peak stresses and life values is shown in Table XII for all five stages of blades and disks. Life requirements are met for all stages.

4.2.3 Disks

Each disk is sized in proportion to the centrifugal loading of the blade row. The spacer arms are forged integrally with the disks and are tapered to

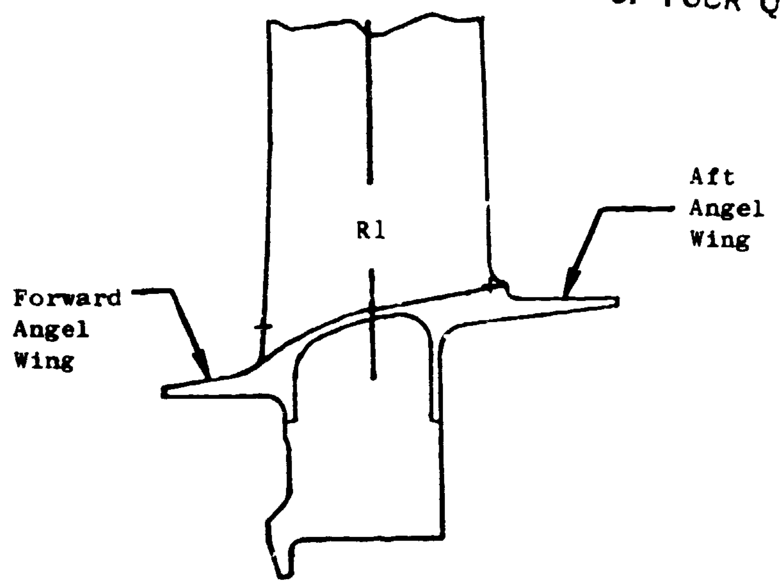

- Other Stage Angel Wings Also Meet Stress and Frequency Requirements

	Stress, MPa (ksi)		Frequency	
Section	Actual	Creep Limit	Actual, (Hz)	% Margin Over 102 S2*
Forward Angel Wing	40.7 (5.9)	162 (23.5)	12,725	50%
Aft Angel Wing	67.6 (9.8)	162 (23.5)	8,170	23%

*Stage 2 Vane Forced Vibration, 102 per Revolution

Figure 67. LPT Stage 1 Blade Angel Wing Stress/Life and Frequency.

ORIGINAL PAGE IS
OF POOR QUALITY

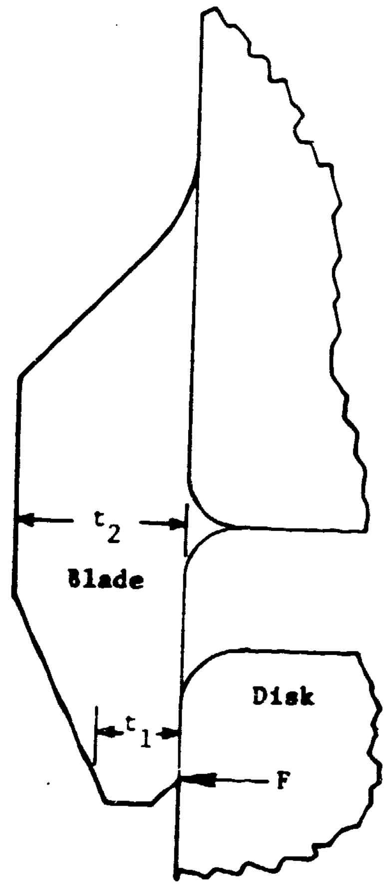

	t_1, cm (in.)	t_2, cm (in.)	F, N (lbf)	σ_{max}., MPa (ksi)	Design Allowable: 0.2% Yield Strength at 649° C (1200° F), MPa (ksi)
Stage 1	0.109 (0.043)	0.267 (0.105)	894 (201)	620.5 (90)	634.3 (92)
Stage 2	0.127 (0.050)	0.292 (0.115)	1103 (248)	627.5 (91)	634.3 (92)
Stage 3	0.173 (0.068)	0.343 (0.135)	1561 (351)	634.3 (92)	634.3 (92)

Figure 68. Blade Retainers for Stages 1, 2, and 3.

- Configuration - Sheet Metal
- Material - Inco 718
- Analysis/Design - Utilize CF6-50, -80 Load Tests

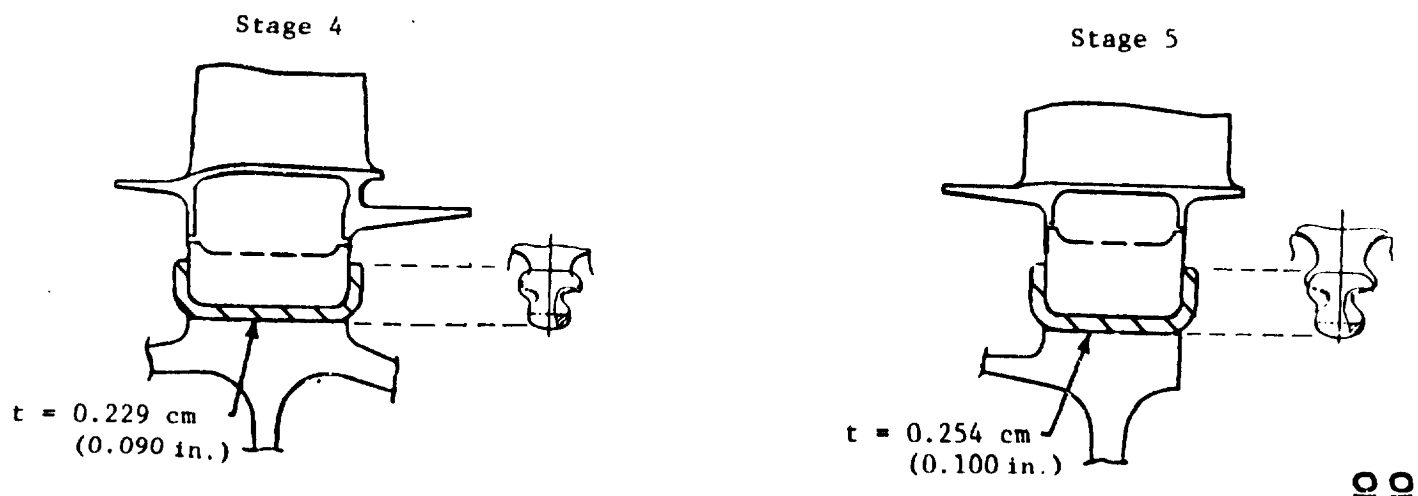

ORIGINAL PAGE IS
OF POOR QUALITY

Figure 69. Blade Retainers - Stages 4 and 5.

ORIGINAL PAGE IS
OF POOR QUALITY

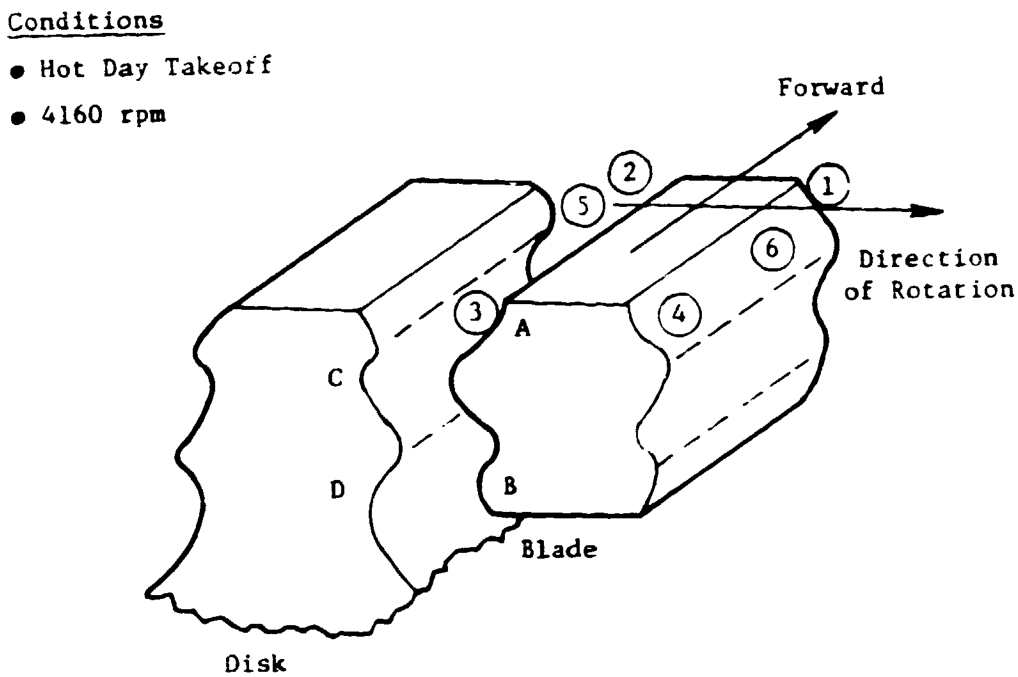

Stresses MPa (ksi)

Location		Position 1	2	3	4	5	6	K_t
Blade	A	118.6 (17.2)	191.8 (27.8)	165.5 (24.0)	91.7 (13.3)	178.6 (25.9)	104.8 (15.2)	1.62
	B	136.5 (19.8)	215.8 (31.3)*	186.2 (27.0)	106.2 (15.4)	201.3 (29.2)	121.4 (17.6)	1.59
Disk	C	66.9 (9.7)	191.7 (27.8)	171.0 (24.8)	46.9 (6.8)	181.3 (26.3)	57.2 (8.3)	1.60
	D	144.8 (21.0)	143.4 (20.8)*	180.0 (26.1)	116.5 (16.9)	194.4 (28.2)	130.3 (18.9)	1.60

$\boxed{}$* = Maximum Stress

Figure 70. LPT Stage 1 Dovetail Stress Distribution.

Table XII. Dovetail Life Summary.

Stages	Temp. °C(°F)	Blade: σ_{Max} MPa (ksi)	Blade: K_t	Blade: Calculated LCF Life (36,000 Cycles Life Required)	Disk: σ_{Max} MPa (ksi)	Disk: K_t	Disk: Calculated LCF Life (72,000 Cycles Life Required)
1	596 (1104)	215.8 (31.3)	1.59	$\geq 10^5$	208.2 (30.2)	1.60	$\geq 10^5$
2	607 (1125)	248.2 (36.0)	1.60	$\geq 10^5$	228.2 (33.1)	1.62	$\geq 10^5$
3	593 (1100)	297.2 (43.1)	1.60	$\geq 10^5$	262.0 (38.0)	1.62	$\geq 10^5$
4	593 (1100)	190.3 (27.6)	1.65	$\geq 10^5$	201.3 (29.2)	1.63	$\geq 10^5$
5	560 (1040)	289.6 (42.0)	1.60	$\geq 10^5$	242.7 (35.2)	1.63	$\geq 10^5$

<u>Conclusion:</u>

All Dovetails Meet LCF Life Requirements become thinner in the region away from the disk web attachment. Spacer arm stresses in the LPT rotor were calculated at the limiting time steps and are shown in Figure 71. There are no bolt hole stress concentrations in the main load-carrying disk webs. Instead, the bolt holes are located in the low-stressed spacer arms. A bolt analysis was conducted, and the results are shown in Table XIII. The available clamping load of the bolting was shown to exceed the requirements, even after the relaxation effects of 9000 hours of engine operation. Table XIV describes the bolts and nuts selected for each disk stage and also lists the limiting mode of "failure."

Analyses of transient engine operation were run to identify the critical operating point (combined speed and temperature gradient) for each disk. As a typical example, Figure 72 shows the stress distributions for the Stage 1 disk at the critical operating point. A summary of disk LCF life limits is given in Table XV. All disk designs meet or exceed the minimum life requirement: 72,000 cycles. An overspeed analysis was conducted to determine whether the disks met the 120% redline speed requirement. All disks meet burst-speed requirements with margin to spare.

4.2.4 Seals

LPT rotor seals have several functions. The primary function is to prevent leakage past the vanes. Stages 1, 2, and 3 seals have two other important functions: to prevent forward movement of the blades and to direct cooling flow to the blade/disk dovetails. All seals meet life requirements.

4.3 LPT STATOR

4.3.1 Stage 1 Nozzle Subassembly

The Stage 1 LPT nozzle assembly comprises the inner and outer transition ducts, Stage 1 LPT nozzle, nozzle support, forward inner seal support, aft inner seal support, and miscellaneous parts such as spoolies, windage shields, heat shield, splash shield, nuts, and bolts. A schematic of this assembly is shown in Figure 73.

One unique feature of this assembly is to direct fifth-stage compressor air down through the nozzle airfoils to purge the Stage 2 HPT disk aft cavity and to pressurize and purge the Stages 1 through 3 LPT rotor cavity.

Outer Duct

The outer HPT/LPT transition duct is assembled from 18 René 80 cast and machined segments. The segments are supported in the front by the nozzle support and at the rear by a bolted joint as shown in Figure 74. A transient heat-transfer analysis was completed for the HPT aft case and adjacent hardware including the outer ducts. The forward attachment hook of each duct

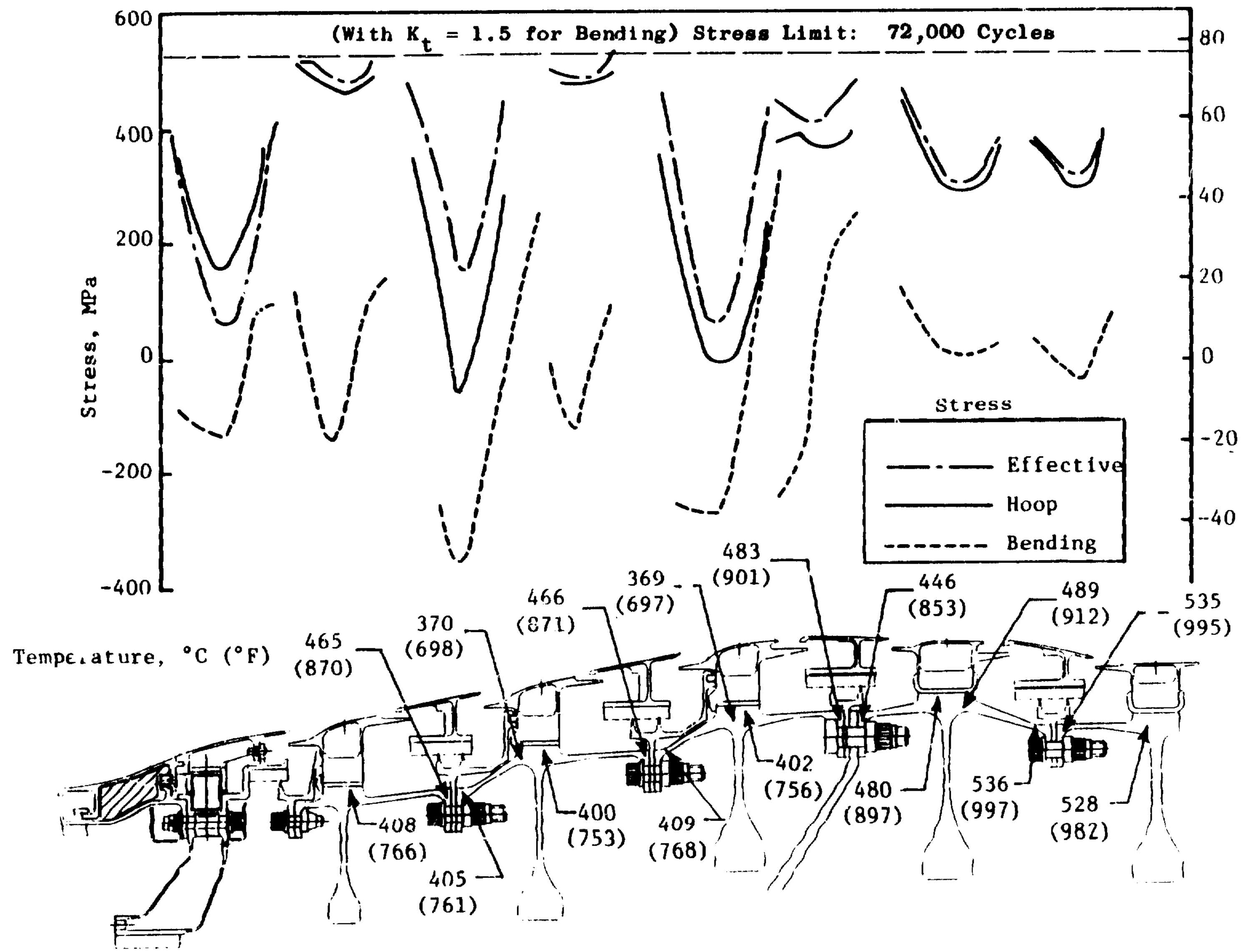

Figure 7i. LPT Rotor Spacer Arm Stresses 60 Seconds into Takeoff Acceleration.

ORIGINAL PAGE IS
OF POOR QUALITY

ORIGINAL PAGE IS
OF POOR QUALITY

Table XIII. LPT Rotor Bolt Analysis.

Stages	Required Clamp Load, N (lb_f)			Available Clamping Load, N (lb_f)	
	Torque and Radial Shear μ = 0.15	Torque μ = 0.10	Separation	Cold Assy. Clamp Load	Residual Cold Clamp Load After 9000 Hr
1-2	11,525 (2,591)	13,745 (3,090)	7,184 (1,615)	34,430 (7,740)	21,796 (4,900)
2-3	13,736 (3,088)	20,017 (4,500)	8,229 (1,850)	34,430 (7,740)	21,796 (4,900)
3-4	29,625 (6,660)	27,525 (6,188)	15,680 (3,525)	53,379 (12,000)	33,139 (7,400)
4-5	10,253 (2,305)	8,398 (1,888)	12,588 (2,830)	34,429 (7,740)	21,796 (4,900)

Table XIV. Selected Bolts for Rotor Flanges.

Stages	Bolt Size cm (in.)	Quantity	Bolt Material	Nut Material	Limiting Mode*
Stage 1 Fwd Flange	0.635 ** (1/4 D-28)	40	Inco 718	Waspaloy	Maximum Bolt Spacing
1-2	0.794 (5/16 D-24)	40	Inco 718	Waspaloy	Torque
2-3	0.794 (5/16 D-24)	52	Inco 718	Waspaloy	Torque
3-4	0.953 (3/8 D-24)	76	Inco 718	Waspaloy	Torque
4-5	0.794 (5/16 D/24)	40	Inco 718	Waspaloy	Flange Separation

*Design requirement which determines bolt selection.

**(¼ Diameter - 28 Threads per inch)

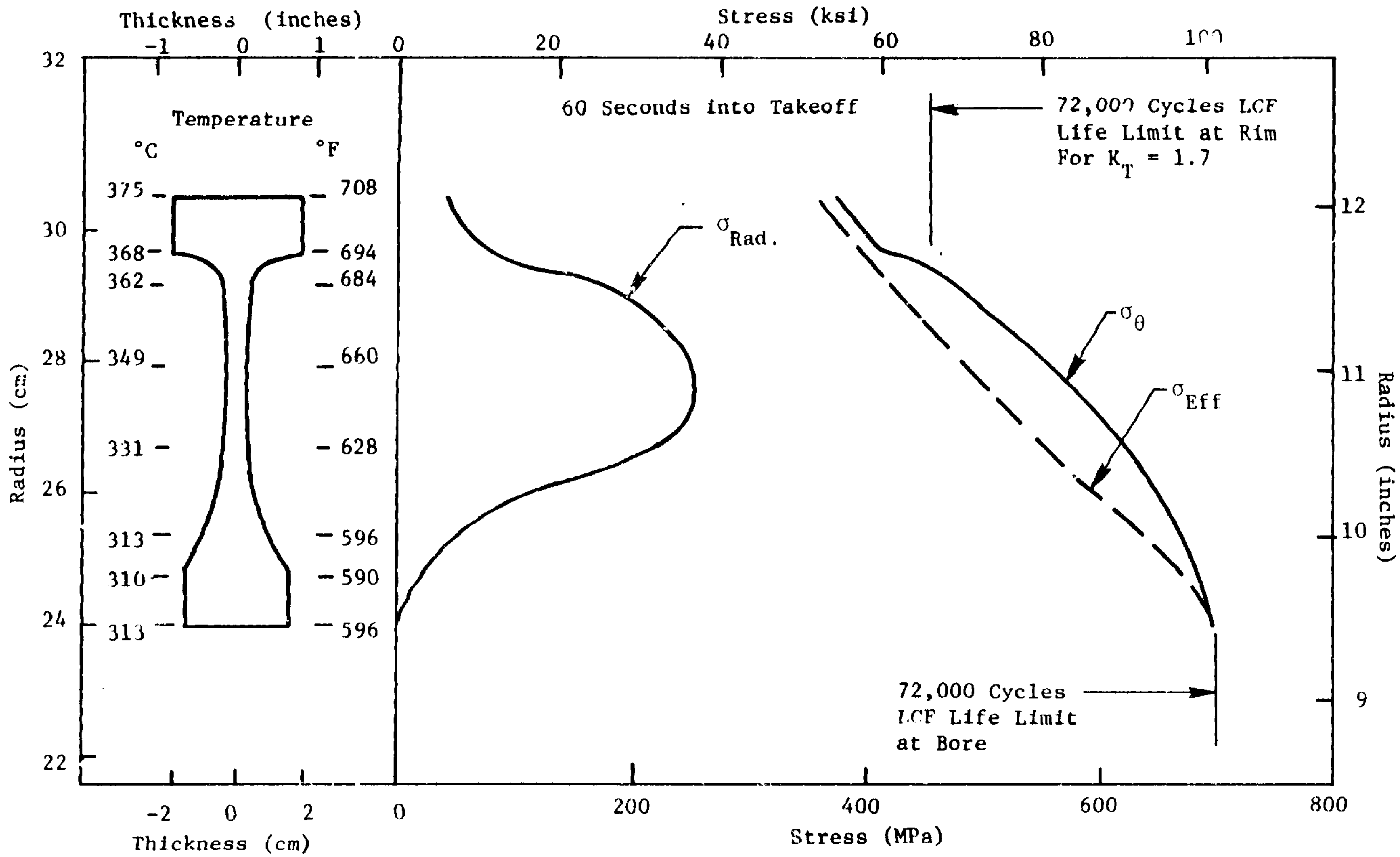

Figure 72. Stage 1 LPT Disk Stress Distribution at Growth Conditions.

Table XV. LPT Rotor Disk Minimum Calculated LCF Life.

Limiting Mission Point	Disk Stage				
	1	2	3	4	5
Time After Takeoff Initiation ➡	60 sec	60 sec	20 sec	60 sec	20 sec
Bore					
Hoop Stress, 1/2 of Peak Value MPa (ksi)	351 (51)	351 (51)	351 (51)	303 (44)	317 (46)
Temperature, °C (°F)	315 (600)	302 (575)	304 (580)	482 (900)	454 (850)
Allowable LCF Cycles	72,000	72,000	72,000	$>10^5$	$>10^5$
Dovetail Slot Bottom K_t = 1.7					
Hoop Stress, 1/2 of Peak Value MPa (ksi)	193 (28)	186 (27)	179 (26)	234 (34)	234 (34)
Temperature, °C (°F)	375 (708)	377 (710)	371 (700)	477 (890)	461 (862)
Allowable LCF Cycles	$>10^5$	$>10^5$	$>10^5$	72,000	72,000

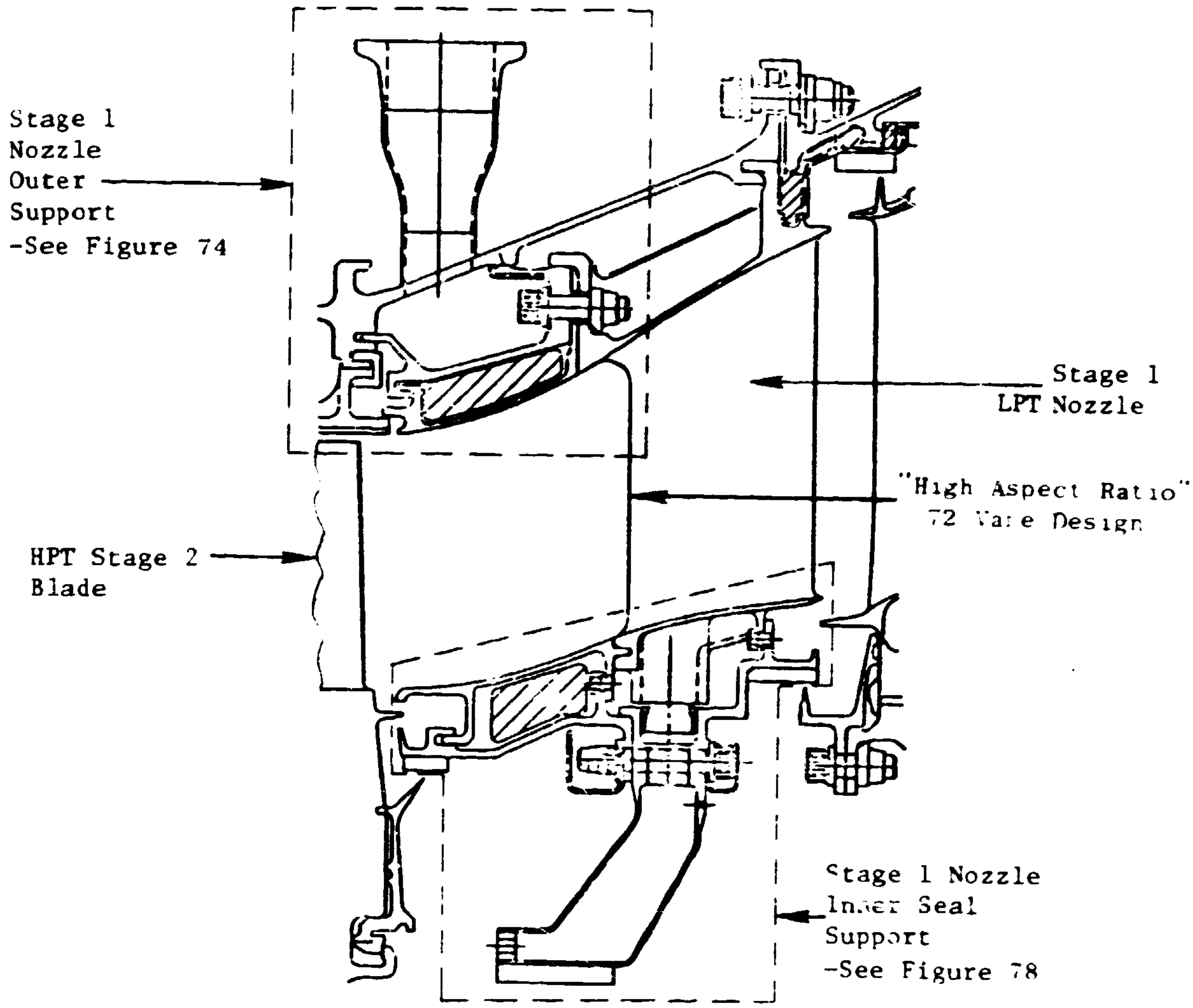

Figure 73. LPT Stage 1 Nozzle Assembly.

ORIGINAL PAGE IS
OF POOR QUALITY

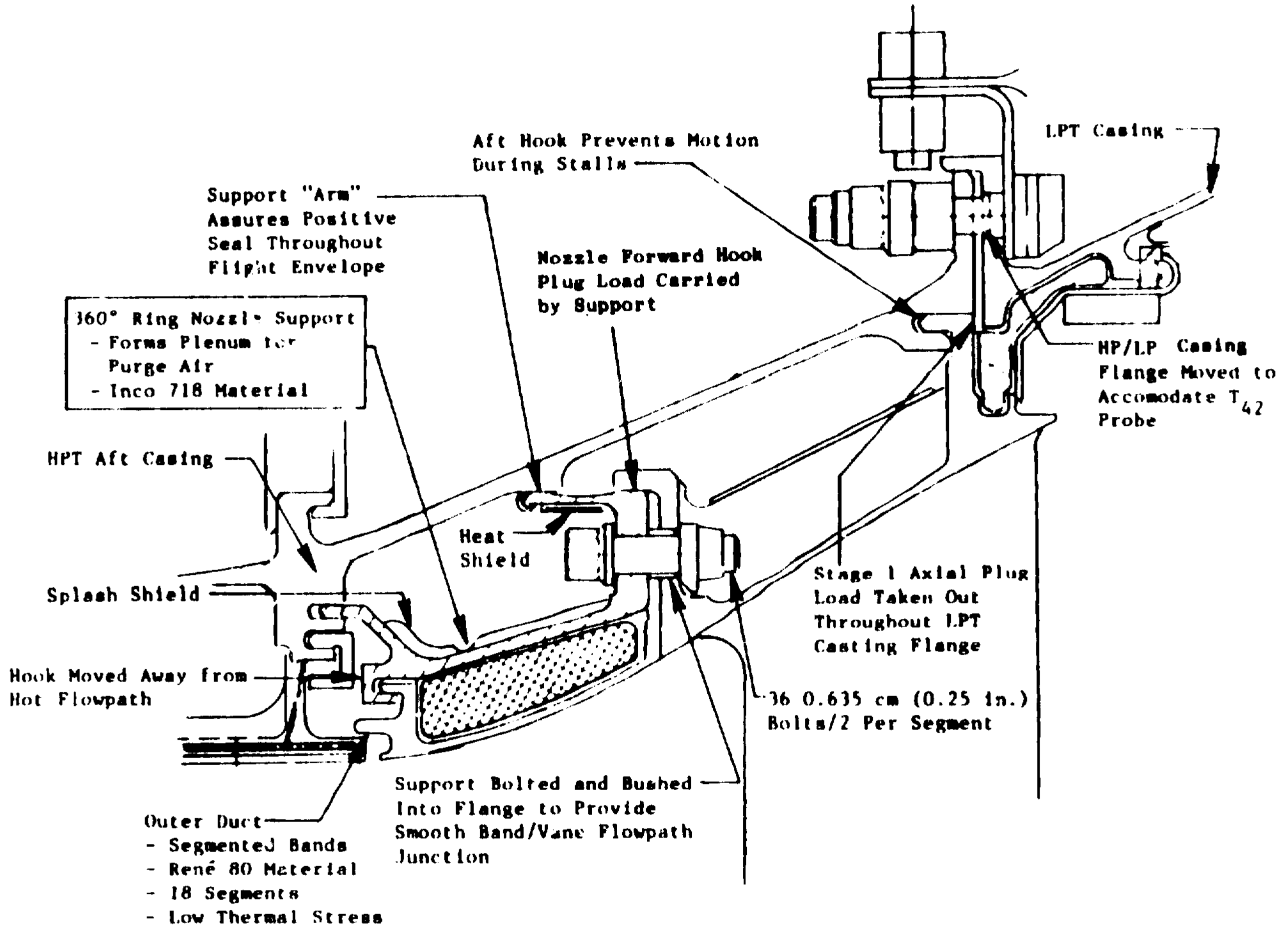

Figure 74. LPT Stage 1 Vane/Support Features.

segment is scalloped to reduce the conduction heat-transfer path into the support. Both the forward attachment hook and the aft attachment flange are saw-cut to reduce thermal stresses. The forward hook is also coated with Triballoy 800 to reduce wear.

All 18 ducts are identical for both the ICLS and the FPS. However, for ICLS testing, provisions were made in the ducts for accepting 14 T_{42} and P_{42} probes spaced circumferentially around the HPT aft casing.

Outer Transition-Duct/Nozzle Support

The final configuration of the outer transition-duct/nozzle support is shown in Figure 74. This support is a 360° ring machined from an Inco 718 forging and forms a plenum for the fifth-stage cooling air. The design features a cylindrical support "arm" that has an interference fit with the HPT casing and allows the support bolted flange to grow radially during accel, thereby maintaining a positive seal with the casing. Figure 75 shows effective stresses at takeoff, as calculated by the GE CLASS/MASS computer program.

The deflection analysis of the support showed that the cylindrical "arm" would not remain in contact with the HPT casing during a portion of the engine decel; fifth-stage air leakage would occur at that point. It was determined that this would occur because of the faster cooling rate of the support compared to the casing, and a thermal shield was added to minimize the probability of this leakage occurring.

To reduce wear, all support surfaces which mate with the HPT casing will be thermal sprayed with Triballoy 800.

The only difference between the FPS and the ICLS designs is the addition of 14 bosses (spaced circumferentially) on the ICLS support. These bosses will provide seating surfaces for the temperature and pressure probes which will be mounted on the HPT casing.

Stage 1 LPT Nozzle

The LPT Stage 1 nozzle design has been modified significantly since the preliminary design phase. The final design (Figure 73) is a high-aspect-ratio, 72-vane design with constant projected axial chord and radial trailing edges. A total of 18 nozzle segments per engine set with 4 vanes per segment will be cast from René 125. The front hook of each segment will be bolted to the outer-duct/nozzle support. The nozzle aft hook radial loads will be carried by the HPT casing. Axial airfoil gas loads and inner seal loads will be resisted by the LPT casing forward flange. The tangential gas load on the airfoils is transmitted through the nozzle outer band, the aft hook, and into the HPT casing via lugs brazed to the aft nozzle hook as shown in Figure 76. The operating conditions and calculated design life for the

ORIGINAL PAGE IS
OF POOR QUALITY

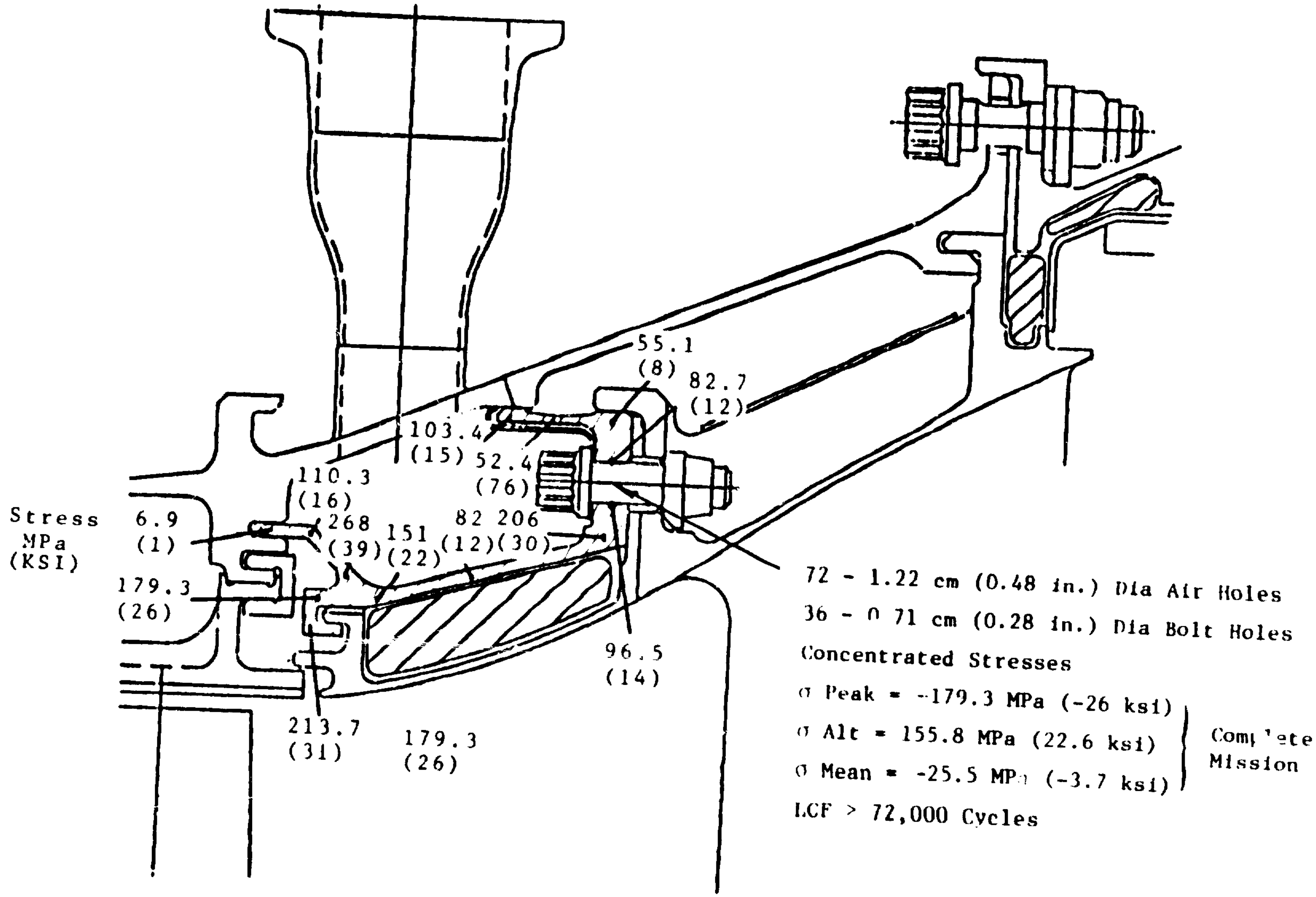

Figure 75. Support for Outer Transition Duct and LPT Stage 1 Nozzle: Effective Stresses at Takeoff.

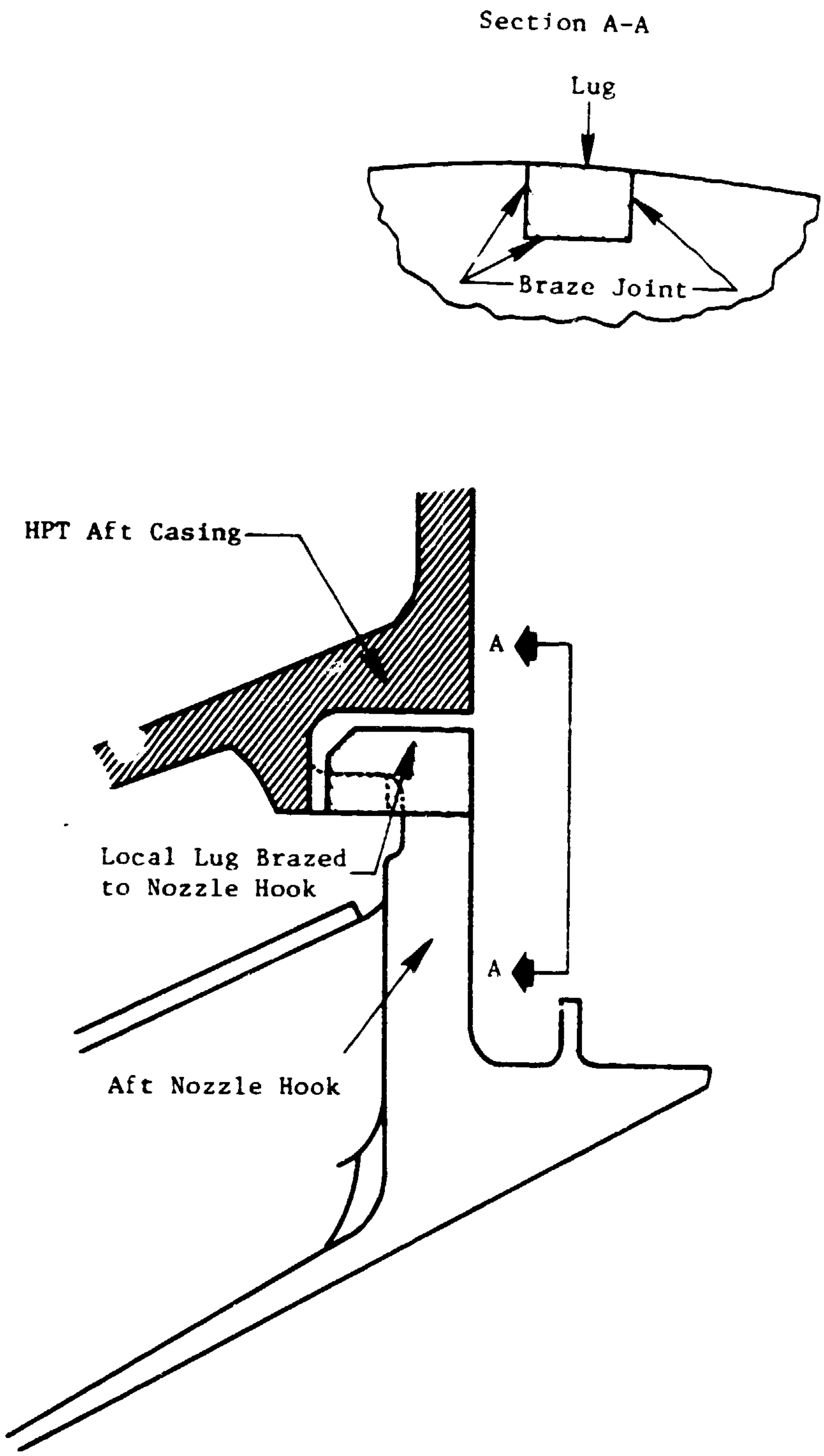

Figure 76. LPT Stage 1 Nozzle Tangential Load Stop.

ORIGINAL PAGE IS
OF POOR QUALITY

Stage 1 nozzle airfoil are displayed in Table XVI and meet all design requirements. The results of a similar analysis of the attachment hooks of the Stage 1 nozzle are given in Figure 77 and are satisfactory.

Table XVI. LPT Stage 1 Nozzle Airfoil Operating Conditions and Calculated Design Life.

● Takeoff, FPS Baseline

Material: René 125

$T_{Gas\ Max.}$ = 957° C (1755° F) at 95% Span

T_{Metal} = 931° C (1708° F), 8° C (47° F) Cooling

$T_{Cooling}$ (Fifth-Stage Purge) = 404° C (760° F)

1.2% Fifth-Stage Purge Air Maximum Cooling Capability = 22° C (72° F)

Axial Gas Load/Vane = 291 N (65.4 lbf)

Tangential Gas Load/Vane = 348 N (78.2 lbf)

ΔP Load/Vane = 263.5 N (59.25 lbf)

Bending Stress at Limiting Section (Tip, Leading Edge)
σ = 118.6 MPa (17.2 ksi)

$$\frac{\text{Rupture Life}}{\text{Required Life}} = 3.4$$

$$\frac{\text{0.5\% Creep Life}}{\text{Required Life}} = 4.3$$

$$\frac{\text{LCF Life}}{\text{Required Life}} \approx 1$$

Leading Edge to Airfoil Radius K_t = 2.02

The inner seal support region is made up of three major components (the aft inner seal support, the forward inner seal support, and the mixer transition duct); features are illustrated in Figure 78.

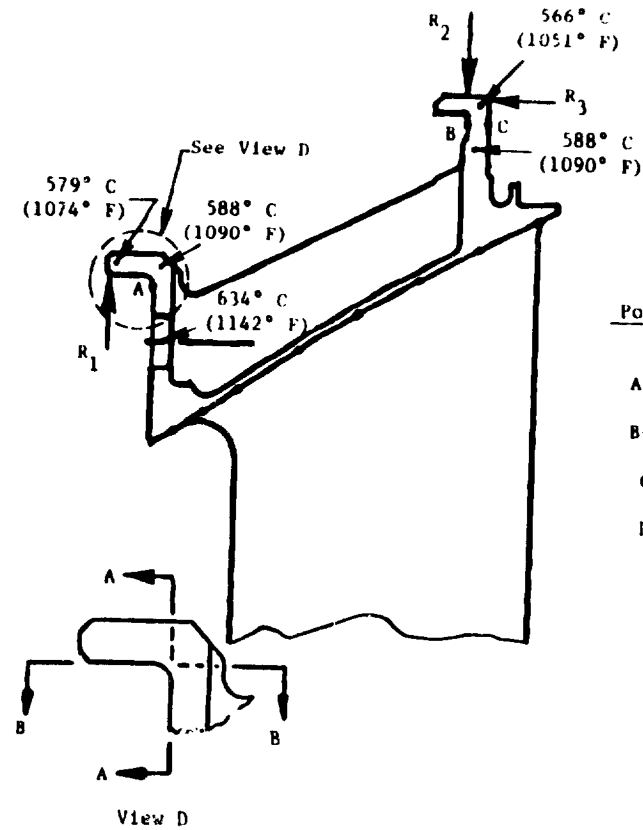

Forces

R_1 = 2.48 MPa (141.87 lb/in.)
R_2 = 2.32 MPa (132.43 lb/in.)
R_3 = 1.41 MPa (80.58 lb/in.)

Point	Stress MPa (ksi)	K_t	Creep/Rupture Life Ratio	LCF Life Ratio
A-A	120.6 (17.5)	1.51	>10	>2
B-B	172.4 (25.0)	1.51	>10	>2
C	-46.9 (-6.8)	1.34	>10	>2
D	34.5 (5.0)	1.0	>10	>2

Figure 77. LPT Stage 1 Nozzle Hook Forces, Temperatures, and Stresses at Takeoff.

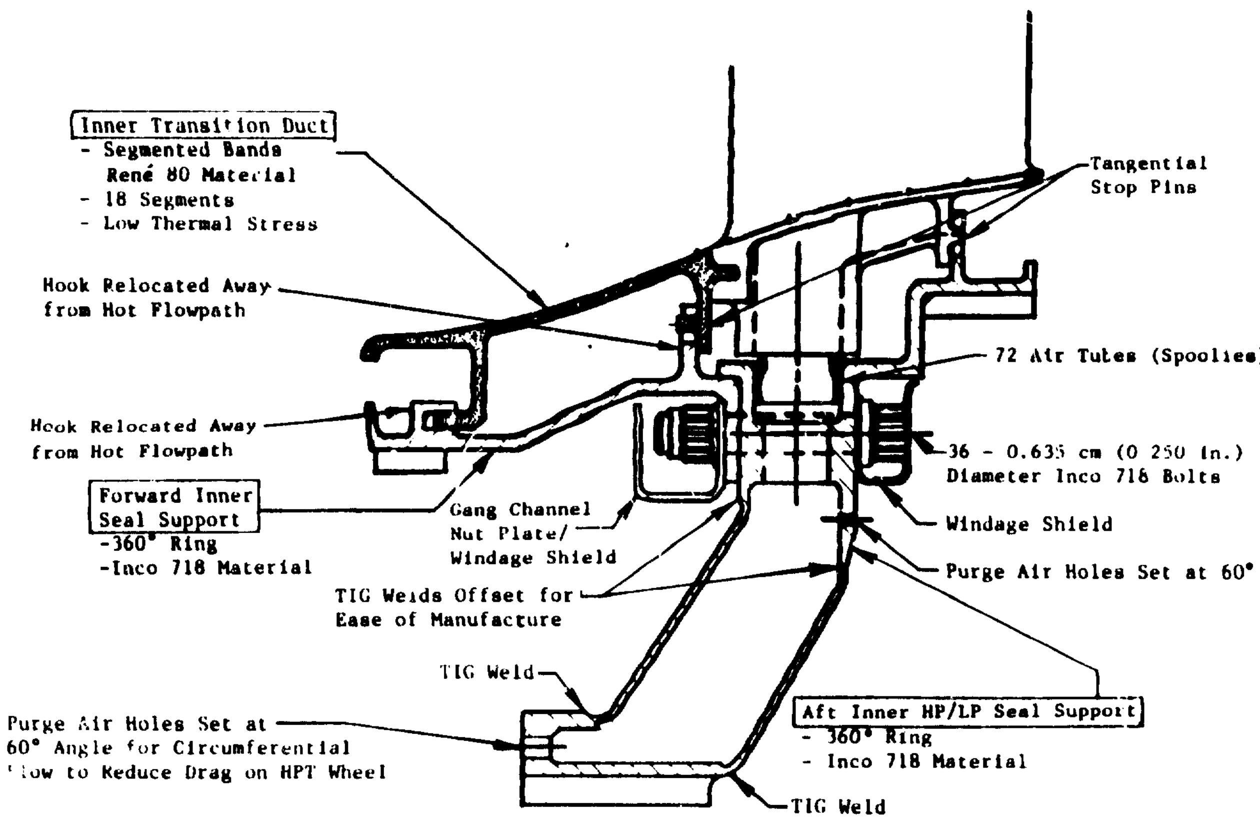

Figure 78. LPT Stage 1 Vane Inner Seal Supports-Features.

One difference between the FPS and ICLS nozzle designs is that the ICLS nozzle will be cast René 77, rather than René 125, in order to reduce cost. The lower creep and rupture life of René 77 will be satisfactory for the planned ICLS testing. Another difference between the two designs is that an integrally cast T_{42} probe pad on the nozzle outer band was eliminated from the ICLS design in order to simplify tooling for the castings. The FPS nozzles will also be Codep coated; the ICLS parts will not.

Inner HPT/LPT Transition Duct

The inner transition duct is similar to the outer in that it is assembled from 18 cast René 80 segments (Figure 78). The duct segments are supported radially in the front by the forward inner seal support and at the rear by slots in the Stage 1 nozzle inner band. The ducts are clamped axially between a flange on the forward inner seal support and the Stage 1 nozzle inner band and are positioned tangentially by pins in the seal-support flange. The duct forward attachment surfaces are coated with Triballoy 800 to reduce wear. The FPS and ICLS designs are identical.

Forward Inner Seal Support

The forward inner seal support configuration (Figure 78) is a 360° ring machined from an Inco 718 forging. This structure provides support for a honeycomb seal located above the Stage 2 HPT blade retainer. Stresses calculated by CLASS/MASS for the maximum stress condition (takeoff) are shown in Figure 79.

Aft Inner Seal Support

The LPT aft inner seal support is shown in Figure 78. This support is fabricated from an Inco 718 ring forging with Inco 718 sheet metal joined to it by tungsten inert gas (TIG) welds. A flash-welded Inco 718 ring that forms the backing for the honeycomb seal is then TIG welded to the sheet metal.

The aft inner seal support has several functions: (1) it provides support for the honeycomb seal over the HPT rotating seals, (2) it ducts fifth-stage cooling air forward to purge the Stage 2 HPT disk cavity, (3) it directs cooling air back to purge the LPT Stage 1-3 rotor cavity, (4) it provides support for a honeycomb seal over the Stage 1 LPT rotating seal, (5) it is a pressure-balance seal between the HPT and LPT, and (6) together with the forward inner seal support, it positions and clamps the inner ducts in place. The calculated temperatures at takeoff along with the predicted pressure loads were used in a CLASS/MASS stress and deflection analysis. Analytical stress values at takeoff are shown in Figure 79.

Miscellaneous Hardware

Other miscellaneous hardware associated with the Stage 1 LPT nozzle subassembly are: (1) air-transfer tubes or "spoolies" which help to seal and

ORIGINAL PAGE IS
OF POOR QUALITY

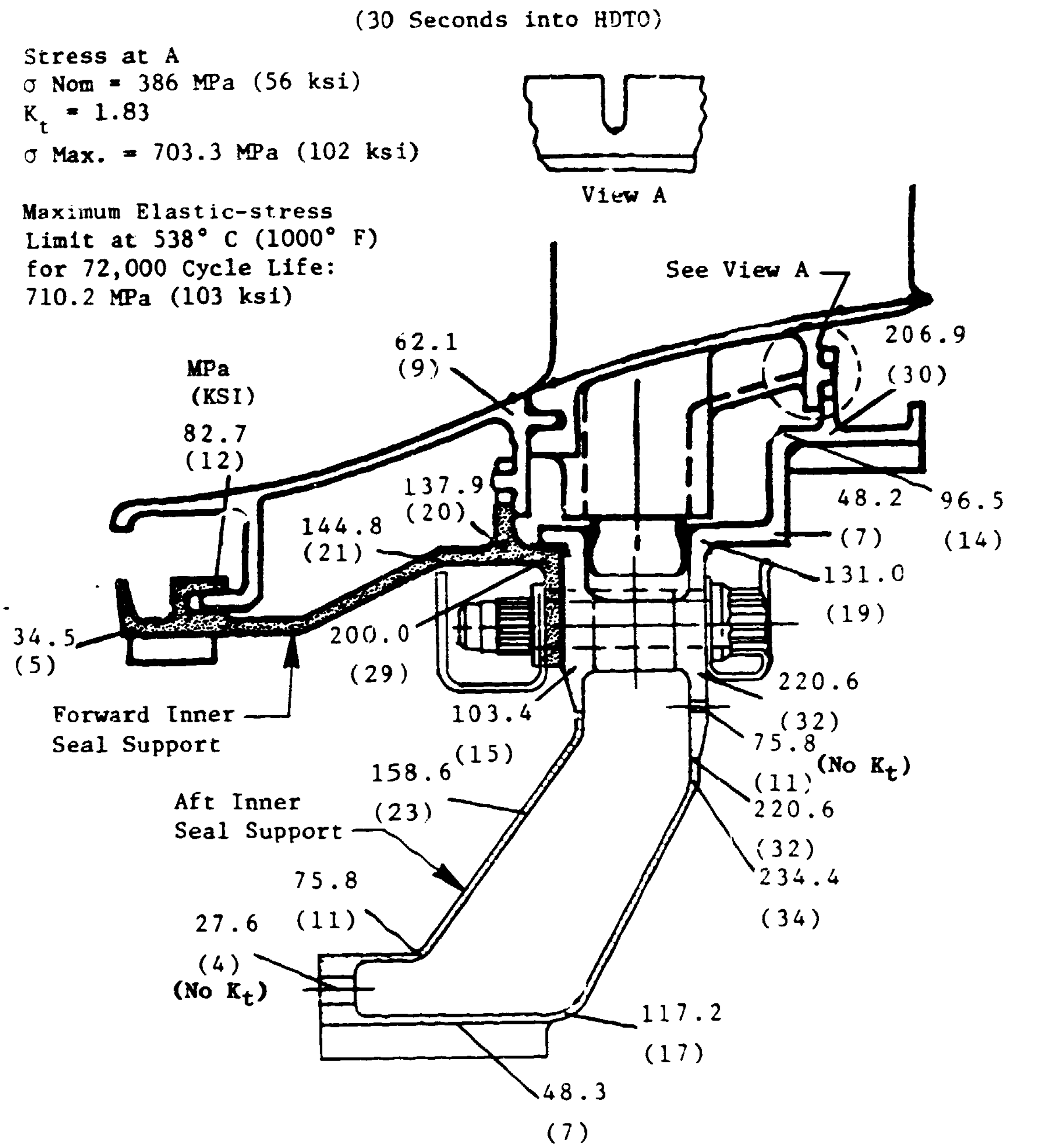

Figure 79. LPT Stage 1 Nozzle Inner Seal Supports: Effective Stresses at 1040 Seconds.

ORIGINAL PAGE IS
OF POOR QUALITY

direct the fifth-stage compressor cooling air from the nozzles into the aft inner seal support, (2) a gang channel nut plate that also serves as a windage shield over the nuts, (3) a windage shield over the heads of the 36 bolts that clamp the forward and aft seal supports together, (4) a heat shield over the flexible arm of the outer-duct support as described earlier, and (5) a splash shield at the fifth-stage purge air inlets to minimize circumferential temperature variations around the outer duct support. Items 1, 2, and 3 are shown in Figure 78, and Items 4 and 5 are shown in Figure 74.

4.3.2 Stages 2 Through 5 Nozzles

Each of the E^3 LPT Stages 2, 3, 4, and 5 stators is cast from René 77. There are six vanes per segment. The quantity of vanes and segments is shown in Figure 80. Stages 2 and 3 nozzle segments have hollow airfoils for reduced weight, but Stages 4 and 5 nozzles are solid. (However, for the ICLS engine, Stages 2 and 3 airfoils will be solid for reduced tooling costs.) All four stages will have uncoated nozzle segments.

Each stage airfoil was analyzed for gas bending stress and life, assuming the airfoil was cantilevered in the axial and tangential directions. The results are shown in Figure 81. Bending stress, LCF, creep, and rupture lives due to reaction loads at the hooks were also calculated for each stage. Figure 82 tabulates the results of the hook calculations for Stage 2. Stresses for Stages 3 through 5 are equal to or less than those shown for Stage 2.

The tangential gas load is transmitted from the nozzle, by means of a slot in the aft rail of each nozzle segment, through a lug brazed into the adjacent shroud. This lug fits into a slot in the LPT casing (Figure 83), thereby transferring the load into the casing. Table XVII shows the tangential gas load for each of the four stages and the resulting shear and bearing stresses.

Table XVII. LPT Stages 2 Through 5 Tangential Load Stop Stresses.

- Hot-Day Takeoff, FPS Baseline

Stages	Tangential Gas Load, N(lbf)/Segment	Load Stop Slug Shear Stress, MPa (ksi)	Nozzle Hook Bearing Stress MPa (ksi)	Casing Hook Bearing Stress, MPa (ksi)
2	2173 (488.5)	63.4 (9.2)	382.6 (55.5)	80.0 (11.6)
3	2288 (514.4)	64.8 (9.4)	443.3 (64.3)	78.6 (11.4)
4	1733 (389.6)	37.2 (5.4)	182.7 (26.5)	55.8 (8.1)
5	1266 (284.7)	33.3 (4.4)	153.3 (22.2)	43.4 (6.3)
Stress Limit		372.3 (54)	517.1 (75)	289.6 (42)

ORIGINAL PAGE IS
OF POOR QUALITY

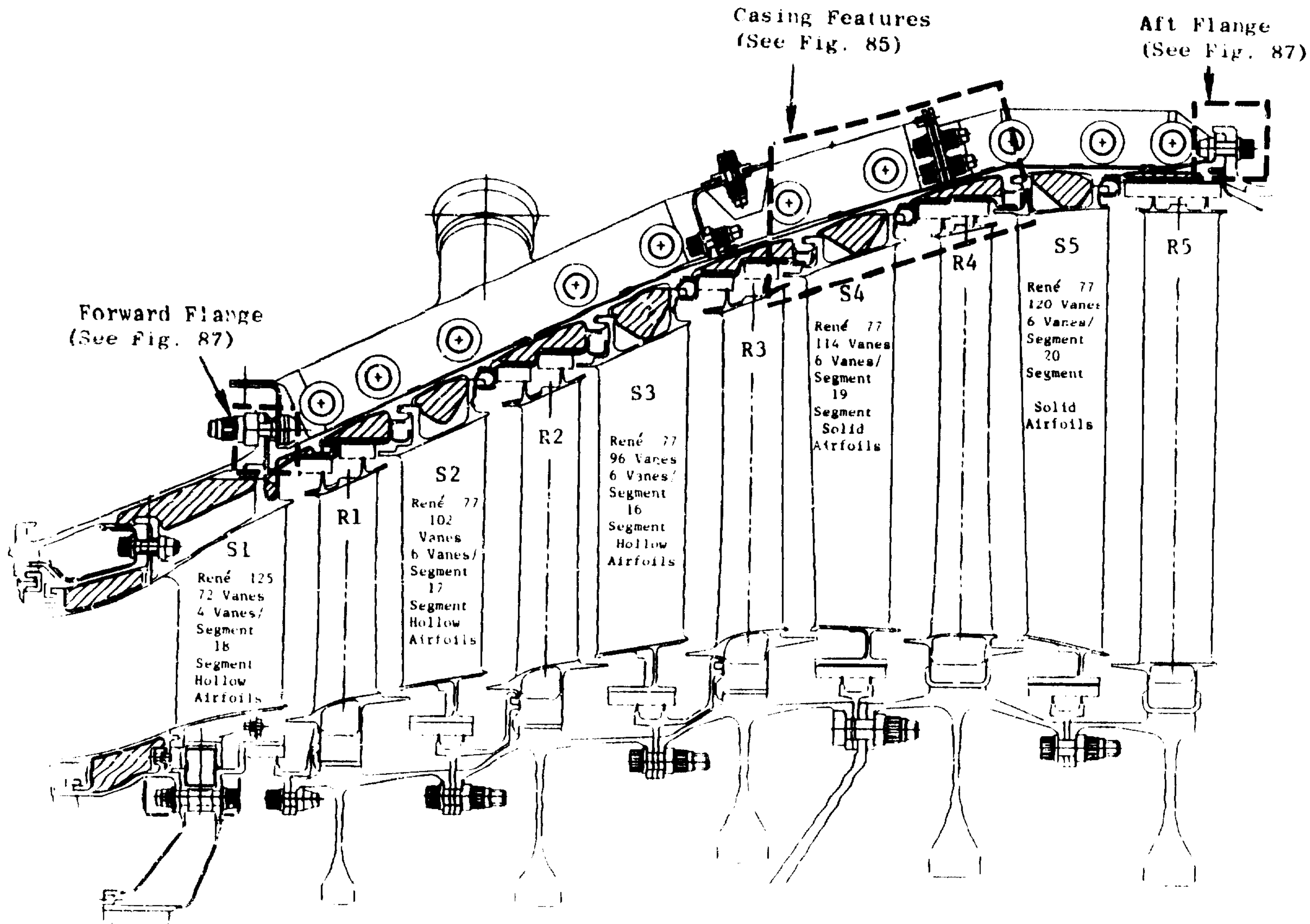

Figure 50. LPT Stator Vane FPS Configuration.

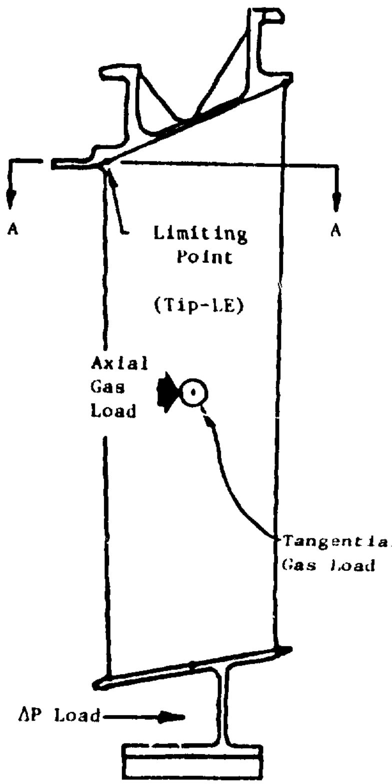

(FPS Baseline)

	Stage 2	Stage 3	Stage 4	Stage 5
Material	Rene' 77	Rene' 77	Rene' 77	Rene' 77
Max. Gas Temp at 95% Span	890° C (1635° F)	821° C (1510° F)	749° C (1380° F)	682° C (1260° F)
Axial Gas Load N/Vane (lb/Vane)	197.8 (44.48)	215.0 (48.33)	139.8 (31.43)	88.4 (19.87)
Tangent Gas Load N/Vane (lb/Vane)	361.3 (81.22)	380.5 (85.53)	288.1 (64.77)	210.5 (47.33)
ΔP Load N/Vane (lb/Vane)	35.9 (8.08)	35.1 (7.90)	14.5 (3.27)	6.0 (1.36)
Stress at LE MPa (ksi), (No K_t)	9.78 (14.18)	10.83 (15.72)	15.5 (22.5)	16.3 (23.70)
K_t	2.02	2.0	2.06	1.98
• Life Margin: Calculated/Allowable				
– 0.2% Creep	1	>10	>10	>10
– Rupture	1.47	>10	>10	>10
– LCF	2	> 2	> 2	> 2

Figure 81. LPT Stages 2 Through 5 Nozzles: Airfoil Stress/Life at Takeoff.

ORIGINAL PAGE IS
OF POOR QUALITY

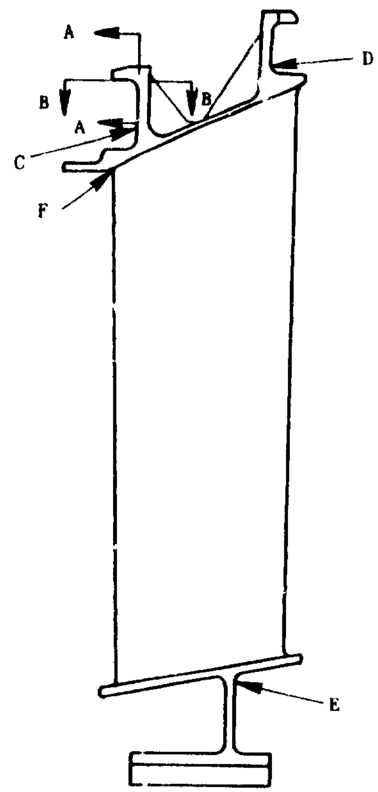

Location	A-A	B-B	C	D	E	F
σ_{Nom} MPa (ksi)	85.5 (12.4)	131 (19.0)	24.1 (3.5)	31.7 (4.6)	62.1 (9.0)	97.8 (14.18)
K_T	1.288	1.288	1.0	≤ 2	≤ 2	2.02
$\sigma_{Max.}$ MPa (ksi)	110.3 (16.0)	168.9 (24.5)	24.1 (3.5)	63.4 (9.2)	124.1 (18.0)	197.5 (28.64)
T, °C (°F)	802 (1475)	802 (1475)	891 (1635)	891 (1635)	835 (1535)	891 (1635)
LCF (Cycles)	$\simeq 10^5$	$\simeq 10^5$	$\geq 10^5$	$\geq 10^5$	$\geq 10^5$	$\simeq 10^5$
0.2% Creep Margin	>10	>10	>10	4.7	3.78	1.0
Rupture Margin	>10	>10	>10	>10	>10	1.47

- Stages 3 - 5 Similar

Figure 82. LPT Stage 2 Nozzle FPS Baseline Stresses/Temperatures at Takeoff.

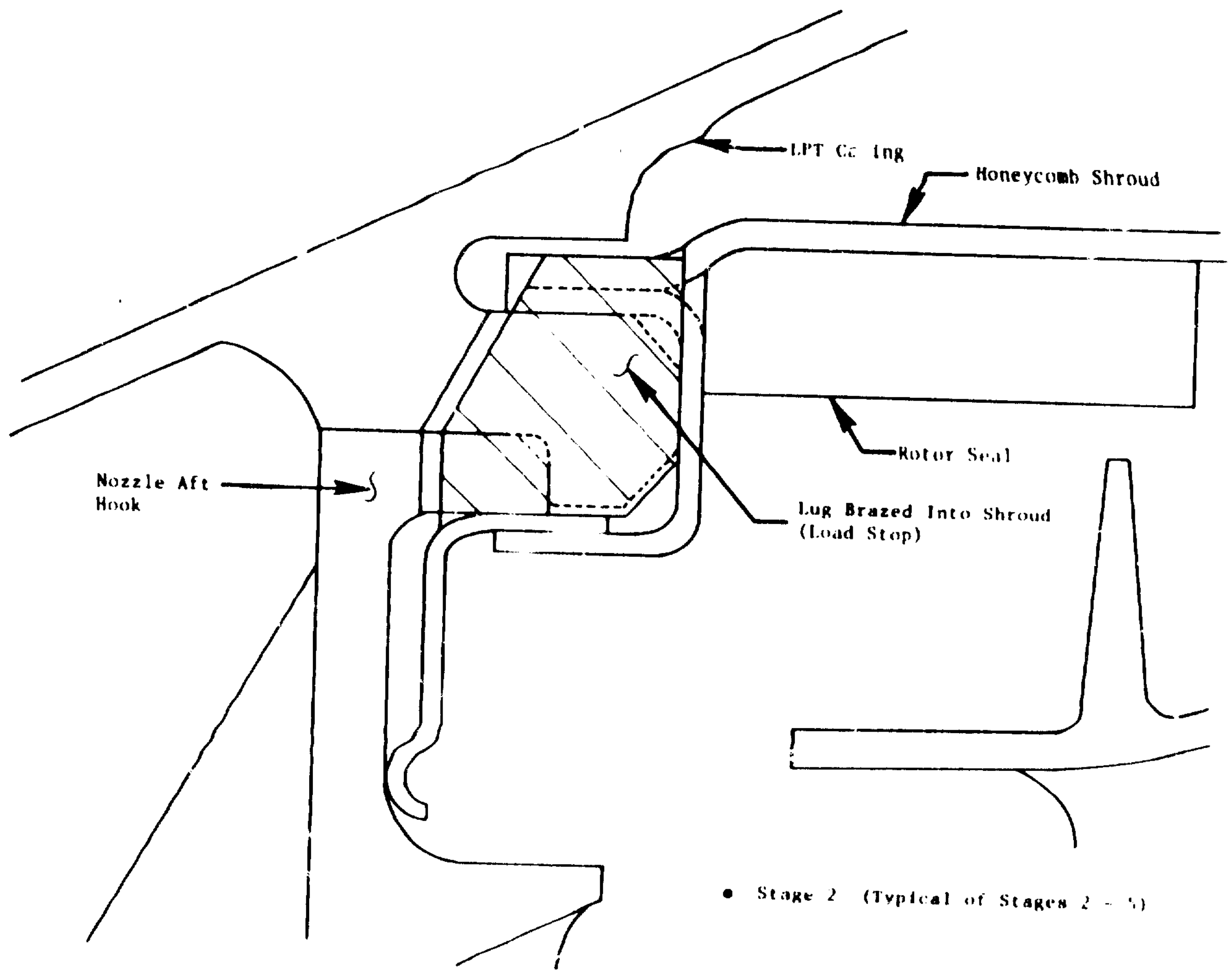

Figure 83. LPT Nozzle and Shroud Tangential Load Stop.

The circumferential gaps between nozzle segments for all five LPT stages were set to minimize leakage between nozzle segments but still prevent arch bind. The overall sealing scheme throughout the LPT stator is shown in Figure 84.

4.3.3 LPT Casing

The E^3 LPT casing is a 360° case fabricated from two Inco 718 cylindrical forgings connected by one circumferential, electron-beam (EB) weld near the axial center. There are no horizontal flanges as on current, commercial turbofan engines. Pads for borescope ports (one for each stage) are EB welded in place. Four local bolt flanges, for attachment of the cooling manifold, are integrally machined into the outer skin. A total of 132 bolts attach the LPT casing flange to the HPT casing flange, and 120 bolts are used to attach the aft frame flange to the aft casing flange. The LPT nozzles attach to the casing by first engaging the front hook with the nozzle segment tilted forward. The nozzle segment is moved forward and tilted back to engage the aft hook. The shroud set is then installed, and this locks the nozzle segments into the casing (Figure 85).

An analysis of the combined effects of thermal and mechanical loads during transient operation was made using the computer model CLASS/MASS. The results were used to calculate stress for "worst case" conditions and to calculate casing deflections. These calculations allowed predictions to be made of cooling effectiveness for the ACC system. Calculated stresses are shown in Figures 86 and 87; LPT clearances based on deflections are addressed later in this report.

Figure 88 indicates that the containment capability of the LPT casing and shrouds is satisfactory for the calculated impact energy of a given E^3 LPT blade, based on the minimum combined thickness for this design.

4.3.4 HPT/LPT Flange Bolt Capability

The HPT/LPT connecting-flange bolts are designed to provide axial containment of the LPT rotor in the event the LPT shaft fails. The bolts selected are 0.79 cm (5/16 in.) in diameter, and in the event of a failure the bolts must absorb the energy generated by the aft motion of the free LPT rotor. This bolt diameter provides more than enough energy aborption capability in the event of failure.

4.4 ACTIVE CLEARANCE CONTROL (ACC)

4.4.1 Approach

The mechanical design of the ACC for the LPT is discussed in Section 3.5 with respect to both purpose and operational characteristics. The basic intent of the design is to allow engine operation with small shroud and seal

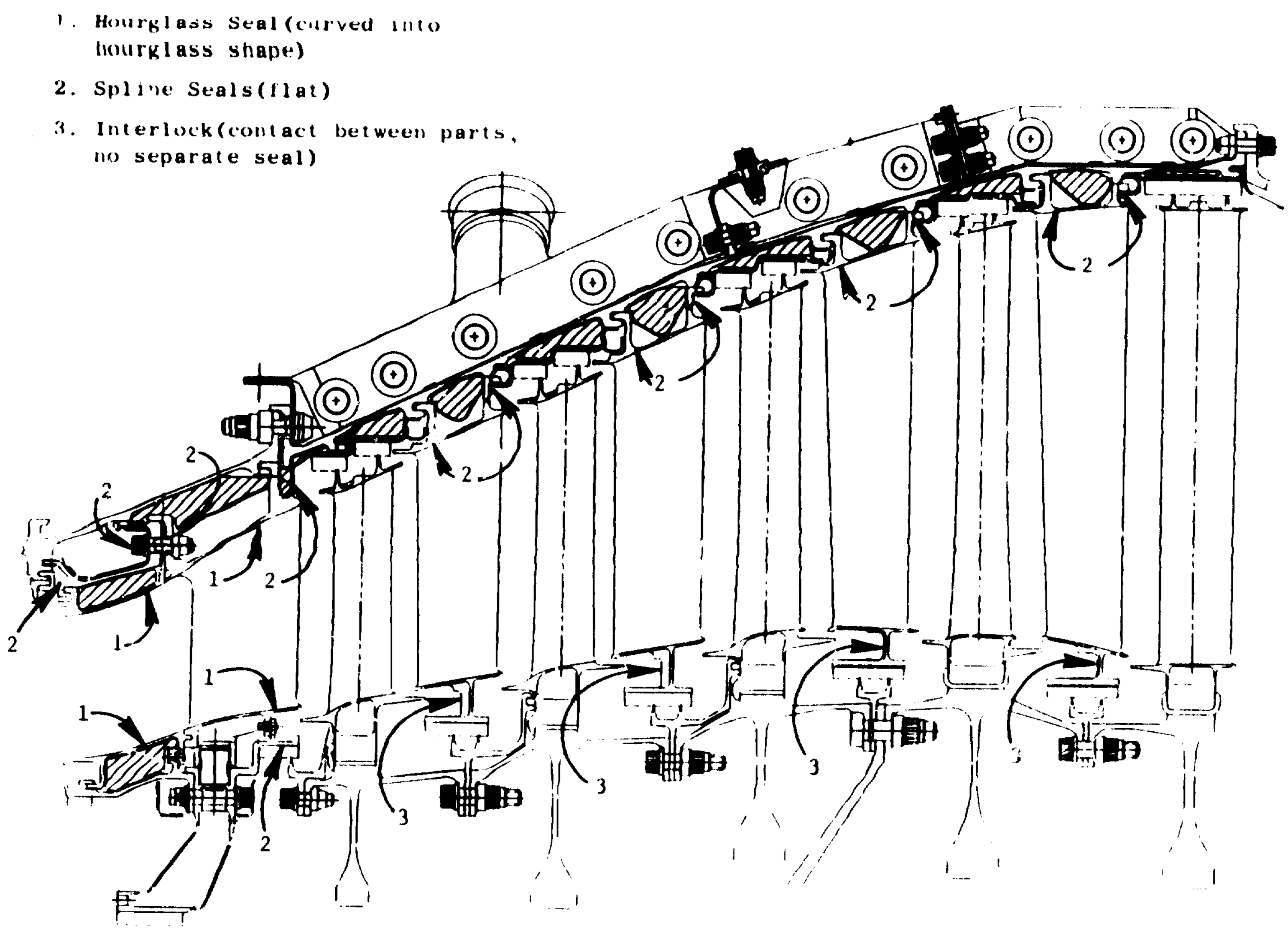

Figure 84. Schematic of LPT Sealing Locations and Configurations.

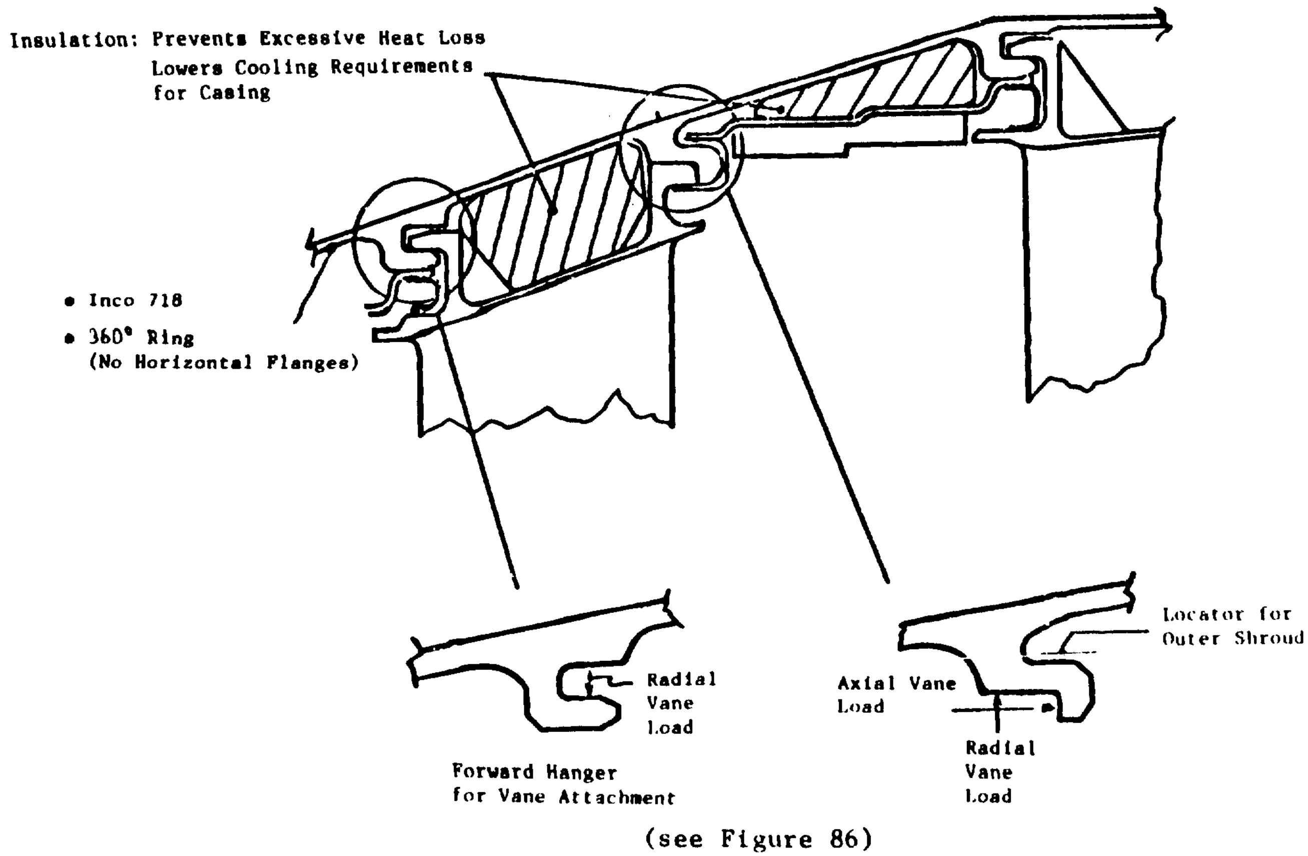

Figure 85. Major Features of the LPT Casing.

(see Figure 80)

Analysis Assumptions:

- Inconel 718 Material Properties Correspond to 72,000 Cycles: A = 1
- 120 Seconds into HDTO

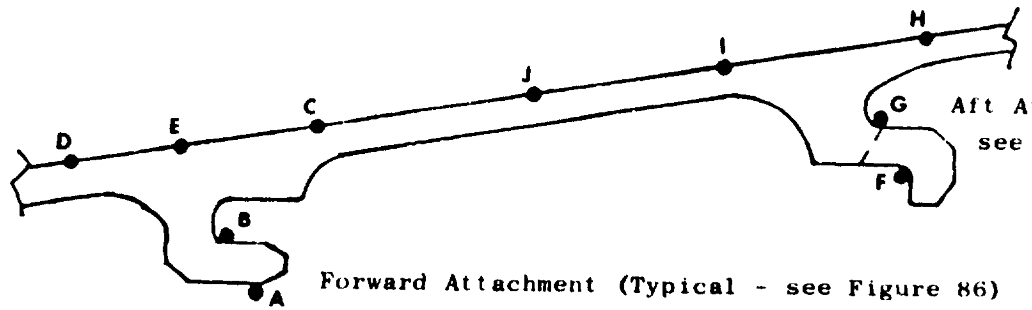

Stresses, MPa (ksi)

	Inner Surfaces					Outer Surfaces						
	Calculated Effective Stress				Allowable Stress at 649° C (1200° F)	Calculated Effective Stress						Allowable Stress at 538° C (1000° F)
Stage	A	B: K_t	F: K_t	G*: K_t		C	D	E	H	I	J	
1	234 (34)	159:1.3 (23:1.3)	- -	- -	786 (114)	- -	- -	276 (40)	- -	- -		703 (102)
2	214 (31)	165:1.8 (24:1.8)	55:1.8 (8:1.8)	241:1.4 (35:1.4)		269 (39)	110 (16)	159 (23)	365 (53)	200 (29)	83 (12)	
3	207 (30)	172:1.8 (25:1.8)	21:1.8 (3:1.8)	303:1.4 (44:1.4)		331 (48)	159 (23)	110 (16)	386 (56)	221 (32)	138 (20)	
4	234 (34)	148:1.8 (21:1.8)	28:1.8 (4:1.8)	372:1.4 (54:1.4)		200 (29)	119 (16)	124 (18)	441 ([illegible])	207 (30)	117 (17)	
5	193 (28)	117:1.8 (17:1.8)	6.9:1.8 (1:1.8)	531:1.4 (77:1.4)		172 (25)	138 (20)	96 (14)	- -	310 (45)	152 (22)	

* Includes Respective K_t Applied to Hoop Stress at Slots for Tangential Load Stops.

Figure 86. Effective Surface Stresses for LPT Casing Attachments.

ORIGINAL PAGE IS OF POOR QUALITY

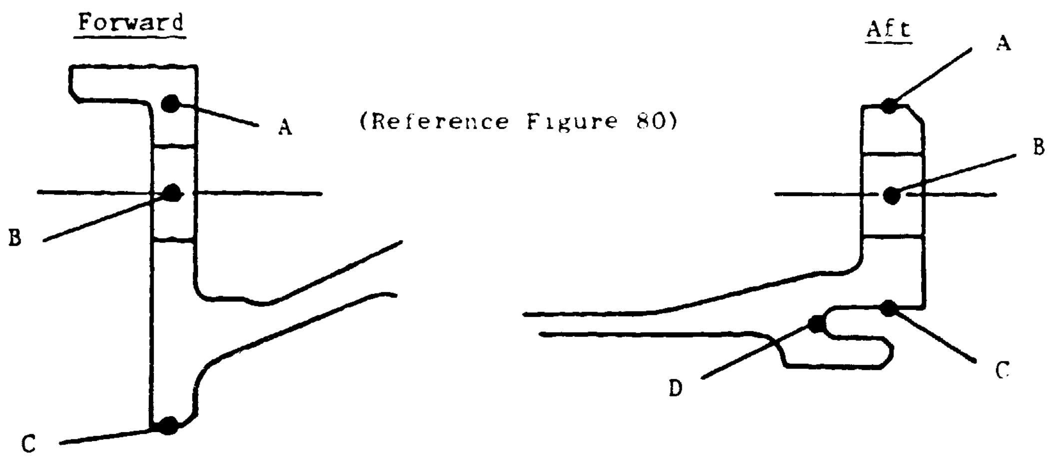

Location		Effective Stress, Most Severe Condition (No K_t) MPa	(ksi)	K_t	LCF Predicted Life, Cycles
Forward:	A	241	(35)	1.4	10^5 or Greater
	B	228	(33)	2.32	
	C*	262	(38)	1.0	
Aft:	A	103	(15)	1.0	
	B	110	(16)	3.02	
	C	75.8	(11)	1	
	D	207	(30)	1.4	

- 120 Seconds into HDTO, Minimum Cooling (Except as Denoted by *)
  (* 30 Seconds into HDTO, Minimum Cooling)
- Conclusion: End Flanges Meet 36,000 Cycle Requirements

Figure 87. End-Flange Stress/Life on LPT Casing Under Maximum Stress Condition.

ORIGINAL PAGE IS
OF POOR QUALITY

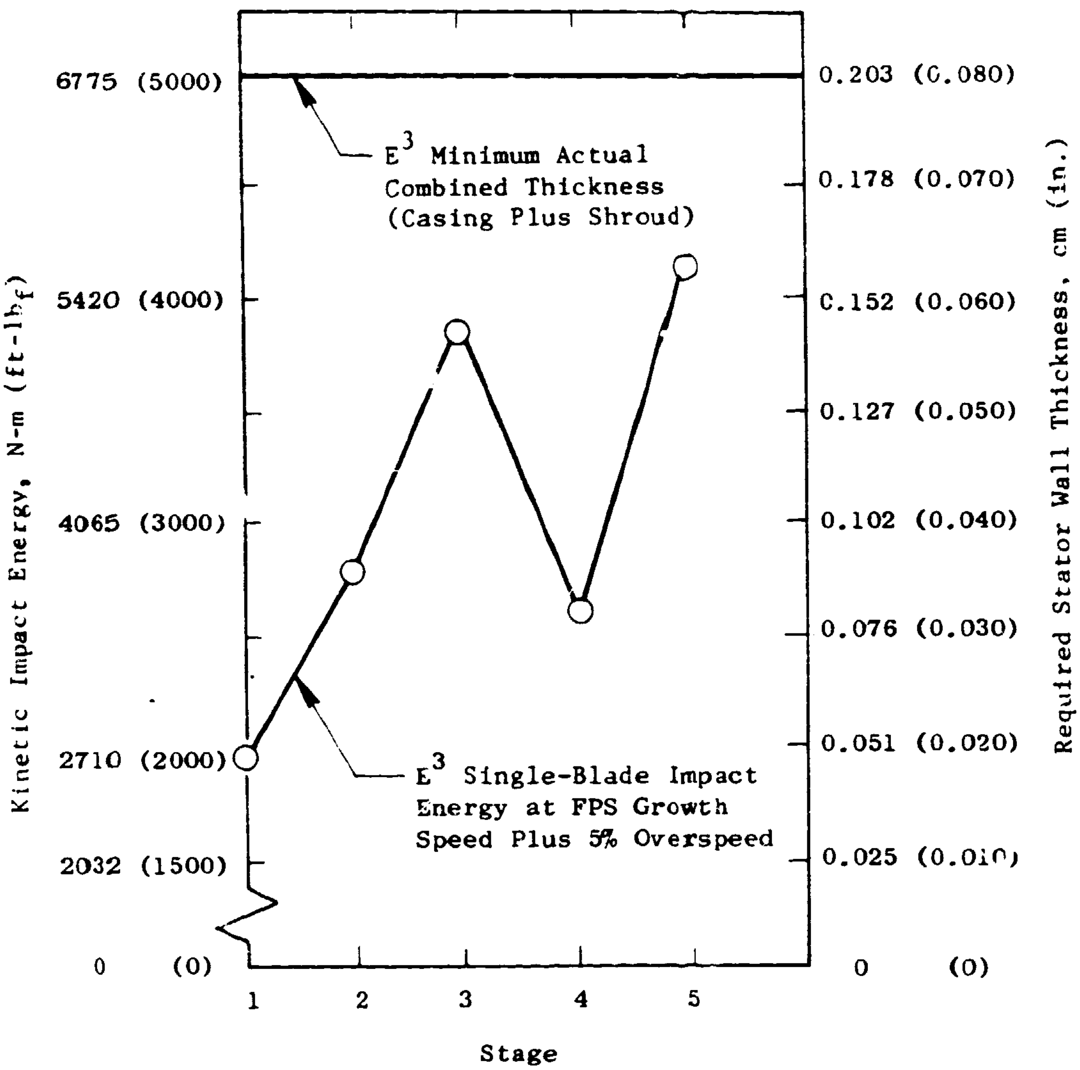

Figure 88. LPT Casing Containment Capability

clearances, compared to current designs, in order to prevent significant deterioration in LPT efficiency. The design provides for the directed distribution of cooling air at appropriate times on the points of shroud and seal attachments, yet the casing configuration will provide adequate life when subjected to the resultant thermal cycling.

The description of the ACC configuration, the LPT clearance improvements it provides, and the stress/life of the components are discussed in the following paragraphs.

4.4.2 Casing Stress/Life

As discussed in Section 4.3.3, the casing, which is the only component significantly stressed by ACC cycling, is fully capable of completing more than the required 36,000 mission cycles.

4.4.3 Cooling Manifold

The air-distribution system for the LPT ACC employs a cooling manifold to deliver air from the fan airflow to be impinged on the LPT case at the outer diameter of the 10 nozzle and shroud support hooks. By controlling the temperatures of these support hooks, the casing size is controlled. This, in turn, controls the shroud seal clearance at the blade tip of all five stages. Thus, the efficiency of the LPT is improved.

The complete LPT cooling manifold is composed of four sectors, each covering a 90° arc (as in Figure 89). Each sector is a backbone/rib-type configuration - i.e., an axial distribution manifold with 10 circumferential tubes extending from each side of the manifold (Figure 90). The axial manifold is further divided into aft and forward parts. The forward part of the manifold contains the seven distribution tubes impinging on the casing over the first four stages of the LPT; the aft portion contains the three distribution tubes impinging on the casing over Stage 5 of the LPT. The forward and aft portions of the manifold are connected by a bolted flange. An orifice plate, installed at engine assembly, allows impingement cooling to be adjusted or eliminated for Stage 5. By testing with various orifice plates, the effectiveness of the ACC cooling and tip clearance control on Stage 5 of the LPT can be assessed accurately.

The cooling manifold, including the tubes and support brackets, is made of 321 stainless steel. The welded and brazed assembly is fabricated of tubing and sheet stock.

The cooling manifold is secured by a forward, middle, and aft mount at the axial manifold backbone and the tube support on each side of the axial manifold. The forward mount is a hard-mounted, bolted joint. The middle mount is a bolted joint spring-mounted to allow axial slip. The aft mount is composed of two pins captured in and protruding from the LPT aft flange.

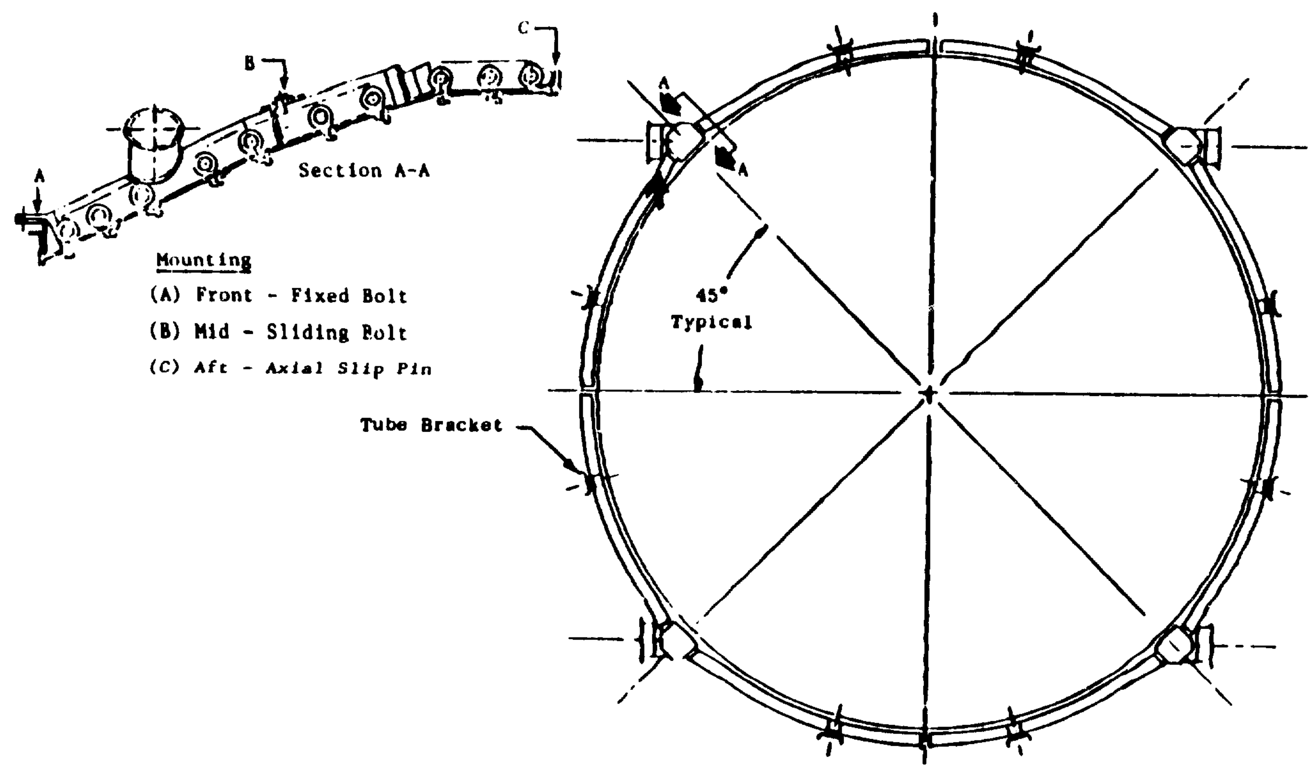

Figure 89. LPT Cooling Manifold (Axial View).

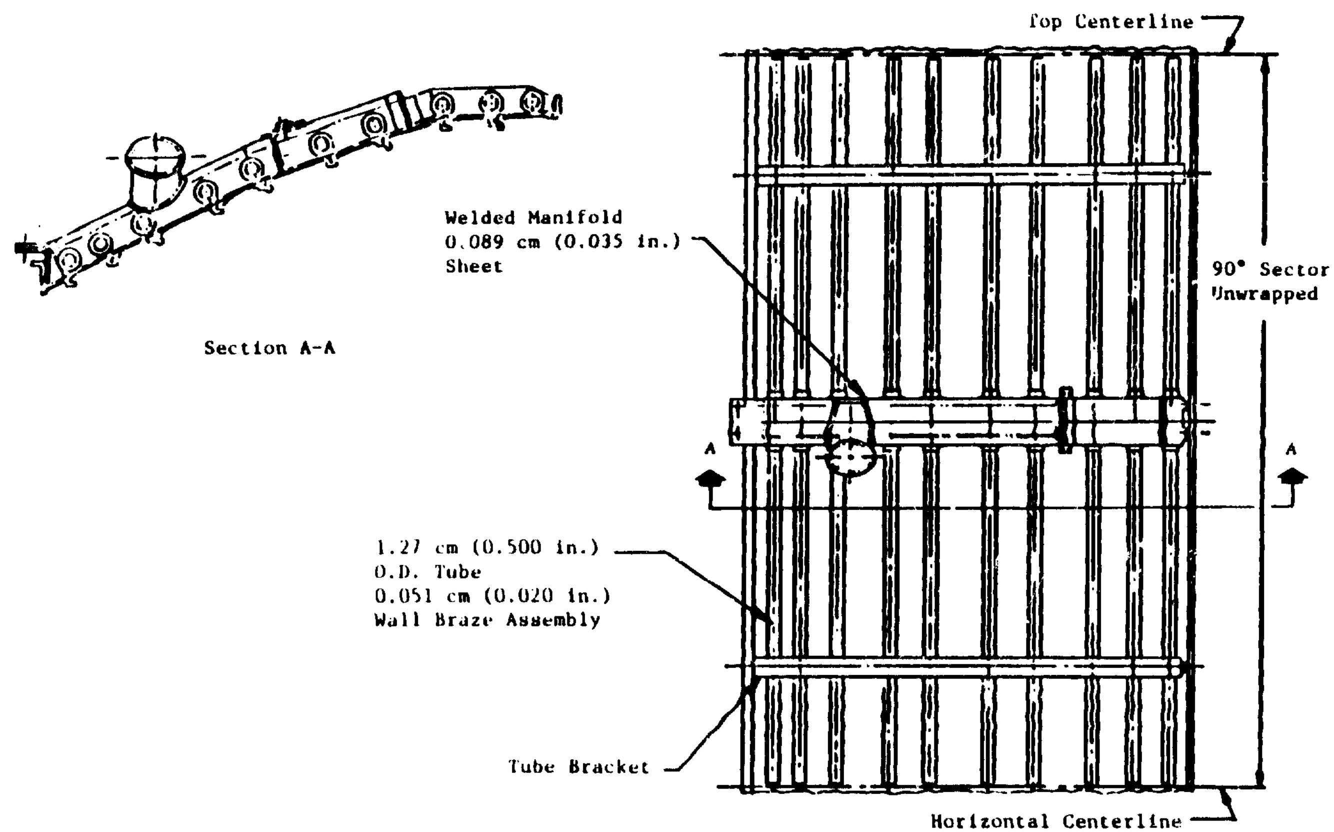

Figure 90. LPT Cooling Manifold (Unwrapped View).

These pins engage the aft end of the manifold and the tube supports, allowing axial slip. By allowing axial slip at the middle and aft supports, differential thermal expansion between the LPT case and the cooling manifold is accommodated.

Another feature of the cooling manifold mounting is the capability of separating the HPT/LPT casing interface flange without requiring the removal of the cooling manifold. This is accomplished by positioning the forward mount brackets on the aft side of the bolted flange and designing the HPT/LPT flange bolts to be inserted from the aft side of the flange. Another important benefit of this bolting arrangement is the small envelope required by the bolt head versus the large envelope required by a nut and protruding bolt threads with the large associated tolerance buildup. The smaller head envelope allows the front tube of the cooling manifold to be positioned over the front shroud support hook without compromising the impingement distance of the cooling air.

4.4.4 Clearance Predictions

Small rotor-to-shroud radial clearances are extremely difficult to achieve and maintain because of the varying dimensional changes of the rotor and shroud that are brought about by operational changes (Figure 91).

With this background, the approach for setting close clearances in the E^3 LPT is as follows:

- For the full aircraft mission, determine radial dimension changes for the rotor and shrouds, separately. These assume "round engine" conditions.
- Determine clearance deviation values from "round engine" values (e.g., maneuvering, concentricity, etc.).
- Evaluate closure capability of ACC system.
- Include abradable characteristics of blade and shroud (e.g., wear ratio).

Using this approach, the results of "round engine" clearances for the Stage 1 rotor and shroud (casing) are illustrated in Figure 92. The presented data cover the range of aircraft operating points from ground idle (GIDLE) through takeoff (T.O.), maximum climb (MXCL), a transient chop to flight idle (FIDLE), then reacceleration (REBURST), out to maximum cruise (MXCR), and cruise (CR). Superimposed on a normal casing-clearance trace are the reduced casing clearances at MXCR and CR with full ACC cooling air on.

Continuing this approach, with Stage 1 as an example, Table XVIII shows the calculated out-of-round deflections. Clearance changes are presented for various sources such as beam bending, vibration, and ovalization and are shown

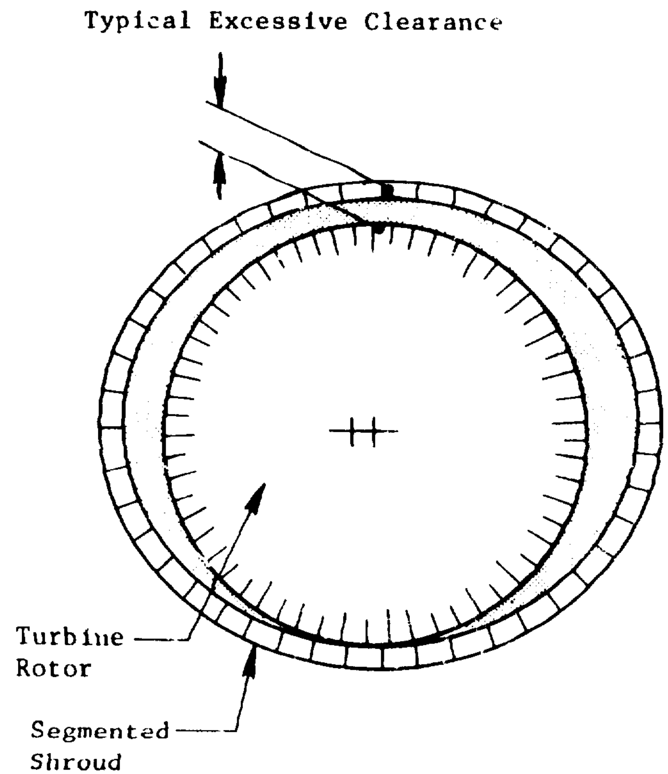

Sources of Excessive Rotor/Shroud Clearance:

Symmetric	Asymmetric
● Transient Heating/ Cooling	Nonconcentricity
● Rotor Centrifugal Field	Out-of-Round
	Maneuver Loads

Figure 91. Schematic of Sources of Excessive Clearance Between the Turbine Rotor and Shroud.

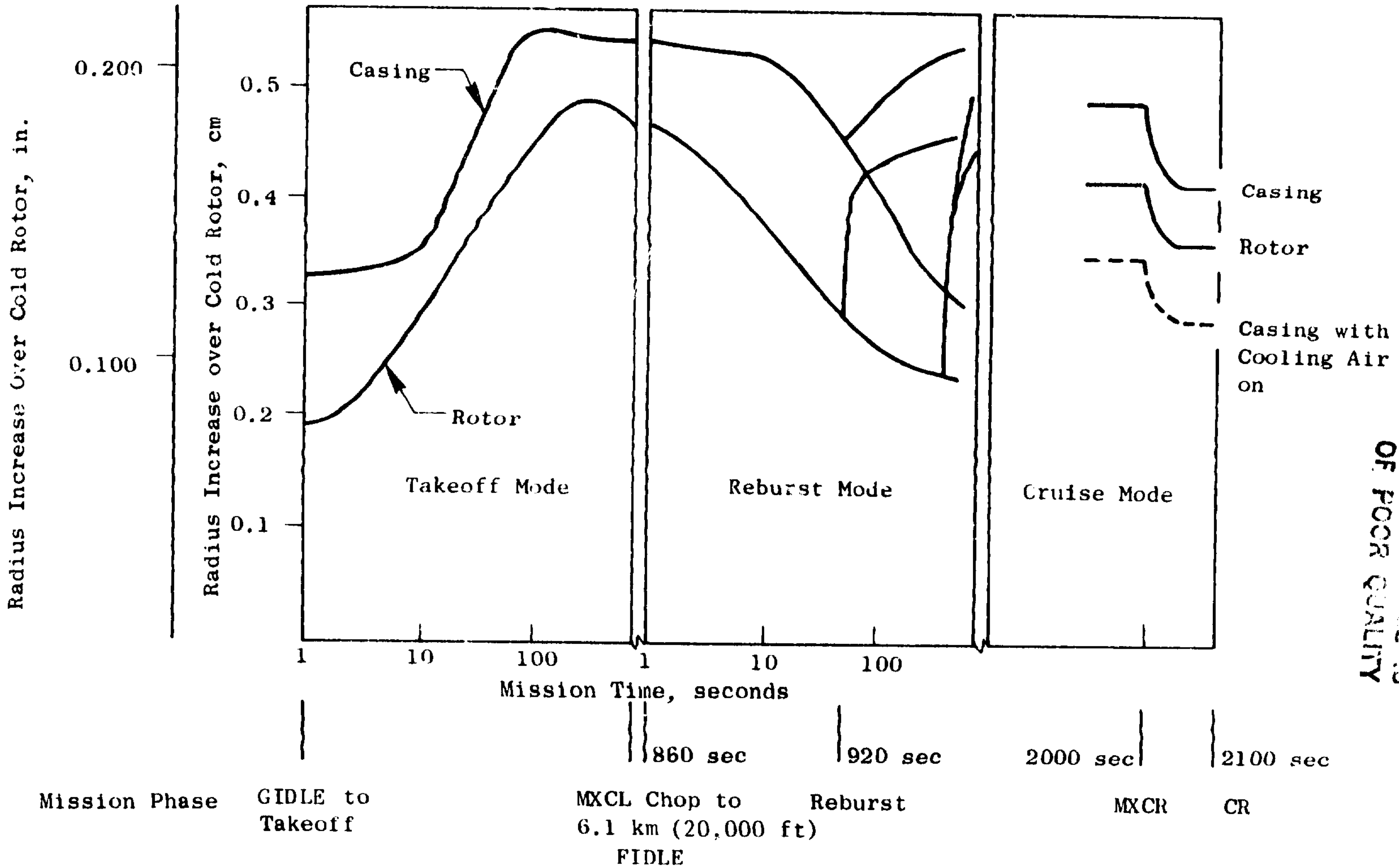

Figure 92. LPT Stage 1 Basic Relative Diameters.

Table XVIII. FPS LPT Stage 1 Clearance Change for Maximum Closure.

Out-of-Round Factors	Clearance Change = mm (mils), Closure = − Clock Position 3	9	12	6
Takeoff Rotation				
Beam Bending	-0.244 (-9.62)	-0.244 (-9.62)	-0.114 (-4.74)	-0.066 (-2.59)
Vibration	-0.076 (-3.00)	-0.076 (-3.00)	-0.076 (-3.00)	-0.076 (-3.00)
Ovalization	-0.028 (-1.12)	-0.037 (-1.47)	+0.027 (+1.05)	+0.041 (+1.60)
Sum	-0.348 (-13.74)	-0.357 (-14.09)	-0.193 (-6.69)	0.031 (-3.99)
2nd Segment Climb				
Beam Bending	-0.330 (-12.99)	-0.330 (-12.99)	-0.390 (-15.36)	-0.460 (-18.12)
Vibration	-0.076 (-3.00)	-0.076 (-3.00)	-0.076 (-3.00)	-0.076 (-3.00)
Ovalization	-0.024 (-0.96)	-0.036 (-1.41)	+0.029 (+1.14)	+0.034 (+1.34)
Sum	-0.430 (-16.95)	-0.442 (-17.40)	-0.437 (-17.22)	-0.502 (-19.78)
Low Mach Cruise				
Beam Bending	-0.104 (-4.09)	-0.104 (-4.09)	-0.139 (-5.49)	-0.182 (-7.15)
Vibration	-0.076 (-3.00)	-0.076 (-3.00)	-0.076 (-3.00)	-0.076 (-3.00)
Ovalization	-0.018 (-0.71)	-0.025 (-1.00)	+0.021 (+0.81)	+0.024 (+0.94)
Sum	-0.198 (-7.80)	-0.205 (-8.09)	-0.194 (-7.68)	-0.234 (-9.21)
Rotor (Root Mean Squares)				
No Assy. Tip Grind	0.0003 (±0.010)	0.0003 (±0.010)	0.0003 (±0.010)	0.0003 (±0.010)
With Assy. Tip Grind	0.00005 (±0.002)	0.00005 (±0.002)	0.00005 (±0.002)	0.00005 (±0.002)

ORIGINAL PAGE IS
OF POOR QUALITY

for engine operation at three major points: takeoff rotation, climb, and cruise. Deflection values are given at each quadrant (3, 6, 9, 12 o'clock); these are the expected peak-deflection locations. Also listed is the cummulative stackup tolerance of the rotor assembly.

The combination of round-engine deflections with out-of-round imposed deflections is shown in Table XIX. The shroud/seal diameters are selected such that round-engine clearance is zero initially (rotor/shroud touching) at the minimum closure point (takeoff), and operating gaps are larger at all other operating conditions. With calculated out-of-round values added, a maximum rub of 0.036 cm (0.014 in.) occurs during takeoff and opens up all clearances to the "resultant gap" values. Reduction of the large resultant gaps (Table XIX) to the desired 0.038 cm (0.015 in.) gap requires ACC closures, as shown, which are well within the capability of the system.

A summary of LPT clearance values is shown in Table XX. This indicates that new engine clearances will be exceptionally good and much better than the 0.038 cm (0.015 in.) goal. With extended operating time and assuming maximum service conditions (imposed out-of-round conditions), clearances would progressively open to slightly greater than the goal value.

4.5 WEIGHT STATUS

A summary of weights for the LPT components in the FPS design is presented in Table XXI. All major components are represented for the rotor and stator assemblies. As indicated, the rotor and stator assemblies are approximately equal in weight (254.4 versus 250.4 kg). Although not indicated, the airfoils account for more than half of the total weight.

Table XIX. Typical LPT Stage 1 Combined Clearance Calculation.

Flight Condition	Tip Clearance Round Engine cm (in.)	Out-of-Round Imposed cm (in.)	Single Point Rub cm (in.)	Resultant Gap cm (in.)	ACC Closure: Need for 0.038 cm Gap (0.015 in.) cm (in.)	ACC Closure: Capability cm (in.)
Cold Assembly	0.050 (0.023)	—	—	0.094 (0.037)	—	—
Takeoff	(0)	0.036 (0.014)	-0.036 (-0.014)*	0.036 (0.014)	—	—
Max. Climb	0.066 (0.026)	0.051 (0.020)	+0.015 (+0.006)	0.102 (0.040)	0.064 (0.025)**	0.163 (0.064)
Cruise	0.091 (0.036)	0.023 (0.009)	+0.069 (+0.027)	0.127 (0.050)	0.089 (0.035)	0.163 (0.064)

*Limiting Rub Point

**Will Be Rubbed Out Again

Table XX. Summary of LPT Clearance Calculations.

Stages	Critical Operating Point	ACC Closure cm (in.)		Operating Clearance with 0.004 Rotor Tolerance cm (in.)	
		Needed	Capability	New	After Max. Service
1	Takeoff	0.064 (0.025)	0.163 (0.064)	0.010 (0.004)	0.061 (0.024)
3	Takeoff	0.069 (0.027)	0.163 (0.064)	0.010 (0.004)	0.038 (0.015)
5	Takeoff	0.114 (0.045)	0.142 (0.056)	0.010 (0.004)	0.094 (0.037)

Goal of 0.038 cm (0.015 in.) Operating Clearance:

- Achieved on All Stages on New Engine
- Over Goal if Subjected to Max. Service Environment

Table XXI. LPT Weight Summary.

Rotor Blade Stage	Weight kg (lb)	Stator Vane Stage	Weight kg (lb)
1	21.3 (47)	1	26.8 (59)
2	24.9 (55)	2	22.7 (50)
3	31.7 (70)	3	27.6 (61)
4	29.0 (64)	4	31.3 (69)
5	28.1 (62)	5	33.1 (73)
Disk Stage			
1	14.1 (31)	Casing, ACC Manifold	59.0 (130)
2	17.7 (39)	Seals, Ring, Fasteners	49.9 (110)
3	22.2 (49)		250.4 (552)
4	23.6 (52)		
5	20.0 (44)		
Seals, Retainers, Fasteners	21.8 (48)		
	254.4 (561)		

Total Weight = 504.8 kg (1113 lb)

APPENDIX

LPT Airfoil Coordinates

ORIGINAL PAGE IS
OF POOR QUALITY

Suction Surface

Z	R	RTHETA
2.694786	13.122117	0.030561
2.696492	13.122778	0.016558
2.703018	13.125302	0.002359
2.714366	13.129676	-0.011913
2.730552	13.135881	-0.026059
2.751585	13.143883	-0.039810
2.777482	13.153642	-0.052830
2.808266	13.165107	-0.064734
2.843956	13.178217	-0.075092
2.884575	13.192898	-0.083455
2.930147	13.209066	-0.089362
2.980693	13.226624	-0.092366
3.036236	13.245463	-0.092053
3.073814	13.257939	-0.089972
3.073814	13.257939	-0.089972
3.130784	13.276438	-0.084117
3.187758	13.294437	-0.075142
3.244626	13.311903	-0.063115
3.301316	13.328817	-0.048166
3.357746	13.345099	-0.030356
3.413857	13.360700	-0.009794
3.469594	13.375772	0.013460
3.524908	13.390312	0.039347
3.579780	13.404324	0.067763
3.634173	13.417810	0.098678
3.688089	13.430779	0.131991
3.741512	13.443240	0.167661
3.794449	13.455096	0.205622
3.846904	13.466571	0.245827
3.898903	13.477725	0.288205
3.950445	13.488562	0.332736
4.001573	13.499098	0.379347
4.052293	13.509339	0.428027
4.102650	13.519299	0.478724
4.152678	13.528989	0.531400
4.202398	13.538452	0.586041
4.251360	13.547836	0.642604
4.301093	13.557159	0.701074
4.350142	13.566429	0.761415
4.399054	13.575655	0.823624
4.447862	13.584844	0.887682
4.496606	13.594004	0.953568
4.545331	13.603142	1.021258
4.594090	13.612388	1.090703
4.642917	13.621965	1.161862
4.691873	13.631642	1.234685
4.741005	13.641427	1.309137
4.782538	13.649756	1.373048

Pressure Surface

Z	R	RTHETA
2.694786	13.122117	0.030561
2.697191	13.123049	0.040420
2.703402	13.125450	0.050067
2.713414	13.129310	0.059448
2.727224	13.134609	0.068494
2.744829	13.141320	0.077134
2.766226	13.149413	0.085330
2.791417	13.158850	0.093110
2.820410	13.169590	0.100619
2.853220	13.181587	0.108169
2.897383	13.197474	0.117819
2.944431	13.214067	0.127954
2.991263	13.230245	0.138285
3.037883	13.246015	0.149255
3.037883	13.246015	0.149255
3.084424	13.261422	0.161003
3.131018	13.276513	0.1736[illegible]4
3.177773	13.291319	0.187395
3.224764	13.305859	0.202235
3.272073	13.320154	0.213286
3.319756	13.334212	0.235653
3.367871	13.347946	0.254404
3.416465	13.361415	0.274397
3.465558	13.374695	0.296331
3.515188	13.387787	0.319647
3.565352	13.400680	0.344633
3.616064	13.413365	0.371327
3.667320	13.425830	0.399821
3.719114	13.438063	0.430134
3.771422	13.449988	0.462344
3.824244	13.461642	0.496469
3.877536	13.473168	0.532577
3.931292	13.484560	0.570681
3.985469	13.495803	0.610832
4.040031	13.506883	0.653068
4.094959	13.517791	0.697403
4.150202	13.528514	0.743880
4.205728	13.539084	0.792516
4.261496	13.549662	0.843336
4.317459	13.560254	0.896364
4.373582	13.570853	0.951622
4.429826	13.581451	1.009148
4.486146	13.592040	1.068936
4.542489	13.602610	1.130990
4.598818	13.613312	1.195277
4.655072	13.624361	1.261774
4.711[illegible]05	13.635483	1.330465
4.758318	13.644892	1.389989

LPT Stator 1 Airfoil Coordinates,

10% From Hub

Suction Surface
Suction Surface

Z	R	RTHETA
2.695141	14.432846	0.030556
2.696609	14.433523	0.017093
2.703456	14.436673	0.003187
2.715697	14.442292	-0.011030
2.733349	14.450362	-0.025339
2.756441	14.460863	-0.039438
2.785008	14.473766	-0.052949
2.819094	14.489033	-0.065419
2.858742	14.506616	-0.076340
2.904007	14.526460	-0.085142
2.954944	14.548498	-0.091216
3.011612	14.572652	-0.093923
3.016001	14.574507	-0.093971
3.016001	14.574507	-0.093971
3.073725	14.598685	-0.092561
3.131757	14.622590	-0.087396
3.189947	14.646156	-0.078559
3.248138	14.669318	-0.066073
3.306200	14.692024	-0.050051
3.364014	14.714167	-0.030547
3.421471	14.735717	-0.007625
3.478493	14.756759	0.018624
3.533014	14.777279	0.048121
3.590980	14.797265	0.080776
3.646358	14.816717	0.116520
3.701114	14.835633	0.155286
3.755255	14.854011	0.196988
3.808775	14.871592	0.241560
3.861673	14.888852	0.288954
3.913972	14.905804	0.339103
3.965695	14.922459	0.391961
4.016865	14.938828	0.447482
4.067528	14.954930	0.505612
4.117719	14.970777	0.566312
4.167458	14.986380	0.629564
4.216813	15.001891	0.695310
4.265810	15.017432	0.763541
4.314506	15.033017	0.834213
4.362938	15.048657	0.907299
4.411159	15.064366	0.982811
4.459218	15.080158	1.060684
4.507159	15.096047	1.140902
4.555017	15.112044	1.223441
4.602860	15.128425	1.308234
4.650716	15.145297	1.395230
4.698645	15.162444	1.484369
4.746698	15.179887	1.575613
4.788324	15.195200	1.656095

Pressure Surface

Z	R	RTHETA
2.695141	14.432846	0.030556
2.698338	14.434319	0.040522
2.706045	14.437863	0.050009
2.718250	14.443461	0.058872
2.734937	14.451086	0.066936
2.756093	14.460705	0.074084
2.781728	14.472289	0.080389
2.811879	14.485813	0.086285
2.846640	14.501269	0.092763
2.851788	14.503546	0.093786
2.899306	14.524411	0.104099
2.945928	14.544620	0.114636
2.992048	14.564357	0.125868
2.992048	14.564357	0.125868
3.037780	14.583676	0.138157
3.083273	14.602645	0.151587
3.128677	14.621331	0.166278
3.174149	14.639798	0.182296
3.219820	14.658097	0.199777
3.265810	14.676271	0.218820
3.312226	14.694357	0.239495
3.359149	14.712327	0.261937
3.406645	14.730189	0.286237
3.454766	14.748045	0.312499
3.503548	14.765897	0.340819
3.553023	14.783746	0.371263
3.603186	14.801581	0.403933
3.654041	14.819390	0.438907
3.705592	14.837165	0.476231
3.757813	14.854854	0.515976
3.810682	14.872216	0.558189
3.864178	14.889666	0.602918
3.918252	14.907186	0.650219
3.972871	14.924761	0.700124
4.028013	14.942380	0.752650
4.083613	14.960019	0.807845
4.139641	14.977666	0.865718
4.196042	14.995346	0.926304
4.252780	15.013285	0.989608
4.309801	15.031505	1.055651
4.367055	15.049993	1.124445
4.424499	15.068736	1.196053
4.482097	15.087724	1.270405
4.539780	15.106936	1.347498
4.597517	15.126557	1.427273
4.655248	15.146908	1.509682
4.712922	15.167601	1.594699
4.762657	15.185736	1.670210

LPT Stage 1 Airfoil Coordinates

50% From Hub

ORIGINAL PAGE IS
OF POOR QUALITY

Suction Surface

Z	R	RTHETA
2.695176	15.657798	0.030556
2.696574	15.658738	0.018183
2.703170	15.663172	0.005333
2.714975	15.671089	-0.007896
2.732002	15.682474	-0.021345
2.754276	15.697303	-0.034793
2.781824	15.715543	-0.047959
2.814679	15.737152	-0.060497
2.852882	15.762079	-0.072010
2.896477	15.790265	-0.082048
2.945512	15.821638	-0.090106
3.000044	15.856117	-0.095633
3.014307	15.865064	-0.096537
3.014307	15.865064	-0.096537
3.071924	15.900903	-0.097962
3.130124	15.936614	-0.095757
3.188708	15.972061	-0.089890
3.247524	16.007145	-0.080351
3.306421	16.041773	-0.067124
3.365245	16.075771	-0.050206
3.423842	16.109067	-0.029634
3.482073	16.141716	-0.005424
3.539831	16.173669	0.022349
3.597011	16.204877	0.053634
3.653540	16.235316	0.086352
3.709365	16.264971	0.126417
3.764449	16.293799	0.167755
3.818758	16.321775	0.212306
3.872289	16.[illegible]9129	0.259982
3.925053	16.375878	0.310703
3.977061	16.402034	0.364409
4.028346	16.427624	0.421029
4.078947	16.452676	0.480505
4.128905	16.477218	0.542778
4.178268	16.501300	0.607801
4.227097	16.525100	0.675509
4.275458	16.548644	0.745857
4.323394	16.571954	0.818801
4.370996	16.595074	0.894281
4.418315	16.618031	0.972286
4.465419	16.640857	1.052759
4.512385	16.663590	1.135658
4.559269	16.686257	1.220937
4.606137	16.709060	1.308521
4.653073	16.732050	1.398317
4.700163	16.755153	1.490242
4.747464	16.778398	1.584247
4.788697	16.798692	1.667427

Pressure Surface

Z	R	RTHETA
2.695176	15.657798	0.030556
2.698280	15.659886	0.039654
2.705744	15.664899	0.048271
2.717558	15.672819	0.056294
2.733707	15.683611	0.063591
2.754186	15.697244	0.070100
2.779007	15.713683	0.075941
2.808215	15.732913	0.081573
2.841908	15.754940	0.087977
2.851944	15.761469	0.090064
2.900030	15.792550	0.101185
2.947201	15.822712	0.112763
2.993695	15.852125	0.125029
2.993695	15.852125	0.125029
3.039509	15.880800	0.138348
3.084805	15.908849	0.152704
3.129784	15.936407	0.168166
3.174599	15.963570	0.184816
3.219401	15.990433	0.202714
3.264348	16.017088	0.221967
3.309592	16.043623	0.242665
3.355275	16.070062	0.264917
3.401504	16.096426	0.288853
3.448386	16.122882	0.314578
3.495992	16.149456	0.342229
3.544379	16.176166	0.371929
3.593581	16.203017	0.403787
3.643637	16.230013	0.437915
3.694546	16.257138	0.474408
3.746299	16.284371	0.513379
3.798886	16.311565	0.554896
3.852273	16.338927	0.599044
3.906422	16.366457	0.645884
3.961291	16.394125	0.695479
4.016833	16.421897	0.747873
4.072986	16.449735	0.803119
4.129684	16.477599	0.861249
4.186883	16.505501	0.922277
4.244493	16.533572	0.986240
4.302463	16.561779	1.053139
4.360723	16.590086	1.122982
4.419196	16.618438	1.195836
4.477827	16.646865	1.271632
4.536546	16.675274	1.350337
4.595268	16.703742	1.431895
4.653904	16.732457	1.516241
4.712397	16.761161	1.603328
4.762961	16.786021	1.681049

LPT Stator 1 Airfoil Coordinates

90% From Hub

Suction Surface

Z	R	RTHETA
5.473056	13.800044	0.
5.469523	13.799177	0.005729
5.468323	13.798883	0.013794
5.469537	13.799181	0.024116
5.473290	13.800101	0.036573
5.479733	13.801679	0.051019
5.489018	13.803948	0.067308
5.501269	13.806933	0.085322
5.515539	13.810638	0.105009
5.534772	13.815042	0.126428
5.552902	13.819397	0.146528
5.552902	13.819397	0.146528
5.579050	13.825639	0.173780
5.605876	13.831994	0.199706
5.633443	13.838472	0.224410
5.661801	13.845081	0.247888
5.691013	13.851831	0.270057
5.721131	13.858692	0.290691
5.752169	13.865692	0.309568
5.784160	13.872854	0.325481
5.817127	13.880179	0.341202
5.851046	13.887656	0.353480
5.885841	13.895263	0.363037
5.921364	13.902964	0.369608
5.957405	13.910728	0.372980
5.993737	13.918529	0.373016
6.030085	13.926305	0.369618
6.066067	13.933975	0.362800
6.101331	13.941465	0.352703
6.135642	13.948729	0.339525
6.168872	13.955729	0.323515
6.201007	13.962451	0.304905
6.232074	13.968975	0.283866
6.262163	13.975316	0.260559
6.291371	13.981493	0.235114
6.319781	13.987522	0.207668
6.347477	13.993419	0.178298
6.374609	13.999215	0.147053
6.401316	14.004961	0.113909
6.427758	14.010759	0.078819
6.454089	14.016574	0.041717
6.480403	14.022424	0.002585
6.506762	14.028324	-0.038537
6.533138	14.034268	-0.081571
6.559509	14.040250	-0.126307
6.585888	14.046274	-0.172518
6.612296	14.052345	-0.220030
6.631968	14.056892	-0.256137

Pressure Surface

Z	R	RTHETA
5.473056	13.800044	0.
5.477397	13.801107	-0.002693
5.483228	13.802534	-0.003789
5.490483	13.804306	-0.003225
5.499083	13.806401	-0.000924
5.508991	13.808809	0.003153
5.520275	13.811542	0.008937
5.533204	13.814664	0.016170
5.553284	13.819489	0.027149
5.585935	13.827275	0.044108
5.618165	13.834888	0.060296
5.618165	13.834888	0.060296
5.649855	13.842304	0.075893
5.680865	13.849493	0.090894
5.711136	13.856427	0.105048
5.740615	13.863092	0.118078
5.769240	13.869520	0.129731
5.796959	13.875704	0.139919
5.823759	13.881645	0.148623
5.849606	13.887339	0.155853
5.874476	13.892785	0.161669
5.898394	13.897992	0.166160
5.921436	13.902980	0.169464
5.943750	13.907789	0.171723
5.965547	13.912479	0.173049
5.987052	13.917096	0.173470
6.008541	13.921699	0.172976
6.030397	13.926371	0.171465
6.052970	13.931186	0.168781
6.076496	13.936193	0.164761
6.101103	13.941417	0.159230
6.126806	13.946860	0.152027
6.153576	13.952515	0.143044
6.181324	13.958331	0.132140
6.209954	13.964328	0.119165
6.239381	13.970513	0.103952
6.269522	13.976870	0.086413
6.300227	13.983370	0.066466
6.331358	13.989985	0.044005
6.362753	13.996680	0.018838
6.394259	14.003424	-0.009294
6.425783	14.010325	-0.040630
6.457261	14.017277	-0.075154
6.488722	14.024282	-0.112599
6.520188	14.031344	-0.152540
6.551647	14.038462	-0.194520
6.583076	14.045630	-0.238211
6.606412	14.050989	-0.271702

LPT Rotor 1 Airfoil Coordinates

10% From Hub

ORIGINAL ... OF POOR QUALITY

Suction Surface

Z	R	RTHETA
5.491467	15.465573	0.
5.488070	15.464274	0.005048
5.486897	15.463826	0.012695
5.488038	15.464262	0.022865
5.491634	15.465637	0.035440
5.497852	15.468014	0.050284
5.506861	15.471454	0.067257
5.518797	15.476007	0.086248
5.533721	15.481692	0.107211
5.542783	15.485139	0.119055
5.542783	15.485139	0.119055
5.567559	15.494547	0.148827
5.593048	15.504201	0.176088
5.619287	15.514111	0.201197
5.646559	15.524381	0.224343
5.675059	15.535082	0.245552
5.704991	15.546284	0.264670
5.736282	15.557899	0.281286
5.768699	15.569907	0.294924
5.802051	15.582240	0.305291
5.836105	15.594809	0.312133
5.870606	15.607521	0.315248
5.905259	15.620264	0.314565
5.939759	15.632919	0.310059
5.973823	15.645422	0.301793
6.007263	15.657730	0.289945
6.039929	15.669786	0.274713
6.071616	15.681513	0.256395
6.102215	15.692867	0.235356
6.131624	15.703806	0.211966
6.159856	15.714394	0.186554
6.187192	15.724729	0.159184
6.213870	15.734857	0.129807
6.240027	15.744828	0.098489
6.265762	15.754677	0.065306
6.291127	15.764423	0.030363
6.316161	15.774079	-0.006244
6.340967	15.783683	-0.044496
6.365671	15.793283	-0.084433
6.390415	15.802927	-0.126133
6.415315	15.812668	-0.169715
6.440434	15.822530	-0.215186
6.465777	15.832516	-0.262394
6.491269	15.842598	-0.311013
6.516788	15.852726	-0.360531
6.542162	15.862834	-0.410480
6.567264	15.872869	-0.460530
6.585714	15.880268	0.497669

Pressure Surface

Z	R	RTHETA
5.491467	15.465573	0.
5.495138	15.466977	-0.001890
5.499917	15.468802	-0.002379
5.505731	15.471023	-0.001402
5.512487	15.473601	0.001117
5.520125	15.476513	0.005228
5.528684	15.479774	0.010900
5.538391	15.483469	0.017945
5.56746	15.494511	0.038299
5.598196	15.506147	0.057987
5.598196	15.506147	0.057987
5.627972	15.517385	0.075366
5.657034	15.528318	0.091068
5.685346	15.538936	0.105379
5.712626	15.549124	0.118160
5.738677	15.558787	0.129012
5.763297	15.567907	0.137517
5.786558	15.576514	0.143597
5.808692	15.584693	0.147563
5.829891	15.592517	0.149743
5.850389	15.600075	0.150473
5.870440	15.607459	0.150034
5.890338	15.614780	0.148534
5.910389	15.622149	0.145994
5.930877	15.629665	0.142308
5.951988	15.637404	0.137200
5.973873	15.645440	0.130309
5.996738	15.653852	0.121216
6.020690	15.662681	0.109586
6.045833	15.671969	0.095295
6.072152	15.681712	0.078532
6.099368	15.691809	0.059707
6.127241	15.702[illegible]74	0.039005
6.155636	15.712802	0.016303
6.184452	15.723691	-0.008554
6.213638	15.734769	-0.035663
6.243155	15.746023	-0.064969
6.272901	15.757417	-0.096361
6.302748	15.768901	-0.129865
6.332556	15.780423	-0.165657
6.362207	15.791935	-0.203975
6.391640	15.803406	-0.245005
6.420848	15.814838	-0.288615
6.449908	15.826259	-0.334354
6.478940	15.837717	-0.381497
6.508118	15.849281	-0.429216
6.537567	15.861001	-0.476893
6.559658	15.869825	-0.512080

LPT Rotor 1 Airfoil Coordinates

50% From Hub

Suction Surface

Z	R	RTHETA
5.483884	17.134516	0.
5.481210	17.133305	0.005321
5.480966	17.133194	0.012825
5.483213	17.134212	0.022443
5.488047	17.136402	0.034074
5.495580	17.139811	0.047596
5.505922	17.144486	0.062889
5.519159	17.150462	0.079865
5.535316	17.157743	0.098498
5.539410	17.159586	0.102988
5.539410	17.159586	0.102988
5.564354	17.170794	0.128786
5.589870	17.182225	0.152729
5.616036	17.193912	0.175007
5.643061	17.205943	0.195786
5.671102	17.218386	0.215023
5.700269	17.231282	0.232571
5.730458	17.244498	0.247990
5.761434	17.258037	0.260933
5.793280	17.271934	0.271215
5.826121	17.286241	0.278620
5.859822	17.300897	0.282837
5.894107	17.315780	0.283631
5.928644	17.330761	0.280843
5.963036	17.345724	0.274406
5.996780	17.360439	0.264427
6.029492	17.3747[illegible]5	0.251201
6.061046	17.388556	0.235021
6.091451	17.401901	0.216146
6.120871	17.414839	0.194703
6.149488	17.427467	0.170791
6.177398	17.439843	0.144534
6.204684	17.451990	0.116065
6.231323	17.463893	0.085563
6.257329	17.475556	0.053230
6.282822	17.487030	0.019143
6.307920	17.498365	-0.016706
6.332783	17.509632	-0.054345
6.357564	17.520905	-0.093854
6.382372	17.532259	-0.135264
6.407283	17.543705	-0.178543
6.432336	17.555263	-0.223629
6.457533	17.566933	-0.270395
6.482817	17.578691	-0.318648
6.508151	17.590518	-0.368094
6.533508	17.602403	-0.418451
6.558881	17.614343	-0.469511
6.577914	17.623331	-0.508169

Pressure Surface

Z	R	RTHETA
5.483884	17.134516	0.
5.487163	17.136001	-0.002306
5.491670	17.138042	-0.003427
5.497342	17.140608	-0.003292
5.504098	17.143662	-0.001815
5.511884	17.147179	0.001065
5.520723	17.151167	0.005325
5.530785	17.155703	0.010776
5.556774	17.167392	0.024742
5.587161	17.181013	0.040235
5.587161	17.181013	0.040235
5.616724	17.194219	0.054381
5.645714	17.207123	0.067525
5.674055	17.219694	0.079830
5.701535	17.231837	0.091036
5.728001	17.243423	0.100779
5.753340	17.254502	0.108688
5.777657	17.265119	0.114806
5.801187	17.275381	0.119399
5.823847	17.285251	0.122639
5.845513	17.294677	0.124556
5.866318	17.303719	0.125186
5.886539	17.312497	0.124515
5.906508	17.321157	0.122482
5.926622	17.329883	0.118987
5.947385	17.338911	0.113866
5.969178	17.348400	0.106944
5.992131	17.358410	0.098163
6.016233	17.368937	0.087511
6.041318	17.379912	0.075019
6.067207	17.391258	0.060563
6.093804	17.402934	0.043899
6.121024	17.414906	0.024776
6.148891	17.427202	0.003054
6.177391	17.439840	-0.021160
6.206405	17.452758	-0.047580
6.235812	17.465904	-0.076037
6.265456	17.479210	-0.106569
6.295181	17.492607	-0.139387
6.324879	17.506046	-0.174771
6.354474	17.519494	-0.212822
6.383927	17.532972	-0.253478
6.413237	17.546448	-0.296518
6.442459	17.559946	-0.341601
6.471631	17.573483	-0.388302
6.500781	17.587072	-0.436190
6.529914	17.600716	-0.484956
6.551741	17.610979	-0.521977

LPT Rotor 1 Airfoil Coordinates

90 % From Hub

ORIGINAL PAGE IS
OF POOR QUALITY

Suction Surface

Z	R	RTHETA
7.356423	14.205098	0.
7.352095	14.204351	-0.007793
7.351199	14.204195	-0.018871
7.353842	14.204653	-0.033125
7.360189	14.205743	-0.050388
7.370435	14.207518	-0.070463
7.384775	14.209993	-0.093152
7.403362	14.213199	-0.118302
7.426252	14.217144	-0.145859
7.453344	14.221810	-0.175925
7.461118	14.223149	-0.184263
7.461118	14.223149	-0.184263
7.495488	14.229061	-0.219789
7.530938	14.235153	-0.253824
7.566676	14.241286	-0.285767
7.602673	14.247492	-0.316009
7.640136	14.253872	-0.344781
7.678788	14.260356	-0.371852
7.719027	14.267073	-0.396878
7.760910	14.274118	-0.419367
7.804401	14.281492	-0.438788
7.849385	14.289191	-0.454567
7.895592	14.297[illegible]45	-0.466179
7.942576	14.305311	-0.473227
7.989794	14.313838	-0.475548
8.036790	14.322537	-0.473175
8.083153	14.331251	-0.466266
8.128504	14.339901	-0.455133
8.172617	14.348435	-0.440173
8.215535	14.356851	-0.421703
8.257374	14.365167	-0.399898
8.298275	14.373415	-0.374747
8.338293	14.381552	-0.346137
8.377377	14.389561	-0.314016
8.415503	14.397433	-0.278391
8.452719	14.405175	-0.239454
8.489179	14.412814	-0.197412
8.525018	14.420375	-0.152455
8.560300	14.427862	-0.104773
8.595099	14.435224	-0.054548
8.629494	14.4425[illegible]4	-0.002019
8.663604	14.449815	0.052513
8.697522	14.457087	0.108748
8.731344	14.464369	0.166382
8.765214	14.471694	0.225079
8.799324	14.479101	0.284521
8.833907	14.486645	0.344422
8.861738	14.492739	0.392176

Pressure Surface

Z	R	RTHETA
7.356423	14.205098	0.
7.362579	14.206161	0.003728
7.371271	14.207662	0.004962
7.382500	14.209600	0.003705
7.396278	14.211977	-0.000034
7.412630	14.214797	-0.006229
7.431617	14.218069	-0.014821
7.453345	14.221811	-0.025700
7.477993	14.226052	-0.038689
7.503339	14.230411	-0.052248
7.545494	14.237652	-0.074739
7.545494	14.237652	-0.074739
7.586325	14.244656	-0.095955
7.626074	14.251465	-0.115399
7.665537	14.258155	-0.133793
7.704540	14.264649	-0.151358
7.742478	14.271011	-0.167728
7.779027	14.277183	-0.182517
7.813989	14.283125	-0.195359
7.847306	14.288824	-0.206071
7.879015	14.294280	-0.214673
7.909231	14.299508	-0.221349
7.938225	14.304552	-0.226375
7.966441	14.309566	-0.230015
7.994424	14.314689	-0.232425
8.022629	14.319902	-0.233619
8.051466	14.325251	-0.233515
8.081315	14.330903	-0.231898
8.112403	14.336815	-0.228518
8.144685	14.343017	-0.223169
8.178047	14.349493	-0.215654
8.212347	14.356222	-0.205769
8.247529	14.363199	-0.193192
8.283645	14.370457	-0.177406
8.320720	14.377971	-0.157820
8.358704	14.385726	-0.133809
8.397445	14.393697	-0.105047
8.436807	14.401858	-0.071585
8.476725	14.410198	-0.033854
8.517126	14.418706	0.007538
8.557931	14.427362	0.052047
8.599022	14.436056	0.099248
8.640305	14.444838	0.148726
8.681684	14.453687	0.200116
8.723014	14.462573	0.253118
8.764105	14.471453	0.307510
8.804721	14.480276	0.363190
8.836547	14.487222	0.408206

LPT Stator 2 Airfoil Coordinates

10 % From Hub

ORIGINAL PAGE IS
OF POOR QUALITY

Suction Surface

Z	R	RTHETA
7.306841	16.162008	0.
7.300594	16.159725	-0.008878
7.297937	16.158752	-0.021903
7.298385	16.159136	-0.038974
7.303922	16.160942	-0.059939
7.312972	16.164241	-0.084609
7.326379	16.169098	-0.112780
7.344368	16.175561	-0.144266
7.367101	16.183640	-0.178937
7.394629	16.193290	-0.216754
7.399384	16.194942	-0.222985
7.399384	16.194942	-0.222985
7.433762	16.206757	-0.265776
7.469963	16.218953	-0.306525
7.507122	16.231210	-0.344484
7.545344	16.243541	-0.379972
7.585329	16.256140	-0.413103
7.627317	16.268936	-0.443517
7.671469	16.281910	-0.470640
7.718261	16.295344	-0.493959
7.768135	16.309304	-0.512781
7.820794	16.323642	-0.526030
7.875373	16.338068	-0.532822
7.930663	16.352227	-0.532603
7.985291	16.365910	-0.525339
8.037950	16.378940	-0.511662
8.087815	16.391133	-0.492329
8.134877	16.402513	-0.468197
8.179413	16.413166	-0.439997
8.221672	16.423171	-0.408264
8.262043	16.432703	-0.373479
8.301072	16.441978	-0.335809
8.339145	16.451074	-0.295178
8.376375	16.460015	-0.251397
8.412839	16.468818	-0.204299
8.448514	16.477473	-0.153805
8.483571	16.486019	-0.099968
8.518244	16.494512	-0.042833
8.552729	16.503053	0.017538
8.587195	16.511833	0.081023
8.621694	16.520710	0.147454
8.656316	16.529[illegible]09	0.216560
8.691034	16.538832	0.288060
8.725889	16.54806[illegible]	0.361564
8.760955	16.557450	0.436623
8.796327	16.567013	0.512821
8.832168	16.576798	0.589812
8.862335	16.585108	0.654202

Pressure Surface

Z	R	RTHETA
7.306841	16.162008	0.
7.313075	16.164278	0.002983
7.321593	16.167368	0.003315
7.332461	16.171290	0.001049
7.345782	16.176067	-0.003730
7.361[illegible]93	16.181727	-0.010906
7.380360	16.188306	-0.020344
7.401965	16.195837	-0.031889
7.426697	16.204347	-0.045388
7.466516	16.217803	-0.067065
7.511846	16.232749	-0.090937
7.511846	16.232749	-0.090937
7.555245	16.246689	-0.112283
7.596822	16.259705	-0.130455
7.637441	16.271937	-0.146198
7.676996	16.283514	-0.159744
7.714739	16.294358	-0.170943
7.750578	16.304432	-0.17[illegible]824
7.784205	16.313723	-0.186689
7.815190	16.322136	-0.191702
7.843093	16.329590	-0.194987
7.868213	16.336201	-0.196980
7.891411	16.342223	-0.198119
7.913899	16.347985	-0.198689
7.937048	16.353835	-0.198620
7.962167	16.360139	-0.197582
7.990079	16.367101	-0.195067
8.020795	16.374712	-0.190717
8.054037	16.382889	-0.184133
8.089555	16.391556	-0.175005
8.126963	16.400608	-0.163002
8.165711	16.409900	-0.147885
8.205416	16.419334	-0.129310
8.245963	16.428897	-0.106790
8.287277	16.438694	-0.079701
8.329380	16.448736	-0.047454
8.372100	16.458986	-0.009685
8.415206	16.469391	0.033630
8.458498	16.479902	0.082268
8.501809	16.490481	0.135863
8.545088	16.501118	0.193896
8.588244	16.512102	0.255871
8.631304	16.523199	0.321191
8.674226	16.534399	0.389310
8.716938	16.545681	0.459682
8.759343	16.557017	0.531823
8.801280	16.568360	0.605431
8.835693	16.577766	0.667519

LPT Stator 2 Airfoil Coordinates

50 % From Hub

ORIGINAL PAGE IS
OF POOR QUALITY

Suction Surface

Z	R	RTHETA
7.263435	17.955466	0.
7.258673	17.953174	-0.008071
7.257204	17.952466	-0.019374
7.259076	17.953368	-0.033861
7.264367	17.955914	-0.051454
7.273180	17.960147	-0.072050
7.285642	17.966111	-0.095525
7.301894	17.973855	-0.121740
7.322089	17.983422	-0.150545
7.345378	17.994848	-0.181792
7.374906	18.008154	-0.215342
7.407795	18.023342	-0.251078
7.440959	18.038493	-0.284726
7.440959	18.038493	-0.284726
7.479079	18.055704	-0.320805
7.517927	18.073019	-0.354955
7.558188	18.090724	-0.387325
7.600123	18.108814	-0.417536
7.643834	18.127357	-0.445097
7.689537	18.146491	-0.469479
7.737375	18.166240	-0.490182
7.787345	18.186565	-0.506462
7.839208	18.207331	-0.517684
7.892520	18.228328	-0.523210
7.946566	18.249115	-0.522560
8.000245	18.269620	-0.515558
8.052541	18.289475	-0.502470
8.102983	18.308514	-0.483704
8.151372	18.326674	-0.459766
8.197688	18.343961	-0.431150
8.241986	18.360459	-0.398247
8.284401	18.376367	-0.361482
8.325121	18.391747	-0.321160
8.364343	18.406660	-0.277480
8.402339	18.421201	-0.230595
8.439379	18.435463	-0.180520
8.475717	18.449540	-0.127217
8.511581	18.463516	-0.070722
8.547142	18.477549	-0.011063
8.582510	18.491835	0.051646
8.617738	18.506208	0.117171
8.652872	18.520684	0.185270
8.688002	18.535301	0.255652
8.723232	18.550103	0.328011
8.758761	18.565174	0.402002
8.794780	18.580601	0.477333
8.831526	18.596494	0.553750
8.862685	18.610092	0.618012

Pressure Surface

Z	R	RTHETA
7.263435	17.955466	0.
7.269163	17.958219	0.003310
7.277351	17.962146	0.004186
7.288014	17.967244	0.002637
7.301179	17.973515	-0.001310
7.316889	17.980965	-0.007615
7.335214	17.989607	-0.016209
7.356257	17.999469	-0.026988
7.380170	18.010596	-0.039808
7.418533	18.028266	-0.060708
7.463920	18.048886	-0.085139
7.507762	18.068510	-0.107609
7.550218	18.087238	-0.127368
7.550218	18.087238	-0.127368
7.592136	18.105399	-0.144992
7.633326	18.122921	-0.160646
7.673104	18.139641	-0.173978
7.711208	18.155473	-0.184848
7.747535	18.170398	-0.193346
7.781870	18.184354	-0.199657
7.814071	18.197308	-0.203941
7.844139	18.209288	-0.206560
7.872315	18.220412	-0.207819
7.899041	18.230857	-0.208026
7.925033	18.240855	-0.207396
7.951393	18.250964	-0.205925
7.979136	18.261571	-0.203413
8.008732	18.272850	-0.199580
8.040381	18.284869	-0.193982
8.074104	18.297628	-0.186100
8.109845	18.311096	-0.175422
8.147468	18.325213	-0.161337
8.186786	18.339900	-0.143337
8.227603	18.355091	-0.121024
8.269646	18.370821	-0.094086
8.312644	18.387023	-0.062351
8.356345	18.403611	-0.025668
8.400519	18.420502	0.016100
8.444996	18.437634	0.062900
8.489667	18.454967	0.114502
8.534477	18.472481	0.170418
8.579382	18.490566	0.230077
8.624291	18.508897	0.292954
8.669099	18.527419	0.358631
8.713608	18.546045	0.426800
8.757628	18.564691	0.497211
8.800920	18.583246	0.569736
8.836291	18.598566	0.631540

LPT Stator 2 Airfoil Coordinates

90% From Hub

ORIGINAL PAGE IS
OF POOR QUALITY

Suction Surface

Z	R	RTHETA
9.387539	14.614119	0.
9.383391	14.613030	0.006358
9.381896	14.612637	0.015580
9.383161	14.612969	0.027570
9.387346	14.614068	0.042185
9.394645	14.615982	0.059250
9.405259	14.618755	0.078587
9.419351	14.622423	0.100051
9.437001	14.626993	0.123572
9.458154	14.632435	0.149203
9.464258	14.633998	0.156299
9.464258	14.633998	0.156299
9.490591	14.640705	0.185661
9.517731	14.647555	0.213769
9.545644	14.654535	0.240621
9.574293	14.661628	0.266154
9.603704	14.668838	0.290207
9.633911	14.676199	0.312614
9.664980	14.683702	0.333159
9.697034	14.691336	0.351724
9.730220	14.699130	0.368113
9.764552	14.707070	0.382037
9.799966	14.715132	0.393123
9.836286	14.723264	0.401035
9.873255	14.731351	0.405470
9.910607	14.739325	0.406245
9.948015	14.747136	0.403233
9.985029	14.754691	0.396434
10.021225	14.761914	0.386025
10.056355	14.768763	0.372245
10.090245	14.775149	0.355378
10.122952	14.780971	0.335664
10.154574	14.786558	0.313267
10.185244	14.791936	0.288307
10.215076	14.797130	0.260894
244069	14.802142	0.231231
272270	14.806983	0.199501
10.299792	14.811676	0.165794
10.326749	14.816358	0.130166
10.353258	14.821142	0.092647
10.379450	14.825900	0.053281
10.405401	14.830645	0.012085
10.431200	14.835393	-0.030908
10.456922	14.840156	-0.075670
10.482664	14.844952	-0.122161
10.508544	14.849805	-0.170331
10.534629	14.854726	-0.220175
10.554520	14.858501	-0.258966

Pressure Surface

Z	R	RTHETA
9.387539	14.614119	0.
9.392686	14.615469	0.002894
9.399520	14.617257	-0.003832
9.407952	14.619458	-0.002734
9.417875	14.622040	0.000497
9.429230	14.624985	0.005915
9.442090	14.628306	0.013456
9.456776	14.632082	0.022831
9.470537	14.635603	0.031523
9.503430	14.643953	0.051566
9.535996	14.652130	0.070950
9.535996	14.652130	0.070950
9.567916	14.660056	0.089578
9.599030	14.667697	0.107223
9.629370	14.675094	0.123526
9.658974	14.682260	0.138214
9.687816	14.689153	0.151194
9.715862	14.695773	0.162458
9.743046	14.702110	0.172102
9.769246	14.708146	0.180114
9.794312	14.713853	0.186487
9.818233	14.719239	0.191277
9.841073	14.724325	0.194672
9.863006	14.729132	0.196863
9.884290	14.733725	0.198052
9.905192	14.738180	0.198328
9.926036	14.742568	0.197720
9.947275	14.746983	0.196148
9.969321	14.751506	0.193428
9.992455	14.756186	0.189368
10.016819	14.761042	0.183763
10.042365	14.766053	0.176424
10.068995	14.771190	0.167153
10.096579	14.776280	0.155096
10.125000	14.781334	0.141707
10.154260	14.786503	0.124816
10.184313	14.791774	0.104892
10.215043	14.797124	0.082037
10.246339	14.802533	0.056415
10.278084	14.807377	0.028188
10.310145	14.813432	-0.002568
10.342447	14.819187	-0.035807
10.374901	14.825072	-0.071491
10.407432	14.831018	-0.109587
10.439944	14.837008	-0.150075
10.472316	14.843021	-0.192954
10.504485	14.849042	-0.238200
10.528635	14.853593	-0.273971

LPT Rotor 2 Airfoil Coordinates

10% From Hub

ORIGINAL PAGE IS
OF POOR QUALITY

Suction Surface

Z	R	RTHETA
9.403337	16.759952	0.
9.399696	16.758581	0.005106
9.398257	16.758039	0.012922
9.399108	16.758360	0.023380
9.402384	16.759593	0.036370
9.408256	16.761804	0.051761
9.416903	16.765060	0.069411
9.428489	16.769425	0.089193
9.443129	16.774942	0.111020
9.460843	16.781623	0.134877
9.479573	16.788691	0.158304
9.479573	16.788691	0.158304
9.505755	16.798579	0.188368
9.532647	16.808744	0.216153
9.560306	16.819211	0.241770
9.588743	16.829982	0.265034
9.617919	16.841044	0.285741
9.647977	16.852579	0.303771
9.679063	16.864491	0.318945
9.711250	16.876778	0.330999
9.744373	16.889394	0.339673
9.778255	16.902263	0.344669
9.812598	16.915270	0.345733
9.847027	16.928227	0.342708
9.881164	16.940868	0.335609
9.914728	16.953209	0.324590
9.947520	16.965180	0.3098[illegible]4
9.979405	16.976741	0.291597
10.010314	16.987883	0.270138
10.040304	16.998601	0.245725
10.069325	17.008862	0.218663
10.097452	17.018686	0.189169
10.124757	17.028200	0.157426
10.151518	17.037502	0.123352
10.178015	17.046691	0.086743
10.204298	17.055785	0.047755
10.230270	17.064751	0.006677
10.255929	17.073588	-0.036309
10.281289	17.082322	-0.081146
10.306486	17.091112	-0.127797
10.331709	17.099922	-0.176271
10.357030	17.108777	-0.226582
10.382440	17.117674	-0.278665
10.407905	17.126601	-0.332332
10.433405	17.135552	-0.387260
10.458931	17.144523	-0.443128
10.484488	17.153516	-0.499700
10.504130	17.160436	-0.543531

Pressure Surface

Z	R	RTHETA
9.403337	16.759952	0.
9.407841	16.761647	-0.002090
9.413717	16.763860	-0.002320
9.420827	16.766538	-0.000581
9.428991	16.769614	0.003271
9.438061	16.773032	0.009353
9.448029	16.776790	0.017672
9.459158	16.780987	0.028021
9.479892	16.788811	0.047241
9.509882	16.800138	0.073623
9.539189	16.811219	0.097416
9.539189	16.811219	0.097416
9.567877	16.822077	0.118688
9.595856	16.832678	0.137474
9.623068	16.843017	0.153518
9.649500	16.853163	0.166872
9.675195	16.86300[illegible]	0.1778[illegible]8
9.700008	16.872488	0.186843
9.723772	16.881552	0.193954
9.746476	16.890194	0.199348
9.768223	16.898457	0.203133
9.789211	16.906417	0.205433
9.809739	16.914189	0.206318
9.830180	16.921914	0.205750
9.850913	16.929671	0.203524
9.872219	16.937565	0.199262
9.894298	16.945708	0.192532
9.917284	16.954145	0.182861
9.941215	16.962885	0.169878
9.966126	16.971936	0.153400
9.991975	16.981277	0.133504
10.018718	16.990885	0.110556
10.046284	17.000732	0.085038
10.074393	17.010634	0.057333
10.102766	17.020539	0.027214
10.131354	17.030495	-0.005864
10.160253	17.040534	-0.041795
10.189464	17.050655	-0.080075
10.218974	17.060854	-0.120364
10.248647	17.071082	-0.162622
10.278295	17.081279	-0.207007
10.307845	17.091537	-0.253671
10.337305	17.101878	-0.302555
10.360710	17.112165	-0.353425
10.396081	17.122455	-0.405898
10.425425	17.132750	-0.459549
10.454739	17.143049	-0.514067
10.477231	17.150961	-0.556396

LPT Rotor 2 Airfoil Coordinates

50% From Hub

ORIGINAL PAGE IS
OF POOR QUALITY

Suction Surface

Z	R	RTHETA
9.399739	18.856664	0.
9.396793	18.855297	0.005103
9.396036	18.854945	0.012361
9.397523	18.855636	0.021720
9.401338	18.857407	0.033097
9.407581	18.860303	0.046391
9.416362	18.864374	0.061497
9.427775	18.869660	0.078321
9.441877	18.876182	0.096808
9.458669	18.883937	0.116962
9.478056	18.892873	0.138741
9.478056	18.892873	0.138741
9.503562	18.904602	0.165349
9.529653	18.916569	0.190360
9.556488	18.928843	0.213833
9.584168	18.941468	0.235651
9.612799	18.954489	0.255616
9.642524	18.967997	0.273505
9.673488	18.982016	0.289031
9.705766	18.996570	0.301879
9.739354	19.011648	0.311635
9.774032	19.027146	0.317876
9.809410	19.042882	0.320213
9.844966	19.058589	0.318394
9.880154	19.073975	0.312411
9.914551	19.088954	0.302393
9.947848	19.103395	0.288614
9.979841	19.117217	0.271448
10.010480	19.130405	0.251223
10.039953	19.143045	0.228150
10.068507	19.155182	0.202313
10.096472	19.167015	0.173630
10.124063	19.178717	0.141976
10.151227	19.190265	0.107506
10.177943	19.201650	0.070867
10.204114	19.212829	0.031983
10.229640	19.223756	0.008759
10.254713	19.234513	-0.051324
10.279622	19.245270	-0.095969
10.304510	19.256212	-0.142797
10.329464	19.267219	-0.191707
10.354467	19.278373	-0.242602
10.379509	19.289582	-0.295327
10.404597	19.300877	-0.349654
10.429765	19.312275	-0.405292
10.455028	19.323783	-0.461983
10.480332	19.335378	-0.519572
10.499930	19.344405	-0.564669

Pressure Surface

Z	R	RTHETA
9.399739	18.856664	0.
9.403614	18.858463	-0.002426
9.408881	18.860906	-0.003370
9.415444	18.863949	-0.002737
9.423180	18.867532	-0.000403
9.431993	18.871612	0.003728
9.441891	18.876189	0.009648
9.453087	18.881360	0.017146
9.474386	18.891182	0.031382
9.504896	18.905215	0.050788
9.534725	18.918891	0.068374
9.534725	18.918891	0.068374
9.564014	18.932279	0.084311
9.592718	18.945360	0.098675
9.620677	18.958071	0.111337
9.647792	18.970386	0.122199
9.673956	18.982228	0.131262
9.699026	18.993536	0.138537
9.722857	19.004251	0.144066
9.745373	19.014344	0.147871
9.766580	19.023822	0.150077
9.786697	19.032788	0.150638
9.806114	19.041419	0.150354
9.825353	19.049949	0.148768
9.844959	19.058585	0.146064
9.865357	19.067513	0.142132
9.886855	19.076898	0.136723
9.909657	19.086826	0.[illegible]9526
9.933812	19.097315	0.120314
9.959135	19.108278	0.108909
9.985375	19.119603	0.095065
10.012205	19.131146	0.078392
10.039409	19.142812	0.058186
10.067040	19.154562	0.033644
10.095118	19.166441	0.004762
10.123742	19.178581	-0.027698
10.153011	19.191025	-0.062767
10.182732	19.203694	-0.099709
10.212619	19.216467	-0.138623
10.242525	19.229281	-0.180082
10.272366	19.242101	-0.224290
10.302158	19.255175	-0.271090
10.3[illegible]1910	19.268334	-0.320218
10.361618	19.281567	-0.371379
10.391244	19.294857	-0.424238
10.420776	19.308196	-0.478457
10.450267	19.321609	-0.533757
10.473058	19.332038	-0.577177

LPT Rotor 2 Airfoil Coordinates

90% From Hub

Suction Surface

Z	R	RTHETA
11 161983	14 973300	0
11 156902	14 972407	-0 008475
11 155286	14 972123	-0 020356
11 157240	14 972466	-0 035540
11 162922	14 973465	-0 053869
11 172536	14 975159	-0 075142
11 186306	14 977590	-0 099137
11 204452	14 980803	-0 125638
11 227153	14 984838	-0 154472
11 254508	14 989723	-0 185540
11 286492	14 995466	-0 218871
11 316976	15 000971	-0 248803
11 316976	15 000971	-0 248803
11 356805	15 008211	-0 285654
11 397265	15 015619	-0 320672
11 438437	15 023214	-0 353889
11 480553	15 031041	-0 385220
11 523838	15 039205	-0 414397
11 568521	15 047700	0 441022
11 614765	15 056535	0 464737
11 662677	15 065736	0 485183
11 712293	15 075315	501920
11 763573	15 085269	0 [illegible]14373
11 816339	15 095569	0 [illegible]21867
11 870106	15 106052	523866
11 923778	15 116515	-0 519896
11 976262	15 126759	-0 510311
12 027102	15 136694	-0 495672
12 076141	15 146287	-0 476629
12 123342	15 155531	-0 453768
12 168856	15 164401	-0 427607
12 213100	15 172824	0 398353
12 256447	15 181145	-0 365965
12 299167	15 189412	0 330180
12 341303	15 197632	-0 290685
12 382609	15 205752	-0 247455
12 423011	15 213754	-0 200688
12 462457	15 221624	-0 150737
12 500978	15 229398	-0 098058
12 538829	15 237319	-0 042760
12 576264	15 245255	0 015210
12 613459	15 253241	0 075753
12 650632	15 261323	0 138607
12 688042	15 269557	0 203390
12 725825	15 277977	0 269700
12 764100	15 286612	0 337165
12 802928	15 295480	0 405530
12 835123	15 302316	0 462001

Pressure Surface

Z	R	RTHETA
11 161983	14 973300	0
11 169746	14 974667	0 004550
11 180655	14 976591	0 005895
11 194664	14 979068	0 003989
211726	14 982094	-0 001215
11 231826	14 985671	-0 009737
11 255026	14 989816	-0 021513
11 [illegible]1541	14 994575	-0 036334
11 3[illegible]908	15 000036	-0 053767
11 3[illegible]6067	15 002619	-0 061863
11 371512	15 010898	-0 086752
11 416128	15 019092	-0 109801
11 416128	15 019092	-0 109801
11 459926	15 027200	-0 130712
11 503092	15 035275	-0 149501
11 [illegible]545	15 043326	-0 166164
11 587055	15 051235	-0 180673
11 627396	15 058956	-0 193079
11 666339	15 066441	-0 203526
11 703722	15 073656	-0 212073
11 739435	15 080577	-0 218751
11 773445	15 087192	-0 223633
11 805791	15 093506	0 226921
11 836652	15 099536	-0 228895
11 866510	15 105351	-0 229708
11 896454	15 111189	-0 229618
11 927606	15 117262	-0 228414
11 960392	15 123661	-0 225843
11 994979	15 130416	-0 221564
12 031404	15 137535	-0 215288
12 069516	15 144991	-0 206789
12 108897	15 152701	-0 195968
12 149177	15 160594	-0 182622
12 190088	15 168434	-0 166358
12 231573	15 176362	-0 146417
12 273893	15 184514	-0 121786
12 317116	15 192906	-0 091744
12 361297	15 201555	-0 056201
12 406402	15 210458	-0 015891
12 452176	15 219568	0 028103
12 498368	15 228855	0 075368
12 544799	15 238578	0 126022
12 591251	15 248461	0 180063
12 637467	15 258449	0 237316
12 683310	15 268510	0 297339
12 728661	15 278613	0 359637
12 773459	15 288739	0 423832
12 809658	15 297028	0 477580

LPT Stator 3 Airfoil Coordinates

10% From Hub

Suction Surface

Z	R	RTHETA
11.129883	17.387064	0
11.122328	17.384333	-0.009847
11.118483	17.382939	-0.024179
11.118478	17.382937	-0.042889
11.122517	17.384401	-0.065811
11.130671	17.387421	-0.092729
11.143849	17.392092	-0.123396
11.161776	17.398505	-0.157554
11.184961	17.406731	-0.19496
11.213659	17.416806	-0.235417
11.248026	17.428715	-0.278802
11.267990	17.435556	-0.302298
11.267990	17.435556	-0.302298
11.308188	17.449155	-0.346426
11.349594	17.462921	-0.387844
11.392411	17.476897	-0.426543
11.436967	17.491162	-0.462378
11.483371	17.505655	-0.494932
11.531684	17.520371	-0.523835
11.582611	17.535565	-0.548871
11.637041	17.551444	-0.569357
11.694911	17.567917	-0.583932
11.75544	17.584696	-0.591341
11.81734	17.601317	-0.590528
11.878758	17.617259	-0.530983
11.937175	17.632210	-0.563483
11.991112	17.645829	-0.539581
12.041446	17.658380	-0.510530
12.089194	17.670144	-0.477009
12.134492	17.681175	-0.439629
12.177623	17.691810	-0.399114
12.219079	17.702090	-0.355722
12.259294	17.712052	-0.309389
12.298728	17.721911	-0.259740
12.337714	17.731451	-0.206264
12.376528	17.741039	-0.148484
12.415435	17.750640	-0.085946
12.454307	17.760224	-0.019030
12.492915	17.769742	0.051218
12.531108	17.779197	0.124375
12.569041	17.788590	0.200573
12.607035	17.798000	0.279816
12.645352	17.807492	0.361892
12.684013	17.817072	0.446481
12.722886	17.826707	0.533100
12.762043	17.836415	0.621143
12.801651	17.846236	0.710114
12.835800	17.854706	0.786335

Pressure Surface

Z	R	RTHETA
11.129883	17.387064	0
11.138199	17.390062	0.003774
11.149389	17.394079	0.003975
11.163446	17.399101	0.000594
11.180382	17.405113	-0.006361
11.200267	17.412119	-0.016837
11.223280	17.420157	-0.030690
11.249779	17.429318	-0.047638
11.280384	17.439774	-0.067184
11.306234	17.448500	-0.082951
11.354097	17.464404	-0.109978
11.400635	17.479552	-0.133539
11.400635	17.479552	-0.133539
11.445829	17.493965	-0.153587
11.489815	17.507635	-0.170367
11.532391	17.520584	-0.184119
11.573227	17.532790	-0.195022
11.612215	17.544247	-0.203473
11.649295	17.554967	-0.209868
11.693760	17.564775	-0.214238
11.714722	17.573459	-0.216624
11.742244	17.581077	-0.217534
11.767107	17.587877	-0.217543
11.790598	17.594230	-0.217171
11.814575	17.600594	-0.216614
11.841550	17.607628	-0.215246
11.873006	17.615776	-0.212340
11.908064	17.624785	-0.207521
11.945708	17.634376	-0.200408
11.985802	17.644496	-0.190412
12.028064	17.655058	-0.176914
12.072000	17.665923	-0.159701
12.117177	17.676973	-0.138625
12.163135	17.688215	-0.113362
12.209542	17.699726	-0.083044
12.256120	17.711266	-0.046271
12.302606	17.722771	-0.001484
12.349126	17.734271	0.052055
12.395910	17.745823	0.112616
12.443110	17.757464	0.177476
12.490569	17.769161	0.245731
12.537967	17.780895	0.317744
12.585043	17.792553	0.393624
12.631774	17.804128	0.473009
12.678293	17.815655	0.555155
12.724528	17.827114	0.639343
12.770313	17.838465	0.725095
12.808836	17.848018	0.799092

LPT Stator 3 Airfoil Coordinates

50% From Hub

Suction Surface

Z	R	RTHETA
11.099155	19.634012	0
11.093014	19.630962	-0.009709
11.090810	19.629866	-0.023519
11.092624	19.630768	-0.041350
11.098593	19.633733	-0.063077
11.108895	19.638834	-0.088532
11.123746	19.646154	-0.117514
11.143388	19.655771	-0.149802
11.168070	19.667756	-0.185166
11.198038	19.682155	-0.223380
11.233511	19.698985	-0.264247
11.274663	19.718217	-0.307611
11.288110	19.724433	-0.321066
11.288110	19.724433	-0.321066
11.329916	19.743545	-0.360880
11.372582	19.762716	-0.398476
11.416522	19.782108	-0.433815
11.462046	19.801643	-0.466672
11.503570	19.821551	-0.496571
11.559719	19.842213	-0.523021
11.613142	19.863833	-0.545119
11.669698	19.886281	-0.561665
11.728662	19.909204	-0.571781
11.788964	19.932129	-0.574831
11.849322	19.954614	-0.570662
11.908403	19.976492	-0.559447
11.965283	19.997433	-0.541959
12.019877	20.017420	-0.518747
12.072233	20.036484	-0.490144
12.122175	20.054574	-0.456451
12.169637	20.071890	-0.418038
12.214754	20.088514	-0.375242
12.257787	20.104485	-0.328385
12.299153	20.119942	-0.277834
12.339247	20.135024	-0.223768
12.378397	20.149843	-0.166273
12.416852	20.164490	-0.105302
12.454842	20.179048	-0.040849
12.492612	20.193683	0.027063
12.530356	20.208606	0.098493
12.568075	20.223659	0.173573
12.605877	20.238883	0.252213
12.643963	20.254364	0.334092
12.682564	20.270199	0.418687
12.721714	20.286407	0.505407
12.761393	20.302987	0.593693
12.801609	20.319949	0.683122
12.836328	20.334720	0.760089

Pressure Surface

Z	R	RTHETA
11.099155	19.634012	0
11.106404	19.637603	0.003912
11.116581	19.642627	0.004723
11.129689	19.649071	0.002431
11.145747	19.656922	-0.002947
11.164806	19.666178	-0.011368
11.186974	19.676859	-0.022730
11.212450	19.689021	-0.036850
11.241563	19.702773	-0.053425
11.269928	19.716020	-0.069374
11.318711	19.738454	-0.095716
11.366053	19.759804	-0.119435
11.412038	19.780145	-0.139763
11.412038	19.780145	-0.139763
11.457245	19.799614	-0.157099
11.501592	19.818232	-0.171760
11.544666	19.836048	-0.183870
11.586155	19.852962	-0.193535
11.625644	19.868834	-0.201009
11.662508	19.883452	-0.206347
11.696099	19.896605	-0.209774
11.726556	19.908394	-0.211710
11.754605	19.919134	-0.212468
11.781316	19.929259	-0.212286
11.807971	19.939224	-0.211154
11.835906	19.949627	0.208929
11.866037	19.960817	-0.205117
11.898456	19.972818	-0.199451
11.933114	19.985605	-0.191665
11.970185	19.999232	-0.181404
12.009735	20.013716	-0.168226
12.051633	20.028995	-0.151665
12.095613	20.044964	-0.131171
12.141260	20.061498	-0.106062
12.188179	20.078707	-0.075774
12.236042	20.096401	-0.039865
12.284601	20.114493	0.001872
12.333624	20.132903	0.049489
12.382867	20.151541	0.102863
12.432136	20.170336	0.161745
12.481431	20.189289	0.225845
12.530642	20.208720	0.295019
12.579569	20.228273	0.368914
12.627982	20.247851	0.447006
12.675849	20.267432	0.528469
12.723179	20.287016	0.512451
12.769976	20.306594	0.698352
12.809453	20.323276	0.772843

LPT Stator 3 Airfoil Coordinates

90% From Hub

Suction Surface

Z	R	RTHETA
13.364055	15.425972	0.
13.360089	15.424932	0.006079
13.358675	15.424562	0.014924
13.359914	15.424887	0.026445
13.363959	15.425947	0.040505
13.370992	15.427786	0.056941
13.381195	15.430446	0.075593
13.394706	15.433952	0.096337
13.411571	15.438302	0.119135
13.431687	15.443453	0.144082
13.449066	15.447871	0.164645
13.449066	15.447871	0.164645
13.477386	15.455004	0.196390
13.506625	15.462283	0.226694
13.536553	15.469644	0.255380
13.567202	15.477089	0.282519
13.598751	15.484653	0.308065
13.631227	15.492508	0.331782
13.664606	15.500504	0.353421
13.699027	15.508546	0.372814
13.734661	15.516654	0.389727
13.771513	15.524809	0.403875
13.809498	15.532966	0.414922
13.848438	15.541070	0.422528
13.888058	15.548738	0.426390
13.927996	15.555972	0.426306
13.967847	15.562815	0.422176
14.007244	15.569209	0.414061
14.045869	15.575120	0.402101
14.083483	15.580537	0.386514
14.119917	15.585427	0.367587
14.155012	15.589777	0.345677
14.188731	15.593741	0.321081
14.221274	15.597368	0.293981
14.252818	15.600695	0.264445
14.283509	15.603756	0.232604
14.313454	15.606575	0.198551
14.342728	15.609169	0.162411
14.371414	15.611619	0.124288
14.399658	15.614002	0.084178
14.427612	15.616249	0.042053
14.455387	15.618372	-0.002083
14.483061	15.620377	-0.048216
14.510722	15.622272	-0.096298
14.538450	15.624062	-0.146260
14.566321	15.625751	-0.198036
14.594409	15.627341	-0.251579
14.616308	15.628503	-0.294168

Pressure Surface

Z	R	RTHETA
13.364055	15.425972	0.
13.368981	15.427261	-0.002741
13.375526	15.428370	-0.003592
13.383601	15.431072	-0.002471
13.393096	15.433535	0.000721
13.403946	15.436339	0.006042
13.416217	15.439495	0.013435
13.430218	15.443079	0.022623
13.451127	15.448393	0.036090
13.486479	15.457277	0.057873
13.521515	15.465957	0.078905
13.521515	15.465957	0.078905
13.555706	15.474308	0.098750
13.588977	15.482320	0.117080
13.621559	15.490157	0.133820
13.653419	15.497846	0.148822
13.684380	15.505149	0.161895
13.714414	15.512074	0.173028
13.743545	15.518642	0.182376
13.771634	15.524835	0.190039
13.798510	15.530632	0.196086
13.824167	15.536050	0.200588
13.848693	15.541122	0.203691
13.872263	15.545772	0.205573
13.8951[illegible]	15.550050	0.206401
13.917725	15.554148	0.206269
13.940384	15.558140	0.205204
13.963497	15.562086	0.203084
13.987381	15.566031	0.199711
14.012277	15.569999	0.194814
14.038354	15.573998	0.188060
14.065768	15.578028	0.179117
14.094559	15.582069	0.167832
14.124527	15.586011	0.154162
14.155492	15.589835	0.138054
14.187311	15.593578	0.119320
14.219876	15.597216	0.097813
14.253112	15.600726	0.073431
14.286935	15.604087	0.046235
14.321202	15.607277	0.016360
14.355758	15.610273	-0.016209
14.390493	15.613241	-0.051587
14.425328	15.616070	-0.089806
14.460178	15.618727	-0.130836
14.494959	15.621205	-0.174581
14.529598	15.623503	-0.220912
14.564020	15.625616	-0.269741
14.590447	15.627124	-0.309168

LPT Rotor 3 Airfoil Coordinates

10% From Hub

ORIGINAL PAGE IS
OF POOR QUALITY

Suction Surface

Z	R	RTHETA
13.398751	18.022804	0
13.394760	18.021491	0.005699
13.393111	18.020949	0.014104
13.393897	18.021208	0.025137
13.397260	18.022314	0.038676
13.403377	18.024328	0.054575
13.412436	18.027316	0.072675
13.424606	18.031339	0.092838
13.439999	18.036442	0.114971
13.458628	18.042641	0.139065
13.476381	18.048570	0.160408
13.476381	18.048570	0.160408
13.503494	18.057669	0.190328
13.531684	18.067183	0.218126
13.560867	18.077092	0.243702
13.591084	18.087415	0.266983
13.622465	18.098203	0.287802
13.655179	18.109778	0.305952
13.689391	18.121913	0.321122
13.725108	18.134559	0.332914
13.762185	18.147660	0.340897
13.800240	18.161079	0.344634
13.[illegible]38716	18.174618	0.343841
13.8[illegible]5987	18.187890	0.338469
13.91[illegible]463	18.200559	0.328666
13.95[illegible]666	18.212632	0.314805
13.985342	18.224042	0.297378
14.018467	18.234802	0.276795
14.050169	18.244972	0.253357
14.080830	18.254688	0.227158
14.110728	18.263883	0.198163
14.139927	18.272699	0.166568
14.168466	18.281251	0.132532
14.196446	18.289574	0.096158
14.223932	18.297689	0.057487
14.251071	18.305644	0.016582
14.277964	18.313469	-0.026528
14.304641	18.321176	-0.071753
14.331122	18.328827	-0.118940
14.357459	18.336549	-0.167981
14.383697	18.344232	-0.218818
14.409878	18.351886	-0.271377
14.436071	18.359533	-0.325525
14.462306	18.367180	-0.381109
14.488632	18.374843	-0.437939
14.515089	18.382533	-0.495839
14.541707	18.390257	-0.554688
14.562573	18.396304	-0.601187

Pressure Surface

Z	R	RTHETA
13.398751	18.022804	0
13.403529	18.024378	-0.002476
13.409788	18.026442	-0.003106
13.417434	18.028967	-0.001809
13.426349	18.031916	0.001514
13.436460	18.035268	0.006926
13.447826	18.039044	0.014378
13.460750	18.043348	0.023615
13.481237	18.050196	0.037960
13.513915	18.061180	0.059528
13.545831	18.071979	0.079279
13.545831	18.071979	0.079279
13.576743	18.082508	0.097053
13.606578	18.092732	0.112739
13.635419	18.102758	0.126311
13.663228	18.112635	0.137798
13.689872	18.122084	0.147279
13.715182	18.131047	0.154781
13.738996	18.139469	0.160336
13.761304	18.147349	0.163990
13.782251	18.154739	0.165847
13.802221	18.161776	0.166058
13.821771	18.168659	0.164720
13.841524	18.175605	0.161792
13.862073	18.182799	0.157143
13.883895	18.190238	0.150545
13.907245	18.198133	0.141770
13.932144	18.206476	0.130759
13.958467	18.215212	0.117557
13.985831	18.224202	0.102210
14.013958	18.233346	0.084520
14.042783	18.242614	0.063972
14.072269	18.251987	0.040281
14.102314	18.261370	0.013385
14.132854	18.270570	-0.016618
14.163740	18.279840	-0.049637
14.194871	18.289107	-0.085587
14.226219	18.298362	-0.124368
14.257763	18.307596	-0.165758
14.289451	18.31679[illegible]	-0.209485
14.321238	18.325942	-0.255385
14.353082	18.335267	-0.303385
14.384914	18.344588	-0.353379
14.416703	18.353879	-0.405202
14.448403	18.363129	-0.458651
14.479971	18.372323	-0.513518
14.511378	18.381455	-0.569649
14.535757	18.388531	-0.614221

LPT Rotor 3 Airfoil Coordinates

50% From Hub

Suction Surface

Z	R	RTHETA
13.379752	20.568110	0.
13.376703	20.566803	0.006110
13.376333	20.566644	0.014544
13.378703	20.567660	0.025231
13.383912	20.569892	0.038060
13.392080	20.573390	0.052898
13.403337	20.578209	0.069599
13.417800	20.584395	0.088031
13.435554	20.591981	0.108105
13.456616	20.600970	0.129801
13.463873	20.604064	0.136925
13.463873	20.604064	0.136925
13.491464	20.615817	0.162562
13.519865	20.627894	0.186517
13.548967	20.640247	0.208619
13.578866	20.652915	0.228825
13.609774	20.665987	0.246977
13.641870	20.679558	0.262854
13.675282	20.693649	0.276131
13.709853	20.708188	0.286400
13.745282	20.723047	0.293308
13.781294	20.738106	0.296520
13.817528	20.753214	0.295820
13.853566	20.768199	0.291109
13.889006	20.782881	0.282444
13.923603	20.797151	0.270064
13.957211	20.810954	0.254180
13.989793	20.824279	0.234963
14.021439	20.837170	0.212575
14.052406	20.849733	0.186988
14.082904	20.861998	0.158152
14.112836	20.873904	0.126261
14.142187	20.885556	0.091613
14.170945	20.896953	0.054299
14.199151	20.908111	0.014449
14.226938	20.919083	-0.027862
14.254450	20.929923	-0.072630
14.281719	20.940660	-0.119755
14.308730	20.951294	-0.169039
14.335528	20.961938	-0.220319
14.362159	20.972525	-0.273509
14.388684	20.983078	-0.328509
14.415156	20.993619	-0.385190
14.441619	21.004165	-0.443391
14.468109	21.014730	-0.502927
14.494684	21.025338	-0.563614
14.521382	21.036004	-0.625328
14.542514	21.044452	-0.674611

Pressure Surface

Z	R	RTHETA
13.379752	20.568110	0.
13.384064	20.569957	-0.003096
13.390086	20.572536	-0.004587
13.397720	20.575805	-0.004360
13.406835	20.579705	-0.002268
13.417331	20.584194	0.001803
13.429209	20.589271	0.007851
13.442682	20.595024	0.015639
13.457956	20.601541	0.024603
13.489823	20.615119	0.043032
13.520991	20.628372	0.060591
13.520991	20.628372	0.060591
13.551328	20.641248	0.076986
13.580855	20.653757	0.092093
13.609681	20.665948	0.105938
13.637710	20.677801	0.118457
13.664730	20.689203	0.129493
13.690561	20.700079	0.138763
13.715077	20.710382	0.145962
13.738434	20.720178	0.150917
13.760932	20.729596	0.153626
13.782849	20.738755	0.154242
13.804542	20.747805	0.152888
13.826432	20.756920	0.149653
13.848920	20.766269	0.144562
13.872251	20.775948	0.137498
13.896571	20.786006	0.128370
13.921917	20.796457	0.117092
13.948198	20.807258	0.103485
13.975160	20.818301	0.087311
14.002589	20.829498	0.067986
14.030585	20.840885	0.044820
14.059162	20.852468	0.017648
14.088332	20.864159	-0.013110
14.118053	20.875976	-0.047009
14.148194	20.887938	-0.083715
14.178610	20.899987	-0.123157
14.209269	20.912108	-0.165360
14.240186	20.924308	-0.210130
14.271315	20.936568	-0.257182
14.302613	20.948869	-0.306343
14.334016	20.961337	-0.357557
14.365471	20.973842	-0.410716
14.396936	20.986363	-0.465673
14.428374	20.998885	-0.522235
14.459727	21.011386	-0.580216
14.490957	21.023850	-0.639478
14.515455	21.033636	-0.687000

LPT Rotor 3 Airfoil Coordinates

90% From Hub

Suction Surface

Z	R	RTHETA
15.435551	15.657863	0.
15.433051	15.657811	-0.005376
15.433642	15.657823	-0.014111
15.437351	15.657901	-0.026181
15.444227	15.658045	-0.041540
15.454343	15.658260	-0.060122
15.467802	15.658551	-0.081833
15.484742	15.658925	-0.106548
15.505342	15.659392	-0.134102
15.529834	15.659964	-0.164284
15.558510	15.660658	-0.196827
15.591736	15.661494	-0.231399
15.613944	15.662072	-0.252837
15.613944	15.662072	-0.252837
15.650540	15.663059	-0.285299
15.688028	15.664112	-0.314898
15.726373	15.665216	-0.341375
15.765568	15.666291	-0.364529
15.805581	15.667477	-0.384157
15.846393	15.668780	-0.400173
15.887952	15.670205	-0.412529
15.930106	15.671750	-0.421100
15.972639	15.673411	-0.425806
16.015308	15.675189	-0.426508
16.057826	15.677387	-0.423180
16.099859	15.679655	-0.415887
16.141166	15.681977	-0.404905
16.181703	15.684346	-0.390494
16.221533	15.686760	-0.372834
16.260858	15.689228	-0.351956
16.299793	15.691754	-0.327716
16.338273	15.694287	-0.300062
16.376267	15.696788	-0.269045
16.413637	15.699251	-0.234890
16.450302	15.701671	-0.197952
16.486419	15.704057	-0.158343
16.522159	15.706420	-0.116016
16.557649	15.708770	-0.071112
16.592947	15.711110	-0.023824
16.628070	15.713333	0.025706
16.662985	15.715492	0.077374
16.697729	15.717614	0.131003
16.732348	15.719702	0.186392
16.766896	15.721760	0.243318
16.801427	15.723791	0.301544
16.835994	15.725797	0.360867
16.870654	15.727783	0.421132
16.898251	15.729346	0.469581

Pressure Surface

Z	R	RTHETA
15.435551	15.657863	0.
15.439271	15.657941	0.001702
15.444646	15.658054	0.001520
15.451595	15.658201	-0.000621
15.460014	15.658382	-0.004813
15.469833	15.658595	-0.011123
15.481084	15.658843	-0.019521
15.493997	15.659133	-0.029796
15.5255[illegible]	15.659862	-0.054264
15.565345	15.660827	-0.083902
15.605312	15.661846	-0.113200
15.644174	15.662884	-0.141267
15.681815	15.663935	-0.166744
15.681815	15.663935	-0.166744
15.718461	15.665000	-0.189046
15.754217	15.665970	-0.207986
15.789115	15.666978	-0.223721
15.823163	15.668027	-0.236591
15.856393	15.669114	-0.247036
15.888824	15.670236	-0.255355
15.920508	15.671389	-0.261680
15.951597	15.672576	-0.266148
15.982307	15.673803	-0.268841
16.012881	15.675077	-0.269897
16.043606	15.676641	-0.269347
16.074816	15.678292	-0.267158
16.106752	15.680036	-0.263157
16.139458	15.681879	-0.257158
16.172871	15.683822	-0.248932
16.206789	15.685857	-0.238152
16.241097	15.687978	-0.224326
16.275860	15.690192	-0.206780
16.311109	15.692501	-0.184952
16.346982	15.694860	-0.158656
16.383560	15.697269	-0.128373
16.420686	15.699716	-0.094896
16.458190	15.702191	-0.058528
16.495942	15.704686	-0.019157
16.533887	15.707197	0.023140
16.572007	15.709722	0.068109
16.610336	15.712226	0.115475
16.648835	15.714620	0.165045
16.687458	15.716990	0.216619
16.726154	15.719331	0.269985
16.764866	15.721640	0.324917
16.803541	15.723914	0.381204
16.842125	15.726151	0.438698
16.872671	15.727898	0.485130

LPT Stator 4 Airfoil Coordinates

10% From Hub

Suction Surface

Z	R	RTHETA
15.311727	18.597028	0.
15.308790	18.596312	-0.006098
15.309153	18.596400	-0.015595
15.312868	18.597307	0.028441
15.320028	18.599053	-0.044548
15.330765	18.601665	-0.063791
15.345257	18.605182	-0.086000
15.363733	18.609649	-0.110957
15.386483	18.615124	-0.138390
15.413861	18.621676	-0.167960
15.446299	18.629387	-0.199258
15.484317	18.638352	-0.231791
15.516309	18.645836	-0.256185
15.516309	18.645836	-0.256185
15.557442	18.655378	-0.283661
15.599505	18.665042	-0.307386
15.642352	18.674813	-0.327326
15.685933	18.684667	-0.343399
15.730214	18.694560	-0.355425
15.775082	18.704459	-0.363188
15.820345	18.714319	-0.366506
15.865776	18.724087	-0.365331
15.911140	18.733714	-0.359645
15.956220	18.743141	-0.349517
16.000843	18.752310	-0.335062
16.044888	18.761215	-0.316411
16.088287	18.769848	-0.293721
16.131010	18.778211	-0.267143
16.173062	18.786309	-0.236831
16.214474	18.794156	-0.202909
16.255302	18.801768	-0.165309
16.295582	18.809001	-0.124734
16.335374	18.816052	-0.080712
16.374734	18.822942	-0.033552
16.413713	18.829681	0.016647
16.452359	18.836282	0.069780
16.490721	18.842754	0.125730
16.528835	18.849104	0.184381
16.566745	18.855342	0.245596
16.604493	18.861599	0.309251
16.642120	18.867822	0.375220
16.679654	18.873986	0.443374
16.717139	18.880098	0.513541
16.754606	18.886165	0.585528
16.792094	18.892192	0.659115
16.829649	18.898186	0.734098
16.867300	18.904154	0.810331
16.898673	18.909090	0.874525

Pressure Surface

Z	R	RTHETA
15.311727	18.597028	0.
15.316607	18.598219	0.002267
15.323822	18.599977	0.001948
15.333203	18.602258	-0.001120
15.344525	18.605005	-0.007154
15.357607	18.608170	-0.016328
15.372434	18.611746	-0.028657
15.389330	18.615807	-0.043830
15.408887	18.620488	-0.061145
15.449583	18.630164	-0.094751
15.490017	18.639689	-0.124274
15.530018	18.649026	-0.150167
15.569224	18.658095	-0.172974
15.569224	18.658095	-0.172974
15.607465	18.666860	-0.192730
15.644774	18.675364	-0.209347
15.681301	18.683626	-0.222722
15.717093	18.691641	-0.232855
15.752184	18.699422	-0.239819
15.786689	18.706999	-0.243732
15.820798	18.714417	-0.244693
15.854740	18.721726	-0.242718
15.888749	18.728979	-0.237802
15.923042	18.736219	-0.229870
15.957792	18.743467	-0.218833
15.993120	18.750734	-0.204592
16.029093	18.758038	-0.187035
16.065743	18.765381	-0.166074
16.103064	18.772756	-0.141647
16.141025	18.780151	-0.113737
16.179570	18.787551	-0.082329
16.218663	18.794943	-0.047460
16.258244	18.802306	0.009172
16.298257	18.809477	0.032454
16.338650	18.816628	0.077331
16.379377	18.823749	0.125370
16.420388	18.830827	0.176472
16.461647	18.837856	0.230514
16.503110	18.844827	0.287368
16.544734	18.851730	0.346894
16.586480	18.858605	0.408968
16.628319	18.865545	0.473458
16.670207	18.872438	0.540209
16.712113	18.879281	0.609029
16.753998	18.886067	0.679696
16.795816	18.892788	0.752003
16.837529	18.899438	0.825797
16.872080	18.904907	0.888137

LPT Stator 4 Airfoil Coordinates

50% From Hub

Suction Surface

Z	R	RTHETA
15.194873	21.296166	0.
15.192670	21.295379	-0.005925
15.193923	21.295827	-0.014903
15.198678	21.297525	-0.026884
15.207009	21.300496	-0.041784
15.219018	21.304774	0.059492
15.234835	21.310397	-0.079864
15.254614	21.317411	-0.102732
15.278528	21.325865	-0.127904
15.306773	21.335814	-0.155164
15.339557	21.347311	-0.184287
15.377339	21.360494	-0.215096
15.377339	21.360494	-0.215096
15.419928	21.375268	-0.246325
15.463455	21.390275	-0.274404
15.507838	21.405479	-0.299233
15.552941	21.420885	-0.320820
15.598762	[illegible]436474	-0.339037
15.645318	2[illegible]452169	-0.353654
15.692554	21.[illegible]67944	-0.364414
15.740343	21.[illegible]3751	-0.371071
15.788514	21.499529	-0.373507
15.836866	21.515209	-0.371598
15.885186	21.530682	-0.365301
15.933267	21.545786	-0.354625
15.980930	21.560569	-0.339622
16.028031	21.574990	-0.320392
16.074480	21.589031	-0.297067
16.120223	21.602682	-0.269781
16.165246	21.615947	-0.238662
16.209571	21.628841	-0.203849
16.253234	21.641104	-0.165454
16.296287	21.653106	-0.123588
16.338779	21.664886	0.078352
16.380761	21.676461	-0.029845
16.422300	21.687851	0.021825
16.463439	21.699070	0.076568
16.504244	21.710138	0.134266
16.544767	21.721069	0.194793
16.585056	21.732163	0.258048
16.625172	21.743285	0.323908
16.665137	21.754388	0.392248
16.705057	21.765484	0.462948
16.744925	21.776588	0.535729
16.784818	21.787716	0.610468
16.824798	21.798886	0.686939
16.864915	21.810110	0.765003
16.898620	21.819553	0.831510

Pressure Surface

Z	R	RTHETA
15.194873	21.296166	0.
15.200546	21.298191	0.003552
15.208933	21.301182	0.004545
15.219877	21.305080	0.002803
15.233164	21.309803	-0.001915
15.248590	21.315277	-0.009836
15.266058	21.321460	-0.021073
15.285701	21.328395	-0.035476
15.308032	21.336256	-0.052474
15.345593	21.349422	-0.079134
15.389259	21.364638	-0.106968
15.432490	21.379609	-0.131898
15.432490	21.379609	-0.131898
15.474900	21.394205	-0.154441
15.516372	21.408391	-0.174530
15.556988	21.422267	-0.191945
15.596885	21.435838	-0.206452
15.636063	21.449060	-0.217994
15.674506	21.461934	-0.226597
15.712269	21.474483	-0.232331
15.749479	21.486755	-0.235269
15.786308	21.498810	-0.235416
15.822955	21.510714	-0.232782
15.859634	21.522538	-0.227321
15.896552	21.534270	-0.218971
15.933888	21.545980	-0.207631
15.971786	21.557747	-0.193187
16.010337	21.569594	-0.175513
16.049593	21.581530	-0.154503
16.089569	21.593553	-0.130084
16.130243	21.605649	-0.102189
16.171579	21.617799	-0.070798
16.213525	21.629975	-0.035899
16.256032	21.641886	0.002488
16.299050	21.653874	0.044320
16.342510	21.665917	0.089548
16.386369	21.678002	0.138088
16.430564	21.690110	0.189868
16.475041	21.702223	0.244779
16.519750	21.714328	0.302700
16.564633	21.726507	0.363528
16.609647	21.738979	0.427153
16.654746	21.751496	0.493424
16.699878	21.764043	0.562167
16.744984	21.776605	0.633180
16.790004	21.789164	0.706265
16.834885	21.801706	0.781282
16.872331	21.812187	0.845488

LPT Stator 4 Airfoil Coordinates

90% From Hub

Suction Surface

Z	R	RTHETA
17.618050	15.758063	0.
17.615121	15.757894	0.005103
17.614500	15.757859	0.012528
17.616270	15.757961	0.022193
17.620557	15.758208	0.033976
17.627515	15.758608	0.047728
17.637299	15.759170	0.063302
17.650032	15.759897	0.080578
17.665767	15.760792	0.099505
17.684443	15.761847	0.120142
17.700133	15.762728	0.136667
17.700133	15.762728	0.136667
17.726316	15.764188	0.162837
17.752928	15.765657	0.187617
17.779940	15.767133	0.210961
17.807387	15.768618	0.232912
17.835361	15.770116	0.253451
17.863931	15.771721	0.272435
17.893145	15.773321	0.289699
17.923017	15.774908	0.305123
17.953562	15.776481	0.318537
17.984775	15.778036	0.329766
18.016620	15.779567	0.338603
18.049015	15.781068	0.344832
18.081825	15.782436	0.348304
18.114912	15.783685	0.348910
18.148094	15.784838	0.346557
18.181110	15.785884	0.341238
18.213694	15.786819	0.333006
18.245628	15.787640	0.322022
18.276771	15.788351	0.308456
18.307099	15.788882	0.292484
18.336641	15.789329	0.274[illegible]37
18.365479	15.789706	0.253[illegible]10
18.393701	15.790020	0.231[illegible]78
18.421375	15.790274	0.206757
18.448545	15.790471	0.180301
18.475296	15.790616	0.151979
18.501704	15.790710	0.121826
18.527883	15.790838	0.089848
18.553925	15.790935	0.056016
18.579861	15.791002	0.020324
18.605748	15.791040	-0.017145
18.631621	15.791048	-0.056258
18.657516	15.791026	-0.096815
18.683430	15.790975	0.138658
18.709312	15.790895	-0.181704
18.727962	15.790818	-0.213468

Pressure Surface

Z	R	RTHETA
17.618050	15.758063	0.
17.622063	15.758295	-0.00237[illegible]
17.627529	15.758609	-0.003139
17.634338	15.759000	-0.002194
17.642342	15.759458	0.000605
17.651428	15.759977	0.005369
17.661597	15.760555	0.012094
17.673085	15.761206	0.020554
17.691641	15.762252	0.034137
17.721618	15.763927	0.055112
17.751259	15.765565	0.074734
17.751259	15.765565	0.074734
17.780488	15.767163	0.092922
17.809288	15.768721	0.109650
17.837688	15.770244	0.124950
17.865653	15.771817	0.138780
17.893091	15.773318	0.151047
17.919933	15.774747	0.161737
17.946130	15.776103	0.170886
17.971670	15.777389	0.178506
17.996537	15.778607	0.184678
18.020736	15.77976[illegible]	0.189494
18.044303	15.780853	0.193078
18.067320	15.781857	0.195564
18.089921	15.782751	0.197019
18.112247	15.783589	0.197455
18.134476	15.784377	0.196843
18.156872	15.785126	0.195082
18.179700	15.785841	0.192062
18.203177	15.786528	0.187630
18.227447	15.787184	0.181675
18.252530	15.787805	0.174107
18.278400	15.788386	0.164843
18.304974	15.788848	0.153777
18.332164	15.789265	0.140736
18.359902	15.789638	0.125482
18.388143	15.789962	0.107879
18.416805	15.790235	0.087830
18.445808	15.790454	0.065315
18.475041	15.790615	0.040330
18.504411	15.790725	0.012833
18.533886	15.790863	-0.017200
18.563412	15.790963	-0.049715
18.592950	15.791025	-0.084539
18.622467	15.791048	-0.121402
18.651965	15.791033	-0.159976
18.681495	15.790980	-0.199990
18.702822	15.790918	-0.229672

LPT Rotor 4 Airfoil Coordinates

10% From Hub

Suction Surface

Z	R	RTHETA
17.677414	19.046764	0
17.675326	19.046380	0.004258
17.675086	19.046336	0.010086
17.676739	19.046640	0.017435
17.680351	19.047305	0.026227
17.686013	19.048349	0.036357
17.693830	19.049796	0.047706
17.703914	19.051671	0.060143
17.716379	19.054002	0.073539
17.731327	19.056817	0.087777
17.749822	19.060330	0.103515
17.749822	19.060330	0.103515
17.772899	19.064759	0.120871
17.796268	19.069295	0.136380
17.820202	19.073995	0.150288
17.844929	19.078909	0.162536
17.870563	19.084110	0.173108
17.896968	19.089588	0.181662
17.923908	19.095207	0.187953
17.951183	19.100925	0.191805
17.978578	19.106699	0.193135
18.005948	19.112498	0.191908
18.033157	19.118293	0.188102
18.060085	19.124009	0.181809
18.086618	19.129579	0.173090
18.112640	19.135017	0.162047
18.138117	19.140318	0.148817
18.163174	19.145510	0.133387
18.187953	19.150622	0.115747
18.212445	19.155654	0.095967
18.236657	19.160593	0.074167
18.260482	19.165345	0.050466
18.283870	19.169995	0.025067
18.306908	19.174560	-0.002005
18.329710	19.179063	0.030826
18.352368	19.183523	-0.061341
18.374897	19.187943	-0.093481
18.397297	19.192323	-0.127157
18.419571	19.196665	-0.162250
18.441739	19.201034	-0.198674
18.463842	19.205389	-0.236368
18.485893	19.209733	-0.275264
18.507916	19.214070	-0.315236
18.529924	19.218404	-0.356110
18.551931	19.222736	-0.397671
18.573926	19.227066	-0.439738
18.595882	19.231386	-0.482193
18.611173	19.234395	-0.512013

Pressure Surface

Z	R	RTHETA
17.677414	19.046764	0
17.680359	19.047306	-0.002172
17.684485	19.048067	-0.003257
17.689720	19.049034	-0.003173
17.695974	19.050194	-0.001815
17.703175	19.051533	0.000899
17.711328	19.053056	0.004964
17.720588	19.054792	0.010202
17.738261	19.058130	0.020184
17.762926	19.062838	0.033287
17.786681	19.067428	0.044662
17.786681	19.067428	0.044662
17.810096	19.072004	0.054923
17.833219	19.076575	0.064486
17.855776	19.081083	0.073333
17.877542	19.085555	0.081227
17.898399	19.089886	0.087673
17.918486	19.094074	0.092380
17.938037	19.098166	0.095310
17.957255	19.102203	0.096552
17.976351	19.106229	0.096234
17.995473	19.110275	0.094493
18.014756	19.114371	0.091439
18.034320	19.118541	0.087049
18.054279	19.122787	0.081311
18.074749	19.127090	0.074182
18.095763	19.131492	0.065602
18.117198	19.135967	0.055534
18.138910	19.140483	0.043682
18.160910	19.145042	0.029618
18.183190	19.149641	0.013031
18.205857	19.154303	-0.006090
18.228960	19.159035	-0.027477
18.252414	19.163738	-0.050707
18.276104	19.168453	-0.075667
18.299938	19.173181	-0.102523
18.323900	19.177917	-0.131302
18.347992	19.182663	-0.161913
18.372210	19.187416	-0.194196
18.396534	19.192174	-0.227981
18.420923	19.196932	-0.263188
18.445363	19.201748	-0.299760
18.469832	19.206569	-0.337600
18.494316	19.211392	-0.376541
18.518800	19.216213	-0.416360
18.543297	19.221037	-0.456805
18.567833	19.225866	-0.497680
18.584988	19.229243	-0.528395

LPT Rotor 4 Airfoil Coordinates

50% From Hub

Suction Surface

Z	R	RTHETA
17.664443	22.030995	0.
17.663537	22.030762	0.004841
17.664742	22.031073	0.010605
17.668080	22.031933	0.017243
17.673585	22.033352	0.024677
17.681305	22.035344	0.032804
17.691295	22.037924	0.041500
17.703614	22.041108	0.050631
17.718326	22.044914	0.060059
17.735487	22.049361	0.069655
17.755148	22.054463	0.079308
17.768036	22.057812	0.085030
17.768036	22.057812	0.085030
17.792032	22.064058	0.094531
17.816258	22.070377	0.102680
17.840813	22.076794	0.109468
17.865844	22.083443	0.114779
17.891374	22.090245	0.118471
17.917372	22.097144	0.120384
17.943718	22.104107	0.120390
17.970259	22.111093	0.118354
17.996848	22.118063	0.114244
18.023326	22.124974	0.107986
18.049541	22.131690	0.099588
18.075381	22.138182	0.089123
18.100831	22.144508	0.076638
18.125905	22.150677	0.062141
18.150692	22.156711	0.045638
18.175239	22.162624	0.027079
18.199505	22.168409	0.006587
18.223426	22.174037	-0.015730
18.247050	22.179456	-0.039841
18.270412	22.184788	-0.065775
18.293561	22.190047	-0.093491
18.316530	22.195239	-0.122927
18.339321	22.200366	-0.154001
18.361913	22.205424	-0.186603
18.384311	22.210414	-0.220606
18.406527	22.215347	-0.255900
18.428602	22.220345	-0.292425
18.450570	22.225323	-0.330191
18.472462	22.230286	-0.369159
18.494323	22.235246	-0.409204
18.516205	22.240214	-0.450122
18.538100	22.245188	-0.491676
18.559961	22.250158	-0.533663
18.581719	22.255108	-0.575964
18.596818	22.258545	-0.605602

Pressure Surface

Z	R	RTHETA
17.664443	22.030995	0.
17.666973	22.031648	-0.003348
17.671193	22.032736	-0.005869
17.677044	22.034245	-0.007431
17.684447	22.036155	-0.007857
17.693337	22.038451	-0.007000
17.703704	22.041131	-0.004840
17.715654	22.044223	-0.001612
17.720024	22.045354	-0.000391
17.743822	22.051523	0.006068
17.766976	22.057537	0.011781
17.789687	22.063447	0.016702
17.789687	22.063447	0.016702
17.812086	22.069288	0.020884
17.834255	22.075075	0.024413
17.856094	22.080838	0.027323
17.877459	22.086541	0.029551
17.898324	22.092092	0.030930
17.918720	22.097501	0.031275
17.938770	22.102802	0.030405
17.958624	22.108034	0.028221
17.978470	22.113238	0.024613
17.99[illegible]347	22.118455	0.019581
18.0[illegible]8528	22.123724	0.013124
18.039082	22.129043	0.005244
18.060027	22.134333	-0.004029
18.081349	22.139671	-0.014700
18.102957	22.145034	-0.026888
18.124804	22.150407	-0.040812
18.146934	22.155800	-0.056802
18.169408	22.161225	-0.074914
18.192179	22.166669	-0.095041
18.215212	22.172121	-0.117108
18.238458	22.177488	-0.141151
18.261884	22.182845	-0.167170
18.285488	22.188215	-0.195105
18.309291	22.193605	-0.224798
18.333288	22.199011	-0.256059
18.357467	22.204430	-0.288711
18.381787	22.209853	-0.322636
18.406214	22.215276	-0.357823
18.430718	22.220824	-0.394315
18.455252	22.226384	-0.432075
18.479764	22.231942	-0.470969
18.504265	22.237503	-0.510729
18.528799	22.243075	-0.551037
18.553436	22.248674	-0.591634
18.570689	22.252598	-0.620034

LPT Rotor 4 Airfoil Coordinates

90% From Hub

ORIGINAL PAGE IS
OF POOR QUALITY

Suction Surface

Z	R	RTHETA
19.617719	15.756459	0.
19.614491	15.756645	-0.005925
19.613723	15.756690	-0.014075
19.615479	15.756588	-0.024381
19.619855	15.756335	-0.036740
19.626960	15.755922	-0.051034
19.636889	15.755340	-0.067158
19.649697	15.754582	-0.085056
19.665350	15.753644	-0.104761
19.695599	15.751795	-0.139449
19.695599	15.751795	-0.139449
19.730685	15.749592	-0.175114
19.766671	15.747267	-0.207195
19.803423	15.744823	-0.236628
19.841450	15.742221	-0.263561
19.880417	15.739477	-0.287680
19.919873	15.736644	-0.308699
19.959917	15.733738	-0.326302
20.000525	15.730680	-0.340669
20.041705	15.727465	-0.351871
20.083461	15.724087	-0.359800
20.125597	15.720558	-0.364311
20.167850	15.716899	-0.365382
20.209958	15.713101	-0.362949
20.251688	15.709021	-0.357103
20.292941	15.704881	-0.347942
20.333629	15.700693	-0.335573
20.373586	15.696478	-0.320186
20.412797	15.692244	-0.302077
20.451634	15.687955	-0.281298
20.490363	15.683584	-0.257694
20.528742	15.679113	-0.231268
20.566576	15.674675	-0.202197
20.603861	15.670296	-0.170414
20.640597	15.665976	-0.135787
20.677002	15.661690	-0.098578
20.713283	15.657414	-0.059032
20.749349	15.653158	-0.017170
20.785040	15.648942	0.026941
20.820542	15.644897	0.072953
20.855933	15.640962	0.120668
20.891171	15.637087	0.169974
20.926359	15.633259	0.220633
20.961405	15.629488	0.272551
20.996396	15.625765	0.325493
21.031469	15.622076	0.379220
21.066893	15.618391	0.433451
21.094615	15.615538	0.475859

Pressure Surface

Z	R	RTHETA
19.617719	15.756459	0.
19.621630	15.756232	0.002389
19.627333	15.755900	0.003050
19.634749	15.755466	0.001895
19.643775	15.754933	-0.001186
19.654326	15.754306	-0.006283
19.666400	15.753580	-0.013400
19.680150	15.752745	-0.022372
19.713356	15.750688	-0.044566
19.753664	15.748115	-0.071149
19.753664	15.748115	-0.071149
19.792408	15.745562	-0.095403
19.830253	15.742994	-0.118161
19.867332	15.740407	-0.139370
19.903136	15.737841	-0.158387
19.937999	15.735342	-0.174681
19.972373	15.732812	-0.188504
20.006160	15.730247	-0.200512
20.039383	15.727649	-0.210673
20.072034	15.725023	-0.218850
20.104108	15.722373	-0.224907
20.135803	15.719685	-0.228722
20.167381	15.716940	-0.230179
20.199104	15.714114	-0.229349
20.231204	15.711038	-0.226271
20.263782	15.707819	-0.221035
20.296925	15.704476	-0.213670
20.330799	15.700987	-0.204182
20.365418	15.697348	-0.192589
20.400412	15.693592	-0.178885
20.435513	15.689747	-0.162684
20.470966	15.685785	-0.143442
20.506963	15.681666	-0.121040
20.543508	15.677382	-0.095809
20.580602	15.673028	-0.067924
20.618028	15.668631	-0.037084
20.655578	15.664213	-0.003112
20.693342	15.659765	0.033758
20.731482	15.655267	0.073115
20.769811	15.650741	0.114765
20.808251	15.646274	0.158471
20.846843	15.641969	0.203962
20.885486	15.637709	0.251096
20.924270	15.633485	0.299578
20.963111	15.629306	0.349251
21.001868	15.625187	0.400009
21.040274	15.621156	0.451885
21.069852	15.618086	0.492838

LPT Stator 5 Airfoil Coordinates

10% From Hub

ORIGINAL PAGE IS
OF POOR QUALITY

Suction Surface

Z	R	RTHETA
19.472147	19.378800	0.
19.469239	19.378395	-0.007904
19.469927	19.378491	-0.018263
19.474305	19.379101	-0.030341
19.482519	19.380239	-0.045735
19.494749	19.381923	-0.062386
19.511189	19.384163	-0.080621
19.532016	19.386963	-0.100191
19.557353	19.390312	-0.120922
19.587229	19.394180	-0.142773
19.605781	19.396538	-0.155435
19.603781	19.396538	-0.155435
19.646496	19.401594	-0.181218
19.687694	19.406545	-0.204733
19.729575	19.411408	-0.226002
19.772124	19.416173	-0.244708
19.815261	19.420867	-0.260474
19.858898	19.425444	-0.273233
19.902966	19.429853	-0.282989
19.947433	19.434087	-0.289636
19.992255	19.438136	-0.293039
20.037348	19.441987	-0.293101
20.082608	19.445628	-0.289682
20.127905	19.448988	-0.282644
20.173066	19.451975	-0.271875
20.217838	19.454726	-0.257390
20.262020	19.457234	-0.239335
20.305603	19.459507	-0.217963
20.348601	19.461556	-0.193485
20.390946	19.463783	-0.166198
20.432653	19.465000	-0.136451
20.474064	19.466388	-0.104484
20.515402	19.467654	-0.070189
20.556339	19.468807	-0.033140
20.596786	19.469844	0.006611
20.636772	19.470773	0.048916
20.676352	19.471596	0.093603
20.715557	19.472317	0.140524
20.754481	19.472941	0.189467
20.793205	19.473605	0.240264
20.831786	19.474264	0.292798
20.870274	19.474873	0.346934
20.908736	19.475432	0.402500
20.947219	19.475942	0.459311
20.985783	19.476403	0.517152
21.024504	19.476817	0.575815
21.063534	19.477184	0.635092
21.094832	19.477441	0.682612

Pressure Surface

Z	R	RTHETA
19.472147	19.378800	0.
19.475609	19.379282	0.002544
19.481257	19.380065	0.003450
19.488982	19.381131	0.002566
19.498644	19.382456	-0.000308
19.510123	19.384019	-0.005343
19.523398	19.385809	-0.012569
19.538646	19.387845	-0.021735
19.565605	19.391389	-0.037817
19.607012	19.396693	-0.060975
19.648063	19.401785	-0.081496
19.648063	19.401785	-0.081496
19.686676	19.406661	-0.100138
19.728805	19.411320	-0.116896
19.768251	19.415746	-0.131395
19.807030	19.419981	-0.143416
19.845221	19.424032	-0.153090
19.882910	19.427873	-0.160417
19.920171	19.431517	-0.165350
19.957030	19.434973	-0.167950
19.993536	19.438248	-0.168263
20.029771	19.441355	-0.166278
20.065838	19.444305	-0.162011
20.101868	19.447109	-0.155458
20.138035	19.449676	-0.146594
20.174590	19.452072	-0.135337
20.211735	19.454363	-0.121633
20.249480	19.456542	-0.105382
20.287810	19.458603	-0.086488
20.326792	19.460541	-0.064892
20.366412	19.462348	-0.040725
20.406328	19.464001	-0.014099
20.446318	19.465479	0.015020
20.486708	19.466786	0.046491
20.527589	19.468008	0.080426
20.568931	19.469140	0.116861
20.610678	19.470178	0.155761
20.652800	19.471117	0.197008
20.695204	19.471954	0.240499
20.737807	19.472685	0.286097
20.780554	19.473378	0.333680
20.823393	19.474125	0.383151
20.866258	19.474812	0.434394
20.909102	19.475437	0.487244
20.951866	19.476000	0.541513
20.994472	19.476501	0.597027
21.036770	19.476938	0.653721
21.070159	19.477241	0.699605

LPT Stator 5 Airfoil Coordinates

50% From Hub

Suction Surface

Z	R	RTHETA
19.343773	22.402337	0
19.343104	22.402235	-0.005493
19.345849	22.402653	0.012819
19.351950	22.403582	-0.022092
19.361323	22.405003	-0.033473
19.373879	22.406896	-0.047133
19.389555	22.409243	-0.063193
19.408352	22.412034	-0.081655
19.430378	22.415270	-0.102308
19.455907	22.418977	-0.124627
19.489064	22.423718	-0.150471
19.489064	22.423718	-0.150471
19.532609	22.429821	-0.179306
19.578347	22.436080	-0.204034
19.624457	22.442232	-0.224388
19.670843	22.448263	-0.24134
19.718042	22.454312	-0.255411
19.765891	22.460300	-0.266115
19.813946	22.466103	-0.273320
19.862097	22.471705	-0.277162
19.910319	22.477103	-0.277780
19.958467	22.482281	-0.275272
20.006389	22.487224	-0.269778
20.053954	22.491861	-0.261425
20.101077	22.496082	-0.250402
20.147748	22.500043	-0.236930
20.194061	22.503758	-0.221293
20.240282	22.507251	-0.203617
20.286570	22.510535	-0.183708
20.332762	22.513599	-0.161303
20.378612	22.516428	-0.136180
20.423881	22.518839	-0.108116
20.468503	22.521038	-0.077208
20.512590	22.523120	-0.043738
20.556276	22.525093	-0.007943
20.599534	22.526958	0.030141
20.642312	22.528716	0.070481
20.684753	22.530375	0.112814
20.726956	22.531941	0.156956
20.768928	22.533645	0.202879
20.810725	22.535447	0.250522
20.852444	22.537241	0.299736
20.894140	22.539030	0.350353
20.935847	22.540816	0.402169
20.977434	22.542592	0.455067
21.019026	22.544364	0.508734
21.060947	22.546146	0.562757
21.094363	22.547564	0.605333

Pressure Surface

Z	R	RTHETA
19.343773	22.402337	0
19.347963	22.402975	0.004074
19.355377	22.404102	0.006367
19.365915	22.405696	0.006687
19.379448	22.407732	0.004783
19.395873	22.410184	0.000456
19.415189	22.413042	-0.006293
19.437603	22.416324	-0.015068
19.446408	22.417603	-0.018520
19.493841	22.424394	-0.036148
19.541240	22.431014	-0.051675
19.541240	22.431014	-0.051675
19.585306	22.437018	-0.066785
19.627181	22.442591	-0.079822
19.668682	22.447985	-0.091188
19.709907	22.453273	-0.101043
19.750320	22.458374	-0.108947
19.790082	22.463248	-0.114990
19.829639	22.467952	-0.119328
19.869100	22.472502	-0.122011
19.908490	22.476902	-0.122939
19.947953	22.481169	-0.122002
19.987643	22.485315	-0.119107
20.027689	22.489353	-0.114245
20.068177	22.493159	-0.107414
20.109118	22.496780	-0.098608
20.150417	22.500263	-0.087739
20.191808	22.503582	-0.074693
20.233131	22.506725	-0.059366
20.274550	22.509703	-0.041664
20.316312	22.512532	-0.021657
20.358654	22.515222	0.000430
20.401644	22.517708	0.024615
20.445168	22.519900	0.051069
20.489095	22.522022	0.079929
20.533448	22.524073	0.111109
20.578281	22.526052	0.144460
20.623452	22.527951	0.180023
20.668860	22.529764	0.217732
20.714500	22.531488	0.257412
20.760314	22.533273	0.299025
20.806207	22.535252	0.342603
20.852123	22.537227	0.388064
20.898027	22.539197	0.435215
20.944052	22.541167	0.4[illegible]3643
20.990072	22.543131	0.533133
21.035762	22.545076	0.583715
21.071317	22.546588	0.624350

LPT Stator 5 Airfoil Coordinates

90% From Hub

Suction Surface

Z	R	RTHETA
21.710133	15.575004	0
21.707451	15.575044	0.006885
21.707884	15.575037	0.016019
21.711491	15.574984	0.027324
21.718365	15.574882	0.040673
21.728637	15.574732	0.055888
21.742473	15.574533	0.072743
21.760077	15.574284	0.090962
21.781686	15.573987	0.110222
21.807571	15.573640	0.130155
21.838035	15.573248	0.150349
21.873412	15.572812	0.170352
21.891989	15.572592	0.179618
21.891989	15.572592	0.179618
21.928785	15.572174	0.195805
21.965821	15.571777	0.209545
22.003443	15.571381	0.221019
22.041506	15.571000	0.230110
22.079750	15.570651	0.236719
22.118131	15.570335	0.240864
22.156655	15.570053	0.242567
22.195252	15.569804	0.241796
22.233829	15.569591	0.238549
22.272301	15.569421	0.232849
22.310584	15.569316	0.224742
22.348589	15.569254	0.214307
22.386266	15.569234	0.201619
22.423680	15.569257	0.186688
22.460902	15.569319	0.169502
22.497952	15.569423	0.150145
22.534775	15.569565	0.128699
22.571092	15.569733	0.105397
22.606667	15.569938	0.080532
22.641683	15.570180	0.054065
22.676493	15.570460	0.025985
22.711072	15.570778	-0.003605
22.745294	15.571132	-0.034569
22.779179	15.571520	-0.066851
22.812860	15.571943	-0.100353
22.846318	15.572414	-0.135076
22.879560	15.572925	-0.170948
22.912605	15.573473	-0.207851
22.945481	15.574057	-0.245627
22.978207	15.574677	-0.284091
23.010792	15.575333	-0.323047
23.043319	15.576026	-0.362266
23.075954	15.576760	-0.401491
23.099690	15.577318	-0.429778

Pressure Surface

Z	R	RTHETA
21.710133	15.575004	0
21.713532	15.574953	-0.002593
21.718845	15.574875	-0.003738
21.726028	15.574770	-0.003377
21.735033	15.574640	-0.001443
21.745835	15.574485	0.002098
21.758475	15.574307	0.007189
21.773121	15.574104	0.013603
21.793224	15.573831	0.022335
21.829692	15.573354	0.037653
21.865399	15.572909	0.052238
21.899509	15.572505	0.065361
21.932669	15.572131	0.076173
21.932669	15.572131	0.076173
21.965648	15.571779	0.085272
21.998387	15.571435	0.092902
22.030540	15.571107	0.098923
22.062252	15.57080[illegible]	0.103269
22.093784	15.570532	0.106094
22.125177	15.570281	0.107530
22.156428	15.570054	0.107609
22.187607	15.569851	0.106348
22.218804	15.569670	0.103735
22.250108	15.569511	0.099729
22.281600	15.569392	0.094268
22.313370	15.569310	0.087275
22.345467	15.569257	0.078711
22.377829	15.569235	0.068539
22.410381	15.569244	0.056594
22.443106	15.569284	0.042569
22.476058	15.569357	0.026224
22.509516	15.569463	0.007521
22.543717	15.569604	-0.013083
22.578475	15.569772	-0.034868
22.613440	15.569981	-0.057815
22.648637	15.570233	-0.082205
22.684190	15.570528	-0.108007
22.720080	15.570868	-0.135011
22.756174	15.571252	-0.163218
22.792490	15.571683	-0.192605
22.829024	15.572164	-0.223159
22.865754	15.572708	-0.254835
22.902653	15.573304	-0.287532
22.939702	15.573951	-0.321078
22.976892	15.574651	-0.355228
23.014140	15.575403	-0.389781
23.051279	15.576202	-0.424683
23.078015	15.576808	-0.450128

LPT Rotor 5 Airfoil Coordinates

10% From Hub

ORIGINAL PAGE IS
OF POOR QUALITY

Suction Surface

Z	R	RTHETA
21.702990	19.485240	0.
21.701674	19.485213	0.006602
21.703330	19.485247	0.014585
21.707989	19.485342	0.023884
21.715701	19.485500	0.034390
21.726546	19.485725	0.045936
21.740638	19.486022	0.058285
21.758128	19.486399	0.071113
21.779220	19.486864	0.083993
21.791797	19.487147	0.090581
21.791797	19.487147	0.090581
21.829715	19.488027	0.106474
21.867672	19.488948	0.117705
21.905394	19.489901	0.125598
21.943396	19.490901	0.130861
21.981648	19.491948	0.133517
22.019953	19.493079	0.133640
22.058222	19.494236	0.131361
22.096405	19.495416	0.126755
22.134474	19.496619	0.119906
22.172409	19.497844	0.110888
22.210168	19.499088	0.099752
22.247710	19.500350	0.086547
22.285006	19.501620	0.071349
22.322039	19.502879	0.054234
22.358816	19.504131	0.035275
22.395334	19.505375	0.014513
22.431571	19.506610	-0.007991
22.467517	19.507836	-0.032156
22.503206	19.509053	-0.057930
22.538652	19.510264	-0.085304
22.573817	19.511404	-0.114272
22.608681	19.512528	-0.144766
22.643254	19.513640	-0.176683
22.677548	19.514740	-0.209916
22.711615	19.515831	-0.244350
22.745482	19.516911	-0.279913
22.779163	19.517983	-0.316537
22.812672	19.519047	-0.354150
22.846041	19.520123	-0.392699
22.879286	19.521202	-0.432164
22.912400	19.522279	-0.472501
22.945395	19.523355	-0.513306
22.978272	19.524429	-0.555345
23.010902	19.525498	-0.597665
23.043477	19.526568	-0.640262
23.076352	19.527650	-0.682743
23.100588	19.528449	-0.713929

Pressure Surface

Z	R	RTHETA
21.702990	19.485240	0
21.707036	19.485322	-0.005137
21.713691	19.485458	-0.008978
21.722902	19.485649	-0.011411
21.734597	19.485894	-0.012784
21.748713	19.486195	-0.011[illegible]65
21.765233	19.486554	-0.008915
21.784230	19.486976	-0.004792
21.805931	19.487471	0.000427
21.823510	19.487880	0.004433
21.823510	19.487880	0.004433
21.855368	19.488645	0.010678
21.887187	19.489436	0.015294
21.919240	19.490261	0.018540
21.951014	19.491107	0.020196
21.982537	19.491973	0.020220
22.014008	19.492902	0.018565
22.045515	19.493849	0.015223
22.077107	19.494816	0.010234
22.108314	19.495806	0.003608
22.140655	19.496817	-0.004659
22.172671	19.497852	-0.014555
22.204905	19.498913	-0.026060
22.237385	19.500001	-0.039163
22.270127	19.501114	-0.053846
22.303126	19.502236	-0.070090
22.336383	19.503367	-0.087866
22.369922	19.504509	-0.107154
22.403752	19.505662	-0.127921
22.437839	19.506824	-0.150123
22.472168	19.507994	-0.173726
22.506779	19.509175	-0.198704
22.541690	19.510365	-0.22[illegible]42
22.576893	19.511503	-0.25[illegible]2
22.612375	19.512647	-0.281648
22.648084	19.513796	-0.311792
22.683992	19.514947	-0.343072
22.720086	19.516101	-0.375426
22.756353	19.517257	-0.408784
22.792760	19.518415	-0.443088
22.829291	19.519580	-0.478309
22.865953	19.520769	-0.514425
22.902733	19.521964	-0.551381
22.939632	19.523167	-0.589050
22.976778	19.524380	-0.627133
23.013978	19.525599	-0.665581
23.050879	19.526811	-0.704528
23.077893	19.527700	-0.733305

LPT Rotor 5 Airfoil Coordinates

50% From Hub

Suction Surface

Z	R	RTHETA
21.702999	22.563210	0
21.703526	22.563218	0.005956
21.706883	22.563270	0.012331
21.713078	22.563365	0.019074
21.722123	22.563505	0.026104
21.734036	22.563689	0.033305
21.748841	22.563917	0.040524
21.766567	22.564189	0.047572
21.787249	22.564507	0.054219
21.803407	22.564756	0.058454
21.803407	22.564756	0.058454
21.840916	22.565331	0.065345
21.878847	22.565913	0.068462
21.916780	22.566493	0.068545
21.954608	22.567071	0.065976
21.992308	22.567656	0.060989
22.029883	22.568260	0.053782
22.067258	22.568849	0.044479
22.104389	22.569423	0.033286
22.141315	22.569982	0.020366
22.178059	22.570527	0.005756
22.214628	22.571059	-0.010484
22.251027	22.571577	-0.028293
22.287748	22.572056	-0.047648
22.323285	22.572502	-0.068529
22.359142	22.572923	-0.090899
22.394815	22.573320	-0.114742
22.430297	22.573693	-0.140031
22.465590	22.574042	-0.166729
22.500697	22.574368	-0.194814
22.535623	22.574671	-0.224266
22.570359	22.574899	-0.255053
22.604903	22.575110	-0.287117
22.639269	22.575311	-0.320396
22.673476	22.575504	-0.354822
22.707527	22.575689	-0.390346
22.741453	22.575865	-0.426887
22.775263	22.576032	-0.464374
22.808955	22.576192	-0.502733
22.842569	22.576386	-0.541870
22.876122	22.576604	-0.581718
22.909614	22.576827	-0.622217
22.943053	22.577056	-0.663288
22.976447	22.577290	-0.704849
23.009744	22.577530	-0.746813
23.042982	22.577776	-0.789107
23.076233	22.578028	-0.831603
23.100651	22.578217	-0.862941

Pressure Surface

Z	R	RTHETA
21.702999	22.563210	0.
21.705121	22.563243	-0.005409
21.709750	22.563314	-0.010390
21.716872	22.563424	-0.014852
21.726466	22.563572	-0.018667
21.738516	22.563758	-0.021718
21.753012	22.563981	-0.023954
21.769970	22.564242	-0.025456
21.789440	22.564541	-0.026582
21.811915	22.564887	-0.027852
21.811915	22.564887	-0.027852
21.844181	22.565382	-0.030079
21.876025	22.565870	-0.033005
21.907866	22.566357	-0.037032
21.939813	22.566845	-0.042199
21.971889	22.567334	-0.048500
22.004088	22.567847	-0.056004
22.036488	22.568365	-0.064738
22.069132	22.568878	-0.074770
22.101981	22.569386	-0.086126
22.135011	22.569887	-0.098774
22.168217	22.570382	-0.112740
22.201593	22.570871	-0.128058
22.235147	22.571352	-0.144719
22.268885	22.571820	-0.162718
22.302803	22.572251	-0.182063
22.336904	22.572664	-0.202745
22.371197	22.573060	-0.224756
22.405679	22.573136	-0.248090
22.440347	22.573794	-0.272724
22.475195	22.574133	-0.298646
22.510235	22.574453	-0.325842
22.545465	22.574743	-0.354290
22.580874	22.574964	-0.383948
22.616442	22.575178	-0.414776
22.652166	22.575385	-0.446714
22.688011	22.575584	-0.479729
22.723980	22.575775	-0.513762
22.760062	22.575958	-0.548728
22.796223	22.576133	-0.584561
22.832445	22.576322	-0.621195
22.868728	22.576555	-0.658557
22.905064	22.576796	-0.696571
22.941449	22.577044	-0.735141
22.977921	22.577301	-0.774122
23.014459	22.577565	-0.813418
23.050983	22.577836	-0.853008
23.077848	22.578040	-0.882231

LPT Rotor 5 Airfoil Coordinates

90% From Hub

END

DATE

FILMED

JAN 8 1985